DEPARTMENT OF PHYSICS
UNIVERSITY OF JYVÄSKYLÄ
RESEARCH REPORT No. 15/2016

APPLICATION OF TIME-DEPENDENT MANY-BODY PERTURBATION THEORY TO EXCITATION SPECTRA OF SELECTED FINITE MODEL SYSTEMS

BY
NIKO SÄKKINEN

Academic Dissertation
for the Degree of
Doctor of Philosophy

To be presented, by permission of the
Faculty of Mathematics and Natural Sciences
of the University of Jyväskylä,
for public examination in Auditorium FYS-1 of the
University of Jyväskylä on December 21, 2016
at 12 o'clock noon

Jyväskylä, Finland
December 2016

JYFL Research Report 15/2016
ISBN 978-951-39-6813-7 (paper copy)
ISBN 978-951-39-6814-4 (pdf)
ISSN 0075-465X

Preface

In this thesis, the research work done in the course of 2010-2016 at the University of Jyväskylä is documented. In the beginning, the work was supervised by Professors Matti Manninen and Robert van Leeuwen of whom the former become the Rector of the University in 2012 and the task of supervising was left to Professor van Leeuwen. I owe thanks to both for the opportunity to study, learn and do the research which culminated into this doctoral dissertation. I would like to thank the pre-examiners of this thesis Professor Michael Bonitz and Doctor Hervé Ness for their valuable work and Doctor Guy Cohen for accepting the duties of the opponent.

In addition, I owe thanks the coauthors of the enclosed publications Yang Peng and Doctor Heiko Appel for their work without which this thesis would not exist. I would like to thank Professors Jussi Timonen, Hannu Häkkinen and Ilari Maasilta for trusting me with the tasks of the demo assistantships of several courses. For the same reason, I thank Doctor Vesa Apaja who has also been of a great help in problems related to the use of the local computer clusters. Also, I owe a debt of gratitude to the current and former administrative staff of the physics department, in particular, to the departmental coordinators Soili Leskinen, Minttu Haapaniemi and Sanna Boman for their help in various things, not the least of, for organizing my funding on several occasions. Also, other colleagues, in particular, Doctors Riku Tuovinen, Daniel Karlsson and Gianluca Stefanucci are acknowledged for collaboration.

A special thanks goes to my family, parents and siblings, who have helped to stay tuned on things other than research. It is for the same reason as well as for her love, support and understanding that I thank Hanna.

Tampere, December 2016
Niko Säkkinen

Abstract

In this thesis, an approximate method introduced to solve time-dependent many-body problems known as time-dependent many-body perturbation theory is studied. Many-body perturbation theory for interacting electrons and phonons is reviewed. In particular, the electron propagator G and an unconventional two-component phonon propagator, which satisfy coupled integral Dyson equations, are introduced. In practice, the associated integral kernels known as the electron Σ and phonon self-energies need to be approximated. The conserving approximations known as the Hartree(-Fock) and the first and second Born approximations, which respect the continuity equation between the electron density and current, are considered in this work.

Time-dependent systems of interest are studied in this thesis by using the integro-differential forms of the Dyson equations referred to as the Kadanoff-Baym Equations (KBE). The Kadanoff-Baym equations are introduced for the electron and phonon propagators unconventionally as coupled first-order integro-differential equations. It is reviewed how these equations are solved numerically by describing an integration rule, a class of practical methods and a parallel implementation of the numerical method. In addition, documentation of how the Kadanoff-Baym equations allow to solve the Bethe-Salpeter Equation (BSE) with the kernel $\delta\Sigma/\delta G$ for the density response function, is provided.

In two of the enclosed publications, we benchmarked observables obtained by using the Hartree and partially and fully self-consistent Born approximations against numerically exact results for the two-site, two-electron Holstein model. In this model, the two electrons which are constrained to move between two lattice sites interact indirectly via the electron-phonon coupling. It was observed that only the fully self-consistent Born approximation could cope qualitatively correctly with the competition between the delocalizing and localizing effects of the kinetic and interaction energies. For the other two approximations, spurious bifurcative symmetry breaking with an associated unbounded density response was observed. Nevertheless, also the self-consistent Born approximation was concluded to fail in describing the bipolaronic behavior of the true system. In the third publication, we benchmarked the Hartree-Fock and second Born approximations against an exact method for the few-site Hubbard and Pariser-Parr-Pople models in which the underlying lattice is inert and the electrons interact amongst themselves directly. It was found that the second Born approximation is capable of describing the so-called correlation induced doubly-excited states. This is not possible for time-local approximations such as Hartree-Fock.

In addition to the qualitative results, which highlight successes of the applied simple self-energy approximations, the approximate and exact results were also compared on a more quantitative level. It is the quantitative and qualitative results combined which are used in this thesis to assess the quality of the many-body approximations used, with the aim to better understand when these methods are predictive.

Author Niko Säkkinen
Department of Physics
University of Jyväskylä
Finland

Supervisor Professor Robert van Leeuwen
Department of Physics
University of Jyväskylä
Finland

Reviewers Professor Michael Bonitz
Institute for Theoretical Physics und Astrophysics
Christian-Albrechts-Universität Kiel
Germany

Doctor Hervé Ness
Department of Physics
King's College London
United Kingdom

Opponent Doctor Guy Cohen
School of Chemistry
Tel Aviv University
Israel

List of Publications

I Säkkinen N, Peng Y, Appel H, and van Leeuwen R,
Many-body Green's function theory for electron-phonon interactions:
Ground state properties of the Holstein dimer,
J. Chem. Phys. 143, 234101 (2015) [SPAL15a]

The author is the principal investigator and main writer: with the exceptions of writing the subsection 'Exact Properties' and obtaining the exact diagonalization results, the author has done all of the theoretical and numerical work.

II Säkkinen N, Peng Y, Appel H, and van Leeuwen R,
Many-body Green's function theory for electron-phonon interactions:
The Kadanoff-Baym approach to spectral properties of the Holstein dimer,
J. Chem. Phys. 143, 234102 (2015) [SPAL15b]

The author is the principal investigator and main writer: with the exceptions of obtaining majority of the exact diagonalization results, the author has done all of the theoretical and numerical work

III Säkkinen N, Manninen M, and van Leeuwen R,
Kadanoff-Baym approach to double excitations in finite systems,
New. J. Phys. 14, 013203 (2012) [SML12]

The author is the principal investigator and main writer: with the exception of the content of the appendix, the author has done all of the theoretical and numerical work.

Other Publications

IV Tuovinen R, Säkkinen N, Karlsson D, Stefanucci G, and van Leeuwen R,
Phononic heat transport in the transient regime: An analytic solution,
Phys. Rev. B 93, 214301 (2016) [TSK+16]

The author provided background information for the theory development part of the article, was primarily responsible for deriving and implementing the exact embedding technique and provided the reference numerical results by using the exact embedding technique.

Contents

1 Introduction

In atomic and molecular, or solid state, physics, there exist many theoretical and computational methods to study both time-independent and -dependent phenomena in a variety of physical situations. Often these methods are overlapping, that is, they exist to describe essentially identical physical situations. The reason for this is that although in principle a unique methodology exists, it is in practice impossible to use it to model all but the smallest of atoms. In particular, in non-relativistic quantum mechanics, it would be ideal to be able to solve the time-independent or -dependent Schrödinger equation; however, as the complexity of this task scales exponentially with the number of degrees of freedom, it is usually not possible to do so. It has been then a general practice to develop approximate methods by, in one way or another, eliminating some hopefully redundant degrees of freedom. Intuitively, it is plausible that the more degrees of freedom that are washed out, the further the results are from the exact methodology. This leads naturally to a trade-off between the accuracy and computational feasibility, which determines the method used in practice. In atomic and molecular physics, or in quantum chemistry, it is possible to study small to modest size molecules by applying, e.g., the time-independent or -dependent variants of the Multi-Configurational Hartree (TD)MCH [BJWM00] or Coupled-Cluster (TD)CC [BM07] methods in which it is straightforward, up to a limit, to increase the accuracy at the expense of the computational cost. In particular, it is possible to obtain numerically exact results if convergence with respect to configurations is guaranteed. If larger molecules, or clusters, are studied, then less accurate methods, such as the time-independent or -dependent Density Functional Theory (TD)DFT [MMN+12], are needed to overcome computational limitations. However, by using these methods, it is typically not possible to achieve numerically exact results in practice. Moreover, some observables cannot be evaluated and, in addition to quantitative errors, also qualitative deficiencies are often found; e.g., incorrect dissociation [CHR12], problems with conical intersections [UY14], and related problems to describe doubly-excited states [UY14]. These problems are offset by the advantage of such methods, that it is possible to use them also to study solid state physics.

If understood in the sense of infinite partial resummations, time-independent and -dependent many-body perturbation theory (TD)MBPT [SL13] is a theoretical and computational methodology which lies roughly speaking in between methods such as coupled-cluster and density functional theory. In fact, its time-independent version has been applied in the context of both atomic and molecular physics [SDL06, NBRG07, CRR+12, CRR+13] and solid state physics in which it has been used for quite a long time to routinely calculate, e.g., (inverse-)photoemission and photoabsorption spectra [AG98, ORR02]. It is common to such applications to realistic systems that often the simplest, non-self-consistent variants of the many-body approximations are used as they are computationally more tractable than their self-consistent counterparts or the more complicated approximations. In its self-consistent form, there are fewer published works on the time-independent, and considerably less on the time-dependent, many-body perturbation theory, especially regarding inhomogeneous systems. If infinite partial resummations are conducted at least by introducing the self-energy then time-dependent many-body perturbation theory can be used by taking advantage of the Kadanoff-Baym formalism [KB62]. In order to name a few applications, which do not make additional approximations and focus on typical condensed matter systems, works concentrating on small atoms and molecules [DSL06, DLS06, DL07, BBB10b, BBB10a, BHB12], semiconductor quantum kinetics [GBH99, BGL+01, GSJ06], few-electron quantum dots [BBL+09, BB09], phonon-mediated

superconductors [KSM+15, SKGK16] and plasmon-accompanied spectroscopy [SBP16, SP16] are noteworthy. The Kadanoff-Baym Equations (KBE), on which the formalism is based, have also been applied recently to studying electron correlation in transient quantum transport in model systems [MSSL08, MSSL09, UKS+10, MSSL10, MTK+12].

In particular, the applications to model systems, such as in the transport problem, invoked interest in benchmarking time-dependent many-body perturbation theory (i) against numerically exact methods to ascertain that the method can be considered predictive. Since an experimental confirmation is out of the question, in order for benchmarking to be conducted in practice, the results in some standard approximations for the electron self-energy beyond the mean-field level, i.e., in the second Born (2B), GW and T-matrix approximations, were compared to numerically exact results directly in the transport context [UKS+11], as well as by investigating finite lattice systems typically used as central systems in a transport setting [FVA09, FVA10a, FVA10b]. In the latter case, a serious deficiency was found, as the time-dependent densities following a strong excitation were shown to exhibit artificial damping to an unphysical steady-state for strongly interacting few-site lattices with a local, Hubbard-type electron-electron interaction. It was also soon after that this observation was confirmed by independent sources, e.g, in [HSB14]. However, in [FVA10b], it is also stated that no artificial damping is found in the linear response regime (ii) in which the dynamics of one-body observables is dominantly dictated by the response function $\delta G/\delta v$. In [KB00], it had been shown that such $\delta G/\delta v$ corresponds to a solution of the Bethe-Salpeter Equation (BSE) with the four-point kernel $\delta\Sigma/\delta G$ but it had been hardly explored [DL07] (iii) if the Kadanoff-Baym approach was a potential method for calculating linear response functions, similarly as done, e.g., in density functional theory [SLR+12]. It was in particular observations (ii) and (iii), in addition to the need (i) to understand when the many-body approximations are predictive, which initiated the work summarized in this thesis.

It is highlighted, e.g., in [UY14] that time-dependent density functional theory has in practice, i.e., when a frequency-independent kernel f_{xc} is used, issues describing absorption spectra of systems in which doubly-excited states play a significant role. In [RSB+09, SROM11], state of the art methods as of that time based on time-dependent density functional theory and time-independent many-body perturbation theory, or more precisely on solving the Bethe-Salpeter equation in frequency-domain, were been developed and shown to be able to describe double-excitations. In our chronologically first publication **III** [SML12] contained in this thesis, motivated by this, in addition to the desire to benchmark time-dependent many-body perturbation theory, we summarize some results regarding the density-density response functions of small, few-site Hubbard and Pariser-Parr-Pople models obtained by solving of the Kadanoff-Baym equations. In this publication, we confirm that for the accessed time-scales, the response function does not show artificial damping, in agreement with [FVA10b], and as the main result show that already the simplest correlated self-consistent approximation for the electron self-energy, i.e., the second Born approximation, comes with the ability to describe doubly-excited states. At the time, a qualitatively similar observation had been made for a few-electron quantum dot in [BHB12] where, in addition, it is highlighted that the second Born approximation also gives rise to spurious excitations, as also speculated in **III** [SML12] and reported more throughly in another context [RSB+09, SROM11]. Next in the chronological order, we studied in **I** [SPAL15a] time-independent many-body perturbation theory by considering the ground state properties of the two-site and -electron Holstein model. It was our motivation to explore other many-body approximations capable of describing the effects of the electron-phonon interaction ultimately to be applied to quantum transport. In the transport context, it has been debated, see [WWTR14] and references therein, whether the electron-phonon interaction or its incorrect approximate description is responsible for the observed bistability, in which two different steady-state solutions are found, which highlights why it is important to study the many-body approximations. In our publication, for one, we summarize the main steps needed to take phononic degrees of freedom into account when solving the equilibrium Dyson equation. For another, it was found that the many-body approxima-

tions, i.e., the Hartree (H), and partially (Gd) and fully (GD) self-consistent Born approximations, support multiple solutions exhibiting spontaneous symmetry-breaking. It was also observed that the symmetry-broken solutions, which were concluded to mimic the bipolaronic crossover of the exact solution, emerged continuously in the manner of a bifurcation in all but the fully self-consistent Born approximation. In **II** [SPAL15b], which is the chronologically latest work included in this thesis, we continued to investigate the many-body approximations by using the same two-site and -electron Holstein model but now focused on the electron and phonon spectral function and the density-density response function. In this publication, we summarize how the non-equilibrium Kadanoff-Baym equations can be solved when the electron-phonon interaction is present. In regard to the application, it is observed, by using analytical and numerical means, that only a single bounded response function, belonging to either a symmetric or symmetry broken solution **I** [SPAL15a], exists for a fixed interaction strength in the Hartree and partially self-consistent Born approximation. In contrast, in the fully self-consistent Born approximation bounded response functions were observed for all co-existing solutions showing, by example, that multiple stable solutions are possible, as also found for a related method in the context of bistability [WWTR14]. Also, to address the question when the approximations are qualitatively, or even quantitatively, predictive, a substantial effort was put on comparing the approximate results against exact results for a relatively wide range of parameters in both **I** [SPAL15a] and **II** [SPAL15b].

In this thesis, in addition to summarizing the content of the enclosed publications, the theoretical and computational background behind this work is, in accord with a good scientific practice, documented in a greater detail than what was possible in the publications. It is, in the first place, reviewed how time-independent and -dependent many-body perturbation theory, especially for the phonon propagator, is derived when both the electron-electron and electron-phonon interactions are present. It is felt that a more detailed description of many-body perturbation theory is entitled as some of the simplifications made for the extended, (quasi-)homogeneous and time-translationally invariant systems considered in many standard sources [AGD65, FW71, Mah00, HJ08] do not apply to the finite, inhomogeneous and time-dependent systems studied in this work. Another point in favor of a more thorough exposition is that we have chosen an unconventional representation of the phononic degrees of freedom in terms of both the displacement and momentum components. It was initially an open problem for us how the Kadanoff-Baym equations should be formulated and subsequently solved for the phonon propagator, which lead to the unconventional choice, and it is only recently that complementary approaches to do so have emerged in the literature known to us, cf., [WWTR14, SBP16]. Hence, it is also documented here in some detail how we have solved the Kadanoff-Baym equations numerically for the coupled phonon field and electron and phonon propagators. In particular, a numerical integration rule, similar to [Bal07, SDL09b], designed to solve the initial-value problem for the real- and mixed-time components of the propagators is proposed and an algorithm relying on this rule and aimed at solving the Kadanoff-Baym equations is summarized. It is finally documented, in order to review the methodology used in the publications, how a density response function satisfying the Bethe-Salpeter is obtained in practice by solving the Kadanoff-Baym equations.

An outline of the thesis is provided below for the convenience of the reader. In Part. I, the many-body problem and time-dependent many-body theory is reviewed starting by introduction of the physical systems in Ch. 2 followed by an introduction to the observables used in the enclosed publication in Ch. 3, and ending with a review of many-body perturbation theory in Ch. 4. In Ch. 4, the Keldysh contour and components, diagrammatic perturbation expansions, conserving many-body approximations and the Kadanoff-Baym equations are introduced with some of the more technical details, e.g., a proof of Wick's theorem, placed in the appendix. In Part. II, in Ch. 5, the numerical methods used in the publications are reviewed by specifying how the field, propagators and equations are represented, summarizing the algorithms used to solve the imaginary-, real and mixed-time components of the field and propagators and reviewing the parallel implementation of these algorithms.

Moreover, in Ch. 6, the numerical integration rule and a class of two-stage methods used to solve the initial value problem for real- and mixed-time components are motivated and presented. In Part. III, it is explained, in Ch. 7, how the density response functions shown in the publications have been obtained and, finally in Ch. 8, a summary of some of the main results of Pubs. **I-III** is represented. An erratum to the enclosed publications is provided in the appendix of Ch. 8. Finally, a summary of this thesis and an outlook is presented in Ch. 9.

Part I

Theory

2 System

Non-relativistic, quantum mechanical, condensed matter systems of interacting electrons and nuclei are used in this thesis as a platform to investigate time-independent and -dependent many-body perturbation theory. In order to be more specific, the nuclei are treated in this work at the level of the harmonic approximation which allows one to use phonons to characterize their properties. Similarly, the dynamic interaction between the electrons and nuclei is treated at the level of the electron-phonon interaction. Moreover, it is noted that unless otherwise stated, a finite, or infinite but enumerable, Hilbert space is assumed in this thesis which essentially means that electrons are treated in a finite basis. However, most of the results apply also for systems with both discrete and continuous spectra,. In what follows, a brief summary of some fundamental aspects of how such many-body systems are specified and described theoretically is given.

2.1 Hamiltonian Operator

In the exact quantum theory, the solution of time-independent or -dependent Schrödinger equation [Mes61a, Mes61b] determines how physical quantities behave statically and dynamically. In this equation, the Hamiltonian operator incorporates the information about the particular physical system and it is responsible for generating the time-evolution. It is therefore natural to begin by introducing the Hamiltonian operator whose role, as an object specifying the physical system, remains invariant when transitioning to the approximate many-body perturbation theory. Here, it is remarked that the units are chosen henceforth such that $\hbar$ is replaced by unity. In the language of the second quantization [BF04, SL13], it is possible to describe a generic system of electrons interacting amongst themselves and nuclei, which experience a harmonic potential, by introducing the Hamiltonian operator

$$\begin{aligned}\widehat{H} = &\frac{1}{2}\sum_{\mu} m_{\mu}^{-1}\hat{p}_{\mu}^{2} + \frac{1}{2}\sum_{\mu\nu} k_{\mu\nu}\hat{u}_{\mu}\hat{u}_{\nu} \\ &+ \sum_{pq} h_{pq}\hat{c}_{p}^{\dagger}\hat{c}_{q} + \frac{1}{2}\sum_{pqst} w_{pqst}\hat{c}_{p}^{\dagger}\hat{c}_{q}^{\dagger}\hat{c}_{s}\hat{c}_{t} \\ &+ \sum_{pq}\sum_{\mu} g_{pq}^{\mu}\hat{u}_{\mu}\hat{c}_{p}^{\dagger}\hat{c}_{q}\,. \end{aligned} \tag{2.1}$$

Here, the first row describes the nuclei, with the first and second terms corresponding to the kinetic and potential energies, the second row describes the electrons, with the first and second terms corresponding to the combined kinetic and potential energy and the electron-electron interaction, and the term on the third line describes the interaction between the electrons and the nuclei. The properties of the nuclei are encoded in the nuclear masses satisfying $m_{\mu} = m_{\mu}^{*}$ and in the curvature, or simply the spring constant, matrix whose elements are denoted by $k_{\mu\nu} = k_{\nu\mu}^{*} = k_{\nu\mu}$. The electronic system is characterized by the combined kinetic and potential energy matrix whose elements are denoted by $h_{pq} = h_{qp}^{*}$ and by the electron-electron interaction with the elements $w_{pqst} = w_{qpts} = w_{tsqp}^{*}$. Finally, the last elements $g_{pq}^{\mu} = g_{qp}^{\mu\,*}$ describe the strength of the interaction between electrons and nuclei. In

addition, in second quantization, the operators $\hat{c}_p$ and $\hat{c}_p^\dagger$ annihilate an electron from and create an electron to a single-particle state denoted with the label p, respectively. The fermionic statistics of the electrons is incorporated into the canonical anti-commutation relations $[\hat{c}_p, \hat{c}_q]_+ = 0$, $[\hat{c}_p^\dagger, \hat{c}_q^\dagger]_+ = 0$, and $[\hat{c}_p, \hat{c}_q^\dagger]_+ = \delta_{pq}$, where the plus sign in the subscript stands for the anti-commutator. The nuclei are on the other hand described by the momentum $\hat{p}_\mu$ and displacement $\hat{u}_\mu$ operators, which commute with the electronic operators and obey the canonical commutation relations $[\hat{u}_\mu, \hat{u}_\nu]_- = 0$, $[\hat{p}_\mu, \hat{p}_\nu]_- = 0$, $[\hat{u}_\mu, \hat{p}_\nu]_- = \imath\delta_{\mu\nu}$. Here the minus sign in the subscript denotes the standard commutator. In many applications, one is interested in time-dependent processes which can result from an interaction with an electromagnetic potential. In other applications and model systems, one explores an idealization of a physical process, e.g., an interaction quench. It is therefore preferable to generalize the Hamiltonian operator by adding a possible time-dependence to all matrix elements, as well as by adding a term describing an external force acting on the nuclei. In its time-dependent form, the Hamiltonian operator is then given by

$$\begin{aligned}\widehat{H}(t) = &\frac{1}{2}\sum_\mu m_\mu^{-1}(t)\hat{p}_\mu^2 + \frac{1}{2}\sum_{\mu\nu} k_{\mu\nu}(t)\hat{u}_\mu\hat{u}_\nu + \sum_\mu f_\mu(t)\hat{u}_\mu \\ &+ \sum_{pq} h_{pq}(t)\hat{c}_p^\dagger\hat{c}_q + \frac{1}{2}\sum_{pqst} w_{pqst}(t)\hat{c}_p^\dagger\hat{c}_q^\dagger\hat{c}_s\hat{c}_t \\ &+ \sum_{pq}\sum_\mu g_{pq}^\mu(t)\hat{u}_\mu\hat{c}_p^\dagger\hat{c}_q\,, \end{aligned} \tag{2.2}$$

where f_p denotes the amplitude of the added external nuclear force. All of the models investigated in this thesis are completely characterizable by this time-dependent Hamiltonian operator.

2.2 Introducing a Two-Component Notation

In this thesis, a two-component notation is chosen for the displacement and momentum operators in order to arrive at a compact representation of many-body perturbation theory. In the first place, this choice was motivated by the desire of the author, due to numerical reasons, to arrive at equations of motion with only first order time derivatives as opposed to the standard second order equations. It later turned out that the two-component notation is, in addition to Hamilton's equations of classical mechanics, used also in the quantum mechanical context in many-body perturbation theory [WALT14]. It is then for the stated reason that the displacement and momentum operators are defined as the components

$$\begin{aligned}\widehat{\phi}_{1,\mu} &\equiv \hat{u}_\mu\,, \\ \widehat{\phi}_{2,\mu} &\equiv \hat{p}_\mu\,, \end{aligned}$$

of the two-component phononic field operators $\widehat{\phi}_\mu$. It follows by defining an isomorphism between the pairs $\{\varsigma_i, \mu_i\}$, where $\varsigma_i = 1, 2$, and indices i that the two-component operators are referred to with the collective indices i when it is more convenient. It is noted that in the following, at the risk of ambiguity, also the collective indices are denoted, e.g., by μ to distinguish them from the electronic indices, e.g., p. That said, it is possible to rewrite the commutation relations satisfied by the displacement and momentum operators in the compact form

$$\left[\widehat{\phi}_\mu, \widehat{\phi}_\nu\right]_- \equiv \alpha_{\mu\nu}\,,$$

such that the matrix α with the elements

$$\alpha_{1\mu,1\nu} = \alpha_{2\mu,2\nu} = 0\,,$$

$$\alpha_{1\mu,2\nu} = -\alpha_{2\mu,1\nu} = \imath\delta_{\mu\nu}\,,$$

equals the imaginary unit times the standard symplectic matrix [AKN06]. It is noted that the matrix α is hermitian and idempotent and the symbol $\delta_{\mu\nu}$ denotes the Kronecker delta. It then remains to rewrite the Hamiltonian operator in terms of these new operators in order to complete the introduction of the two-component notation. In the abbreviated notation, it then follows that the Hamiltonian operator is given by

$$\begin{aligned}\widehat{H}(t) = &\sum_{\mu\nu} \Omega_{\mu\nu}(t)\widehat{\phi}_\mu\widehat{\phi}_\nu + \sum_{\mu} F_\mu(t)\widehat{\phi}_\mu \\ &+ \sum_{pq} h_{pq}(t)\hat{c}_p^\dagger\hat{c}_q + \frac{1}{2}\sum_{pqst} w_{pqst}(t)\hat{c}_p^\dagger\hat{c}_q^\dagger\hat{c}_s\hat{c}_t \\ &+ \sum_{pq}\sum_{\mu} M_{pq}^{\mu}(t)\widehat{\phi}_\mu\hat{c}_p^\dagger\hat{c}_q\,,\end{aligned} \tag{2.3}$$

where

$$\begin{aligned}\Omega_{\varsigma\mu,\varsigma'\nu}(t) &\equiv \frac{1}{2}\delta_{\varsigma\varsigma'}\left(\delta_{\varsigma 1}k_{\mu\nu}(t) + \delta_{\varsigma 2}\delta_{\mu\nu}m_\mu^{-1}(t)\right)\,,\\ F_{\varsigma\mu}(t) &\equiv \delta_{\varsigma 1}f_\mu(t)\,,\\ M_{pq}^{\varsigma\mu}(t) &\equiv \delta_{\varsigma 1}g_{pq}^{\mu}(t)\,.\end{aligned}$$

provide the connection between the new and original matrix elements. It is worthwhile to remark that although the two-component notation was originally motivated by technical reasons rather than physical arguments, the new Hamiltonian is an extension of the original Hamiltonian operator and can also be used to address more complicated physical situations in possibly alternative unconventional bases, see the outlook in Ch. 9 for examples.

2.3 Selected Lattice Models

In this thesis, the theoretical framework presented in the forthcoming is based on systems which can be described with the Hamiltonian operator of Eq. (2.3). However, the applications of the theory discussed in the present work relate to selected model Hamiltonians which are simplified versions of the so far discussed Hamiltonian. A model typically arises from the need to simplify the real problem such that it can be analyzed and explained with the available toolbox. In particular, the lattice models discussed in the present work and introduced in the following arise by neglecting electronic degrees of freedom such that only a minimal set remains.

2.3.1 Hubbard Model

The Hubbard model [Hub63, SL13] was initially introduced to study electron correlation in the d- and f-bands of transition metal oxides but has since then been applied to a variety of physical situations. In the simplest variant of this model, one considers a uniform system of atoms or molecules, hereon referred to as sites, described by taking a single electronic basis function per site, and only retaining local, on-site electron-electron interactions. The Hamiltonian operator is given by

$$\widehat{H}_{\mathrm{H}} \equiv -t_{\mathrm{kin}}\sum_{\langle i,j\rangle}\sum_{\sigma}\left(\hat{c}_{i\sigma}^\dagger\hat{c}_{j\sigma} + \hat{c}_{j\sigma}^\dagger\hat{c}_{i\sigma}\right)$$

$$+ U \sum_i \hat{n}_{i\uparrow}\hat{n}_{i\downarrow} \,, \tag{2.4}$$

where the indices i and σ denote the site and spin while $\langle i,j\rangle$ indicates that the summed site indices i and j must refer to neighboring sites. The operators $\hat{c}_{i\sigma}$ and $\hat{c}^\dagger_{i\sigma}$ therefore annihilate an electron from and create an electron to the site i with the spin σ, respectively, whereas $\hat{n}_{i\sigma} \equiv \hat{c}^\dagger_{i\sigma}\hat{c}_{i\sigma}$ denotes the site spin-density operator. Here, t_{kin} and U are the hopping and electron-electron interaction strength parameters which model respectively the electron kinetic energy and the Coulomb interaction between the electrons.

2.3.2 Pariser-Parr-Pople Model

The Hubbard model can be extended to also describe long range interactions between the electrons. In this case, one typically talks about the extended Hubbard model or sometimes more specifically about the Pariser-Parr-Pople (PPP) model. The Pariser-Parr-Pople model was originally tailored to describe complex organic dyes [PP53a, PP53b, Pop53]. Its simplest form can be described by the Hamiltonian operator

$$\begin{aligned}\widehat{H}_{\mathrm{PPP}} \equiv & -t_{\mathrm{kin}} \sum_{\langle i,j\rangle} \sum_\sigma \left(\hat{c}^\dagger_{i\sigma}\hat{c}_{j\sigma} + \hat{c}^\dagger_{j\sigma}\hat{c}_{i\sigma}\right) \\ & + U \sum_i \hat{n}_{i\uparrow}\hat{n}_{i\downarrow} \\ & + \frac{1}{2}\sum_{ij} V_{ij}\left(\hat{n}_i - Z\right)\left(\hat{n}_j - Z\right) ,\end{aligned}$$

where V_{ij} describes the Coulomb interaction between the electrons at the sites i and j while Z is a term which describes a uniform background potential induced by the positive ions. Moreover, $\hat{n}_i \equiv \sum_\sigma \hat{n}_{i\sigma}$ denotes the site density operator

2.3.3 Holstein Model

The Holstein model was originally introduced to describe polaronic physics in molecular crystals [Hol00a, Hol00b]. The model Hamiltonian can be written in its simplest form for a uniform system as

$$\begin{aligned}\widehat{H}_{\mathrm{hol}} \equiv & -t_{\mathrm{kin}} \sum_{\langle i,j\rangle} \sum_\sigma \left(\hat{c}^\dagger_{i\sigma}\hat{c}_{j\sigma} + \hat{c}^\dagger_{j\sigma}\hat{c}_{i\sigma}\right) \\ & + \frac{1}{2}\sum_i \left(M^{-1}\hat{p}_i^2 + K\hat{u}_i^2\right) \\ & - g\sum_i \hat{u}_i\hat{n}_i \,,\end{aligned}$$

where $\hat{p}_i$ and $\hat{u}_i$ are the momentum and displacement operators for the site i. The parameters M and K are the mass and spring constant associated with each site and g is a local electron-phonon interaction strength. In the diagonal representation, which is obtained by introducing the phonon annihilation and creation operators

$$\hat{a}_i \equiv \sqrt{\frac{M\omega_0}{2}}\left(\hat{u}_i + \frac{\imath}{M\omega_0}\hat{p}_i\right) ,$$

$$\hat{a}_i^\dagger \equiv \sqrt{\frac{M\omega_0}{2}}\left(\hat{u}_i - \frac{\imath}{M\omega_0}\hat{p}_i\right),$$

where $\omega_0 \equiv \sqrt{K/M}$ is the phonon frequency, the Hamiltonian operator is given by

$$\begin{aligned}\widehat{H}_{\mathrm{hol}} = &-t_{\mathrm{kin}} \sum_{\langle i,j\rangle} \sum_{\sigma} \left(\hat{c}_{i\sigma}^\dagger \hat{c}_{j\sigma} + \hat{c}_{j\sigma}^\dagger \hat{c}_{i\sigma}\right) \\ &+ \omega_0 \sum_i \left(\hat{a}_i^\dagger \hat{a}_i + \frac{1}{2}\right) \\ &- \frac{g}{\sqrt{2M\omega_0}} \sum_i \left(\hat{a}_i + \hat{a}_i^\dagger\right)\hat{n}_i \,. \end{aligned} \tag{2.5}$$

which is another often used useful representation. Here, it is found noteworthy that certain restrictions of the Fock space make this Hamiltonian operator isomorphic to several textbook quantum optics models [Rab36, Rab37, Dic54].

3 Observables

In this chapter, some basic concepts familiar from quantum mechanics and (non-)equilibrium quantum statistical mechanics are reviewed in order to provide a reference point for the subsequent chapters. It is noteworthy that although quantum statistical mechanics provides the formal framework for many-body perturbation theory, in the applications, only its zero-temperature limit, i.e., pure state quantum mechanics, is used. Hence, it is the intention to keep the discussion here brief and to highlight points which are relevant for reviewing the theory behind the publications. In addition to the general theory, also some one- and two-body observables, as well as correlation functions, which are used, analyzed and discussed in Pubs. **I-III** are introduced. In particular, emphasis is put in this thesis on the so-called spectral functions which contain, as their name implies, energetic information on a given physical system. It is often that a spectral function is valuable as it is closely related to an experimentally measurable response property. In the following, the spectral functions associated with photoemission and -absorption spectroscopies are introduced and some of their properties are described.

3.1 Grand Canonical Ensemble Average

Quantum statistical mechanics is concerned with, traditionally macroscopic, statistical properties of large numbers of particles obeying laws of quantum mechanics with large being typically of the order of Avogadro's number $\sim 10^{23}$. In the ensemble theory [Kar07, PB11], it is the ensemble averages of quantum mechanical expectation values, or other probabilistic measures, corresponding to some physical quantity which are relevant. In particular, the ensemble average of an observable O described by the self-adjoint operator $\widehat{O}$ for a time-independent system whose total energy and electron number are allowed to fluctuate, is the grand canonical ensemble average

$$\begin{aligned} O &\equiv \langle \widehat{O} \rangle_{\mathrm{G}} \\ &\equiv Z^{-1} \sum_k e^{-\beta(E_k - \mu N_k)} \langle \Psi_k | \widehat{O} | \Psi_k \rangle \,, \\ Z &\equiv \sum_k e^{-\beta(E_k - \mu N_k)} \,, \end{aligned}$$

where Z is the partition function, $\beta = 1/k_B T$ is the inverse temperature, μ the chemical potential, and E_k and N_k the energy and electron number corresponding to an eigenstate $|\Psi_k\rangle$ of the Hamiltonian operator $\widehat{H}$ of Eq. (2.1) describing the system. It is said that a system the observables of which are described by the grand canonical ensemble is at an equilibrium with temperature T and chemical potential μ. However, it is often interesting to consider situations in which the system is at some point driven out of the state described by equilibrium quantum statistical mechanics. In particular, this can be achieved by initially at time t_0 preparing the system in equilibrium and subsequently perturbing the system such that each quantum state in the ensemble evolves in time for times $t > t_0$ according to the time-dependent Schrödinger equation with the time-dependent Hamiltonian operator $\widehat{H}(t)$ of

Eq. (2.2). It then follows that the time-dependent ensemble average of the observable O is given by

$$O(t) \equiv Z^{-1} \sum_k e^{-\beta(E_k - \mu N_k)} \langle \Psi_k(t) | \widehat{O} | \Psi_k(t) \rangle \,,$$

where $|\Psi_k(t)\rangle$ satisfies the time-dependent Schrödinger equation $\imath \partial_t |\Psi_k(t)\rangle = \widehat{H}(t) |\Psi_k(t)\rangle$ with the initial condition $|\Psi_k(t_0)\rangle = |\Psi_k\rangle$. In this thesis, all observables are defined as the grand canonical ensemble average suggests but in the applications only its zero-temperature limit $\beta \to \infty$ is used, in which

$$\lim_{\beta \to \infty} O(t) = \frac{\sum_{k: E_k - \mu N_k = \Omega_0} \langle \Psi_k(t) | \widehat{O} | \Psi_k(t) \rangle}{\sum_{k: E_k - \mu N_k = \Omega_0} 1} \,,$$

where $\Omega_0 \equiv \min_k (E_k - \mu N_k)$. In particular, if for a fixed number of electrons N, the system has a non-degenerate lowest energy state, i.e., the ground state, with the energy E_0^N then it is possible to extract this ground expectation value by using

$$\lim_{\beta \to \infty} O(t) = \langle \Psi_0^N(t) | \widehat{O} | \Psi_0^N(t) \rangle \,,$$

where $|\Psi_0^N\rangle$ is the corresponding eigenstate, provided that the chemical potential satisfies

$$-\Omega_R < \mu < \Omega_A \,,$$

where $\Omega_R \equiv \min_{N' < N} \left(E_0^{N'} - E_0^N \right) / (N - N')$ and $\Omega_A \equiv \min_{N' > N} \left(E_0^{N'} - E_0^N \right) / (N' - N)$ denote respectively the lowest multi-electron removal and addition energies per electron. It is noteworthy that for a non-interacting system with a spin-compensated ground state following the Aufbau principle, this condition reduces to fixing the chemical potential between the highest occupied and lowest unoccupied single-electron levels.

In the remaining section, some fundamental aspects of the treatment of ensembles in quantum mechanics are reviewed. To begin with, it is, instead of the Schrödinger picture, more convenient to use the Heisenberg picture as it, e.g., allows a more concise representation of correlation functions on which many-body perturbation theory is based on. In the Heisenberg picture, the time-evolution of quantum states is mapped to the time-evolution of operators by introducing the time-evolution operator $U(t, t')$ for all $t, t' \geq t_0$ as the solution to

$$\begin{aligned} \imath \partial_t U(t, t') &= \widehat{H}(t) U(t, t') \,, \\ -\imath \partial_{t'} U(t, t') &= U(t, t') \widehat{H}(t') \end{aligned}$$

with the initial condition $U(t_0, t_0) = \mathbb{1}$. It follows from this definition that the time-evolution operator maps a quantum state at t' to another state at t such that this state satisfies the time-dependent Schrödinger equation. It further satisfies the closure property $U(t, t') = U(t, t'') U(t'', t')$ and is unitary $U^{-1}(t, t') = U^\dagger(t, t') = U(t', t)$ which are easy to see for time-independent Hamiltonian operators $\widehat{H}$ as then $U(t, t') = \exp\left(-\imath \widehat{H} (t - t') \right)$ but can be shown to hold also for time-dependent Hamiltonian operators [SL13]. It is then possible to rewrite the time-dependent ensemble average by using the time-evolution operator as

$$\begin{aligned} O(t) &= Z^{-1} \sum_k e^{-\beta(E_k - \mu N_k)} \langle \Psi_k | \widehat{O}_H(t) | \Psi_k \rangle \\ &= \langle \widehat{O}_H(t) \rangle_{\mathrm{G}} \,, \end{aligned}$$

where $\widehat{O}_H(t) \equiv U(t_0, t) \widehat{O} U(t, t_0)$ defines a Heisenberg operator. Moreover, if Tr refers to a trace over a complete set of quantum states, $\widehat{N}$ is the electron number operator and $\widehat{\rho}_{\mathrm{G}} \equiv Z^{-1} \exp\left(-\beta (\widehat{H} - \mu \widehat{N}) \right)$

the grand canonical density operator then $\langle \ldots \rangle_{\mathrm{G}} \equiv \mathrm{Tr}\big[\widehat{\rho}_{\mathrm{G}} \ldots\big]$ defines a convenient standard shorthand notation for the ensemble average. It is noted that, at the risk of ambiguity, in this thesis the subscript G specifying the statistical density operator is often neglected although the grand canonical density operator is implied. It is then possible to treat the time-dependence of ensemble averages by introducing equations of motion for the Heisenberg picture operators. If $\widehat{O}(t)$ denotes a possibly explicitly time-dependent operator in the Schrödinger picture then

$$\imath\partial_t \widehat{O}_H(t) = \Big[\widehat{O}_H(t), \widehat{H}(t)\Big]_- + U(t_0,t)\big(\imath\partial_t \widehat{O}(t)\big)U(t,t_0)\,.$$

is the Heisenberg equation of motion for the corresponding Heisenberg picture operator $\widehat{O}_H(t)$. In order to close the section, it is noted that the Heisenberg equations of motion are an important element in the derivation of the governing equations of time-independent and -dependent many-body perturbation theory.

3.2 Time-Local Observables

Here, a few time-local observables which are relevant for this work are briefly introduced. It is perhaps motivating to keep in mind that the observables to be introduced can be, and have been in Pubs. **I-III**, evaluated from the knowledge of objects obtained in many-body perturbation theory as is described in the next chapter. It is also remarked that in the electronic case, a choice has been made to work in a general basis instead of the spin-position basis [BF04, SL13] and while some observables are basis independent, others are specific to the latter basis and are hence represented here in terms of more general objects. It is left until Ch. 8 on the applications to translate these more general objects to the more natural basis specific objects, e.g., the electron density. In the case of purely electronic observables, in the second quantized theory, the more general objects from which all electronic one- and two-body observables can be in principle obtained are the time-dependent electron one- and two-body reduced density matrices. In a general basis, they are defined by

$$\gamma_{pq}(t) \equiv \langle \hat{c}^\dagger_{Hq}(t)\hat{c}_{Hp}(t)\rangle\,,$$

and

$$\Gamma_{pqst}(t) = \langle \hat{c}^\dagger_{Ht}(t)\hat{c}^\dagger_{Hs}(t)\hat{c}_{Hq}(t)\hat{c}_{Hp}(t)\rangle\,,$$

respectively. If the spin-position basis characterized by the position vector r and spin label σ would be chosen by $p \to \{r,\sigma\}$ and $q \to \{r',\sigma'\}$ such that $\gamma_{pq}(t) \to \gamma(r\,\sigma, r'\,\sigma', t)$ then, e.g., the electron spin-density would be given by $n(r\,\sigma,t) \equiv \gamma(r\,\sigma, r\,\sigma; t)$ and the spin-current by $j(r\,\sigma,t) \equiv -\imath\big(\nabla_r - \nabla_{r'}\big)\gamma(r\,\sigma, r'\,\sigma, t)\big|_{r'=r}/2m_e$, where m_e is the electron mass [BF04, SL13]. In general, the pth diagonal element of the density matrix, i.e., $\gamma_{pp}(t)$, describes the population of the pth single-electron state in the chosen basis, and then naturally its trace

$$N(t) \equiv \sum_p \gamma_{pp}(t)$$

is equal to the electron number, which is an example of a basis invariant quantity. In principle, also the electron energy is a basis invariant quantity, however its definition in the presence of time-dependent electromagnetic potentials relies on gauge-invariance, and therefore, in a general basis, without a concrete model or a physical system in mind, it is not completely clear to the author how to define it unambiguously. That said, in this thesis, its one-body part is defined as

$$E_{\mathrm{e}}(t) - E_{\mathrm{ee}}(t) \equiv \sum_{pq} h_{pq}(t)\gamma_{qp}(t)\,,$$

where E_{ee} denotes the electron-electron interaction energy. It is emphasized that, e.g., in the spin-position basis and in the presence of time-varying electromagnetic potentials it would instead be correct to define $E_{\mathrm{e}}(t) \equiv \langle \widehat{H}_{\mathrm{e}}(t) + e\sum_{\sigma}\int dr\, \big(v(r,t) - v(r,t_0)\big)\hat{n}(r\,\sigma,t)\rangle$, where $\widehat{H}_e(t)$ is the electronic Hamiltonian containing the one- and two-body parts, e is the elementary charge and $v(r,t)$ is the scalar potential, since then gauge-invariance would be guaranteed [SL13]. In **III** [SML12], and in the next chapter, also the electron-electron interaction energy, which is defined as

$$E_{\mathrm{ee}}(t) \equiv \frac{1}{2}\sum_{pqst} w_{pqst}(t)\Gamma_{tsqp}(t)\,,$$

is relevant and it will be reviewed that despite it being a two-body observable, it is possible to evaluate it in many-body perturbation theory. In addition to the electronic observables, the phonon field expectation value

$$\phi_{\mu}(t) \equiv \langle \widehat{\phi}_{H\mu}(t)\rangle\,,$$

and covariance matrix

$$\Phi_{\mu\nu}(t) \equiv \langle \Delta\widehat{\phi}_{H\nu}(t)\Delta\widehat{\phi}_{H\mu}(t)\rangle\,,$$

where $\Delta\widehat{\phi}_{\mu}(t) \equiv \widehat{\phi}_{\mu} - \phi_{\mu}(t)$ is a fluctuation operator, are of notable interest in this work since they contain information on the properties of the joint-probability distributions of the nuclei. In contrast to a change of the electronic basis obtained via a similarity transformation, in the harmonic approximation a change of basis is typically achieved by a symplectic transformation, as it preserves the canonical commutation relations, which does not preserve the trace of the covariance matrix, i.e., it is not a basis invariant quantity. It is instead reasonable to discuss the energy of the nuclei, or alternatively of the phonons, which is defined here as

$$E_{\mathrm{p}}(t) \equiv \sum_{\mu\nu}\Omega_{\mu\nu}(t)\big(\Phi_{\nu\mu}(t) + \phi_{\nu}(t)\phi_{\mu}(t)\big) + \sum_{\mu}F_{\mu}(t)\phi_{\mu}(t)\,,$$

with the disclaimer that a more accurate definition may be introduced if a more specific physical situation is described. It is finally possible to define the electron-nuclei, or alternatively electron-phonon, interaction energy as

$$E_{\mathrm{ep}}(t) \equiv \sum_{pq}\sum_{\mu} M^{\mu}_{pq}(t)\Lambda_{0;qp,\mu}(t)\,,$$

where also the so-called electron-phonon correlation function

$$\Lambda_{0;pq,\mu}(t) \equiv \langle \hat{c}^{\dagger}_{Hq}(t)\hat{c}_{Hp}(t)\widehat{\phi}_{H\mu}(t)\rangle$$

was introduced. It is concluded here with the definition that by summing the electron, phonon, electron-electron interaction and electron-phonon interaction energies the total energy of the system is obtained under the disclaimers regarding, e.g., the gauge-invariance.

3.3 Electronic Spectral Functions

3.3.1 Non-neutral Excitation Spectra

It is possible to measure single-electron properties, e.g., ionization potentials in atoms and molecules or band structures in solids, by (Angle-Resolved) PhotoEmission Spectroscopy (AR)PES. In such

experiments, basically by relying on the photoelectric effect, electrons are electrically excited outside the sample and the resulting photocurrent is recorded, in particular, as a function of the electric field frequency. In order to keep track with the experiments, a considerable effort has been invested to describe photoemission spectra theoretically. This has lead to several models relating the photocurrent to theoretically more or less accessible quantities [CLRRSJ73, Alm85, HL02, Alm06]. In the simplest case [HL02], if the so-called extrinsic losses due to the interaction of the excited electron with other charges are neglected then the photocurrent is proportional to the function $A^{<}_{pq}(t;t') = \langle \hat{c}^{\dagger}_{Hq}(t')\hat{c}_{Hp}(t)\rangle$ or, to be more precise, if it depends on the time difference only, as in $A^{<}_{pq}(t;t') \equiv A^{<}_{pq}(t-t')$, to its frequency-domain representation. It is noteworthy that often this function is used directly to interpret photoemission spectra amounting to the omission of the so-called optical dipole matrix elements. Having said that, in **II** [SPAL15b] and **III** [SML12], it is $A^{<}_{pq}$, or its extension

$$A_{pq}(t;t') \equiv \langle \left[\hat{c}_{Hp}(t), \hat{c}^{\dagger}_{Hq}(t')\right]_{+}\rangle$$

henceforth simply referred to as the spectral function, which is used to describe non-neutral excitation spectra of the studied systems. Moreover, in this work, only the equilibrium spectral functions corresponding to the time-independent Hamiltonian operator $\widehat{H}$ of Eq. (2.1) are considered. It is then perhaps more convenient to view the spectral function in the frequency-representation which is known in the exact theory as the Lehmann representation, In this representation, the spectral function is given by

$$\begin{aligned}\hat{A}_{pq}(\omega)/2\pi = &\sum_{N=0}^{\infty}\sum_{k\in\varsigma_N}\sum_{l\in\varsigma_{N+1}} \rho^{N}_{\mathrm{G},k} f^{N>}_{kl,p} f^{N>*}_{kl,q}\delta(\omega-\Omega^{N+1}_{lk}) \\ &+\sum_{N=0}^{\infty}\sum_{k\in\varsigma_N}\sum_{l\in\varsigma_{N-1}} \rho^{N}_{\mathrm{G},k} f^{N<}_{lk,p} f^{N<*}_{lk,q}\delta\left(\omega+\Omega^{N-1}_{lk}\right),\end{aligned}$$

where $\Omega^{N\pm1}_{lk} \equiv E^{N\pm1}_{l} - E^{N}_{k}$ denote addition (+) and removal (-) energies and $f^{N>}_{kl,p} \equiv \langle \Psi^{N}_{k}|\hat{c}_{p}|\Psi^{N+1}_{l}\rangle$ and $f^{N<}_{kl,p} \equiv \langle \Psi^{N-1}_{k}|\hat{c}_{p}|\Psi^{N}_{l}\rangle$ the corresponding intensities, respectively. Here, E^{N}_{k} and $|\Psi^{N}_{k}\rangle$ refer to the k labeled eigenenergy and -state of the N electron system, ς_N is the set of all labels for the eigenstates of the N electron system and $\rho^{N}_{\mathrm{G},k} = e^{-\beta(E^{N}_{k}-\mu N)}/Z$ is a diagonal matrix element of the grand canonical density operator. It is evident from this representations that the spectral function contains information about single-electron properties as it obtains non-zero values only at the electron removal and addition energies. Its intensity spectrum is hence referred to in the following as the non-neutral excitation spectrum.

3.3.2 Neutral Excitation Spectra

In contrast to photoemission spectroscopy, in a typical experiment in optical spectroscopy, electrons are excited by an electric field without ionizing the system and either the reflected or transmitted field is recorded. In this way only charge conserving, i.e., neutral, excitations are observed which gives complementary information about the physical system when compared to the photoemission case. In particular, in a finite system, it is possible to evaluate the optical absorption spectra theoretically or computationally from the knowledge of the photoabsorption cross section which is proportional to the retarded density-density response function [ORR02]. In the spin-position basis, the retarded density-density response function of a system described by the unperturbed Hamiltonian operator $\widehat{H}(t)$ is defined by $\chi^{R}(r\,\sigma,t;r'\,\sigma',t') \equiv -\imath\theta(t-t')\langle[\hat{n}_{H}(r\,\sigma,t),\hat{n}_{H}(r'\,\sigma',t')]_{-}\rangle$ [SL13]. In a general basis, this density response function can be obtained from the knowledge of the retarded response function

$$\chi^{R}_{pq,st}(t;t') \equiv -\imath\theta(t-t')\langle[\widehat{\gamma}_{Hpq}(t),\widehat{\gamma}_{Hst}(t')]_{-}\rangle\,, \tag{3.1}$$

where $\widehat{\gamma}_{pq} \equiv \hat{c}_q^\dagger \hat{c}_p$ is the one-body reduced density matrix operator. If the unperturbed Hamiltonian operator is time-independent and commutes with the initial state statistical density operator then it follows, by the invariance under time-translations, that this response function depends on the time-difference $t - t'$ only. It is then reasonable to introduce its frequency representation which is given for the Hamiltonian operator $\widehat{H}$ of Eq. (2.1) by

$$\hat{\chi}^R_{pq,st}(\omega) = \sum_{N=0}^{\infty} \sum_{k,l \in \varsigma_N} \rho^N_{\mathrm{G},k} \left(\frac{h^N_{kl,pq} h^N_{lk,st}}{\omega - \Omega^N_{lk} + \imath\eta} - \frac{h^N_{lk,pq} h^N_{kl,st}}{\omega + \Omega^N_{lk} + \imath\eta} \right)$$

where $\Omega^N_{kl} \equiv E^N_k - E^N_l$ denotes an excitation energy and $h^N_{kl,pq} \equiv \langle \Psi^N_k | \widehat{\gamma}_{pq} | \Psi^N_l \rangle$ the corresponding intensity or oscillator strength. Moreover, the positive infinitesimal η arises from an integral representation of the Heaviside function, or equivalently by adding an exponential convergence factor prior to the Fourier transform, and enforces the correct causal structure of a retarded function [SL13]. It is clear from the above Lehmann representation that only (charge) neutral excitations contribute to the response function and hence its spectral content is referred to as the neutral excitation spectrum in this work. It is concluded by a more technical statement that, for a system described by the Hamiltonian operator of Eq. (2.1), the retarded response function satisfies the sum rule

$$\begin{aligned} -\int_{-\infty}^{\infty} \frac{d\omega}{\imath\pi}\, \omega \hat{\chi}^R_{pq,st}(\omega) = \langle \hat{h}_{pt} \widehat{\gamma}_{sq} \rangle + \langle \widehat{\gamma}_{pt} \hat{h}_{sq} \rangle - \sum_{p'} \left(\delta_{qs} \langle \hat{h}_{pp'} \widehat{\gamma}_{p't} \rangle + \delta_{pt} \langle \widehat{\gamma}_{sp'} \hat{h}_{p'q} \rangle \right) \\ + \sum_{p'q'} \left(w_{psp'q'} \Gamma_{q'p'qt} + \Gamma_{psp'q'} w_{q'p'qt} \right) \\ + \sum_{p'q'} \left((w_{pp'q't} - w_{pp'tq'}) \Gamma_{sq'p'q} + \Gamma_{pp'q't} (w_{sq'p'q} - w_{q'sp'q}) \right) \\ - \sum_{p'q's'} \left(\delta_{sq} w_{pp'q's'} \Gamma_{s'q'p't} + \delta_{tp} \Gamma_{sp'q's'} w_{s'q'p'q} \right), \end{aligned}$$

where $\hat{h}_{pq} \equiv h_{pq} + \sum_\mu M^\mu_{pq} \widehat{\phi}_\mu$ denotes an effective one-body Hamiltonian operator. In the absence of the electron-phonon interaction, it reduces to the f-sum rule, or the Thomas-Reiche-Kühn sum rule, and, if a spin-position representation [LD04] or a lattice model with only two-index interactions [SML12] is chosen, to a relation between the retarded density-density response function and the one-body reduced density matrix.

4 Many-Body Perturbation Theory

An exact solution of a time-independent or -dependent many-body problem becomes quickly unmanageable as the computational complexity of solving the time-independent or dependent Schrödinger equation scales exponentially with the particle number. It is this fact which has made physicists turn to reduced objects, that is, objects which are related to the full solution such that most of the degrees of freedom have been integrated out. In this thesis, the focus is on reduced objects know as the electron and phonon propagators. It is their simplest variants which admit a closed representation of many-body perturbation theory and still contain enough information to extract some of the most important time-independent and -dependent properties of a physical system. In particular, it appears to be primarily due to the fact that both the photoemission and -absorption spectrum, cf., Sec.3.3, are readily available once the electron propagator is known that many-body perturbation theory has become ubiquitous in contemporary solid state physics [ORR02].

It was however already in the 1950's that time-independent diagrammatic many-body perturbation theory made its breakthrough into solid state physics. For instance, in [GMB57] it was shown that an infinite partial summation prevents divergences for the correlation energy of the electron gas. Following its success, today, a number of textbooks describing both zero- and finite-temperature formalisms of many-body perturbation theory in particular for the fermion-boson and fermion-fermion interactions exist [AGD65, FW71, Mah00, BF04, DVN05, HJ08, SL13]. It was also soon after, in the mid 1960's, when an extension to adiabatically switched-on time-dependent perturbations was popularized by Keldysh in [Kel65]. In [Dan84], a formalism which also enabled the inclusion of switch-on effects as well as uncorrelated, correlated zero- and finite-temperature, and general initial states was introduced. Concerning general initial states, further progress was made the 1990's by relying on an exponential representation of the initial statistical density operator [Wag91, MR99] and a bit later by using n-body initial correlation functions [SKB99, LS12, LS13]. In essence, all but the approach to general initial states with correlation functions were introduced by extending the domains of definition of the propagators without any changes to the formal structure of the time-independent theory. It was only until very recently that textbooks summarizing time-independent and -dependent variations of many-body perturbation theory have been published [Ram07, SL13]. It should be also mentioned that the source-field method, which can be used to derive many-body perturbation theory without explicit invocation of perturbative arguments, was developed in parallel with the diagrammatic theory [MS59]. It can be also applied to treat both electron-electron [HL70, Str88] and electron-phonon interactions [Blo67, HL70].

Some comments on the suitability of approaches known to the author to the work presented in this thesis are in order. Firstly, in some texts many-body perturbation theory for the electron-phonon interaction is introduced for translationally invariant, or quasi-invariant, systems [AGD65, FW71, Mah00, HJ08] which leads to some simplifications not suitable for truly inhomogeneous systems, e.g., the neglect of the Hartree (tadpole) diagram in the case of electron-phonon interactions [AGD65, FW71]. Secondly, in addition to a demand of a theory for inhomogeneous systems also the capability to deal with time-dependence is an essential requirement in the present work. In principle, as reviewed above, only domains of the propagators are affected, however due to the desire of the author to

work with first order integro-differential equations, also the momentum and displacement-momentum components of the phonon propagator need to be considered. It is due to these reasons that an alternative representation, which is equivalent to one used in [WALT14] for purely phononic systems, is chosen in the present work and it is this which obliges to a more thorough representation of the theory.

In what follows, many-body perturbation theory is presented in a manner which is consistent with the background information discussed in **I-III**. In addition to a review of all of the relevant basic concepts, some more technical details are presented in the appendices of this chapter. In particular, the appendix contains a proof of Wick's theorem for the non-interacting phonon propagator, a derivation of the Galitski-Migdal total energy functional and a discussion on the sufficient conditions for obtaining conserving approximations.

4.1 Keldysh Contour

In [Kel65], it was shown that time-independent many-body perturbation theory for the real-time electron propagator could be extended to adiabatic non-equilibrium situations by defining a (complex) contour on which the time-arguments are defined. It has been since then shown that all of the different flavors, i.e., the zero- and finite-temperature and non-equilibrium formalisms, of many-body perturbation theory can be described on an equal footing by defining an appropriate complex contour which is here called the Keldysh contour [LS13, SL13]. In the case that the initial state is described by a grand canonical ensemble, see Sec. 3.1, the contour idea arises naturally if it is recognized that the corresponding density operator $\widehat{\rho}_{\mathrm{G}}$ resembles the imaginary time time-evolution operator $U_{H^M}(t_0 - \imath\tau, t_0 - \imath\tau') \equiv \exp\big(-\widehat{H}^M(\tau - \tau')\big)$ where $\widehat{H}^M \equiv \widehat{H} - \mu\widehat{N}$. It then follows that a grand canonical ensemble average can be written as

$$O(t) = \frac{\mathrm{Tr}\Big[U_{H^M}(t_0 - \imath\beta, t_0)U(t_0, t)\widehat{O}U(t, t_0)\Big]}{\mathrm{Tr}\Big[U_{H^M}(t_0 - \imath\beta, t_0)\Big]},$$

which is readily understood to consist of a forward time-evolution up to time t, after action of the operator $\widehat{O}$ follows a backward time-evolution back to the initial time t_0, and finally an imaginary time time-evolution up to time $t_0 - \imath\beta$. It is possible to formally describe this sequence of time-evolutions by defining the Hamiltonian operator

$$\widehat{H}(z) \equiv \begin{cases} \widehat{H}^M & z \in C^M \\ \widehat{H}(t) & z = t_\pm \in C^\pm \end{cases}, \tag{4.1}$$

where z is a complex-valued time argument which can have values on the Keldysh contour of Fig. 4.1.1. The Keldysh contour consists of two real time branches: the forward C^- and backward C^+ branch, and a single imaginary time branch C^M which is usually called the Matsubara branch explaining the abbreviation M. Moreover, by definition, the contour-time t_{0-} corresponding to the real-time t_0 and lying on the forward $(-)$ branch is the starting point and the contour-time $t_0 - \imath\beta$ the ending point of the contour. It thus makes sense to order contour-times, e.g., a contour-time t_+ on the backward branch is always later than a contour-time t'_- on the forward branch. Here on, the notation $t_\pm$ with $\pm$ denoting the branch on which the contour-time lies and t the corresponding real-time is used without the explanation. It is then possible to extend the domain of the time-evolution operator for the contour-times by requiring that it solves the differential equation pair

$$\imath\partial_z U(z, z') = \widehat{H}(z)U(z, z'),$$

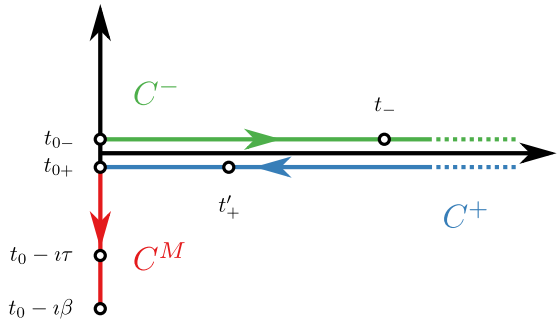

Figure 4.1.1: The Keldysh contour C and some of the contour-time naming conventions are illustrated. The contour consists of the vertical, imaginary-time branch C^M responsible for the initial equilibrium preparation and of the horizontal forward C^- and backward C^+ real-time branches related to the real-time time-evolution.

$$-\imath\partial_{z'}U(z,z') = U(z,z')\widehat{H}(z')\,,$$

with the initial condition $U(z,z) = \mathbb{1}$. It follows from this definition that the contour time-evolution operator satisfies the semi-group property $U(z,z') = U(z,z'')U(z'',z')$ but is not unitary if a contour time lies on the imaginary track. The formal solution to these equations is given by

$$U(z,z') = \begin{cases} T\exp\left(-\imath\int_{C(z,z')}d\bar{z}\;\widehat{H}(\bar{z})\right) & z \geq z' \\ \bar{T}\exp\left(\imath\int_{C(z',z)}d\bar{z}\;\widehat{H}(\bar{z})\right) & z < z' \end{cases},$$

where T and $\bar{T}$ are the chronological and anti-chronological contour time-ordering operators and $C(z,z')$ with $z \geq z'$ denotes the part of the contour extending from z' to z. If two operators are given then by their (anti-)chronological order, it is meant that if $z > z'$ then the operator with z goes to the (right) left of the operator with z'. Hence, the (anti)-chronological time-ordering operator acts by reordering operators to the (anti-)chronological order by repeated use the binary relation for neighboring operators such that every transposition of two fermionic operators changes the sign of the result. Moreover, by a (non-)fermionic operator, it is meant here an operator consisting of strings of (even) odd numbers of annihilation $\hat{c}_p$ and creation $\hat{c}_p^\dagger$ operators satisfying the fermionic anti-commutation relations. It then follows, by extending the domain of the ensemble averages to contour times, that

$$\langle\widehat{O}_H(z)\rangle \equiv \frac{\mathrm{Tr}\left[T\left\{e^{-\imath\int_C d\bar{z}\;\widehat{H}(\bar{z})}\widehat{O}(z)\right\}\right]}{\mathrm{Tr}\left[T\left\{e^{-\imath\int_C d\bar{z}\;\widehat{H}(\bar{z})}\right\}\right]}\,,$$

where $\widehat{O}(z)$ refers to a Schrödinger picture operator with an explicit contour-time argument, even if the operator itself would be time-independent, to keep track of the time-ordering [SL13]. This contour-time extension generalizes to strings of operators such that a time-ordered ensemble average of an arbitrary string $\widehat{O}_1\ldots\widehat{O}_n$ of n fermionic or non-fermionic operators given by

$$\langle T\{\widehat{O}_{H1}(z_1)\ldots\widehat{O}_{Hn}(z_n)\}\rangle \equiv \frac{\mathrm{Tr}\left[T\left\{e^{-\imath\int_C d\bar{z}\;\widehat{H}(\bar{z})}\widehat{O}_1(z_1)\ldots\widehat{O}_n(z_n)\right\}\right]}{\mathrm{Tr}\left[T\left\{e^{-\imath\int_C d\bar{z}\;\widehat{H}(\bar{z})}\right\}\right]}$$

reduces to $n!$ ensemble averages when its arguments are given a definite order. Finally, it is particularly noteworthy that if such a string of operators is given and $\widehat{O}_k(t_0 - \imath\beta) = \widehat{O}_k(t_{0-})$ then it holds that

$$\begin{aligned}&\langle T\{\widehat{O}_{H1}(z_1)\dots\widehat{O}_{Hk}(t_0-\imath\beta)\dots\widehat{O}_{Hn}(z_n)\}\rangle \\ &\quad = \kappa_1\dots\kappa_{k-1}\kappa_{k+1}\dots\kappa_n\langle T\{\widehat{O}_{H1}(z_1)\dots\widehat{O}_{Hk}(t_{0-})\dots\widehat{O}_{Hn}(z_n)\}\rangle\end{aligned} \tag{4.2}$$

where κ_j equals the sign obtained by transposing the kth operator with the jth operator under the time-ordering. It is the contour-time machinery reviewed here which turns out to be an important tool for handling the complexity of the perturbation approach presented in the next sections.

4.2 Contour-Ordered Propagators

In many-body perturbation theory, the central object is the propagator or the Green's function which, roughly speaking, describes the time-evolution (propagation) of added particles, holes or fields in the physical system. In the case that electron-electron and electron-phonon interactions are considered there are several relevant propagators which can be classified as electron, phonon or mixed propagators. In this thesis, only observables which can extracted from the simplest electron and phonon propagators, that is the one-body electron and one- and two-field phonon propagators, are considered. Moreover, these propagators are especially important as they are the simplest objects which form a closed theory and allow one to represent also higher order propagators as shown in the next sections. In here, by using the results of the previous section, the simplest propagators are introduced and more general mixed propagators are defined. To begin with, in order to define the phonon propagator, the phonon field

$$\phi_\mu(z) \equiv \frac{\mathrm{Tr}\left[T\left\{e^{-\imath\int_C d\bar{z}\ \widehat{H}(\bar{z})}\widehat{\phi}_\mu(z)\right\}\right]}{\mathrm{Tr}\left[T\left\{e^{-\imath\int_C d\bar{z}\ \widehat{H}(\bar{z})}\right\}\right]},$$

is introduced so that the two-field phonon propagator, or simply the phonon propagator D, can be defined as

$$D_{\mu\nu}(z,z') \equiv \frac{1}{\imath}\frac{\mathrm{Tr}\left[T\left\{e^{-\imath\int_C d\bar{z}\ \widehat{H}(\bar{z})}\Delta\widehat{\phi}_\mu(z)\Delta\widehat{\phi}_\nu(z')\right\}\right]}{\mathrm{Tr}\left[T\left\{e^{-\imath\int_C d\bar{z}\ \widehat{H}(\bar{z})}\right\}\right]},$$

where $\Delta\widehat{\phi}_\mu(z) \equiv \widehat{\phi}_\mu - \phi_\mu(z)$ is a fluctuation operator. It is possible to view the phonon propagator as an object describing the propagation of displacement-momentum fields in the system. The phonon field and propagator are also directly related to observable quantities, e.g., the covariance matrix introduced in Sec. 3.2 is readily obtained, and hence any derivable observable, by using $\Phi_{\mu\nu}(t) = \imath D_{\mu\nu}(t_-, t_+)$. It is noted that often [AGD65, FW71, Mah00, BF04] the phonon propagator is not defined by using fluctuation operators, which is in particular justifiable for time-independent translationally invariant systems, but in the work contained in this thesis the definition in terms of fluctuation operators, which arises naturally in the source-field method [Blo67, HL70, SBP16], is found more convenient. The one-body electron propagator which describes the propagation of

electrons, or holes, in the system is instead defined as usual by

$$G_{pq}(z;z') \equiv \frac{1}{\imath} \frac{\mathrm{Tr}\left[T\left\{e^{-\imath\int_C d\bar{z}\ \widehat{H}(\bar{z})}\hat{c}_p(z)\hat{c}_q^\dagger(z')\right\}\right]}{\mathrm{Tr}\left[T\left\{e^{-\imath\int_C d\bar{z}\ \widehat{H}(\bar{z})}\right\}\right]},$$

and is here on often referred to simply as the electron propagator [BF04, SL13]. Its physical relevance comes, for instance, from the possibility to evaluate the one-body reduced density matrix, and derivable observables, by using $\gamma_{pq}(t) = -\imath G_{pq}(t_-;t_+)$. Moreover, in contrast to some other methods based on reduced objects, e.g., density functional theory, both photoemission and -absorption spectra discussed in Sec. 3.3 can be deduced directly from the knowledge of the electron propagator. It is also possible to define a generic mixed propagator from which the phonon field and propagator and the electron propagator can be obtained as special cases. However, in order to facilitate a compact representation of the diagrammatic theory, a short-hand notation similar to the routinely employed short-hand $1 \equiv (x_1, z_1)$, where x_1 denotes a spin-position variable, used in [BF04, SL13] is introduced first. In the present work, this standard notation is sometimes inconvenient or ambiguous due to the equations having both electronic and phononic degrees of freedom. It is therefore proposed that when an ambiguity exists, to overcome it, a set of quantum numbers and/or contour times is instead referred to according to the convention that if $i,j,k \in \mathbb{Z}_{\geq 0}$ then $i_{z\mu} \equiv (z_i, \mu_i)$, $j'_{zpq} \equiv (z'_j, p'_j, q'_j)$, $\bar{k}_{z\mu pq} \equiv (\bar{z}_k, \bar{\mu}_k, \bar{p}_k, \bar{q}_k)$, etc. . It is then possible, by using this abbreviated notation, to define that $\widehat{\phi}(i_{z\mu}) \equiv \widehat{\phi}_{\mu_i}(z_i)$ and $\hat{c}^{(\dagger)}(i_{zp}) \equiv \hat{c}^{(\dagger)}_{p_i}(z_i)$ and to introduce the mixed propagator

$$\begin{aligned} &X_{i,j}(\bar{1}_{z\mu},\ldots,\bar{i}_{z\mu};1_{zp},\ldots,j_{zp};1'_{zp},\ldots,j'_{zp}) \\ &\quad\equiv \frac{1}{\imath^{i/2+j}} \frac{\mathrm{Tr}\left[T\left\{e^{-\imath\int_C dz\ \widehat{H}(z)}\widehat{\phi}(\bar{1}_{z\mu})\ldots\widehat{\phi}(\bar{i}_{z\mu})\hat{c}(1_{zp})\ldots\hat{c}(j_{zp})\hat{c}^\dagger(j'_{zp})\ldots\hat{c}^\dagger(1'_{zp})\right\}\right]}{\mathrm{Tr}\left[T\left\{e^{-\imath\int_C dz\ \widehat{H}(z)}\right\}\right]} \end{aligned} \tag{4.3}$$

in terms of which it is further possible to define higher order phonon and electron propagators. Firstly, the j-field phonon propagator D_j is defined as

$$D_j(1_{z\mu},\ldots,j_{z\mu}) \equiv \frac{1}{\imath^{j/2}} \frac{\mathrm{Tr}\left[T\left\{e^{-\imath\int_C dz\ \widehat{H}(z)}\Delta\widehat{\phi}(1_{z\mu})\ldots\Delta\widehat{\phi}(j_{z\mu})\right\}\right]}{\mathrm{Tr}\left[T\left\{e^{-\imath\int_C dz\ \widehat{H}(z)}\right\}\right]}$$

in terms of which $D_{\mu_1\mu_2}(z_1,z_2) \equiv D(1_{z\mu},2_{z\mu}) \equiv D_2(1_{z\mu},2_{z\mu})$, and the j-field phonon propagator $D_{0;j}$, defined without the fluctuation operators as

$$\begin{aligned} D_{0;j}(1_{z\mu},\ldots,j_{z\mu}) &\equiv X_{j,0}(1_{z\mu},\ldots,j_{z\mu};;) \\ &= \frac{1}{\imath^{j/2}} \frac{\mathrm{Tr}\left[T\left\{e^{-\imath\int_C dz\ \widehat{H}(z)}\widehat{\phi}(1_{z\mu})\ldots\widehat{\phi}(j_{z\mu})\right\}\right]}{\mathrm{Tr}\left[T\left\{e^{-\imath\int_C dz\ \widehat{H}(z)}\right\}\right]}, \end{aligned}$$

is also introduced as it appears naturally in the diagrammatic theory. In order to avoid confusion both phonon propagators are referred explicitly by D_j and $D_{0;j}$ or it is indicated otherwise which

one is in question. Secondly, the j-body electron propagator is defined as

$$\begin{aligned} G_j(1_{zp},\dots,j_{zp};1'_{zp},\dots,j'_{zp}) &\equiv X_{0,j}(;1_{zp},\dots,j_{zp};1'_{zp},\dots,j'_{zp}) \\ &\equiv \frac{1}{\imath^j}\frac{\mathrm{Tr}\left[T\left\{e^{-\imath\int_C dz\ \widehat{H}(z)}\hat{c}(1_{zp})\dots\hat{c}(j_{zp})\hat{c}^\dagger(j'_{zp})\dots\hat{c}^\dagger(1'_{zp})\right\}\right]}{\mathrm{Tr}\left[T\left\{e^{-\imath\int_C dz\ \widehat{H}(z)}\right\}\right]} \end{aligned}$$

such that $G_{p_1p'_1}(z_1;z'_1)\equiv G(1_{zp};1'_{zp})\equiv G_1(1_{zp};1'_{zp})$ is obtained as a special case. It is noted here that, by defining the j-field phonon propagator in terms of j two-component operators, propagators with both even and odd numbers of phononic operators can be considered, but at the same time a possible confusion with the more common terminology in which a j-body propagator consists of $2j$ operators is introduced. In the next sections, the strategy is to formulate perturbation theory for the mixed propagator as far as needed and then specialize to the electron and phonon propagators. It is possible to do this, i.e., to formulate perturbation theory for the contour time-ordered propagators introduced here, since the mixed propagator satisfies specific boundary conditions. It can be concluded by using Eq. (4.2) that the generic mixed propagator satisfies the boundary conditions

$$\begin{aligned} &X_{i,j}(\bar{1}_{z\mu},\dots,t_0-\imath\beta\,\mu_k,\dots,\bar{i}_{z\mu};1_{zp},\dots,j_{zp};1'_{zp},\dots,j'_{zp}) \\ &\quad= X_{i,j}(\bar{1}_{z\mu},\dots,t_{0-}\,\mu_k,\dots,\bar{i}_{z\mu};1_{zp},\dots,j_{zp};1'_{zp},\dots,j'_{zp})\,, \\ &X_{i,j}(\bar{1}_{z\mu},\dots,\bar{i}_{z\mu};1_{zp},\dots,t_0-\imath\beta\,p_k,\dots,j_{zp};1'_{zp},\dots,j'_{zp}) \\ &\quad= -X_{i,j}(\bar{1}_{z\mu},\dots,\bar{i}_{z\mu};1_{zp},\dots,t_{0-}\,p_k,\dots,j_{zp};1'_{zp},\dots,j'_{zp})\,, \\ &X_{i,j}(\bar{1}_{z\mu},\dots,\bar{i}_{z\mu};1_{zp},\dots,j_{zp};1'_{zp},\dots,t_0-\imath\beta\,p'_k,\dots,j'_{zp}) \\ &\quad= -X_{i,j}(\bar{1}_{z\mu},\dots,\bar{i}_{z\mu};1_{zp},\dots,j_{zp};1'_{zp},\dots,t_{0-}\,p'_k,\dots,j'_{zp})\,, \end{aligned}$$

which are known as the Kubo-Martin-Schwinger (KMS) boundary conditions. It is noted that these are in fact the usual symmetric (bosonic) and anti-symmetric (fermionic) boundary conditions for the electron and phonon propagators [BF04, SL13].

4.3 Perturbation Theory for Contour-Ordered Propagators

In what follows, it is reviewed how diagrammatic perturbation expansions with respect to the electron-electron and electron-phonon interactions are carried out in many-body perturbation theory. It is the strategy to proceed by first showing that an expansion of the mixed propagator of Eq. (4.3) exists in terms of the non-interacting electron and phonon propagators of all orders and then by proving that this expansion can be rewritten in terms of the lowest order non-interacting electron and phonon propagators by using Wick's theorems. It is then shown by using standard diagrammatic arguments, i.e., by arguing that only the connected, topologically inequivalent, irreducible and skeletonic diagrams are relevant, that a closed formal solution in the form of coupled Dyson equations for the electron and phonon propagators follows as a special case of the more general expansion. Finally, it is reviewed that an electronic generalized response function, and hence the density-density response function, has a similar closed solution, provided that the electron and phonon propagators are given, as it satisfies the Bethe-Salpeter equation. In the process, it is the intention to keep the reader informed, if the presentation chosen here differs non-trivially from ones found in the literature known to the author.

In order to introduce the perturbation expansions, the Hamiltonian operator of the non-interacting

system is defined as $\widehat{H}_0(z_1) = \widehat{H}_{0\mathrm{e}}(z_1) + \widehat{H}_{0\mathrm{p}}(z_1)$ where, in terms of the two-component notation,

$$\widehat{H}_{0\mathrm{e}}(z_1) \equiv \sum_{p_1 q_1} h(1_{zpq}) \hat{c}^\dagger_{p_1} \hat{c}_{q_1} \,,$$
$$\widehat{H}_{0\mathrm{p}}(z_1) \equiv \sum_{\mu_1 \nu_1} \Omega(1_{z\mu\nu}) \widehat{\phi}_{\mu_1} \widehat{\phi}_{\nu_1} + \sum_{\mu_1} F(1_{z\mu}) \widehat{\phi}_{\mu_1} \,,$$

denote the Hamiltonian operators for the non-interacting electron (e) and phonon (p) systems. Here, the abbreviations $F(1_{z\mu}) \equiv F_{\mu_1}(z_1)$, $\Omega(1_{z\mu\nu}) \equiv \Omega_{\mu_1\nu_1}(z_1)$ and $h(1_{zpq}) \equiv h_{p_1q_1}(z_1)$, with the right-hand sides defined piece-wise on the contour analogously to Eq. (4.1), were introduced. It is then meant by perturbation theory with respect to the many-body interactions that the operator $\widehat{H}(z) - \widehat{H}_0(z)$ containing only the many-body interactions plays the role of the perturbation with respect to which the perturbation expansions are introduced. In order to keep the expressions for the perturbation expansions a bit shorter, it is convenient to introduce the short-hands

$$\int d1_{zp} \ \ldots \equiv \sum_{p_1} \int_C dz_1 \ \ldots \,,$$
$$\int d1_{z\mu pq} \ \ldots \equiv \sum_{\mu_1} \sum_{p_1 q_1} \int_C dz_1 \ \ldots \,.$$

and their straightforward generalizations to additional indices to abbreviate combinations of sums and a contour-time integral. Moreover, for the same reason, the abbreviations $M(1_{z\mu pq}) \equiv M^{\mu_1}_{p_1q_1}(z_1)$ and $w(1_{zpq}, 1'_{zpq}) \equiv w_{p_1p'_1q'_1q_1}(z_1)\delta(z_1, z'_1)$, where $\delta(z, z')$ is a delta function on the contour, are introduced identically to the above defined other abbreviated elements. It is then possible to proceed by expanding the time-ordered exponentials in the numerator and denominator of Eq. (4.3) with respect to the perturbation by relying on the commutativity of non-fermionic operators under the time-ordering [BF04, SL13]. In particular, the denominator, i.e., the partition function, can be shown to have the expansion

$$\begin{aligned} Z =& Z_0 \sum_{i,j=0}^{\infty} \frac{(-1)^i \imath^{i/2+j}}{i! j! 2^j} \int d\underline{1}_{z\mu pq} \ldots d\underline{i}_{z\mu pq} d\underline{1}'_{zpq} \ldots d\underline{j}'_{zpq} d\underline{1}''_{zpq} \ldots d\underline{j}''_{zpq} \\ & \times M(\underline{1}_{z\mu pq}) \ldots M(\underline{i}_{z\mu pq}) w(\underline{1}'_{zpq}, \underline{1}''_{zpq}) \ldots w(\underline{j}'_{zpq}, \underline{j}''_{zpq}) \\ & \times d_{0,i}(\underline{1}_{z\mu}, \ldots, \underline{i}_{z\mu}) g_{i+2j} \begin{pmatrix} \underline{1}_{zq}, \ldots, \underline{i}_{zq}, \underline{1}'_{zq}, \underline{1}''_{zq}, \ldots, \underline{j}'_{zq}, \underline{j}''_{zq}; \\ \underline{1}^+_{zp}, \ldots, \underline{i}^+_{zp}, \underline{1}'^+_{zp}, \underline{1}''^+_{zp}, \ldots, \underline{j}'^+_{zp}, \underline{j}''^+_{zp} \end{pmatrix} \,, \end{aligned} \tag{4.4}$$

where Z_0 is the partition function of the non-interacting system and the superscript $+$ $(-)$ denotes an infinitesimal increment (decrement) of the contour-time to which it is attached to. Here, to arrive at the result, it was acknowledged that a non-interacting ensemble average of a time-ordered string of electronic and phononic operators is equal to the product of the non-interacting ensemble averages of the strings of electronic and phononic operators, respectively. Moreover, in the process, the non-interacting j-field phonon propagator

$$d_{0;j}(1_{z\mu}, \ldots, j_{z\mu}) \equiv \frac{1}{\imath^{j/2}} \frac{\mathrm{Tr}\left[T\left\{ e^{-\imath \int_C dz \ \widehat{H}_{0\mathrm{p}}(z)} \widehat{\phi}(1_{z\mu}) \ldots \widehat{\phi}(j_{z\mu}) \right\} \right]}{\mathrm{Tr}\left[T\left\{ e^{-\imath \int_C dz \ \widehat{H}_{0\mathrm{p}}(z)} \right\} \right]} \tag{4.5}$$

and the non-interacting j-body electron propagator

$$g_j(1_{zp},\ldots,j_{zp};1'_{zp},\ldots,j'_{zp}) \equiv \frac{1}{\imath^j}\frac{\mathrm{Tr}\left[T\left\{e^{-\imath\int_C dz\ \widehat{H}_{0e}(z)}\hat{c}(1_{zp})\ldots\hat{c}(j_{zp})\hat{c}^\dagger(j'_{zp})\ldots\hat{c}^\dagger(1'_{zp})\right\}\right]}{\mathrm{Tr}\left[T\left\{e^{-\imath\int_C dz\ \widehat{H}_{0e}(z)}\right\}\right]} \tag{4.6}$$

were introduced. It is noted that the arguments of the latter were divided into two rows to fit the expression on a single line in the expansion of the partition function. It then follows by a similar expansion of the numerator of Eq. (4.3) that the mixed propagator $X_{i,j}$ has the perturbation expansion

$$\begin{aligned}
&X_{i,j}(\bar{1}_{z\mu},\ldots,\bar{i}_{z\mu};1_{zp},\ldots,j_{zp};1'_{zp},\ldots,j'_{zp})\\
&=\frac{Z_0}{Z}\sum_{k,l=0}^{\infty}\frac{(-1)^k\imath^{k/2+l}}{k!l!2^l}\int d\underline{1}_{z\mu pq}\ldots d\underline{k}_{z\mu pq}d\underline{1}'_{zpq}d\underline{1}''_{zpq}\ldots d\underline{l}'_{zpq}d\underline{l}''_{zpq}\\
&\quad\times M(\underline{1}_{z\mu pq})\ldots M(\underline{k}_{z\mu pq})w(\underline{1}'_{zpq},\underline{1}''_{zpq})\ldots w(\underline{l}'_{zpq},\underline{l}''_{zpq})\\
&\quad\times d_{0,i+k}(\bar{1}_{z\mu},\ldots,\bar{i}_{z\mu},\underline{1}_{z\mu},\ldots,\underline{k}_{z\mu})g_{j+k+2l}\begin{pmatrix}1_{zp},\ldots,j_{zp},\underline{1}_{zq},\ldots,\underline{k}_{zq},\underline{1}'_{zq},\underline{1}''_{zq},\ldots,\underline{l}'_{zq},\underline{l}''_{zq};\\ 1'_{zp},\ldots,j'_{zp},\underline{1}^+_{zp},\ldots,\underline{k}^+_{zp},\underline{1}'^+_{zp},\underline{1}''^+_{zp},\ldots,\underline{l}'^+_{zp},\underline{l}''^+_{zp}\end{pmatrix},
\end{aligned} \tag{4.7}$$

which serves as the basis for the subsequent steps, of which the next, is the decomposition of this expansion into a sum of products of the non-interacting one-body electron and two-field phonon propagators. In order to accomplish this, Wick's theorems need to be introduced.

4.3.1 Wick's Theorems

It is possible to rewrite the j-body electron and j-field phonon propagators of the non-interacting system, which appear in the perturbation expansions of Eqs. (4.4) and (4.7), in terms of the one-body electron and two-field phonon propagators by invoking Wick's theorem. It was originally introduced in [Wic50] in a form suitable for the zero-temperature formalism and extended in [Mat55] to cover also the finite-temperature case and stands today as one of the corner stones of diagrammatic perturbation theory. In its original form, the theorem is usually formulated algebraically by introducing the normal ordering and by defining contractions [FW71]. Here, as the propagators are defined on an extended non-equilibrium contour, it is found more convenient to use an approach based on solving the equations of motion for the propagators, cf., [BF04, SL13]. In the following, Wick's theorem for the electron and phonon propagators are stated and, by following [BF04, SL13], a proof of the latter invented by the author is presented in App. 4.C.1.

In order to express Wick's theorems diagrammatically, the reader is reminded that a diagram is a graph which consists of a given number of vertices connected to each other by edges. Here, by the edge referred to as the g-line, which connects a vertex with the label $1'_{zp}$ to a vertex with the label 1_{zp}, it is referred to the relation

$g(1_{zp};1'_{zp})\ \simeq$ 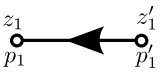

(4.8)

where $g(1_{zp};1'_{zp}) \equiv g_1(1_{zp};1'_{zp})$, and similarly, by the d-line, which connects vertices with the labels

$1_{z\mu}$ and $1'_{z\mu}$, to the relation

$$d(1_{z\mu}, 1'_{z\mu}) \simeq \overset{z_1}{\underset{\mu_1}{\circ}} \cdots\cdots \overset{z'_1}{\underset{\mu'_1}{\circ}} \tag{4.9}$$

where $d(1_{z\mu}, 1'_{z\mu}) \equiv d_2(1_{z\mu}, 1'_{z\mu})$. In this context, the symbol $\simeq$ is used to denote an isomorphism between the algebraic and diagrammatic representations. It is also necessary to introduce the notion of topologically (in-)equivalent diagrams by the statement that topologically equivalent diagrams can be deformed into each other by continuous transformations, e.g., rotation, bending, etc. , while topologically inequivalent diagrams cannot. It is then possible to state a Wick's theorem for the non-interacting j-body electron propagator. In the statement, as ambiguity is not an issue, the pair (z_i, p_i) is abbreviated with i instead of i_{zp}. Moreover, it is convenient, for the brevity and clarity of the presentation, to define the $k \times k$ matrix $g_{\alpha_1,\ldots\alpha_k;\alpha'_1,\ldots,\alpha'_k}$ such that for the given sets of row $\{\alpha_1, \ldots, \alpha_k\}$ and column $\{\alpha'_1, \ldots, \alpha'_k\}$ arguments its matrix element (i, j) is defined as $g(\alpha_i; \alpha'_j)$ for $i, j \in [1, k] \cap \mathbb{Z}$. In particular, then it is possible to define the determinant

$$\begin{aligned}\det(g_{1,\ldots,k;1',\ldots,k'}) &\equiv \sum_{j=1}^{k} (-1)^{i+j} g(i; j') \det(g_{1,\ldots,i-1,i+1,\ldots,k;1',\ldots,(j-1)',(j+1)',\ldots,k'}) \\ &\equiv \sum_{\sigma \in S_k} \operatorname{sgn}(\sigma) \prod_{i=1}^{k} g(i, \sigma(i)') \,,\end{aligned}$$

where $k \in \mathbb{Z}_{>1}$ and $i \in [1, k] \cap \mathbb{Z}$ in the recursive Laplace form on the first line while, in the expanded Leibniz form on the second line, S_k refers to the symmetric group of order k and $\operatorname{sgn} : S_k \to \{-1, 1\}$ is the sign function.

Theorem 4.3.1 (Wick's Theorem A)**.** *The non-interacting k-body electron propagator g_k satisfies*

$$\begin{aligned} g_k(1, \ldots, k; 1', \ldots, k') &= \det(g_{1,\ldots,k;1',\ldots,k'}) \\ &\simeq \left\{ \begin{array}{l} \textit{sum of all topologically inequivalent diagrams,} \\ \textit{in which } \{1', \ldots, k'\} \textit{ are pair-wise connected to} \\ \{1, \ldots, k\} \textit{ by g-lines , with the sign } (-1)^C, \textit{ where} \\ C \textit{ is the number of the crossings of the lines when} \\ \{1', \ldots, k'\} \textit{ and } \{1, \ldots, k\} \textit{ are organized to a left and} \\ \textit{right column for a fixed order of the labels} \end{array} \right\} \end{aligned}$$

with the first and second lines being the algebraic and diagrammatic statements.

It is referred to [BF04, SL13], for the proof of this theorem and for its illustration by some simple examples.. It follows analogously that the non-interacting k-field phonon propagator

$$d_k(1_{z\mu}, \ldots, k_{z\mu}) \equiv \frac{1}{\imath^{k/2}} \frac{\operatorname{Tr}\left[T\left\{e^{-\imath \int_C dz\ \widehat{H}_{0\mathrm{p}}(z)} \Delta\widehat{\phi}(1_{z\mu}) \ldots \Delta\widehat{\phi}(k_{z\mu})\right\}\right]}{\operatorname{Tr}\left[T\left\{e^{-\imath \int_C dz\ \widehat{H}_{0\mathrm{p}}(z)}\right\}\right]} \tag{4.10}$$

where $\Delta\widehat{\phi}(i_{z\mu}) \equiv \widehat{\phi}_{\mu_i} - \imath^{1/2} d_{0;1}(i_{z\mu})$, satisfies a Wick's theorem which is stated below by assuming the convention that the pair (z_i, μ_i) is abbreviated with i instead of $i_{z\mu}$. It is convenient, also similarly as above, to define the $k \times k$ symmetric matrix $d_{\alpha_1,\ldots,\alpha_k}$ such that for the given set of row and column arguments $\{\alpha_1, \ldots, \alpha_k\}$ its matrix element (i, j) is defined as $d(\alpha_i, \alpha_j)$ for $i, j \in [1, k] \cap \mathbb{Z}$. It is then possible to define the hafnian

$$\operatorname{haf}(d_{1,\ldots,2k+1}) \equiv 0 \,,$$

$$\begin{aligned}\mathrm{haf}(d_{1,\ldots,2k}) &\equiv \sum_{\substack{j=1\\ j\neq i}}^{2k} d(i,j)\mathrm{haf}(d_{1,\ldots,i-1,i+1,\ldots,j-1,j+1,\ldots,2k}) \\ &\equiv \frac{1}{2^k k!}\sum_{\sigma\in S_{2k}}\prod_{i=1}^{k} d(\sigma(2i-1),\sigma(2i))\,,\end{aligned}$$

where $k \in \mathbb{Z}_{>1}$ and $i \in [1,2k]\cap\mathbb{Z}$ in the recursive statement, which plays an analogous role to the determinant of $g_{1,\ldots,k;1',\ldots,k'}$ in the following.

Theorem 4.3.2 (Wick's theorem B)**.** *The non-interacting k-field phonon propagator d_k satisfies*

$$\begin{aligned}d_k(1,\ldots,k) &= \mathrm{haf}(d_{1,\ldots,k}) \\ &\simeq \left\{\begin{array}{l}\textit{if } k\in 2\mathbb{Z}\textit{, sum of all topologically inequivalent di-}\\ \textit{agrams in which } \{1,\ldots,k\} \textit{ are pair-wise intercon-}\\ \textit{nected by d-lines , else the null diagram}\end{array}\right\},\end{aligned}$$

with the first and second lines representing the algebraic and diagrammatic statements.

Here, by the null diagram it is referred to a diagram which evaluates to zero. It remains to state a Wick's theorem for the more conventional non-interacting phonon propagator defined without the fluctuation operators. In order to do this, a vertex known as the F-vertex is defined by

$$\imath^{-1/2}F(1_{z\mu}) \;\simeq\; \overset{z_1}{\underset{\mu_1}{\times}}\cdots\cdots\,, \tag{4.11}$$

where by the gray dashed line, it is implied that a d-line is the only acceptable joining edge, and it is stated that

$$d_{0;1}(1) = \frac{1}{\imath^{1/2}}\int d2\; d(1,2)F(2)\,,$$

which is shown to be true in the proof of the theorem stated below. It is further useful to define the $k\times k$ diagonal matrix $d_{0;\alpha_1,\ldots,\alpha_k}$ such that for the given set of arguments $\{\alpha_1,\ldots,\alpha_k\}$ its ith diagonal element is defined as $d_{0;1}(\alpha_i)$ for $i\in[1,k]\cap\mathbb{Z}$. In particular, the permanent of $d_{0;1,\ldots,k}$ is then given by

$$\mathrm{per}(d_{0;1,\ldots,k}) \equiv d_{0;1}(1)\ldots d_{0;1}(k)\,,$$

as follows by the usual definition of the permanent. Moreover, if $s\subset\{\alpha_1,\ldots,\alpha_k\}$ then $(d_{(0;)\alpha_1,\ldots,\alpha_k})_s$ refers to a $(k-|s|)\times(k-|s|)$ matrix obtained by removing from $d_{(0;)\alpha_1,\ldots,\alpha_k}$ the arguments contained in s whereas if $s\equiv\{\alpha_1,\ldots,\alpha_k\}$ then the slightly counterintuitive conventions that $\mathrm{haf}(d_{\alpha_1\ldots\alpha_k})_s\equiv 1$ and $\mathrm{per}(d_{0;\alpha_1\ldots\alpha_k})_s\equiv 1$ are used in the statement of the following theorem. It then follows, by taking into account that to convert a diagram into its algebraic representative all internal vertices are labeled and thus obtained arguments are integrated over, that the Wick's theorem for $d_{0;k}$ can be stated as follows.

Theorem 4.3.3 (Wick's theorem C)**.** *The non-interacting k-field phonon propagator $d_{0;k}$ satisfies*

$$\begin{aligned}d_{0;k}(1,\ldots,k) &= \sum_{s\in P_K}\mathrm{haf}(d_{1,\ldots,k})_{K\setminus s}\mathrm{per}(d_{0;1,\ldots,k})_s \\ &\simeq \left\{\begin{array}{l}\textit{sum of all topologically inequivalent diagrams with}\\ l\in[0,k]\cap\mathbb{Z}\textit{, such that } k+l\in 2\mathbb{Z}\textit{, unlabeled F-}\\ \textit{vertices are pair-wise connected to } \{1,\ldots,k\} \textit{ by d-}\\ \textit{lines with the remaining of } \{1,\ldots,k\} \textit{ being pair-wise}\\ \textit{interconnected by d-lines}\end{array}\right\},\end{aligned}$$

where P_K is the set of all subsets of $K \equiv \{1, \ldots, k\}$, with the first and second lines being the algebraic and diagrammatic statements.

The proof of this theorem, and as a corollary that of Thm. 4.3.2, is provided in App. 4.C.1. Its use is illustrated for $d_{0;k}$ with $k \in [1,4] \cap \mathbb{Z}$ by

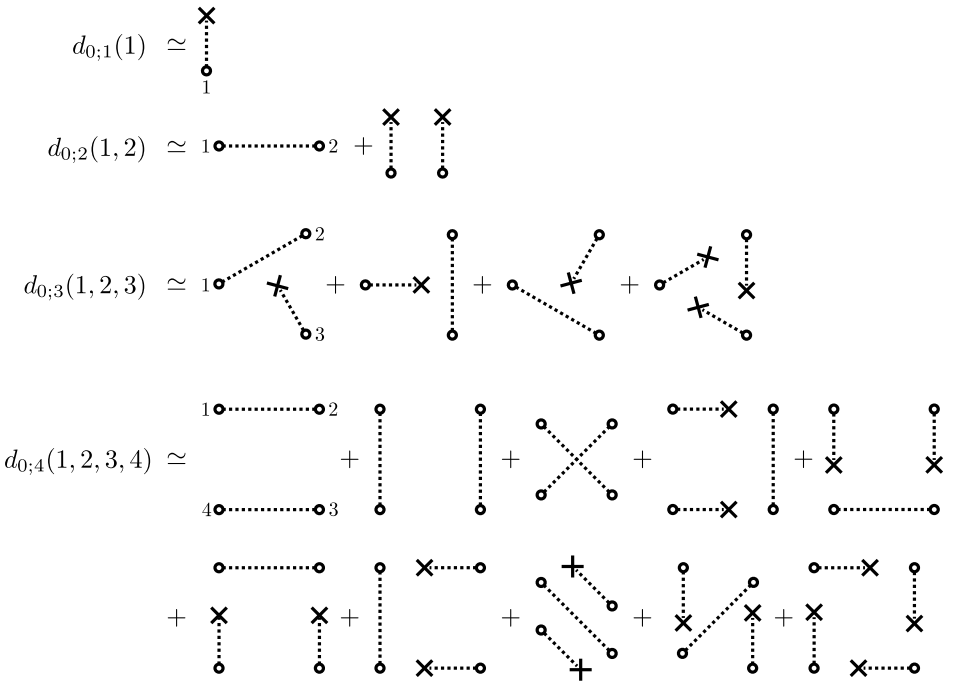

where the labeling of the external vertices of an unlabeled diagram is to be deduced from the first labeled diagram on the right-hand side, It is finally noted that it is possible to extract the decomposition of the corresponding phonon propagator d_k by neglecting all diagrams with F-vertices.

4.3.2 Diagrammatic Perturbation Expansions

It is by virtue of Wick's theorems that the non-interacting j-body electron and j-field phonon propagators can be written in terms of the non-interacting one-body electron and two-field phonon propagators giving rise to an increasing number of terms for the increasing number of interactions in the perturbation expansions of Eqs. (4.4) and (4.7). In order to keep these expansions tractable, it is customary to introduce a graphical method which relies on the diagrammatic statements of Wick's theorems and enables one to write the expansions in a compact and intuitive fashion in terms of graphs known as the Feynman diagrams. If only the electron-phonon and electron-electron interactions are considered, as done in this thesis, then in addition to the g- and d-line and F-vertex, the M-vertex, defined by the relation

$$\imath^{1/2} M(1_{z\mu pq}) \simeq$$

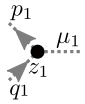

(4.12)

and the w-line, defined by the relation

$$iw(1_{zpq}, 1'_{zpq}) \simeq$$

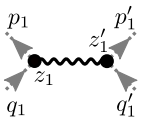

(4.13)

form the edges and vertices of the Feynman diagrams. Here, by the gray dashed lines with arrows, it is implied that an in- or out-going g-line is the only allowed joining edge. It is then possible to represent each term in the expansions as a graph consisting of these elements if it is also taken into account that each graph with j M-vertices and k w-lines comes with the multiplicative prefactor $1/(j!k!2^k)$ and with the sign $(-1)^{j+C}$ where C is the number of the crossings of the g-lines obtained as described in Thm. 4.3.1. The sign of a diagram contributing the perturbation expansion of the propagator $X_{i,j}$ can also be determined more conveniently by taking advantage of a diagrammatic rule known as the loop rule.

Diagrammatic Rule 4.3.1 (Loop Rule)**.** *Given the last $2j$ arguments $(1,\dots,j;1',\dots,j')$ of the propagator $X_{i,j}$, the sign of a diagram contributing to its perturbation expansion is equal to*

$$(-1)^{L-j}$$

where L is the number of closed loops formed by g-lines when the diagram is closed such that the external vertex with the label i' is moved on top of the vertex with the label i for all $i \in [1,j] \cap \mathbb{Z}$.

It is not common that the loop rule is stated as above so a justification of this statement is provided in App. 4.C.2 and it is referred, e.g., to [SL13] for a more usual formulation. In order to proceed, it is noted that the perturbation expansion of the mixed propagator simplifies because some of the diagrams cancel against Z/Z_0 and some are related by changes of integration variables. It is these results, known as the cancellation of disconnected diagrams and the summation of only topologically inequivalent diagrams [BF04, SL13], which lead to a drastic decrease in the complexity of the expansion. In what follows, the consequences of these results are summarized by stating the perturbation expansion of the mixed propagator $X_{i,j}$ of Eq. (4.7) graphically in terms of the Feynman diagrams and by providing the diagrammatic rules, i.e., the so-called Feynman rules, for converting each diagram into an algebraic expression. In order to do this, it is first defined that a diagram whose each internal vertex is connected to at least one of the $i+2j$ labeled external vertices by any combination of edges, i.e., g-, d- or w-lines, is a connected diagram. Moreover, to avoid cluttered notation, by a variable k appearing as an argument of $X_{i,j}$, it is referred to (z_k, μ_k) if it is one the first i arguments and to (z_k, p_k) if it is one the last $2j$ arguments. It is then possible to conclude that

$$X_{i,j}(1,\dots,i;1',\dots,j';1'',\dots,j'') \simeq \left\{ \begin{array}{l} \text{sum of all connected, topologically inequivalent diagrams in which } \{1,\dots,i\}, \text{ unlabeled F-vertices and unlabeled M-vertices are connected pair-wise by d-lines, and the M-vertices and unlabeled end-vertices of w-lines, } \{1'',\dots,j''\} \text{ and } \{1',\dots,j'\} \text{ are connected pair-wise by g-lines such that the elements of } \{1'',\dots,j''\} \text{ and } \{1',\dots,j'\} \text{ are only connected by an out- and in-going g-line} \end{array} \right\} \tag{4.14}$$

which is to be complemented with the following diagrammatic rule.

Diagrammatic Rule 4.3.2. *In order to convert a diagram into an algebraic expression*

i assign dummy labels to all unlabeled F- and M- vertices and end-vertices of w-lines

ii *replace all graphical elements, i.e., the g-, d- and w-lines defined by Eqs. (4.8), (4.9) and (4.13) and the F- and M-vertices defined by Eqs. (4.11) and (4.12), by their algebraic counterparts*

iii *add the superscript + to all second arguments of the electron propagators*

iv *integrate over the dummy labels assigned in ii*

and multiply the result with the sign given by the loop rule 4.3.1.

It is referred to App. 4.C.3 for the justification that the expansion can be indeed represented in terms of connected topologically inequivalent diagrams only. That said, until here, many-body perturbation theory has been treated at a very general level, i.e., the diagrammatic expansion of a generic mixed propagator has been introduced, and most of the steps have been justified, cf. App. 4.C. However, here on, the representation chosen in this thesis becomes better compatible with the standard texts and hence a more brief discussion is deemed more appropriate.

4.3.3 Electron/Phonon Propagators: Dyson Equation

Equation (4.14) is now readily applied to obtain the diagrammatic perturbation expansions of the one- and two-field phonon propagators and the one-body electron propagator. In what follows, it is reviewed, in a brief manner, how the standard resummations of the perturbative series, i.e., the identification of the irreducible and skeletonic diagrams, can be used to arrive at closed coupled equations, known as the Dyson equations, for these objects. As a result of this, another drastic reduction in the complexity of the perturbation expansions is accomplished and the summation of certain classes of diagrams to infinite order with respect to the interactions is made possible. It is the latter, i.e., the infinite partial resummation of the perturbative series beyond the conventional perturbation theory [Mes61b], on which the applications of many-body perturbation theory summarized in this thesis and, to the best knowledge of the author, in the majority of literature are based on. It is recapitulated that the reader is, already in advance, referred to standard literature, e.g., [AGD65, FW71, Mah00, BF04, DVN05, Ram07, SL13], for the most of the details presented in this and the next section. In regard to conventions, it is also noted that here the label i, and its barred or primed variations, refers to i_{zp} when it appears as an argument of an electron propagator or self-energy and to $i_{z\mu}$ when it appears as an argument of a phonon field, propagator or self-energy.

It is found convenient to begin by considering the perturbation expansion of the one-body electron propagator. In order to do so, Eq. (4.14) is used to define, similarly to the g-line, that a G-line which connects a vertex with the label $1'_{zp}$ to a vertex with the label 1_{zp} refers to the relation

$G(1_{zp}; 1'_{zp}) \simeq$ 

$$= \left\{ \begin{array}{l} \text{sum of all connected, topologically inequivalent diagrams} \\ \text{in which external vertices with the labels } 1_{zp} \text{ and } 1'_{zp} \text{ and} \\ \text{unlabeled F-vertices, M-vertices and end-vertices of w-lines} \\ \text{are connected pair-wise by g- and d-lines such that the ex-} \\ \text{ternal vertices with the labels } 1_{zp} \text{ and } 1'_{zp} \text{ are attached re-} \\ \text{spectively to an in- and out-going g-line} \end{array} \right\} \tag{4.15}$$

where the second line defines the diagrammatic perturbation expansion of the one-body electron propagator. The diagrammatic rule 4.3.2 can be then used to convert this expansion into an algebraic perturbation expansion. It is however noted that for the one-body electron propagator the loop

rule 4.3.1 reduces to a form found in most standard textbooks, i.e., a diagram comes with the sign $(-1)^L$ where L is the number of closed loops formed by the g-lines. It is possible to justify this by noticing that when the two external vertices of a connected diagram are placed on top of each other, a single additional loop is created and therefore $(-1)^{L_c-1}$, where L_c is the number of loops in the closed diagram, becomes $(-1)^L$, where $L = L_c - 1$ is he number of loops in the original diagram. In order to resum this perturbative series, it is the next task to identify the so-called one g-line irreducible (1GI) diagrams defined as connected diagrams with two external vertices connected to each other by any combination of edges such that it is not possible to disconnect the external vertices from each other by cutting a single g- or G-line. Moreover, the so-called electron self-energy insertion is defined as a piece of a diagram which can be disconnected from the rest of the diagram by cutting two g- or G-lines. In order to achieve a further resummation, or reduction in the number of diagrams, it is useful to define a G-skeleton diagram as an diagram which does not contain any electron self-energy insertions. It follows by these definitions that the perturbation expansion of the one-body electron propagator can be rewritten diagrammatically in the form

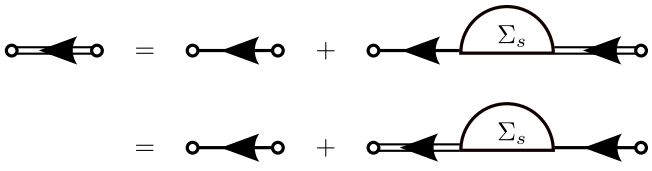

(4.16a)

and, by restoring the omitted external and internal labels and integrating over the internal labels, in the equivalent algebraic form

$$\begin{aligned} G(1;1') &= g(1;1') + \int d2d2'\; g(1;2)\Sigma_s(2;2')G(2';1') \\ &= g(1;1') + \int d2d2'\; G(1;2)\Sigma_s(2;2')g(2';1')\,, \end{aligned} \tag{4.16b}$$

which is just the Dyson equation for the one-body electron propagator. In this equation, the singly-skeletonic electron self-energy Σ_s defined as

$$\Sigma_s(1_{zp};1'_{zp}) \;\simeq\; \underset{p_1}{\overset{z_1}{\circ}} \!\!\leftarrow\!\!\!\!\overset{\Sigma_s}{\frown}\!\!\!\!\leftarrow\!\! \underset{p'_1}{\overset{z'_1}{\circ}}$$

$$\equiv \left\{ \begin{array}{l} \text{sum of all connected, topologically inequivalent, one g-line} \\ \text{irreducible, G-skeletonic diagrams in which external ver-} \\ \text{tices with the labels } 1_{zp} \text{ and } 1'_{zp} \text{ and unlabeled F-vertices,} \\ \text{M-vertices and end-vertices of w-lines are connected pair-} \\ \text{wise by d- and G-lines such that the external vertices with} \\ \text{the labels } 1'_{zp} \text{ and } 1_{zp}\text{, accepting respectively an in- and} \\ \text{out-going g- or G-line, are either M-vertices or end-vertices} \\ \text{of a w-line} \end{array} \right\} \tag{4.17}$$

was introduced. Here, as before, the gray dashed lines with arrows indicate the only allowed joining edges, i.e., out- and in-going g- or G-lines. It is noted that to convert a self-energy diagram to its algebraic form, the diagrammatic rule 4.3.2 and the revised loop rule, i.e., $(-1)^L$ where L is the number of fermionic loops, are to be used.

It is found convenient to continue by introducing first the perturbation expansion of the phonon field ϕ and then by considering the two-field $D_{(0;)2}$ phonon propagator. In terms of these objects, it is also possible to introduce yet another reduction in the number of the electron self-energy diagrams. It is remarked that since these objects are less frequently discussed in the literature known to the

author,when compared to the electronic case, it is felt that a slightly more detailed exposition is in order. In this work, the phonon field $\phi(1_{z\mu}) = \imath^{1/2} D_{0;1}(1_{z\mu})$ is referred to diagrammatically by the relation

$$\imath^{-1/2}\phi(1_{z\mu}) \simeq \bigotimes_{z_1}{}^{\mu_1} = \left\{ \begin{array}{l} \text{sum of all connected, topologically inequivalent diagrams} \\ \text{in which an external vertex with the label } 1_{z\mu} \text{ and unla-} \\ \text{beled F-vertices, M-vertices and end-vertices of w-lines are} \\ \text{connected pair-wise by g- and d-lines such that the external} \\ \text{vertex is attached to a d-line} \end{array} \right\} \tag{4.18}$$

where the second equality follows by using Eq. (4.14). It is possible to resum this diagrammatic expansion by taking advantage of the observation that, in contrast to the g-lines, an internal vertex accepts at most a single d-line, i.e., the number of d-lines is not conserved at an internal vertex. It then holds that a sequence of d-lines, in which any diagrammatic element free of d-lines acts as a vertex, starting from an external vertex can end either to another external vertex, a F-vertex or a M-vertex attached to g-lines forming either a closed loop or terminating to external vertices. If the phonon field is considered then only a single external vertex exists and since any closed dressed fermion loop is related to electron self-energy insertions, it holds diagrammatically that

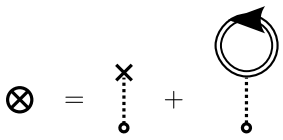

(4.19a)

and, by restoring the omitted external and internal labels and integrating over the internal labels, algebraically that

$$\begin{aligned} \phi(1_{z\mu}) = & \int d1'_{z\mu}\, d(1_{z\mu}, 1'_{z\mu}) F(1'_{z\mu}) \\ & - \imath \int d1'_{z\mu pq}\, d(1_{z\mu}, 1'_{z\mu}) M(1'_{z\mu pq}) G(1'_{zq}; 1'^{+}_{zp})\,. \end{aligned} \tag{4.19b}$$

which is readily verified by checking that the given algebraic form satisfies both the Kubo-Martin-Schwinger boundary conditions and the equations of motion derived in App. 4.A. It is noted that, in the harmonic approximation for the nuclei, the result is physically appealing since it can be understood such that the displacement (momentum) expectation value has possibly non-zero values only in the presence of a (generalized) force F acting on the nuclei or due to the electrically induced force $-\imath MG$ related to the interaction with the electrons. In many standard texts [AGD65, FW71, Mah00], due to the absence of external forces and due to considering extended translationally invariant systems, diagrams such as those found on the right-hand side of Eq. (4.19a) are neglected which amounts to fixing the displacement (momentum) expectation value to zero. It is also argued below that such diagrams have an effect on how the perturbation expansion of the two-field phonon propagator D, which is introduced in the following by using Eq. (4.14) for the phonon propagator $D_{0;2}$, can be resummed. It follows from the diagrammatic arguments used to resum the perturbation expansion of the phonon field that every internal vertex of a diagram in the perturbation expansion of $D_{0;2}$ is connected to only one, when all sequences of d-lines starting from an external vertex end to a F-vertex or a M-vertex attached to closed fermion loop, or both, when a sequence of d-lines starting from an external vertex ends to another external vertex, of the external vertices by any combination of edges. The sum of all connected, topologically inequivalent diagrams of the former kind, i.e., diagrams with each internal vertex connected to only one of the external vertices, is equal to the product of the sums of all connected, topologically inequivalent diagrams attached to the external vertices or, in

other words, equal to the product of two phonon fields of Eq. (4.18). It then follows, by using the definition of the fluctuation operators, that it is possible to refer to the two-field phonon propagator D graphically by the D-line connecting two vertices with the labels $1_{z\mu}$ and $1'_{z\mu}$ such that

$D(1_{z\mu}, 1'_{z\mu}) \simeq$ 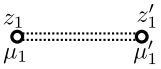

$$= \left\{ \begin{array}{l} \text{sum of all connected, topologically inequivalent diagrams} \\ \text{in which external vertices with the labels } 1_{z\mu} \text{ and } 1'_{z\mu} \text{ and} \\ \text{unlabeled F-vertices, M-vertices and end-vertices of w-lines} \\ \text{are connected pair-wise by g- and d-lines such that the ex-} \\ \text{ternal vertices are attached to d-lines and interconnected} \\ \text{by any combination of lines} \end{array} \right\} \tag{4.20}$$

where the second line defines the perturbation expansion of the two-field phonon propagator. In order to obtain the corresponding algebraic expansion, similarly to the electron propagator, the diagrammatic rule 4.3.2 and the revised loop rule can be used. From this point on, it is possible to proceed also otherwise identically as done in the case of the electron propagator. Firstly, the so-called one d-line irreducible (1DI) diagrams are defined as connected diagrams with two external vertices connected to each other by any combination of edges such that it is not possible to disconnect the external vertices from each other by cutting a single d- or D-line. The so-called phonon self-energy insertion is defined as a piece of a diagram which can be disconnected from the rest of the diagram by cutting two d- or D-lines. Lastly, a D-skeleton diagram is defined as an diagram which does not contain any phonon self-energy insertions. It is then possible to rewrite the perturbation expansion of the phonon propagator diagrammatically as

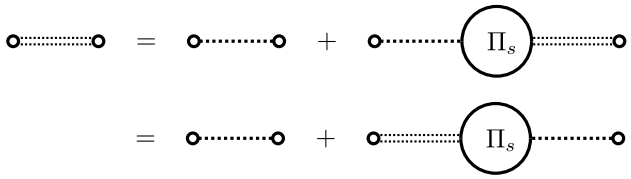

(4.21a)

and, by restoring the omitted external and internal labels and integrating over the internal labels, algebraically as

$$\begin{aligned} D(1,1') &= d(1,1') + \int d2d2'\; d(1,2)\Pi_s(2,2')D(2',1') \\ &= d(1,1') + \int d2d2'\; D(1,2)\Pi_s(2,2')d(2',1')\,, \end{aligned} \tag{4.21b}$$

which is known as the Dyson equation for the phonon propagator D. Here, the singly-skeletonic phonon self-energy Π_s is defined as

$\Pi_s(1_{z\mu}, 1'_{z\mu}) \simeq$ 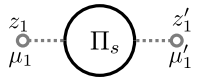

$$\equiv \left\{ \begin{array}{l} \text{sum of all connected, topologically inequivalent, one d-line} \\ \text{irreducible, D-skeletonic diagrams in which external ver-} \\ \text{tices with the labels } 1_{z\mu} \text{ and } 1'_{z\mu} \text{ and unlabeled F-vertices,} \\ \text{M-vertices and end-vertices of w-lines are connected pair-} \\ \text{wise by g- and D-lines such that the external vertices, ac-} \\ \text{cepting a d- or D-line , are M-vertices} \end{array} \right\} \tag{4.22}$$

where the gray dashed lines indicate that a d- or D-line is the only allowed joining edge. In order to convert a self-energy diagram to its algebraic form the diagrammatic rule 4.3.2 and the loop rule

specified in this section are to be used. It is particularly noteworthy, as already stated above, that it is the phonon propagator D, i.e., the propagator defined in terms of the fluctuation operators, which satisfies the Dyson equation and that it reduces to the phonon propagator $D_{0;2}$ only when it is justified to neglect the phonon field.

It is possible to achieve a further standard reduction, and the last one introduced in this thesis, in the number of diagrams by resumming the singly-skeletonic electron and phonon self-energies. This is done by removing all phonon (electron) self-energy insertions from the electron (phonon) self-energy and by replacing all non-interacting phonon (electron) propagators with the interacting phonon (electron) propagators. In order to avoid unnecessary repetition, it is merely stated at this point that the so-called doubly-skeletonic electron Σ_{ss} and phonon Π_{ss} self-energies obtained in this way are defined respectively by adding the term D-skeletonic and G-skeletonic and by replacing d- with D-(lines) and g- with G-(lines) in Eqs. (4.17) and (4.22). In the case of the phonon self-energy, also the term F-vertices in Eq. (4.22) should be removed when defining the doubly-skeletonic self-energy. Moreover, in the case of the electron self-energy, a d-line should not be replaced by a D-line in the diagrams shown in Eq. (4.19a) since, by doing so, a double-counting of diagrams would occur analogously to the purely electronic case [Hed65, SL13]. In addition, the electron and phonon propagators entering the doubly-skeletonic self-energy diagrams satisfy Eqs. (4.16) and (4.21) with the singly- (s) replaced by the doubly-skeletonic (ss) electron and phonon self-energies. In fact, by introducing the doubly-skeletonic self-energies, the Dyson equations for the electron and phonon propagators have been coupled. In order to introduce an alternative, explicit way to construct both doubly-skeletonic self-energies a dressed Φ-functional is defined below. It is first noted that in this context by equivalent G-lines, it is meant lines which lead to topologically equivalent diagrams when removed [SL13]. The dressed Φ-functional is defined by

$-\Phi \simeq$ 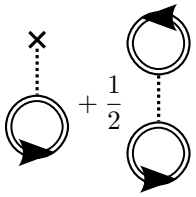 $+\frac{1}{2}$ $+$ { sum of all topologically inequivalent, G- and D-skeletonic diagrams, except the diagrams on the left, in which unlabeled M-vertices and end-vertices of w-lines are connected pair-wise by G- and D-lines such that all vertices are connected to each other by combinations of lines and each diagram is multiplied by $1/N_s$ where N_s is the number of equivalent G-lines } , (4.23)

cf., [SL13]. It then holds that the doubly-skeletonic electron self-energy is given by summing all terms which are obtained by removing a single G-line from each term of the dressed Φ-functional in all possible ways. Similarly, the doubly-skeletonic phonon self-energy is given by summing all diagrams which are obtained by removing a single D-line from each term of the Φ-functional in all possible ways. It is the symmetry prefactor of each Φ-diagram which ensures that each self-energy diagram arises with the correct prefactor. Moreover, it is possible to argue that a functional derivative of a diagram with respect to a propagator corresponds to removing the corresponding line in all possible ways [SL13]. So, to summarize, it holds in both diagrammatic and algebraic terms that

$$\begin{aligned}\Sigma_{ss}(1;1') &= \frac{\delta\Phi}{\delta G(1';1)} \\ &\simeq -\left\{\begin{array}{l}\text{sum of all diagrams obtained by removing a single G-line}\\ \text{from each term of the } \Phi\text{-functional in all possible ways such}\\ \text{that the resulting external vertices accepting an out- and}\\ \text{in-going g- or G-line are labeled by 1 and } 1' \text{ respectively}\end{array}\right\},\\ \Pi_{ss}(1,1') &= -2\frac{\delta\Phi}{\delta D(1,1')}\bigg|_S \\ &\simeq -2\left\{\begin{array}{l}\text{sum of all diagrams obtained by removing a single D-line}\\ \text{from each term of the } \Phi\text{-functional in all possible ways such}\\ \text{that the resulting external vertices accepting a d- or D-line}\\ \text{are labeled by 1 and } 1'\end{array}\right\},\end{aligned}$$

where the subscript S stands for the symmetrized functional derivative $\delta/\delta D(1,1')\big|_S \equiv (\delta/\delta D(1,1') + \delta/\delta D(1',1))/2$ [SL13].

4.3.4 Electronic Response Function: Bethe-Salpeter equation

In addition to the one-body electron and two-field phonon propagators, the perturbation expansions of which were treated in the previous section, also electronic response functions, whose perturbation expansions follow similarly from Eq. (4.14), are of interest in this thesis. In the following, a generalized electronic response function is defined in terms of the one- and two-body electron propagators and its perturbation expansion, along with some standard resummation strategies, is introduced. In particular, by the elimination of the self-energy insertions and by identifying the so-called two g-line irreducible diagrams, it is possible to arrive at a closed equation for this response function known as the Bethe-Salpeter equation [Str88, FW71, SL13]. In Ch. 7, it will be moreover explained, in a detailed way, how a retarded electronic response function satisfying the Bethe-Salpeter equation can also be deduced from the sole knowledge of the one-body electron propagator. In order to define the generalized response function, it is possible to start by considering the perturbation expansion of Eq. (4.14) for the two-body electron propagator G_2 and by making the observation that in a connected diagram a sequence of g-lines starting from an external vertex can only end to another external vertex. It then holds that there exist connected diagrams in which the external vertices associated with the first and third arguments of the two-body propagator are connected to each other by a sequence of g-lines but not, by any combination of lines, to the external vertices labeled with the second and fourth arguments. It is such terms which prevent one from forming a closed equation for the two-body electron propagator analogously to what happens with the diagrams shown in Eq. (4.19a) in the case of the phonon propagator, see Sec.4.3.3. In order to go around this issue, it is possible to define the generalized electronic response function

$$L(1,2;1',2') \equiv -\big[G_2(1,2;1',2') - G(1;1')G(2;2')\big]\,, \tag{4.24a}$$

where the label $i^{(\prime)}$ refers to $i^{(\prime)}_{zp}$, which applies also to the remaining section. It follows from this definition that

$$\begin{aligned} L(1_{zp},2_{zp};1^+_{zq},2^+_{zq}) &= \frac{\mathrm{Tr}\left[T\left\{e^{-\imath\int_C d\bar{z}\ \widehat{H}(\bar{z})}\Delta\widehat{\gamma}_{p_1q_1}(z_1)\Delta\widehat{\gamma}_{p_2q_2}(z_2)\right\}\right]}{\mathrm{Tr}\left[T\left\{e^{-\imath\int_C d\bar{z}\ \widehat{H}(\bar{z})}\right\}\right]} \\ &\equiv \imath\chi(1_{zpq},2_{zpq})\,, \end{aligned}$$

where χ is a contour-time extension of the response function of Eq. (3.1), which, for one, explains why L is referred to here as the generalized electronic response function. In any case, it is clear that this response function does not contain the problematic terms as they cancel against the product of the one-body electron propagators. It then follows from Eq. (4.14) that the generalized electronic response function has the graphical representation

$L(1_{zp},2_{zp};1'_{zp},2'_{zp}) \simeq$

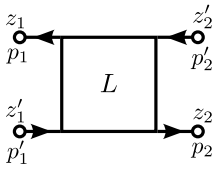

$$\simeq -\left\{\begin{array}{l}\text{sum of all connected, topologically inequivalent diagrams in which the external vertices with the labels } \{1_{zp}, 2_{zp}, 1'_{zp}, 2'_{zp}\} \text{ and unlabeled F-vertices, M-vertices and end-vertices of w-lines are connected pair-wise by d- and g-lines such that the external vertices with the labels } 1_{zp}\ (1'_{zp}) \\ \text{and } 2_{zp}\ (2'_{zp}) \text{ are attached to in(out)-going g-lines and } 1_{zp} \\ \text{and } 1'_{zp} \text{ are connected to } 2_{zp} \text{ and } 2'_{zp} \text{ by any combination of lines}\end{array}\right\} \tag{4.24b}$$

where the second line defines the perturbation expansion of this response function. It is now possible to define the so-called two g-line irreducible (2GI) diagrams as connected diagrams in which the external vertices corresponding to the first and third arguments are connected to the external vertices corresponding to the second and fourth arguments by any combination of lines such that this connection cannot be broken by removing two g- or G-lines. It follows, by removing also all electron self-energy insertions and replacing the g- with G-lines, that the generalized electronic response function satisfies the diagrammatic equation

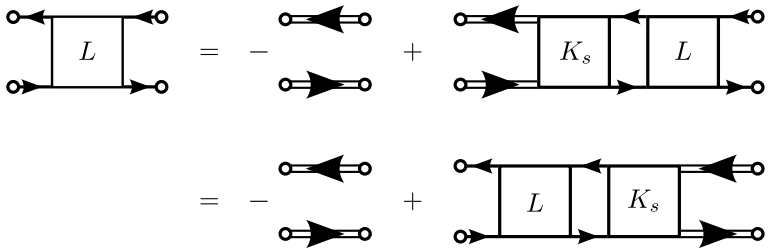

(4.25a)

and, by restoring the external and internal labels and integrating over the latter, the equivalent algebraic equation

$$\begin{aligned} L(1,2;1',2') &= G(1;2')G(2;1') - \int d3d4d3'd4'\ G(1;3')G(3;1')K_s(3',4';3;4)L(4,2;4',2') \\ &= G(1;2')G(2;1') - \int d3d4d3'd4'\ L(1,3;1',3')K_s(3',4';3;4)G(4;2')G(2;4')\,, \end{aligned} \tag{4.25b}$$

which is known as the Bethe-Salpeter equation. Here, the singly-skeletonic four-point kernel K_s was introduced and defined as

$$K_s(1_{zp}, 2_{zp}; 1'_{zp}, 2'_{zp}) \simeq$$

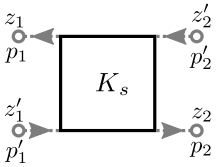

$$\simeq \left\{\begin{array}{l}\text{sum of all connected, G-skeletonic, two g-line irreducible, topologically inequivalent diagrams in which the external vertices with the labels } (1_{zp}, 2_{zp}; 1'_{zp}, 2'_{zp}) \text{ and unlabeled M-vertices and end-vertices of w-lines are connected pair-wise by d- and G-lines such that the external vertices with the labels } 1_{zp},\ 2_{zp} \text{ and } 1'_{zp},\ 2'_{zp}, \\ \text{accepting respectively out- and in-going g- or G-lines, are M-vertices or end-vertices of w-lines}\end{array}\right\} \tag{4.26}$$

where the gray dashed lines with in- or out-going arrows indicate that an in- or out-going g- or G-line is the only acceptable joining edge. It is noted that the diagrammatic rule 4.3.2 applies here if the diagram is closed explicitly by a G-line in the loop rule [SL13]. A further reduction in the number of the kernel diagrams can be achieved by removing all phonon self-energy insertions and replacing all d- with D-lines in all diagrams except in

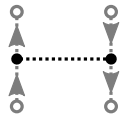

as doing so would lead to double-counting. The doubly-skeletonic four-point kernel K_{ss} obtained in this way is defined by adding the term D-skeletonic and by replacing the d- with D-lines, expect for the above diagram, in the definition of the singly-skeletonic four-point kernel of Eq. (4.26). Finally, in particular with regard to Ch. 7, an important connection between the electron self-energy and the four-point kernel is stated. If the singly-skeletonic electron self-energy is regarded as a functional of the one-body electron propagator then

$$K_s(1,2;1',2') = -\frac{\delta\Sigma_s(1;1')}{\delta G(2';2)}\,,$$

which follows from the proof presented in [SL13] for purely electronic systems.

4.4 Conserving Approximations for Electron and Phonon Propagators

In order to use many-body perturbation theory in practice, it is conventional to introduce approximations by truncating the perturbation expansions of the self-energies or four-point kernels. It is true that, if further resummations are not introduced, the higher order self-energy or four-point kernel diagrams are more difficult to evaluate since there are more internal integrals to calculate. It is partially due to this reason that the number of practical approximations has remained to this day relatively low. In fact, in many applications, it is even necessary to restrict to singly-skeletonic, or insertions containing, self-energies in order to reduce the computational demand. However, as a consequence, it can be that such approximations have undesirable traits such as a failure to respect the conservation laws for the particle number or total energy, which are particularly undesirable deficiencies in some applications. It was in [BK61, Bay62] that a recipe to construct the so-called conserving approximations, which are guaranteed to lead to the fulfillment of the continuity equation for the particle density and to the obedience of the particle number and the total momentum, angular momentum and energy conservation laws, was introduced. In this thesis, only approximations which respect the continuity equation are studied since the present work has been partially motivated by the applications to transient quantum transport in which it is desirable that the change of the charge of a volume element equals minus the charge current through the enclosing surface.

It is shown in [Bay62], for a purely electronic system, that a so-called Φ-derivable approximation, i.e., a self-energy approximation Σ obtained by functional differentiation $\Sigma = \delta\Phi/\delta G$ of an approximation Φ to the exact Φ-functional, is a conserving approximation. In App. 4.D, it is shown explicitly, for a system with both electron-phonon and electron-electron interactions, that if, analogously to the case of the screened interaction for purely electronic systems [SL13], the Ψ-functional is defined as

$-\Psi \equiv -\Phi -$ 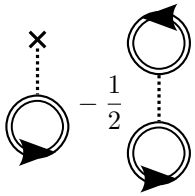 $-\frac{1}{2}$ (4.27)

then the so-called Ψ-derivable approximations are conserving approximations. Here, by conserving, it is meant that the electron one-body reduced density matrix, cf., App. 4.D.1, and total energy, cf., App. 4.D.2, obtained from the approximate propagators satisfy the continuity equations following from the Heisenberg equations of motion. It is noteworthy that the particle number and, in the absence of an explicit time-dependence, total energy conservation arise as special cases of these continuity equations. Moreover, by Ψ-derivability, it is meant here that the phonon field ϕ and propagator D and the electron propagator G satisfy the integro-differential forms of the integral equations (4.19), (4.21) and (4.16), cf., Sec. 4.5.2, with the Ψ-derivable electron and phonon self-energies

$$\Sigma(1_{zp};1'_{zp}) = \Sigma_{\mathrm{epMF}}(1_{zp};1'_{zp}) + \frac{\delta\Psi}{\delta G(1'_{zp};1_{zp})}\,,$$
$$\Pi(1_{z\mu},1'_{z\mu}) = -2\frac{\delta\Psi}{\delta D(1'_{z\mu},1_{z\mu})}\bigg|_S\,,$$

where

$$\Sigma_{ep\mathrm{MF}}(1_{zp};1'_{zp}) \simeq$$

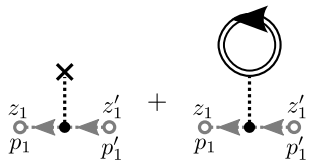

$$= \delta(z_1,z'_1)\sum_{\mu_1} M^{\mu_1}_{p_1p'_1}(z_1)\phi(1_{z\mu}) \tag{4.28}$$

is the electron-phonon interaction induced mean-field part of the electron self-energy. It is assumed that Ψ is a well-defined approximation to the exact Ψ-functional which means here that it is obtained diagrammatically as a sum of diagrams in which M- and end vertices of w-lines are connected pair-wise by D- and G-lines such that a given vertex is connected to all other vertices by some combination of lines. In a general basis, it is also necessary that the electron-phonon correlation function $\Lambda_0 \equiv X_{1,1}$, cf., Sec. 3.2, and the two-body electron propagator G_2, which appear on the right-hand sides of the continuity equations, are Ψ-derivable, i.e.

$$\Lambda_0(1_{z\mu};1_{zp};1^+_{zq}) = \frac{1}{\imath^{1/2}}\left[\phi(1_{z\mu})G(1_{zp};1^+_{zq}) + \frac{\delta\Psi}{\delta M(1_{z\mu qp})}\right],$$
$$G_2(1_{zp},1_{zq};1^+_{zs},1^+_{zt}) = -\frac{2}{\imath}\frac{\delta\Psi}{\delta w(1_{zsp},1_{ztq})}\bigg|_S\,,$$

and that the two-body electron propagator also obeys the exact symmetry $G_2(1_{zp},1_{zq};1^+_{zs},1^+_{zt}) = -G_2(1_{zq},1_{zp};1^+_{zs},1^+_{zt}) = -G_2(1_{zp},1_{zq};1^+_{zt},1^+_{zs})$. It is noted that when Ψ is the exact Ψ-functional, the above relations follow, for instance, by a straightforward use and generalization of the identities $-\imath\chi/2 = \delta\Phi_{\mathrm{xc}}/\delta w\big|_S$ and $-\imath P/2 = \delta\Psi/\delta W\big|_S$ for the proofs and notation of which it is referred to [SL13]. Finally, in the proof regarding the continuity equation for the total energy, cf., App. 4.D.2, the exact symmetries $D(1_{z\mu},1'_{z\mu}) = D(1'_{z\mu},1_{z\mu})$ and $dD(1_{z\mu},1^+_{z\nu})/dz_1 = dD(1_{z\nu},1^+_{z\mu})/dz_1$ were used and hence, unless an alternative proof can be introduced, these symmetries are a prerequisite for a conserving approximation.

In what follows, the conserving approximations, which follow by truncating the exact Ψ-functional up to second order with respect to M-vertices or w-lines and which are studied in the publications contained in this thesis, are summarized. It is noted that here and, unless otherwise stated, from now on, the subscripts referring to singly- or doubly-skeletonic diagrams are omitted.

4.4.1 Hartree and Born Approximations

In **I** [SPAL15a] and **II** [SPAL15b], we have considered the Holstein model in which there is no direct interaction between the electrons but they instead interact with the phonons via the electron-phonon interaction. In this work, we have used conserving many-body self-energy approximations which we call the Hartree and partially and fully self-consistent Born approximations. Here, these approximations are introduced by defining the corresponding many-body contributions, obtained by neglecting the first diagram of Eq. (4.23), of the Φ-functional. The Hartree (H) approximation is obtained by using the Φ-functional

$-\Phi_{\mathrm{H}} \simeq \frac{1}{2}$

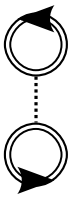

from which the electron self-energy

$\Sigma_{\mathrm{H}}(1_{zp}; 1'_{zp}) \simeq$

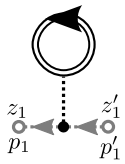

$$= -\imath\delta(z_1, z'_1) \sum_{\mu_1\mu_2} \sum_{p_2 q_2} M^{\mu_1}_{p_1 p'_1}(z_1) \int_C dz_2 \; d_{\mu_1\mu_2}(z_1, z_2) M^{\mu_2}_{p_2 q_2}(z_2) G_{q_2 p_2}(z_2; z_2^+)$$

follows by functional differentiation. It follows from Ψ-derivability with $\Psi_{\mathrm{H}} = 0$ that the phonon self-energy is omitted in the Hartree approximation and that this approximation is conserving in the sense that the continuity equations for the electron one-body reduced density matrix and total energy are guaranteed to be obeyed. If approximations based on an order-by-order truncation of the diagrammatic expansion of the singly-skeletonic electron self-energy are considered then it is the partially self-consistent Born approximation which is the simplest approximation beyond the Hartree approximation. Equivalently, the partially self-consistent Born (Gd) approximation is given by differentiating the functional

$-\Phi_{\mathrm{Gd}} \simeq \frac{1}{2}$

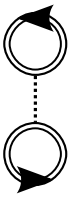

$+ \frac{1}{2}$

such that the electron self-energy

$\Sigma_{\mathrm{Gd}}(1_{zp}; 1'_{zp}) \simeq$

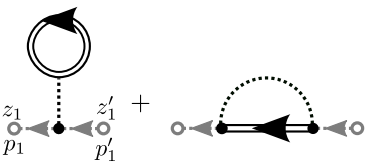

$$= \Sigma_{\mathrm{H}}(1_{zp}; 1'_{zp}) + \imath \sum_{\mu_1\mu'_1} \sum_{q_1 q'_1} M^{\mu_1}_{p_1 q_1}(z_1) d_{\mu_1\mu'_1}(z_1, z'_1) M^{\mu'_1}_{q'_1 p'_1}(z'_1) G_{q_1 q'_1}(z_1; z'_1)$$

and the omission of the phonon self-energy follow. It is the latter, i.e., the neglect of the phonon self-energy, due to which only the continuity equation for the reduced density matrix is guaranteed to be satisfied, cf., [KL16]. In fact, by considering the doubly-skeletonic extension of this approximation, also the continuity equation for the total energy can be shown to be obeyed. In order to obtain the doubly-skeletonic extension, the Φ-functional

$$-\Phi_{\mathrm{GD}} \simeq \frac{1}{2} + \frac{1}{2}$$

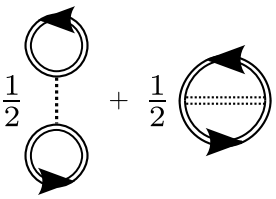

is defined such that, by functional differentiation, the electron

$$\Sigma_{\mathrm{GD}}(1_{zp};1'_{zp}) \simeq$$

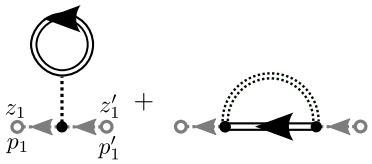

$$= \Sigma_{\mathrm{H}}(1_{zp};1'_{zp}) + \imath \sum_{\mu_1\mu'_1} \sum_{q_1 q'_1} M^{\mu_1}_{p_1 q_1}(z_1) D_{\mu_1\mu'_1}(z_1,z'_1) M^{\mu'_1}_{q'_1 p'_1}(z'_1) G_{q_1 q'_1}(z_1;z'_1)$$

and phonon

$$\Pi_{\mathrm{GD}}(1_{z\mu},1'_{z\mu}) \simeq$$

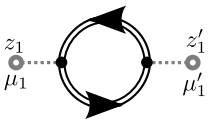

$$= -\imath \sum_{\substack{p_1 q_1 \\ p'_1 q'_1}} M^{\mu_1}_{p_1 q_1}(z_1) G_{q_1 p'_1}(z_1;z'_1) G_{q'_1 p_1}(z'_1;z_1) M^{\mu'_1}_{p'_1 q'_1}(z'_1)$$

self-energies are obtained. It is this both continuity equations respecting approximation which is denoted in this work as the fully self-consistent Born (GD) approximation. It is emphasized here that if, instead of a d-line, the tadpole diagram in Σ_{GD} would be dressed with a D-line then a double-counting of perturbative terms would occur, see Sec. 4.3.3 and cf. [Hed65, SL13]. Finally, it is noted that in other contexts it is perhaps more natural to refer to the fully self-consistent Born approximation as the Migdal(-Eliashberg) approximation [Mig58, Eli60a, Eli60b].

4.4.2 Hartree-Fock and Second Born Approximations

In **III** [SML12], we have considered finite lattice models, i.e., the Hubbard and Pariser-Parr-Pople models, in which the nuclei are assumed to be inert and the electrons interact only amongst themselves. The Hartree-Fock and second Born approximations which are both fully conserving, i.e., the continuity equations for the electron one-body reduced density matrix and total energy are both respected, are used in this work. The Hartree-Fock (HF) approximation is obtained from the Φ-

functional

$-\Phi_{\mathrm{HF}} \simeq \frac{1}{2}$  $+ \frac{1}{2}$ 

such that, by functional differentiation, the electron self-energy

$$\begin{aligned}\Sigma_{\mathrm{HF}}(1_{zp};1'_{zp}) \simeq\ & \\ &= -\imath\delta(z_1,z_1')\sum_{p_2q_2} w_{p_1p_2q_2p_1'}(z_1)G_{q_2p_2}(z_1;z_1^+)\\ &+\imath\delta(z_1,z_1')\sum_{q_1q_1'} w_{p_1q_1'p_1'q_1}(z_1)G_{q_1q_1'}(z_1;z_1^+)\\ &\equiv \Sigma_{\mathrm{eeMF}}(1_{zp};1'_{zp})\end{aligned} \tag{4.29}$$

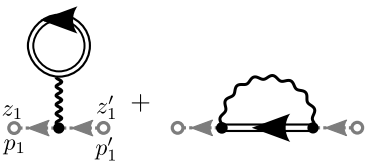

follows. It is due to its time-local dependence on the one-body reduced density matrix that this approximation is referred to as a mean-field approximation and hence denoted above also as the electron-electron interaction (ee) induced mean-field (MF) self-energy. The second Born approximation follows by considering all singly-skeletonic self-energy diagrams which have at most two w-lines hence it represents the simplest order-by-order extension of the Hartree-Fock approximation. It is possible to obtain the second Born approximation by using

$-\Phi_{\mathrm{2B}} \simeq \frac{1}{2}$ 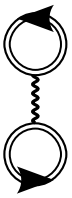 $+ \frac{1}{2}$  $+ \frac{1}{4}$  $+ \frac{1}{4}$ 

such that the electron self-energy

$\Sigma_{\mathrm{2B}}(1_{zp};1'_{zp}) \simeq$ 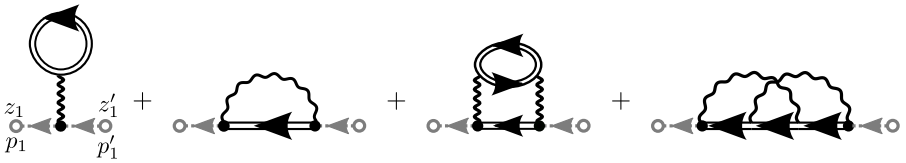

$$\begin{aligned}&= \Sigma_{\mathrm{HF}}(1_{zp},1'_{zp})\\ &+\sum_{\substack{q_1q_1'\\p_2q_2\\p_2'q_2'}} w_{p_1p_2q_2q_1}(z_1)w_{q_1'p_2'q_2'p_1'}(z_1')G_{q_1q_1'}(z_1;z_1')G_{q_2p_2'}(z_1;z_1')G_{q_2'p_2}(z_1';z_1)\\ &-\sum_{\substack{q_1q_1'\\p_2q_2\\p_2'q_2'}} w_{p_1q_2'p_2'q_1}(z_1)w_{q_1'q_2p_2p_1'}(z_1')G_{q_1q_2}(z_1;z_1')G_{p_2q_2'}(z_1';z_1)G_{p_2'q_1'}(z_1;z_1')\end{aligned}$$

follows by functional differentiation. In **III** [SML12], the second Born approximation is referred to as the correlated approximation since it describes electron correlation, and exchange, beyond the mean-field description.

4.5 From Contour-Ordered to Real-, Imaginary- and Mixed-Time Propagators

In the previous sections, time-independent and -dependent many-body perturbation theory has been introduced at a formal and general level which is, in many cases, not suitable or necessary as such for practical applications. Here, by focusing on the one- and two-field phonon propagators and the one-body electron propagator, the standard methodologies to bridge the gap between the formal representation and a practical one are introduced by decomposing the contour-ordered propagators into more amenable real-, imaginary- and mixed-time objects referred to as the Keldysh components [Kel65]. It is particularly noteworthy that the equations of motion for the Keldysh components of the aforementioned propagators known as the Kadanoff-Baym equations are introduces in this section [KB62]. It is these equations whose solutions and the solving of which forms the lion's share of the work published in this thesis and in the enclosed publications. Finally, it is noted that although applications relying on these notions are by no means limited to many-body perturbation theory or only to numerical applications, it is, nevertheless, the context in which they are applied in this thesis.

4.5.1 Keldysh Components

In order to access the physical information contained in the propagators defined on the Keldysh contour, their contour-time structure needs to be decoded back to the original representation based on real and, in some cases, imaginary times. It is common to do this by defining the so-called Keldysh components [Kel65, Wag91, SL13] of the contour-ordered one-

$$k_1(z) = \frac{\mathrm{Tr}\left[T\left\{e^{-\imath\int_C d\bar{z}\ \widehat{H}(\bar{z})}\widehat{O}(z)\right\}\right]}{\mathrm{Tr}\left[T\left\{e^{-\imath\int_C d\bar{z}\ \widehat{H}(\bar{z})}\right\}\right]},$$

and two-time

$$k_2(z;z') = \frac{\mathrm{Tr}\left[T\left\{e^{-\imath\int_C d\bar{z}\ \widehat{H}(\bar{z})}\widehat{O}(z)\widehat{O}'(z')\right\}\right]}{\mathrm{Tr}\left[T\left\{e^{-\imath\int_C d\bar{z}\ \widehat{H}(\bar{z})}\right\}\right]},$$

correlation functions. Here, the operators $\widehat{O}$ and $\widehat{O}'$ are arbitrary fermionic or non-fermionic operators. It is noted that although Keldysh components of more complicated objects could also be defined, they are perhaps not as useful and are, nevertheless, not required in this work. It follows from the piece-wise definition of the Hamiltonian operator that the one-time correlation function has only the two Keldysh components

$$k_1(t) \equiv k_1(t_\pm),$$

$$\begin{aligned} k_1^M(\tau) &\equiv k_1(t_0 - \imath\tau) \\ &= k_1^M\,, \end{aligned} \qquad \text{(Matsubara)}$$

where $t_\pm$ is a contour-time on the backward/forward branch corresponding to the real time t. Here, it has been acknowledged that since the Hamiltonian operator is independent of the imaginary time on the imaginary track, also the Matsubara component is independent of the imaginary time. In contrast to the one-time functions, the two-time correlation functions are also piece-wise defined due to the nature of the contour-time ordering operator. In fact, the two-time correlation function is a special case of a more general Keldysh function which has the contour-time structure

$$k_2(z;z') \equiv \delta(z,z')k_2^\delta(z) + \theta(z,z')k_2^>(z;z') + \theta(z',z)k_2^<(z;z')\,,$$

where δ and θ are the contour-time Dirac delta and Heaviside functions [SL13]. Here, the contour-time function k^δ, such that

$$\begin{aligned} k_2^\delta(t) &\equiv k_2^\delta(t_\pm)\,, \\ k_2^{\delta_M}(\tau) &\equiv k_2^\delta(t_0 - \imath\tau) \\ &= k_2^{\delta_M}\,, \end{aligned} \qquad \text{(Matsubara)}$$

is called the local contour-time component while $k^>$ and $k^<$ are referred to as the greater and lesser contour-time components, respectively. It is possible to further define the real-, imaginary- and mixed-time Keldysh components

$$\begin{aligned} k_2^>(t;t') &\equiv k_2(t_+;t'_-)\,, && \text{(Greater)} \\ k_2^<(t;t') &\equiv k_2(t_-;t'_+)\,, && \text{(Lesser)} \\ k_2^\rceil(t;\tau) &\equiv k_2(t_\pm;t_0 - \imath\tau)\,, && \text{(Right)} \\ k_2^\lceil(\tau;t) &\equiv k_2(t_0 - \imath\tau;t_\pm)\,, && \text{(Left)} \\ k_2^M(\tau;\tau') &\equiv k_2(t_0 - \imath\tau;t_0 - \imath\tau') \\ &\equiv k_2^M(\tau - \tau')\,, && \text{(Matsubara)} \end{aligned}$$

where, similarly to the one-time function, the imaginary-time difference dependence of the Matsubara component follows from the imaginary time independence of the Hamiltonian operator on the imaginary track. The real-time, i.e., the greater and lesser, components can be further used define the retarded and advanced components

$$\begin{aligned} k_2^R(t;t') &\equiv \delta(t-t')k_2^\delta(t) + \theta(t-t')k_2^r(t;t') \\ &\equiv \delta(t-t')k_2^\delta(t) + \theta(t-t')\big[k_2^>(t;t') - k_2^<(t;t')\big]\,, && \text{(Retarded)} \\ k_2^A(t;t') &\equiv \delta(t-t')k_2^\delta(t) + \theta(t'-t)k_2^a(t;t') \\ &\equiv \delta(t-t')k_2^\delta(t) + \theta(t'-t)\big[k_2^<(t;t') - k_2^>(t;t')\big]\,. && \text{(Advanced)} \end{aligned}$$

where the functions with the lower case superscripts r/a are referred to as the regular parts of the retarded/advanced components. It is also possible to define the time-ordered and anti time-ordered components [SL13] but as they are not relevant for this work they are not introduced. However, it is relevant to be able to rewrite contour-time integrals of the one- and two-time correlation functions, in particular integrals such as

$$\begin{aligned} c_1(z) &\equiv [a_2 \circ b_1](z) \\ &\equiv \int_C d\bar{z}\; a_2(z;\bar{z})b_1(\bar{z})\,, \end{aligned}$$

$$\begin{aligned} c_2(z;z') &\equiv [a_2 \circ b_2](z;z') \\ &\equiv \int_C d\bar{z}\; a_2(z;\bar{z}) b_2(\bar{z},z')\,, \end{aligned}$$

where b_1 and c_1 are one- while a_2, c_2 and b_2 are two-time Keldysh functions, in terms of the real-, imaginary- and mixed-time components. It is possible to do this by using a set of rules collectively referred to as the Langreth rules [Lan76, SL13]. In this work, the Langreth rules

$$\begin{aligned} c_1(t) &= \big[a_2^R \bullet b_1\big](t) + \big[a_2^\rceil \star b_1^M\big](t)\,, \\ c_1^M(\tau) &= \big[a_2^M \star b_1^M\big](\tau) \\ &= c_1^M\,, \end{aligned}$$

and

$$\begin{aligned} c_2^\gtrless(t;t') &= \big[a_2^R \bullet b_2^\gtrless\big](t;t') + \big[a_2^\gtrless \bullet b_2^A\big](t;t') + \big[a_2^\rceil \star b_2^\lceil\big](t;t')\,, \\ c_2^\rceil(t;\tau) &= \big[a_2^R \bullet b_2^\rceil\big](t;\tau) + \big[a_2^\rceil \star b_2^M\big](t;\tau)\,, \\ c_2^\lceil(\tau;t) &= \big[a_2^\lceil \bullet b_2^A\big](\tau;t) + \big[a_2^M \star b_2^\lceil\big](\tau;t)\,, \\ c_2^M(\tau;\tau') &= \big[a_2^M \star b_2^M\big](\tau;\tau') \\ &= c_2^M(\tau-\tau')\,, \end{aligned}$$

are particularly convenient. Here, the standard abbreviations

$$\begin{aligned} \big[\alpha_2 \bullet \beta_1\big](t) &\equiv \int_{t_0}^{\infty} d\bar{t}\; \alpha_2(t;\bar{t})\beta_1(\bar{t})\,, \\ \big[\alpha_2 \star \beta_1\big](\tau) &\equiv -\imath \int_0^{\beta} d\bar{\tau}\; \alpha_2(\tau;\bar{\tau})\beta_1(\bar{\tau})\,, \end{aligned}$$

and

$$\begin{aligned} \big[\alpha_2 \bullet \beta_2\big](t;t') &\equiv \int_{t_0}^{\infty} d\bar{t}\; \alpha_2(t;\bar{t})\beta_2(\bar{t};t')\,, \\ \big[\alpha_2 \star \beta_2\big](\tau;\tau') &\equiv -\imath \int_0^{\beta} d\bar{\tau}\; \alpha_2(\tau;\bar{\tau})\beta_2(\bar{\tau};\tau')\,, \end{aligned}$$

were introduced to denote the integrations with respect to the imaginary and real times in a compact way.

4.5.2 Kadanoff-Baym Equations

In their original form, the Kadanoff-Baym equations were introduced in [KB62] as the equations of motion for the greater and lesser components of the one-body electron propagator. In the case of the extended Keldysh contour, i.e., when the contour-times lie also on the imaginary branch, and in the presence of the electron-phonon interaction they are instead the equations of motion for the real- and imaginary-time components of the phonon field as well as for the greater, lesser, right, left and Matsubara components of the electron and phonon propagators. Instead of proceeding to write down all of these equations, it is found useful to first list a few symmetries of the aforementioned components in order to present only the equations the solutions of which are not related by the

symmetries. Firstly, it follows, by their definition and by the Kubo-Martin-Schwinger boundary conditions, that the Keldysh components of the exact electron propagator obey the symmetries

$$G^{\gtrless}_{pq}(t;t') = -\big[G^{\gtrless}_{qp}(t';t)\big]^*\,, \tag{4.30a}$$
$$G^{\rceil}_{pq}(t;\tau) = \big[G^{\lceil}_{qp}(\beta-\tau;t)\big]^*\,, \tag{4.30b}$$
$$\begin{aligned} G^{M}_{pq}(\tau) &= -G^{M}_{pq}(\tau-\beta) \\ &= \big[G^{M}_{qp}(\tau-\beta)\big]^*\,, \qquad \tau\in[0,\beta]\,, \end{aligned} \tag{4.30c}$$

which show that it is sufficient to consider the greater and lesser components for $t \geq t'$ ($t' \geq t$) and the Matsubara component for $\tau \in [0,\beta]$ ($\tau \in [-\beta,0]$) and, moreover, that the left (right) component is fully determined by the right (left) component. Here, it is also remarked that the last equality implies that the Matsubara component is anti-hermitian for a fixed imaginary-time value which effectively follows from the time-independence of the Hamiltonian operator on the imaginary track. It is similarly possible to show that the Keldysh components of the exact phonon propagator obey the symmetries

$$\begin{aligned} D^{\gtrless}_{\mu\nu}(t;t') &= -\big[D^{\gtrless}_{\nu\mu}(t';t)\big]^* \\ &= -\big[D^{\lessgtr}_{\mu\nu}(t;t')\big]^*\,, \end{aligned} \tag{4.30d}$$
$$\begin{aligned} D^{\rceil}_{\mu\nu}(t;\tau) &= -\big[D^{\lceil}_{\nu\mu}(\beta-\tau;t)\big]^* \\ &= -\big[D^{\rceil}_{\mu\nu}(t;\beta-\tau)\big]^*\,, \end{aligned} \tag{4.30e}$$
$$\begin{aligned} D^{M}_{\mu\nu}(\tau) &= D^{M}_{\mu\nu}(\tau-\beta) \\ &= -\big[D^{M}_{\nu\mu}(\tau-\beta)\big]^* \\ &= -\big[D^{M}_{\mu\nu}(\beta-\tau)\big]^*\,, \qquad \tau\in[0,\beta]\,, \end{aligned} \tag{4.30f}$$

where the additional relations follow from the symmetry $D_{\mu\nu}(z;z') = D_{\nu\mu}(z';z)$. It is due to these additional symmetries that the greater (lesser) component is fully determined by the lesser (greater) component and that it is sufficient to consider the right, left and Matsubara components for $\tau \in [0,\beta/2]$ ($\tau \in [-\beta/2,0]$). In order to introduce the Kadanoff-Baym equations, it is first noted that the contour-time equations of motion

$$\sum_{\nu}\big(\imath\alpha_{\mu\nu}\partial_z - \bar{\Omega}_{\mu\nu}(z)\big)\phi_\nu(z) = F_\mu(z) - \imath\sum_{pq} M^{\mu}_{pq}(z)G_{qp}(z;z^+)\,, \tag{4.31a}$$

$$\sum_{\lambda}\big(\imath\alpha_{\mu\lambda}\partial_z - \bar{\Omega}_{\mu\lambda}(z)\big)D(z\,\lambda;z'\,\nu) = \delta_{\mu\nu}\delta(z,z') + \sum_{\lambda}\int_C d\bar{z}\;\Pi(z\,\mu;\bar{z}\,\lambda)D(\bar{z}\,\lambda;z'\,\nu)\,, \tag{4.31b}$$

$$\sum_{\lambda}\big(-\imath\alpha_{\lambda\nu}\partial_{z'} - \bar{\Omega}_{\lambda\nu}(z')\big)D(z\,\mu;z'\,\lambda) = \delta_{\mu\nu}\delta(z,z') + \sum_{\lambda}\int_C d\bar{z}\;D(z\,\mu;\bar{z}\,\lambda)\Pi(\bar{z}\,\lambda;z'\,\nu)\,, \tag{4.31c}$$

$$\sum_{s}\big(\imath\delta_{ps}\partial_z - h_{ps}(z)\big)G(z\,s;z'\,q) = \delta_{pq}\delta(z,z') + \sum_{s}\int_C d\bar{z}\;\Sigma(z\,p;\bar{z}\,s)G(\bar{z}\,s;z'\,q)\,, \tag{4.31d}$$

$$\sum_{s}\big(-\imath\delta_{sq}\partial_{z'} - h_{sq}(z')\big)G(z\,p;z'\,s) = \delta_{pq}\delta(z,z') + \sum_{s}\int_C d\bar{z}\;G(z\,p;\bar{z}\,s)\Sigma(\bar{z}\,s,z'\,q) \tag{4.31e}$$

where $\bar{\Omega}_{\mu\nu}(z) \equiv \Omega_{\mu\nu}(z) + \Omega_{\nu\mu}(z)$, follow by differentiating the integral equations (4.19), (4.21) and (4.16). The Kadanoff-Baym equations are then obtained by choosing the external contour-times to lie on the real- and/or imaginary-time branches of the contour and by applying the Langreth rules summarized in Sec. 4.5.1. It is reasonable, by taking into account the symmetries, to only

introduce the equations, in addition to the real- and imaginary-time components of the phonon field, for the greater, lesser, right, and Matsubara components of the electron and phonon propagators. Moreover, for the same reason, only the equations obtained by differentiating the first time argument are introduced. It then follows by adhering to these guidelines and by taking the Keldysh components of Eqs. (4.31) that

$$\sum_{\nu} \big(-\alpha_{\mu\nu}\partial_\tau - \bar{\Omega}^M_{\mu\nu}\big)\phi^M_\nu(\tau) = F^M_\mu - \imath \sum_{pq} M^{M\,\mu}_{pq} G^M_{qp}(0^-)\,, \tag{4.32a}$$

$$\sum_{\nu} \big(\imath\alpha_{\mu\nu}\partial_t - \bar{\Omega}_{\mu\nu}(t)\big)\phi_\nu(t) = F_\mu(t) - \imath \sum_{pq} M^{\mu}_{pq}(t) G^<_{qp}(t;t)\,, \tag{4.32b}$$

$$\sum_{\lambda} \big(-\alpha_{\mu\lambda}\partial_\tau - \bar{\Omega}^M_{\mu\lambda}\big) D^M_{\lambda\nu}(\tau) = \imath\delta_{\mu\nu}\delta(\tau) + \sum_{\lambda} \big[\Pi^M_{\mu\lambda} \star D^M_{\lambda\nu}\big](\tau)\,, \tag{4.32c}$$

$$\sum_{\lambda} \big(\imath\alpha_{\mu\lambda}\partial_t - \bar{\Omega}_{\mu\lambda}(t)\big) D^\rceil_{\lambda\nu}(t;\tau) = \sum_{\lambda} \big[\Pi^R_{\mu\lambda} \bullet D^\rceil_{\lambda\nu} + \Pi^\rceil_{\mu\lambda} \star D^M_{\lambda\nu}\big](t;\tau)\,, \tag{4.32d}$$

$$\sum_{\lambda} \big(\imath\alpha_{\mu\lambda}\partial_t - \bar{\Omega}_{\mu\lambda}(t)\big) D^{\gtrless}_{\lambda\nu}(t;t') = \sum_{\lambda} \big[\Pi^R_{\mu\lambda} \bullet D^{\gtrless}_{\lambda\nu} + \Pi^{\gtrless}_{\mu\lambda} \bullet D^A_{\lambda\nu} + \Pi^\rceil_{\mu\lambda} \star D^\lceil_{\lambda\nu}\big](t;t')\,, \tag{4.32e}$$

$$\sum_{s} \big(-\delta_{ps}\partial_\tau - h^M_{ps}\big) G^M_{sq}(\tau) = \imath\delta_{pq}\delta(\tau) + \sum_{s} \big[\Sigma^M_{ps} \star G^M_{sq}\big](\tau)\,, \tag{4.32f}$$

$$\sum_{s} \big(\imath\delta_{ps}\partial_t - h_{ps}(t)\big) G^\rceil_{sq}(t;\tau) = \sum_{s} \big[\Sigma^R_{ps} \bullet G^\rceil_{sq} + \Sigma^\rceil_{ps} \star G^M_{sq}\big](t;\tau)\,, \tag{4.32g}$$

$$\sum_{s} \big(\imath\delta_{ps}\partial_t - h_{ps}(t)\big) G^{\gtrless}_{sq}(t;t') = \sum_{s} \big[\Sigma^R_{ps} \bullet G^{\gtrless}_{sq} + \Sigma^{\gtrless}_{ps} \bullet G^A_{sq} + \Sigma^\rceil_{ps} \star G^\lceil_{sq}\big](t;t')\,, \tag{4.32h}$$

where the identities $df(z)/dz|_{t_0-\imath\tau} = \imath df(t_0-\imath\tau)/d\tau$ and $\delta(t_0-\imath\tau, t_0-\imath\tau') = \imath\delta(\tau-\tau')$ were used to obtain the equations for the Matsubara components. Here, by the superscript M to the matrix elements introduced in Eqs. (2.1) and (2.3), it is referred to their imaginary-time (Matsubara) components whose definitions follow straightforwardly from the definition $\widehat{H}^M \equiv \widehat{H} - \mu\widehat{N}$ of the imaginary-time Hamiltonian operator $\widehat{H}^M$, cf., Sec. 4.1. It is this set of integro-differential equations which is collectively referred to as the Kadanoff-Baym equations (KBe) in this work. It is noted here that the so-called collision integrals $[\Pi \circ D]$ and $[\Sigma \circ G]$, the name of which is related to the interpretation that they can be seen as nonlocal potentials describing scattering events, obey the same symmetries as do the propagators in whose equations of motion they appear. It remains to complement the Kadanoff-Baym equations, which only determine how the components of the field and propagators evolve in real- and imaginary-time, with the appropriate boundary and initial conditions. It follows from the Kubo-Martin-Schwinger boundary conditions that the Matsubara components of the phonon field and the phonon and electron propagators are required to satisfy the boundary conditions

$$\begin{aligned} \phi^M_\mu(0) &= \phi^M_\mu(\beta)\,, \\ D^M_{\mu\nu}(\tau) &= D^M_{\mu\nu}(\tau-\beta)\,, \\ G^M_{pq}(\tau) &= -G^M_{pq}(\tau-\beta)\,, \end{aligned}$$

where $\tau \in [0,\beta]$, which guarantee that the integral equations of Eqs. (4.19), (4.21) and (4.16) are satisfied. Moreover, these boundary conditions also ensure, as seen by using the variation of constants formula, that the Matsubara component of the phonon field is independent of the imaginary-time, i.e., $\phi^M(\tau) = \phi^M$, as it should be. It also follows straightforwardly that the phonon field and the electron and phonon propagators satisfy the initial conditions

$$\phi_\mu(t_0) = \phi^M_\mu\,, \tag{4.33a}$$

$$D^{\gtrless}_{\mu\nu}(t_0;t_0) = D^{M}_{\mu\nu}(0^{\pm})\,, \tag{4.33b}$$

$$D^{\rceil}_{\mu\nu}(t_0;\tau) = D^{M}_{\mu\nu}(-\tau)\,, \tag{4.33c}$$

$$G^{\gtrless}_{pq}(t_0;t_0) = G^{M}_{pq}(0^{\pm})\,, \tag{4.33d}$$

$$G^{\rceil}_{pq}(t_0;\tau) = G^{M}_{pq}(-\tau)\,, \tag{4.33e}$$

which are required to be able to numerically solve the real-time Kadanoff-Baym equations. It is finally emphasized that the equations for the Matsubara components are closed on their own and can therefore be solved first such that the greater, lesser and right components can be obtained subsequently from these fixed initial conditions.

Appendix

4.A Martin-Schwinger Hierarchy

In what follows, the equations of motion for the mixed propagator of Eq. (4.3) are derived primarily due to the fact that they are needed in this work to derive Galitski-Migdal total energy functionals, see App. 4.B, and to prove Wick's theorems, see App. 4.C.1. It is characteristic to these equations that a contour-time derivative of the mixed propagator with j electron addition and removal and k phonon field operators depends on propagators with higher numbers of either electron or phonon operators which prevents the propagator to be determined by a finite number of equations of motion. It is the infinite hierarchy of coupled equations of motion obtained in this way which is usually referred to as the Martin-Schwinger hierarchy of equations of motion [MS59]. It is possible to derive this hierarchy by using the Heisenberg equations of motion for the electron and phonon operators [SL13]. In this work, the relevant Heisenberg equations of motion are given by

$$\begin{aligned}
\imath\frac{d}{dz}\hat{c}_{Hp}(z) &= \sum_{q} h_{pq}(z)\hat{c}_{Hq}(z) \\
&\quad + \sum_{q}\sum_{\mu} M^{\mu}_{pq}(z)\widehat{\phi}_{H\mu}(z)\hat{c}_{Hq}(z) \\
&\quad + \sum_{qst} w_{pqst}(z)\hat{c}^{\dagger}_{Hq}(z)\hat{c}_{Hs}(z)\hat{c}_{Ht}(z)\,, \\
-\imath\frac{d}{dz}\hat{c}^{\dagger}_{Hp}(z) &= \sum_{q} \hat{c}^{\dagger}_{Hq}(z)h_{qp}(z) \\
&\quad + \sum_{q}\sum_{\mu} \widehat{\phi}_{H\mu}(z)\hat{c}^{\dagger}_{Hq}(z)M^{\mu}_{qp}(z) \\
&\quad + \sum_{qst} \hat{c}^{\dagger}_{Ht}(z)\hat{c}^{\dagger}_{Hs}(z)\hat{c}_{Hq}(z)w_{tsqp}(z)\,, \\
\imath\frac{d}{dz}\widehat{\phi}_{H\mu}(z) &= \sum_{\nu\lambda} \alpha_{\mu\nu}\bar{\Omega}_{\nu\lambda}(z)\widehat{\phi}_{H\lambda}(z) \\
&\quad + \sum_{\nu} \alpha_{\mu\nu}F_{\nu}(z) \\
&\quad + \sum_{pq}\sum_{\mu} \alpha_{\mu\nu}M^{\nu}_{pq}(z)\hat{c}^{\dagger}_{Hp}(z)\hat{c}_{Hq}(z)\,,
\end{aligned}$$

where $\bar{\Omega}_{\mu\nu}(z) \equiv \Omega_{\mu\nu}(z)+\Omega_{\nu\mu}(z)$. It is further useful to write down explicitly the Heisenberg equation of motion

$$\begin{aligned}
\imath\frac{d}{dz}\Delta\widehat{\phi}_{H\mu}(z) &= \sum_{\nu\lambda} \alpha_{\mu\nu}\bar{\Omega}_{\nu\lambda}(z)\Delta\widehat{\phi}_{H\lambda}(z) \\
&\quad + \sum_{pq}\sum_{\nu} \alpha_{\mu\nu}M^{\nu}_{pq}(z)\big(\hat{c}^{\dagger}_{Hp}(z)\hat{c}_{Hq}(z) - \langle\hat{c}^{\dagger}_{Hp}(z)\hat{c}_{Hq}(z)\rangle\big)\,,
\end{aligned} \tag{4.34}$$

where $\Delta\widehat{\phi}_{H\mu}(z) \equiv \widehat{\phi}_{H\mu}(z) - \langle\widehat{\phi}_{H\mu}(z)\rangle$ is a fluctuation operator. It then follows by using these equations that the mixed propagator $X_{k,l}$ defined in Eq. (4.3) satisfies the equations of motion

$$
\begin{aligned}
&\imath\partial_{z_i} X_{k,l}(1_{z\mu},\ldots,k_{z\mu};1'_{zp},\ldots,l'_{zp};1''_{zp},\ldots,l''_{zp}) \\
&\quad= \sum_{\substack{j=1\\ j\neq i}}^{k} \alpha_{\mu_i\mu_j}\delta(z_i,z_j) X_{k-2,l}(1_{z\mu},\ldots,\overbrace{i_{z\mu}},\ldots,\overbrace{j_{z\mu}},\ldots,k_{z\mu};1'_{zp},\ldots,l'_{zp};1''_{zp},\ldots,l''_{zp}) \\
&\qquad+ \sum_{\mu\nu} \alpha_{\mu_i\mu}\bar{\Omega}_{\mu\nu}(z_i) X_{k,l}(1_{z\mu},\ldots,z_i\,\nu,\ldots,k_{z\mu};1'_{zp},\ldots,l'_{zp};1''_{zp},\ldots,l''_{zp}) \\
&\qquad+ \frac{1}{\imath^{1/2}} \sum_{\mu} \alpha_{\mu_i\mu} F_{\mu}(z_i) X_{k-1,l}(1_{z\mu},\ldots,\overbrace{i_{z\mu}},\ldots,k_{z\mu};1'_{zp},\ldots,l'_{zp};1''_{zp},\ldots,l''_{zp}) \\
&\qquad- \imath^{1/2} \sum_{pq}\sum_{\mu} \alpha_{\mu_i\mu} M^{\mu}_{pq}(z_i) X_{k-1,l+1}(1_{z\mu},\ldots,\overbrace{i_{z\mu}},\ldots,k_{z\mu};1'_{zp},\ldots,l'_{zp},z_i\,q;1''_{zp},\ldots,l''_{zp},z_i^{+}\,p)\,, \\
&\imath\partial_{z'_i} X_{k,l}(1_{z\mu},\ldots,k_{z\mu};1'_{zp},\ldots,l'_{zp};1''_{zp},\ldots,l''_{zp}) \\
&\quad= \sum_{j=1}^{l} (-1)^{i+j} \delta_{p'_i p''_j}\delta(z'_i,z''_j) X_{k,l-1}(1_{z\mu},\ldots,k_{z\mu};1'_{zp},\ldots,\overbrace{i'_{zp}},\ldots,l'_{zp};1''_{zp},\ldots,\overbrace{j''_{zp}},\ldots,l''_{zp}) \\
&\qquad+ \sum_{p} h_{p'_i p}(z'_i) X_{k,l}(1_{z\mu},\ldots,k_{z\mu};1'_{zp},\ldots,z'_i\,p,\ldots,l'_{zp};1''_{zp},\ldots,l''_{zp}) \\
&\qquad+ \imath^{1/2} \sum_{p}\sum_{\mu} M^{\mu}_{p'_i p}(z'_i) X_{k+1,l}(1_{z\mu},\ldots,k_{z\mu},z'_i\,\mu;1'_{zp},\ldots,z'_i\,p,\ldots,l'_{zp};1''_{zp},\ldots,l''_{zp}) \\
&\qquad- \imath \sum_{pqs} w_{p'_i pqs}(z'_i) X_{k,l+1}(1_{z\mu},\ldots,k_{z\mu};1'_{zp},\ldots,z'_i\,s,\ldots,l'_{zp},z'_i\,q;1''_{zp},\ldots,l''_{zp},z'^{+}_i\,p)\,, \\
&-\imath\partial_{z''_i} X_{k,l}(1_{z\mu},\ldots,k_{z\mu};1'_{zp},\ldots,l'_{zp};1''_{zp},\ldots,l''_{zp}) \\
&\quad= \sum_{j=1}^{l} (-1)^{i+j} \delta_{p''_i p'_j}\delta(z''_i,z'_j) X_{k,l-1}(1_{z\mu},\ldots,k_{z\mu};1'_{zp},\ldots,\overbrace{j'_{zp}},\ldots,l'_{zp};1''_{zp},\ldots,\overbrace{i''_{zp}},\ldots,l''_{zp}) \\
&\qquad+ \sum_{p} X_{k,l}(1_{z\mu},\ldots,k_{z\mu};1'_{zp},\ldots,l'_{zp};1''_{zp}.\ldots,z''_i\,p,\ldots,l''_{zp}) h_{pp''_i}(z''_i) \\
&\qquad+ \imath^{1/2} \sum_{p}\sum_{\mu} X_{k+1,l}(1_{z\mu},\ldots,k_{z\mu},z''_i\,\mu;1'_{zp},\ldots,l'_{zp};1''_{zp},\ldots,z''_i\,p,\ldots,l''_{zp}) M^{\mu}_{pp''_i}(z''_i) \\
&\qquad- \imath \sum_{pqs} X_{k,l+1}(1_{z\mu},\ldots,k_{z\mu};1'_{zp},\ldots,l'_{zp},z''_i\,p;1''_{zp},\ldots,z''^{+}_i\,s,\ldots,l''_{zp},z''^{+}_i\,q) w_{sqpp''_i}(z''_i)\,,
\end{aligned}
$$

the derivation of which requires, in addition to the Heisenberg equations of motion, that the contour-time derivative of the time-ordered string of operators is evaluated as shown in [SL13]. Here, by a bracket on top of an argument (index), it is meant that the argument (index) is missing. It is now useful to write down explicitly several relevant special cases of these equations of motion. For instance, by neglecting the electron-electron and electron-phonon interactions, one arrives at the equations of motion for the non-interacting phonon and electron propagators. The equations of motion for the non-interacting phonon propagators $d_{0,k}$ of Eq. (4.5) and d_k of Eq. (4.10) are given by

$$
\begin{aligned}
&\imath\partial_{z_i} d_{0;k}(1_{z\mu},\ldots,k_{z\mu}) \\
&\quad= \sum_{\substack{j=1\\ j\neq i}}^{k} \alpha_{\mu_i\mu_j}\delta(z_i,z_j) d_{0;k-2}(1_{z\mu},\ldots,\overbrace{i_{z\mu}},\ldots,\overbrace{j_{z\mu}},\ldots,k_{z\mu})
\end{aligned}
$$

$$
\begin{aligned}
&+ \sum_{\mu\nu} \alpha_{\mu_i\mu} \bar{\Omega}_{\mu\nu}(z_i) d_{0;k}(1_{z\mu}, \ldots, z_i\,\nu, \ldots, k_{z\mu}) \\
&+ \frac{1}{\imath^{1/2}} \sum_{\mu} \alpha_{\mu_i\mu} F_{\mu}(z_i) d_{0;k-1}(1_{z\mu}, \ldots, \overbrace{i_{z\mu}}, \ldots, k_{z\mu}) \,, \qquad (4.35)
\end{aligned}
$$

and

$$
\begin{aligned}
&\imath\partial_{z_i} d_k(1_{z\mu}, \ldots, k_{z\mu}) \\
&\quad = \sum_{\substack{j=1 \\ i\neq j}}^{k} \alpha_{\mu_i\mu_j} \delta(z_i, z_j) d_{k-2}(1_{z\mu}, \ldots, \overbrace{i_{z\mu}}, \ldots, \overbrace{j_{z\mu}}, \ldots, k_{z\mu}) \\
&\qquad + \sum_{\mu\nu} \alpha_{\mu_i\mu} \bar{\Omega}_{\mu\nu}(z_i) d_k(1_{z\mu}, \ldots, z_i\,\nu, \ldots, k_{z\mu}) \,, \qquad (4.36)
\end{aligned}
$$

respectively. Similarly, the non-interacting k-body electron propagator of Eq. (4.6) satisfies the equations of motion

$$
\begin{aligned}
&\imath\partial_{z_i} g_k(1_{zp}, \ldots, k_{zp}; 1'_{zp}, \ldots, k'_{zp}) \\
&\quad = \sum_{j=1}^{k} (-1)^{i+j} \delta_{p_i p'_j} \delta(z_i, z'_j) g_{k-1}(1_{zp}, \ldots, \overbrace{i_{zp}}, \ldots, k_{zp}; 1'_{zp}, \ldots, \overbrace{j'_{zp}}, \ldots, k'_{zp}) \\
&\qquad + \sum_{p} h_{p_i p}(z_i) g_k(1_{zp}, \ldots, z_i\,p, \ldots, k_{zp}; 1'_{zp}, \ldots, k'_{zp}) \,, \\
&-\imath\partial_{z'_i} g_k(1_{zp}, \ldots, k_{zp}; 1'_{zp}, \ldots, k'_{zp}) \\
&\quad = \sum_{j=1}^{k} (-1)^{i+j} \delta_{p'_i p_j} \delta(z'_i, z_j) g_{k-1}(1_{zp}, \ldots, \overbrace{j_{zp}}, \ldots, k_{zp}; 1'_{zp}, \ldots, \overbrace{i'_{zp}}, \ldots, k'_{zp}) \\
&\qquad + \sum_{p} g_k(1_{zp}, \ldots, k_{zp}; 1'_{zp} \ldots, z'_i\,p, \ldots, k'_{zp}) h_{pp'_i}(z'_i) \,.
\end{aligned}
$$

Moreover, it is convenient to write down explicitly the equations of motion for the interacting two-field phonon and one-body electron propagators. The phonon propagators $D_{0;2}$ and D satisfy respectively the equations of motion

$$
\begin{aligned}
\imath\partial_z D_{0;2;\mu\nu}(z, z') &= \alpha_{\mu\nu}\delta(z, z') \\
&\quad + \sum_{\lambda\gamma} \alpha_{\mu\lambda} \bar{\Omega}_{\lambda\gamma}(z) D_{0;2;\gamma\nu}(z, z') \\
&\quad + \frac{1}{\imath} \sum_{\lambda} \alpha_{\mu\lambda} F_{\lambda}(z) \phi_{\nu}(z') \\
&\quad + \frac{1}{\imath} \sum_{pq} \sum_{\lambda} \alpha_{\mu\lambda} M^{\lambda}_{pq}(z) \langle T\{\widehat{\phi}_{H\nu}(z') \hat{c}^{\dagger}_{Hp}(z^+) \hat{c}_{Hq}(z)\}\rangle \,, \qquad (4.38)
\end{aligned}
$$

and

$$
\begin{aligned}
\imath\partial_z D_{\mu\nu}(z, z') &= \alpha_{\mu\nu}\delta(z, z') \\
&\quad + \sum_{\lambda\gamma} \alpha_{\mu\lambda} \bar{\Omega}_{\lambda\gamma}(z) D_{\gamma\nu}(z, z') \\
&\quad + \frac{1}{\imath} \sum_{pq} \sum_{\lambda} \alpha_{\mu\lambda} M^{\lambda}_{pq}(z) \langle T\{\Delta\widehat{\phi}_{H\nu}(z') \hat{c}^{\dagger}_{Hp}(z^+) \hat{c}_{Hq}(z)\}\rangle \,, \qquad (4.39)
\end{aligned}
$$

as well as the adjoint equations which can be obtained by using the symmetry $D_{(0;2;)\mu\nu}(z,z') = D_{(0;2;)\nu\mu}(z',z)$. Here, the identity $\langle \Delta\widehat{\phi}_{H\nu}(z)\rangle = 0$ was used to obtain the equations for D. The interacting electron propagator G instead satisfies the equations of motion

$$\begin{aligned}
\imath\partial_z G_{pq}(z;z') &= \delta_{pq}\delta(z,z') \\
&\quad + \sum_{p'} h_{pp'}(z) G_{p'q}(z;z') \\
&\quad - \frac{1}{\imath}\sum_{p'}\sum_{\mu} M^{\mu}_{pp'}(z)\langle T\big\{\widehat{\phi}_{H\mu}(z)\hat{c}^{\dagger}_{Hq}(z')\hat{c}_{Hp'}(z)\big\}\rangle \\
&\quad - \frac{1}{\imath}\sum_{p'q's'} w_{pp'q's'}(z)\langle T\big\{\hat{c}^{\dagger}_{Hq}(z')\hat{c}^{\dagger}_{Hp'}(z^{+})\hat{c}_{Hq'}(z)\hat{c}_{Hs'}(z)\big\}\rangle\,, \qquad (4.40a) \\
-\imath\partial_{z'} G_{pq}(z;z') &= \delta_{pq}\delta(z,z') \\
&\quad + \sum_{p'} G_{pp'}(z;z') h_{p'q}(z') \\
&\quad - \frac{1}{\imath}\sum_{p'}\sum_{\mu}\langle T\big\{\widehat{\phi}_{H\mu}(z')\hat{c}^{\dagger}_{Hp'}(z')\hat{c}_{Hp}(z)\big\}\rangle M^{\mu}_{p'q}(z') \\
&\quad - \frac{1}{\imath}\sum_{p'q's'}\langle T\big\{\hat{c}^{\dagger}_{Hp'}(z'^{+})\hat{c}^{\dagger}_{Hq'}(z'^{+})\hat{c}_{Hs'}(z')\hat{c}_{Hp}(z)\big\}\rangle w_{p'q's'q}(z')\,, \qquad (4.40b)
\end{aligned}$$

which concludes the derivation of the relevant equations of motion.

4.B Galitski-Migdal Total Energy

Here, a derivation of a Galitski-Migdal total energy functional [GM58, SL13] for systems with both electron-phonon and electron-electron interactions is presented. It is shown that although the total energy is not a one-body observable, it can be obtained from the contour-time derivatives of the electron and phonon propagators by using the equations of motion derived in App. 4.A. It follows directly from the definitions of the electron and phonon energies, cf., Sec. 3.2, and from the definitions of the one-body electron and two-field phonon propagators that

$$\begin{aligned}
E_{\mathrm{e}}(z) - E_{\mathrm{ee}}(z) &= -\imath\sum_{pq} h_{pq}(z) G(z\,q; z^{+}\,p)\,, \\
E_{\mathrm{p}}(z) &= \imath\sum_{\mu\nu}\Omega_{\mu\nu}(z)\big(D(z\,\nu, z^{+}\,\mu) - \imath\phi(z\,\nu)\phi(z\,\mu)\big) + \sum_{\mu} F_{\mu}(z)\phi(z\,\mu)\,,
\end{aligned}$$

and from Eqs. (4.38) and (4.40) that

$$\begin{aligned}
E_{\mathrm{ep}}(z) + E_{\mathrm{ee}}(z) &= -\frac{\imath}{2}\sum_{pq}\big(\imath\delta_{pq}\partial_z - h_{pq}(z)\big) G(z\,q; z'\,p)\big|_{z'=z^{+}} \\
&\quad + \frac{\imath}{2}\sum_{\mu\nu}\big(\imath\alpha_{\mu\nu}\partial_z - \bar{\Omega}_{\mu\nu}(z)\big)\big(D(z\,\nu, z'\,\mu) - \imath\phi(z\,\nu)\phi(z'\,\mu)\big)_{z'=z^{+}} \\
&\quad - \frac{1}{2}\sum_{\mu} F_{\mu}(z)\phi(z\,\mu) \qquad (4.41a) \\
&= -\frac{\imath}{2}\sum_{pq}\big(-\imath\delta_{pq}\partial_{z'} - h_{pq}(z')\big) G(z\,q; z'\,p)\big|_{z'=z^{+}}
\end{aligned}$$

$$+\frac{\imath}{2}\sum_{\mu\nu}\big(-\imath\alpha_{\mu\nu}\partial_{z'}-\bar{\Omega}_{\mu\nu}(z')\big)\big(D(z\,\nu,z'\,\mu)-\imath\phi(z\,\nu)\phi(z'\,\mu)\big)_{z'=z^+}$$
$$-\frac{1}{2}\sum_{\mu}\phi(z\,\mu)F_\mu(z)\,, \tag{4.41b}$$

where the first and second expressions follow by using Eqs. (4.40a) and (4.40b), respectively. In this work, the total energy is defined to be the sum of the electron, phonon and electron-phonon interaction energies. It is then found by using Eq. (4.41a) that

$$\begin{aligned}E(z)=&-\frac{\imath}{2}\sum_{pq}\big(\imath\delta_{pq}\partial_z+h_{pq}(z)\big)G(z\,q;z'\,p)\big|_{z'=z^+}\\&+\frac{\imath}{2}\sum_{\mu\nu}\big(\imath\alpha_{\mu\nu}\partial_z+\Omega_{\mu\nu}(z)\big)\big(D(z\,\nu,z'\,\mu)-\imath\phi(z\,\nu)\phi(z'\,\mu)\big)_{z'=z^+}\\&+\frac{1}{2}\sum_{\mu}F_\mu(z)\phi(z\,\mu)\,.\end{aligned} \tag{4.42}$$

and by using Eqs. (4.41a) and (4.41b) that

$$\begin{aligned}E(z)=&-\frac{\imath}{4}\sum_{pq}\big(\imath\delta_{pq}(\partial_z-\partial_{z'})+h_{pq}(z)+h_{pq}(z')\big)G(z\,q;z'\,p)\big|_{z'=z^+}\\&+\frac{\imath}{4}\sum_{\mu\nu}\big(\imath\alpha_{\mu\nu}(\partial_z-\partial_{z'})+\Omega_{\mu\nu}(z)+\Omega_{\mu\nu}(z')\big)\big(D(z\,\nu,z'\,\mu)-\imath\phi(z\,\nu)\phi(z'\,\mu)\big)_{z'=z^+}\\&+\frac{1}{2}\sum_{\mu}F_\mu(z)\phi(z\,\mu)\,.\end{aligned} \tag{4.43}$$

where $\Omega_{\mu\nu}(z)\equiv\Omega_{\mu\nu}(z)-\Omega_{\nu\mu}(z)$. It is these equations which are here referred to as the Galitski-Migdal total energy functions or functionals. It is noteworthy that if there are no electron-electron interactions then another expression can be derived for the total energy by using only the equation of motion for the one-body electron propagator. It follows by assuming that no electron-electron interaction is present that the electron-phonon interaction energy can be written as

$$E_{\mathrm{ep}}(z)=-\imath\sum_{pq}\big(\imath\delta_{pq}\partial_z-h_{pq}(z)\big)G(z\,q;z'\,p)\big|_{z'=z^+}\,,$$

and hence the total energy becomes

$$\begin{aligned}E(z)=&\sum_{p}\partial_z G(z\,p;z'\,p)\big|_{z'=z^+}\\&+\imath\sum_{\mu\nu}\Omega_{\mu\nu}(z)\big(D(z\,\nu,z^+\,\mu)-\imath\phi(z\,\nu)\phi(z\,\mu)\big)+\sum_{\mu}F_\mu(z)\phi(z\,\nu)\,,\end{aligned}$$

which is referred to as the Galitski-Migdal total energy functional in **I** [SPAL15a].

4.C Justification of Diagrammatic Rules

4.C.1 Wick's Theorem (B and C)

In the following, Wick's theorem 4.3.3 is proven for the non-interacting phonon propagator d_0 of Eq. (4.5) by following the principles behind the corresponding proof [BF04, SL13] for the non-

interacting electron propagator g of Eq. (4.6). It follows from the relation

$$\begin{aligned} d_k(1,\ldots,k) &= d_{0;k}(1,\ldots,k)\big|_{F=0} \\ &= \mathrm{haf}(d_{1,\ldots,k})\,, \end{aligned}$$

that the proof of the Wick's theorem 4.3.2 is obtained as a special case of this proof. Here, the relation on the first line follows, e.g., by acknowledging that the equations of motion and boundary conditions are the same for the left- and right-hand sides. In the proof, the inverse of the non-interacting two-field phonon propagator d, which is defined by

$$d^{-1}(1_{z\mu},2_{z\mu}) \equiv \big(\imath\alpha_{\mu_1\mu_2}\partial_{z_1} - \bar{\Omega}_{\mu_1\mu_2}(z_1)\big)\delta(z_1,z_2)\,,$$

and, by defining $\delta(1_{z\mu},1'_{z\mu}) \equiv \delta_{\mu_1\mu'_1}\delta(z_1,z'_1)$, satisfies

$$\begin{aligned} \delta(1_{z\mu},1'_{z\mu}) &= \int d2_{z\mu}\, d^{-1}(1_{z\mu},2_{z\mu})d(2_{z\mu},1'_{z\mu}) \\ &= \int d2_{z\mu}\, d(1_{z\mu},2_{z\mu})d^{-1}(2_{z\mu},1'_{z\mu})\,, \end{aligned}$$

is used to arrive at a compact representation. That said, it is the strategy to prove that

$$d_{0;k}(1,\ldots,k) = \sum_{s\in P_K} \mathrm{haf}(d_{1,\ldots,k})_{K\setminus s}\mathrm{per}(d_{0;1,\ldots,k})_s$$

holds by showing that the right-hand side satisfies Eqs. (4.35) and meets the Kubo-Martin-Schwinger boundary conditions. Here, P_K denotes the set of all subsets of $K \equiv \{1,\ldots,k\}$ and a set of arguments $(s,\ K\setminus s)$ as a subscript of a matrix is to be understood as described above Thm. 4.3.3. In what follows, $d_{0;k}$ given above is regarded as a trial solution. It then holds for $i \in [1,k]\cap\mathbb{Z}$ that

$$\begin{aligned} d_{0;k}(1,\ldots,k) = &\sum_{\substack{s\in P_K \\ s\cap\{i\}\neq\emptyset}} \sum_{j\in s\setminus\{i\}} d(i,j)\mathrm{haf}(d_{1,\ldots,k})_{K\setminus(s\setminus\{i,j\})}\mathrm{per}(d_{0;1,\ldots,k})_s \\ &+ \sum_{\substack{s\in P_K \\ s\cap\{i\}=\emptyset}} \mathrm{haf}(d_{1,\ldots,k})_{K\setminus s} d_{0;1}(i)\mathrm{per}(d_{0;1,\ldots,k})_{s\cup\{i\}} \\ = &\sum_{\substack{j=1 \\ j\neq i}}^{k} d(i,j) \sum_{s\in P_{K\setminus\{i,j\}}} \mathrm{haf}(d_{1,\ldots,k})_{K\setminus s}\mathrm{per}(d_{0;1,\ldots,k})_{s\cup\{i,j\}} \\ &+ d_{0;1}(i) \sum_{s\in P_{K\setminus\{i\}}} \mathrm{haf}(d_{1,\ldots,k})_{K\setminus s}\mathrm{per}(d_{0;1,\ldots,k})_{s\cup\{i\}} \\ = &\sum_{\substack{j=1 \\ j\neq i}}^{k} d(i,j) d_{0;k-2}(1,\ldots,\overset{\sqcap}{i},\ldots,\overset{\sqcap}{j},\ldots k) + d_{0;1}(i) d_{0;k-1}(1,\ldots,\overset{\sqcap}{i},\ldots,k) \end{aligned}$$

where the extended recursive definition of the hafnian

$$\mathrm{haf}(d_{1\ldots k}) = \sum_{\substack{j=1 \\ j\neq i}}^{k} d(i,j)\mathrm{haf}(d_{1\ldots k})_{\{i,j\}}\,,$$

which is valid here for $k\in\mathbb{Z}_{\geq 1}$, has been used. Here, also the convention that a bracket on top of an argument (index) indicates that the argument (index) should be excluded. It is then possible to deduce, by using the above recursive form, that

$$\int di'\ d^{-1}(i,i')d_{0;k}(1,\ldots,i',\ldots,k)$$

$$
\begin{aligned}
&= \sum_{\substack{j=1\\ j\neq i}}^{k} \int di'\; d^{-1}(i,i')d(i',j)d_{0;k-2}(1,\ldots,\overset{\sqcap}{i},\ldots,\overset{\sqcap}{j},\ldots,k) \\
&\quad + \int di'\; d^{-1}(i,i')d_{0;1}(i')d_{0;k-1}(1,\ldots,\overset{\sqcap}{i},\ldots,k) \\
&= \sum_{\substack{j=1\\ j\neq i}}^{k} \delta(i,j)d_{0;k-2}(1,\ldots,\overset{\sqcap}{i},\ldots,\overset{\sqcap}{j},\ldots,k) + \frac{1}{\imath^{1/2}}F(i)d_{0;k-1}(1,\ldots,\overset{\sqcap}{i},\ldots,k)\,, \\
&d_{0;k}(1,\ldots,t_0-\imath\beta\,\mu_i,\ldots,k) \\
&= \sum_{\substack{j=1\\ j\neq i}}^{k} d(t_0-\imath\beta\,\mu_i,j)d_{0;k-2}(1,\ldots,\overset{\sqcap}{i},\ldots,\overset{\sqcap}{j},\ldots,k) \\
&\quad + d_{0;1}(t_0-\imath\beta\,\mu_i)d_{0;k-1}(1,\ldots,\overset{\sqcap}{i},\ldots,k) \\
&= \sum_{\substack{j=1\\ j\neq i}}^{k} d(t_{0-}\,\mu_i,j)d_{0;k-2}(1,\ldots,\overset{\sqcap}{i},\ldots,\overset{\sqcap}{j},\ldots,k) + d_{0;1}(t_{0-}\,\mu_i)d_{0,k-1}(1,\ldots,\overset{\sqcap}{i},\ldots,k) \\
&= d_{0;k}(1,\ldots,t_{0-}\,\mu_i,\ldots,k)\,,
\end{aligned}
$$

which shows that the trial solution is the solution since it satisfies the equations of motion of Eqs. (4.35) and meets the Kubo-Martin-Schwinger boundary conditions. It remains to conclude the diagrammatic statement of Thm. 4.3.3. If

$$
d_{0;1}(1) = \frac{1}{\imath^{1/2}}\int d1'\; d(1,1')F(1')
$$

is regarded as a trial solution then

$$
\begin{aligned}
\int d1'\; d^{-1}(1,1')d_{0;1}(1') =& \frac{1}{\imath^{1/2}}\int d1'd2\; d^{-1}(1,1')d(1',2)F(2) \\
=& \frac{1}{\imath^{1/2}}F(1)\,, \\
d_{0;1}(t_0-\imath\beta\,\mu_1) =& \frac{1}{\imath^{1/2}}\int d1'\; d(t_0-\imath\beta\,\mu_1,1')F(1') \\
=& \frac{1}{\imath^{1/2}}\int d1'\; d(t_{0-}\,\mu_1,1')F(1') \\
=& d_{0;1}(t_{0-}\,\mu_1,1')\,,
\end{aligned}
$$

shows that it is the solution since it satisfies Eq. (4.35) for $k=1$ and meets the Kubo-Martin-Schwinger boundary conditions. It then follows, by using $d_k(1,\ldots,k) = \mathrm{haf}(d_{1,\ldots,k})$, from the induction steps

i by definition $d_2(1,2) \equiv d(1,2)$ equals to the sum of all topologically inequivalent diagrams in which the vertices with the labels $\{1,2\}$ are pair-wise interconnected by d-lines

ii by induction assumption $d_{2(k-1)}(1,\ldots,2(k-1))$ equals to the sum of all topologically inequivalent diagrams in which the vertices with the labels $\{1,\ldots,2(k-1)\}$ are pair-wise interconnected by d-lines

iii by definition of the hafnian

$$d_{2k}(1,\ldots,2k) = \sum_{\substack{j=1\\ j\neq i}}^{2k} d(i,j) d_{2(k-1)}(1,\ldots,\overset{\sqcap}{i},\ldots,\overset{\sqcap}{j},\ldots,2k)$$

so that by assuming ii to hold for $d_{2(k-1)}(1,\ldots,\overset{\sqcap}{i},\ldots,\overset{\sqcap}{j},\ldots,2k)$, it is true that

- a any two diagrams in which the same labeled vertex i is connected to different labeled vertices j_1 and j_2, such that $j_1 \neq j_2 \neq i$, are topologically inequivalent
- b the summand equals to the sum of all topologically inequivalent diagrams in which the vertices with the labels $\{i,j\}$ are connected by d-lines and $\{1,\ldots,\overset{\sqcap}{i},\ldots,\overset{\sqcap}{j},\ldots,2k\}$ are pair-wise interconnected by d-lines

and hence it holds that $d_{2k}(1,\ldots,2k)$ is the sum of all topologically inequivalent diagrams in which the vertices with the labels $\{1,\ldots,2k\}$ are pair-wise interconnected by d-lines

that $\mathrm{haf}(d_{1,\ldots,k})$ satisfies the diagrammatic form of Thm. 4.3.2 and, moreover, it holds that

$$\mathrm{per}(d_{0;1,\ldots,k}) = d_{0;1}(1)\ldots d_{0;1}(k) \simeq$$

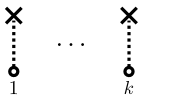

represents a topologically unique diagram in which the vertices with the labels $\{1,\ldots,k\}$ are connected to unlabeled F-vertices. Hence, if $s \in P_K$, such that $|s| \in 2\mathbb{Z}$, then $\mathrm{haf}(d_{1,\ldots,k})_{K\setminus s}\mathrm{per}(d_{0;1,\ldots,k})_s$ is equivalent to the sum of all topologically inequivalent diagrams in which the vertices with the labels s are pair-wise interconnected and vertices with labels K/s are connected to unlabeled F-vertices by d-lines . It then follows from the uniqueness of $\mathrm{per}(d_{0;1,\ldots,k})_s$, i.e., each $s \in P_K$ leads to topologically inequivalent diagrams, that by summing over all $s \in P_K$, as in

$$d_{0;k}(1,\ldots,k) = \sum_{s\in P_K} \mathrm{haf}(d_{1,\ldots,k})_{K\setminus s}\mathrm{per}(d_{0;1,\ldots,k})_s$$

one arrives at the diagrammatic rule of Thm. 4.3.3 which completes the proof.

4.C.2 Loop Rule

Here, the loop rule 4.3.1 is justified by straightforwardly extending the arguments used in [SL13] to justify a more conventional statement of this rule. In order to begin, it is noted that each term contributing to the perturbation expansion of Eq. (4.7) of the propagator $X_{i,j}$ comes with the sign $(-1)^k(-1)^C$ where k is the number of the M-vertices and C is the number of the crossings of the g-lines arising from the application of Wick's theorem 4.3.1 to the propagator g_{j+k+2l} where l is the number of the w-lines. Algebraically, any of the $(j+k+2l)!$ terms arising from the Leibniz expansion of the determinant

$$g_{j+k+2l}\begin{pmatrix} 1_{zp},\ldots,j_{zp},\underline{1}_{zq},\ldots,\underline{k}_{zq},\underline{1}'_{zq},\underline{1}''_{zq},\ldots,\underline{l}'_{zq},\underline{l}''_{zq}; \\ 1'_{zp},\ldots,j'_{zp},\underline{1}^{+}_{zp},\ldots,\underline{k}^{+}_{zp},\underline{1}'^{+}_{zp},\underline{1}''^{+}_{zp},\ldots,\underline{l}'^{+}_{zp},\underline{l}''^{+}_{zp} \end{pmatrix}$$

$$= \det\left(g_{1_{zp}\dots j_{zp}\underline{1}_{zq}\dots\underline{k}_{zq}\underline{1}'_{zq}\underline{1}''_{zq}\dots\underline{l}'_{zq}\underline{l}''_{zq};1'_{zp}\dots j'_{zp}\underline{1}^{+}_{zp}\dots\underline{k}^{+}_{zp}\underline{1}'^{+}_{zp}\underline{1}''^{+}_{zp}\dots\underline{l}'^{+}_{zp}\underline{l}''^{+}_{zp}}\right)$$

can be obtained by a finite sequence of transpositions of the last $j+k+2l$ arguments of g_{j+k+2l} starting from the identity term

$$g(1_{zp};1'_{zp})\dots g(j_{zp};j'_{zp})g(\underline{1}_{zq};\underline{1}^{+}_{zp})\dots g(\underline{k}_{zq};\underline{k}^{+}_{zp})g(\underline{1}'_{zq};\underline{1}'^{+}_{zp})\dots g(\underline{l}'_{zq};\underline{l}'^{+}_{zp})g(\underline{1}''_{zq};\underline{1}''^{+}_{zp})\dots g(\underline{l}''_{zq};\underline{l}''^{+}_{zp})$$

such that each subsequent transposition changes the prefactor of the previous term by a multiple of -1. Graphically, a transposition equals to an interchange of the origins of the corresponding g-lines [SL13] and the identity term corresponds to the identity diagram

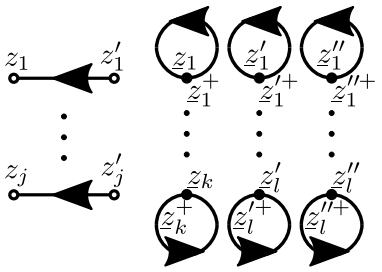

where, for brevity, only contour-time indices are shown. Moreover, any diagram obtained from this diagram by dressing it with F-vertices and d- and w-lines appears in Eq. (4.7) with the same prefactor $(-1)^k$. If the open g-lines are closed such that the vertex with the label z'_i is moved on top of the vertex with the label z_i for all $i \in [1,j] \cap \mathbb{Z}$ one arrives at the closed diagram

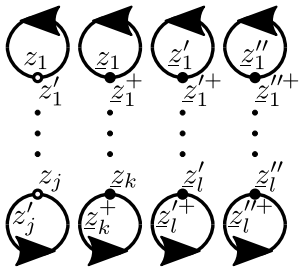

which has $L = j+k+2l$ loops formed by the g-lines, i.e., closed fermion loops, and hence the prefactor $(-1)^{L-j} = (-1)^k$ of the loop rule 4.3.1 is the correct prefactor for the identity diagram. It then follows from the observations that

i each interchange of the origins of two g-lines can be carried-out by closing the diagram, interchanging the origins of the g-lines and finally by reversing the closing of the diagram, e.g,

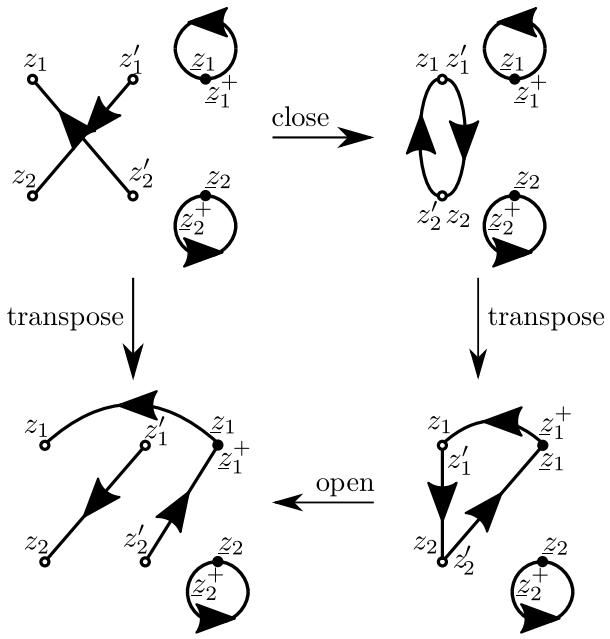

ii in a closed diagram, each interchange of the origins of two g-lines either increases, if the out-going vertices belong to the same loop, or decreases, if the out-going vertices belong to different loops, the number of closed fermion loops by one [SL13].

that the prefactor $(-1)^{L-j}$ of the loop rule 4.3.1, where L is the number of the closed fermion loops when for all $i \in [1,j] \cap \mathbb{Z}$ the vertex with the label z_i' is moved on top of the vertex with the label z_i, is the correct prefactor for any diagram.

4.C.3 Reduction to Connected Topologically Inequivalent Diagrams

In the following, it is justified why it is valid to sum over only connected and topologically inequivalent diagrams in Eq. (4.14). It follows from Wick's theorems 4.3.1 and 4.3.3 that the perturbation expansion of the propagator $X_{i,j}$ given in Eq. (4.7) can be written in the form

$$\frac{Z}{Z_0} X_{i,j} \simeq \sum_{k=0}^{\infty} \sum_{l=0}^{\infty} \frac{1}{k!l!2^l} \sum_{\substack{m=0 \\ i+k+m \in 2\mathbb{Z}}}^{i+k} \left\{ \begin{array}{l} \text{sum of all topologically inequivalent diagrams in which the} \\ i \text{ external labeled vertices, } m \text{ unlabeled F-vertices and } k \\ \text{labeled M-vertices are connected pair-wise by d-lines, and} \\ \text{the } j \text{ external labeled vertices for in- and out-going g-lines,} \\ \text{the M-vertices and } 2l \text{ labeled end-vertices of } l \text{ w-lines are} \\ \text{connected pair-wise by g-lines} \end{array} \right\}$$

where the d- and g-lines are only allowed to connect to the internal vertices as shown in Eqs. (4.11), (4.12) and (4.13) and a d-line is not allowed to connect F-vertices to each other. In order to convert the diagrams into algebraic expressions, the unlabeled vertices are to be given dummy labels and all labels, but the unspecified labels for the external vertices, are to be integrated over. It is possible to express each topologically inequivalent diagram appearing in the above sum as a product of a connected and a disconnected diagram. Moreover, it follows from the loop rule 4.3.1 that the sign of

such a diagram is equal to the product of the signs of its disjoint pieces. Hence, it is found that

$$\left\{\begin{array}{l}\text{sum of all topologically inequivalent diagrams in which the } i \text{ external labeled vertices, } m \text{ unla-}\\ \text{beled F-vertices and } k \text{ labeled M-vertices are connected pair-wise by d-lines, and the } j \text{ external}\\ \text{labeled vertices for in- and out-going g-lines, the M-vertices and } 2l \text{ labeled end-vertices of } l\\ \text{w-lines are connected pair-wise by g-lines}\end{array}\right\}$$

$$=\sum_{k'=0}^{k}\sum_{l'=0}^{l}\sum_{\substack{m'=\max(0,m-(k-k'))\\ i+k'+m'\in 2\mathbb{Z}}}^{\min(m,i+k')}\binom{k}{k'}\binom{l}{l'}\left\{\begin{array}{l}\text{sum of all connected topo-}\\ \text{logically inequivalent dia-}\\ \text{grams in which the } i \text{ ex-}\\ \text{ternal labeled vertices, } m'\\ \text{unlabeled F-vertices and}\\ k' \text{ labeled M-vertices are}\\ \text{connected pair-wise by d-}\\ \text{lines, and the } j \text{ external la-}\\ \text{beled vertices for in- and}\\ \text{out-going g-lines, the M-}\\ \text{vertices and } 2l' \text{ labeled end-}\\ \text{vertices of } l' \text{ w-lines are con-}\\ \text{nected pair-wise by g-lines}\end{array}\right\}\times\left\{\begin{array}{l}\text{sum of all topolog-}\\ \text{ically inequivalent}\\ \text{diagrams in which}\\ m-m' \text{ unlabeled}\\ \text{F-vertices and } k-k'\\ \text{labeled M-vertices}\\ \text{are connected pair-}\\ \text{wise by d-lines, and}\\ \text{the M-vertices and}\\ 2(l-l') \text{ labeled}\\ \text{end-vertices of } l-l'\\ \text{w-lines are connected}\\ \text{pair-wise by g-lines}\end{array}\right\}$$

where the binomial prefactors enumerate the possible ways to pick k' out of the k labeled M-vertices and l' out of the l labeled w-lines. Here, it was taken into account that it follows by relabeling all but the external vertices that when k' and l' are summed over, all choices of the k' labeled M-vertices and l' labeled w-lines to form the connected and, as a consequence, disconnected parts contribute equally. Moreover, it is noted that for some m' in the above sum there are no connected or disconnected diagrams which needs to be understood such that their sum is identically zero. It then follows by using this result and the reordering

$$\sum_{k=0}^{\infty}\sum_{k'=0}^{k}\sum_{l=0}^{\infty}\sum_{l'=0}^{l}\ldots=\sum_{k'=0}^{\infty}\sum_{k=k'}^{\infty}\sum_{l'=0}^{\infty}\sum_{l=l'}^{\infty}\ldots,$$

$$\sum_{\substack{m=0\\ i+k+m\in 2\mathbb{Z}}}^{i+k}\sum_{\substack{m'=\max(0,m-(k-k'))\\ i+k'+m'\in 2\mathbb{Z}}}^{\min(m,i+k')}\ldots=\sum_{\substack{m'=0\\ i+k'+m'\in 2\mathbb{Z}}}^{i+k'}\sum_{\substack{m=m'\\ i+k+m\in 2\mathbb{Z}}}^{m'+(k-k')}\ldots$$

of the summations followed by the sequence $k-k'\equiv\bar{k}$, $l-l'\equiv\bar{l}$ and $m-m'\equiv\bar{m}$ of relabelings of the summation indices that

$$X_{i,j}\simeq\sum_{k=0}^{\infty}\sum_{l=0}^{\infty}\sum_{\substack{m=0\\ i+k+m\in 2\mathbb{Z}}}^{i+k}\frac{1}{k!l!2^l}\left\{\begin{array}{l}\text{sum of all connected topologically inequivalent diagrams in}\\ \text{which the } i \text{ external labeled vertices, } m \text{ unlabeled F-vertices}\\ \text{and } k \text{ labeled M-vertices are connected pair-wise by d-lines,}\\ \text{and the } j \text{ external labeled vertices for in- and out-going g-}\\ \text{lines, the M-vertices and } 2l \text{ labeled end-vertices of } l \text{ w-lines}\\ \text{are connected pair-wise by g-lines}\end{array}\right\}$$

where it was also recognized that

$$\frac{Z}{Z_0}\simeq\sum_{\bar{k}=0}^{\infty}\sum_{\bar{l}=0}^{\infty}\sum_{\substack{\bar{m}=0\\ \bar{k}+\bar{m}\in 2\mathbb{Z}}}^{\bar{k}}\frac{1}{\bar{k}!\bar{l}!2^{\bar{l}}}\left\{\begin{array}{l}\text{sum of all topologically inequivalent diagrams in which } \bar{m}\\ \text{unlabeled F-vertices and } \bar{k} \text{ labeled M-vertices are connected}\\ \text{pair-wise by d-lines, and the M-vertices and } 2\bar{l} \text{ labeled end-}\\ \text{vertices of } \bar{l} \text{ w-lines are connected pair-wise by g-lines}\end{array}\right\}$$

and that if $i+k+m\in 2\mathbb{Z}$ and $i+(k+\bar{k})+(m+\bar{m})\in 2\mathbb{Z}$ then $\bar{k}+\bar{m}\in 2\mathbb{Z}$. It has been thus shown that it is valid to consider only connected diagrams and it remains to justify why the expansion

can be rewritten in terms of connected topologically inequivalent diagrams with unlabeled internal vertices only. Given a connected diagram with k labeled M-vertices and $2l$ labeled end-vertices of l w-lines, there are $k!$ permutations of the labels of the M-vertices and $l!2^l$ permutations of the labels of the end-vertices of the w-lines [SL13] which result into a different connected labeled diagrams but whose value is the same as the value of the original diagram. It is due to this observations that the sum of all connected topologically inequivalent diagram with labeled M-vertices and end-vertices of w-lines is equal to $k!l!2^l$ times the corresponding sum with unlabeled internal vertices. It then follows that

$$X_{i,j} \simeq \sum_{k=0}^{\infty}\sum_{l=0}^{\infty}\sum_{\substack{m=0\\ i+k+m\in 2\mathbb{Z}}}^{i+k} \left\{\begin{array}{l}\text{sum of all connected topologically inequivalent diagrams in}\\ \text{which the } i \text{ external labeled vertices, } m \text{ unlabeled F-vertices}\\ \text{and } k \text{ unlabeled M-vertices are connected pair-wise by d-}\\ \text{lines, and the } j \text{ external labeled vertices for in- and out-}\\ \text{going g-lines, the M-vertices and } 2l \text{ unlabeled end-vertices}\\ \text{of } l \text{ w-lines are connected pair-wise by g-lines}\end{array}\right\}$$

which concludes the justification why only connected topologically inequivalent diagrams can be used in Eq. (4.7).

4.D Continuity Equations and Ψ-derivability

In what follows, it is shown that, under some additional constraints, Ψ-derivable approximations satisfy the continuity equations for the electron one-body reduced density matrix and total energy as argued in Sec. 4.4. It is the strategy, by following [Bay62], to consider variations of the Ψ-functional which, by denoting $\Sigma_{\backslash\text{epMF}}(z\,p;z'\,q) \equiv \Sigma(z\,p;z'\,q) - \Sigma_{\text{epMF}}(z\,p;z'\,q)$ and $\Lambda(z\,\mu;z\,p;z^+\,q) \equiv \Lambda_0(z\,\mu;z\,p;z^+\,q) - \phi(z\,\mu)G(z\,p;z^+\,q)/\imath^{1/2}$, can be written as

$$\begin{aligned}\delta\Psi = &\sum_{pq}\int_C dzdz'\;\Sigma_{\backslash\text{epMF}}(z\,p;z'\,q)\delta G(z'\,q;z\,p)\\ &-\frac{1}{2}\sum_{\mu\nu}\int_C dzdz'\;\Pi(z\,\mu,z'\,\nu)\delta D(z'\,\nu,z\,\mu)\\ &+\imath^{1/2}\sum_{\mu}\sum_{pq}\int_C dz\;\Lambda(z\,\mu;z\,p,z^+\,q)\delta M^{\mu}_{qp}(z)\\ &-\frac{\imath}{2}\sum_{pqst}\int_C dz\;G_2(z\,p,z\,q;z^+\,t,z^+\,s)\delta w_{tsqp}(z)\,.\end{aligned} \tag{4.44}$$

where it was assumed that $\delta D(z\,\mu,z'\,\nu) = \delta D(z'\,\nu,z\,\mu)$ and $\delta w_{pqst}(z) = \delta w_{qpts}(z)$.

4.D.1 One-Body Reduced Density Matrix

It follows from Eqs. (4.40a) and (4.40b) that the exact electron one-body reduced density matrix $\gamma_{pq}(z) = -\imath G(z\,p;z^+\,q)$ satisfies the continuity equation

$$\begin{aligned}\frac{d}{dz}\gamma_{pq}(z) = &\sum_s\Big(G(z\,p;z^+\,s)h_{sq}(z) - h_{ps}(z)G(z\,s;z^+\,q)\Big)\\ &+\imath^{1/2}\sum_s\sum_{\mu}\Big(\Lambda_0(z\,\mu;z\,p;z^+\,s)M^{\mu}_{sq}(z) - M^{\mu}_{ps}(z)\Lambda_0(z\,\mu;z\,s;z^+\,q)\Big)\end{aligned}$$

$$-\frac{1}{\imath}\sum_{stu}\Big(G_2(z\,p,z\,s;z^+\,t,z^+\,u)w_{utsq}(z)-w_{pstu}(z)G_2(z\,u,z\,t;z^+\,s,z^+\,q)\Big) \tag{4.45}$$

or any of its variations obtained by using the exact symmetries of the objects on the right-hand side. It is now shown that the corresponding continuity equation obtained by using Eqs. (4.31d) and (4.31e), i.e.,

$$\begin{aligned}\frac{d}{dz}\gamma_{pq}(z)=&\sum_s\big(G(z\,p;z^+\,s)h_{sq}(z)-h_{ps}(z)G(z\,s;z^+\,q)\big)\\&+\sum_s\sum_\mu\big(G(z\,p;z^+\,s)\phi(z\,\mu)M^\mu_{sq}(z)-M^\mu_{ps}(z)\phi(z\,\mu)G(z\,s;z^+\,q)\big)\\&+\sum_s\int_C dz'\,\big(G(z\,p;z'\,s)\Sigma_{\backslash\mathrm{epMF}}(z'\,s;z^+\,q)-\Sigma_{\backslash\mathrm{epMF}}(z\,p;z'\,s)G(z'\,s;z^+\,q)\big)\,,\end{aligned} \tag{4.46}$$

reduces to the continuity equation of Eq. (4.45) for a Ψ-derivable approximation. In order to do this, by following [Bay62], the gauge transformation

$$\begin{aligned}G_\Theta(z\,p;z'\,q)&\equiv\sum_{p'q'}\big[e^{\imath\Theta(z)}\big]_{pp'}G(z\,p';z'\,q')\big[e^{-\imath\Theta(z')}\big]_{q'q}\,,\\M^\mu_{\Theta;pq}(z)&\equiv\sum_{p'q'}\big[e^{\imath\Theta(z)}\big]_{pp'}M^\mu_{p'q'}(z)\big[e^{-\imath\Theta(z)}\big]_{q'q}\,,\\w_{\Theta;pqst}(z)&\equiv\sum_{p'q's't'}\big[e^{\imath\Theta(z)}\big]_{pp'}\big[e^{\imath\Theta(z)}\big]_{qq'}w_{p'q's't'}(z)\big[e^{-\imath\Theta(z)}\big]_{s's}\big[e^{-\imath\Theta(z)}\big]_{t't}\,,\end{aligned}$$

where the gauge functions $\Theta_{pq}(z)$ satisfy the contour-time boundary conditions $\Theta_{pq}(t_0-\imath\beta)=\Theta_{pq}(t_{0-})$, is introduced. It follows from the facts that each M- or end-vertex of w-line accepts an in- and out-going g-line and that internal variables are integrated over that any well-defined Ψ-functional, cf., Sec 4.4 is invariant under this gauge transformation. Hence, by recognizing that

$$\begin{aligned}\delta G(z\,p,z'\,q)&=\imath\sum_s\big(\Theta_{ps}(z)G(z\,s;z'\,q)-G(z\,p;z'\,s)\Theta_{sq}(z')\big)\,,\\\delta M^\mu_{pq}(z)&=\imath\sum_s\big(\Theta_{ps}(z)M^\mu_{sq}(z)-M^\mu_{ps}(z)\Theta_{sq}(z)\big)\,,\\\delta w_{pqst}(z)&=\imath\sum_u\big(\Theta_{pu}(z)w_{uqst}(z)+\Theta_{qu}(z)w_{pust}(z)-w_{pqut}(z)\Theta_{us}(z)-w_{pqsu}(z)\Theta_{ut}(z)\big)\,,\end{aligned}$$

it follows from the equation $0=\delta\Psi$ by a relabeling of the summation indices that

$$\begin{aligned}0=\sum_{pu}\int_C dz\,\Bigg(&\imath\sum_q\int_C dz'\,\big(G(z\,p;z'\,q)\Sigma_{\backslash\mathrm{epMF}}(z'\,q;z\,u)-\Sigma_{\backslash\mathrm{epMF}}(z\,p;z'\,q)G(z'\,q;z\,u)\big)\\&+\imath^{3/2}\sum_\mu\sum_q\big(M^\mu_{pq}(z)\Lambda(z\,\mu;z\,q;z^+\,u)-\Lambda(z\,\mu;z\,p;z^+\,q)M^\mu_{qu}(z)\big)\\&+\sum_{qst}\big(w_{psqt}(z)G_2(z\,q,z\,t;z^+\,s,z^+\,u)-G_2(z\,p,z\,q;z^+\,s,z^+\,t)w_{stqu}(z)\big)\Bigg)\Theta_{up}(z)\,.\end{aligned}$$

where also the symmetries $w_{pqst}(z)=w_{qpts}(z)$ and $G_2(z\,p,z\,q;z^+\,s,z^+\,t)=G_2(z\,q,z\,p;z^+\,t,z^+\,s)$ were used. It then must be, since $\Theta_{pq}(z)$ is arbitrary, that the content of the parenthesis vanishes identically which, when substituted back to Eq. (4.46), leads to the equation

$$\frac{d}{dz}\gamma_{pq}(z)=\sum_s\big(G(z\,p;z^+\,s)h_{sq}(z)-h_{ps}(z)G(z\,s;z^+\,q)\big)$$

$$
\begin{aligned}
&+ \imath^{1/2} \sum_{\mu} \sum_{s} \Big(\big(\Lambda(z\,\mu; z\,p; z^+\,s) + \imath^{-1/2} G(z\,p; z^+\,s) \phi(\mu\,z) \big) M^{\mu}_{sq}(z) \\
&- M^{\mu}_{ps}(z) \big(\Lambda(z\,\mu; z\,s; z^+\,q) + \imath^{-1/2} G(z\,s; z^+ q) \phi(z\,\mu) \big) \Big) \\
&+ \frac{1}{\imath} \sum_{stu} \big(G_2(z\,p, z\,u; z^+\,s, z^+\,t) w_{stuq}(z) - w_{psut}(z) G_2(z\,u, z\,t; z^+\,s, z^+\,q) \big) \,.
\end{aligned}
$$

showing that Eq. (4.45) is obtained. It is noted that here it was assumed that $G_2(z\,p, z\,q; z^+\,s, z^+\,t) = -G_2(z\,q, z\,p; z^+\,s, z^+\,t) = -G_2(z\,p, z\,q; z^+\,t, z^+\,s)$ without which, in general, an unambiguous relation between the two continuity equations is not achieved. However, as readily checked, it follows only from the symmetry $G_2(z\,p, z\,q; z^+\,s, z^+\,t) = G_2(z\,q, z\,p; z^+\,t, z^+\,s)$, which is obeyed by construction, that $\sum_p d\gamma_{pp}(z)/dz = dN(z)/dz = 0$ showing that the particle number is conserved.

4.D.2 Total Energy

In this work, the total energy is defined as the ensemble average of the Hamiltonian operator and hence, as follows from the Heisenberg equations of motion, it satisfies the continuity equation

$$
\begin{aligned}
\frac{d}{dz} E(z) = &- \imath \sum_{pq} \dot{h}_{pq}(z) G(z\,q; z^+\,p) \\
&+ \imath \sum_{\mu\nu} \dot{\Omega}_{\mu\nu}(z) \big(D(z\,\nu, z^+\,\mu) - \imath \phi(z\,\nu) \phi(z\,\mu) \big) \\
&+ \sum_{\mu} \dot{F}_{\mu}(z) \phi(z\,\mu) \\
&- \imath^{3/2} \sum_{\mu} \sum_{pq} \dot{M}^{\mu}_{pq}(z) \Lambda_0(z\,\mu; z\,q; z^+\,p) \\
&+ \frac{1}{2} \sum_{pqst} \dot{w}_{pqst}(z) G_2(z\,t, z\,s; z^+\,q, z^+\,p) \,,
\end{aligned}
\tag{4.47}
$$

where the overhead dot denotes a contour-time derivative. It is shown below that in a Ψ-derivable approximation, the total energy obtained by using Eq. (4.43) satisfies this continuity equation. Firstly, it follows by differentiation of Eq. (4.43) that

$$
\begin{aligned}
\frac{d}{dz} E(z) = &- \frac{\imath}{2} \sum_{pq} \dot{h}_{pq}(z) G(z\,q; z^+\,p) \\
&+ \frac{\imath}{2} \sum_{\mu\nu} \dot{\Omega}_{\mu\nu}(z) \big(D(z\,\nu, z^+\,\mu) - \imath \phi(z\,\nu) \phi(z\,\mu) \big) \\
&+ \frac{1}{2} \sum_{\mu} \dot{F}_{\mu}(z) \phi(z\,\mu) \\
&- \frac{\imath}{4} \sum_{pq} \big(\imath \delta_{pq} (\partial_z - \partial_{z'}) + h_{pq}(z) + h_{pq}(z') \big) \big(\partial_z + \partial_{z'} \big) G(z\,q; z'\,p) \big|_{z'=z^+} \\
&+ \frac{\imath}{4} \sum_{\mu\nu} \imath \alpha_{\mu\nu} (\partial_z - \partial_{z'}) (\partial_z + \partial_{z'}) \big(D(z\,\nu, z'\,\mu) - \imath \phi(z\,\nu) \phi(z'\,\mu) \big) \big|_{z'=z^+} \\
&+ \frac{1}{2} \sum_{\mu} F_{\mu}(z) \dot{\phi}(z\,\mu) \,, \,,
\end{aligned}
$$

where it was assumed that $dD(z\,\mu, z^+\,\nu)/dz = dD(z\,\nu, z^+\,\mu)/dz$ which is true if the identities $D(z\,\mu, z'\,\nu) = D(z'\,\nu, z\,\mu)$ and $D(z^+\,\mu, z\,\nu) - D(z\,\mu, z^+\,\nu) = -\imath\alpha_{\mu\nu}$ are satisfied. It then follows by using Eqs. (4.31d) and (4.31e) that

$$\begin{aligned}
&-\imath\sum_s \int_C d\bar{z}\,\big(\partial_z G(z\,p;\bar{z}\,s)\Sigma(\bar{z}\,s;z'\,q) + \Sigma(z\,p;\bar{z}\,s)\partial_{z'}G(\bar{z}\,s;z'\,q)\big)\\
&\quad = \sum_{st}\int_C d\bar{z}\,\big(\Sigma(z\,p;\bar{z}\,s)G(\bar{z}\,s;z'\,t)h_{tq}(z') - h_{ps}(z)G(z\,s;\bar{z}\,t)\Sigma(\bar{z}\,t;z'\,q)\big)\,.
\end{aligned}$$

and subsequently by using the relations

$$\begin{aligned}
&(\partial_z - \partial_{z'})\big(\Sigma(z\,p;\bar{z}\,q)G(\bar{z}\,q;z'\,p) - G(z\,p;\bar{z}\,q)\Sigma(\bar{z}\,q;z'\,p)\big)\Big|_{z'=z^+}\\
&\qquad = \frac{d}{dz}\big(\Sigma(z\,p;\bar{z}\,q)G(\bar{z}\,q;z^+\,p) + G(z\,p;\bar{z}\,q)\Sigma(\bar{z}\,q;z^+\,p)\big)\\
&\qquad\quad - 2\big(\Sigma(z\,p;\bar{z}\,q)\partial_z G(\bar{z}\,q;z^+\,p) + \partial_z G(z\,p;\bar{z}\,q)\Sigma(\bar{z}\,q;z^+\,p)\big)\,,\\
&(\partial_z - \partial_{z'})\big(\Pi(z\,\mu;\bar{z}\,\nu)D(\bar{z}\,\nu;z'\,\mu) - D(z\,\mu;\bar{z}\,\nu)\Pi(\bar{z}\,\nu;z'\,\mu)\big)\Big|_{z'=z^+}\\
&\qquad = \frac{d}{dz}\big(\Pi(z\,\mu;\bar{z}\,\nu)D(\bar{z}\,\nu;z^+\,\mu) + D(z\,\mu;\bar{z}\,\nu)\Pi(\bar{z}\,\nu;z^+\,\mu)\big)\\
&\qquad\quad - 2\big(\Pi(z\,\mu;\bar{z}\,\nu)\partial_z D(\bar{z}\,\nu;z^+\,\mu) + \partial_z D(z\,\mu;\bar{z}\,\nu)\Pi(\bar{z}\,\nu;z^+\,\mu)\big)\,,
\end{aligned}$$

and additionally Eqs. (4.31a), (4.31b) and (4.31c) that

$$\begin{aligned}
\frac{d}{dz}E(z) = &-\imath\sum_{pq}\dot{h}_{pq}(z)G(z\,q;z^+\,p)\\
&+\imath\sum_{\mu\nu}\dot{\Omega}_{\mu\nu}(z)\big(D(z\,\nu,z^+\,\mu) - \imath\phi(z\,\nu)\phi(z\,\mu)\big)\\
&+\sum_{\mu}\dot{F}_{\mu}(z)\phi(z\,\mu)\\
&-\frac{\imath}{2}\sum_{\mu}\sum_{pq}\dot{M}^{\mu}_{pq}(z)\phi(z\,\mu)G(z\,q;z^+\,p)\\
&-\frac{\imath}{4}\sum_{pq}\int_C d\bar{z}\,\frac{d}{dz}\big(\Sigma(z\,p;\bar{z}\,q)G(\bar{z}\,q;z^+\,p) + G(z\,p;\bar{z}\,q)\Sigma(\bar{z}\,q;z^+\,p)\big)\\
&+\imath\sum_{pq}\int_C d\bar{z}\,\big(\Sigma(z\,p;\bar{z}\,q)\partial_z G(\bar{z}\,q;z^+\,p) + \partial_z G(z\,p;\bar{z}\,q)\Sigma(\bar{z}\,q;z^+\,p)\big)\\
&+\frac{\imath}{4}\sum_{\mu\nu}\int_C d\bar{z}\,\frac{d}{dz}\big(\Pi(z\,\mu;\bar{z}\,\nu)D(\bar{z}\,\nu;z^+\,\mu) + D(z\,\mu;\bar{z}\,\nu)\Pi(\bar{z}\,\nu;z^+\,\mu)\big)\\
&-\frac{\imath}{2}\sum_{\mu\nu}\int_C d\bar{z}\,\big(\Pi(z\,\mu;\bar{z}\,\nu)\partial_z D(\bar{z}\,\nu;z^+\,\mu) + \partial_z D(z\,\mu;\bar{z}\,\nu)\Pi(\bar{z}\,\nu;z^+\,\mu)\big)\\
&+\frac{\imath}{2}\sum_{\mu}\sum_{pq}M^{\mu}_{pq}(z)\dot{\phi}(z\,\mu)G(z\,q;z^+\,p)\\
&-\frac{\imath}{2}\sum_{\mu}\sum_{pq}M^{\mu}_{pq}(z)\phi(z\,\mu)\dot{G}(z\,q;z^+\,p)\,.
\end{aligned}$$

In order to use Ψ-derivability, the mean-field self-energy corresponding to the electron-phonon interaction is treated explicitly by taking advantage of the result

$$-\frac{\imath}{4}\sum_{pq}\int_C d\bar{z}\,\frac{d}{dz}\big(\Sigma_{\mathrm{epMF}}(z\,p;\bar{z}\,q)G(\bar{z}\,q;z^+\,p) + G(z\,p;\bar{z}\,q)\Sigma_{\mathrm{epMF}}(\bar{z}\,q;z^+\,p)\big)$$

$$
\begin{aligned}
&+\imath\sum_{pq}\int_C d\bar{z}\,\big(\partial_z G(z\,p;\bar{z}\,q)\Sigma_{\mathrm{epMF}}(\bar{z}\,q;z^+\,p)+\Sigma_{\mathrm{epMF}}(z\,p;\bar{z}\,q)\partial_z G(\bar{z}\,q;z^+\,p)\big)\\
=&-\frac{\imath}{2}\sum_{\mu}\sum_{pq}\dot{M}^{\mu}_{pq}(z)\phi(z\,\mu)G(z\,q;z^+\,p)\\
&-\frac{\imath}{2}\sum_{\mu}\sum_{pq}M^{\mu}_{pq}(z)\dot{\phi}(z\,\mu)G(z\,q;z^+\,p)\\
&+\frac{\imath}{2}\sum_{\mu}\sum_{pq}M^{\mu}_{pq}(z)\phi(z\,\mu)\dot{G}(z\,q;z^+\,p)\,.
\end{aligned}
$$

which allows one to arrive at the equation

$$
\begin{aligned}
\frac{d}{dz}E(z)=&-\imath\sum_{pq}\dot{h}_{pq}(z)G(z\,q;z^+\,p)\\
&+\imath\sum_{\mu\nu}\dot{\Omega}_{\mu\nu}(z)\big(D(z\,\nu,z^+\,\mu)-\imath\phi(z\,\nu)\phi(z\,\mu)\big)\\
&+\sum_{\mu}\dot{F}_{\mu}(z)\phi(z\,\mu)\\
&-\imath\sum_{\mu}\sum_{pq}\dot{M}^{\mu}_{pq}(z)\phi(z\,\mu)G(z\,q;z^+\,p)\\
&-\frac{\imath}{4}\sum_{pq}\int_C d\bar{z}\,\frac{d}{dz}\big(\Sigma_{\backslash\mathrm{epMF}}(z\,p;\bar{z}\,q)G(\bar{z}\,q;z^+\,p)+G(z\,p;\bar{z}\,q)\Sigma_{\backslash\mathrm{epMF}}(\bar{z}\,q;z^+\,p)\big)\\
&+\imath\sum_{pq}\int_C d\bar{z}\,\big(\Sigma_{\backslash\mathrm{epMF}}(z\,p;\bar{z}\,q)\partial_z G(\bar{z}\,q;z^+\,p)+\partial_z G(z\,p;\bar{z}\,q)\Sigma_{\backslash\mathrm{epMF}}(\bar{z}\,q;z^+\,p)\big)\\
&+\frac{\imath}{4}\sum_{\mu\nu}\int_C d\bar{z}\,\frac{d}{dz}\big(\Pi(z\,\mu;\bar{z}\,\nu)D(\bar{z}\,\nu;z^+\,\mu)+D(z\,\mu;\bar{z}\,\nu)\Pi(\bar{z}\,\nu;z^+\,\mu)\big)\\
&-\frac{\imath}{2}\sum_{\mu\nu}\int_C d\bar{z}\,\big(\Pi(z\,\mu;\bar{z}\,\nu)\partial_z D(\bar{z}\,\nu;z^+\,\mu)+\partial_z D(z\,\mu;\bar{z}\,\nu)\Pi(\bar{z}\,\nu;z^+\,\mu)\big)\,,
\end{aligned}
\tag{4.48}
$$

which is now shown to reduce to the continuity equation for the total energy, i.e., to Eq. (4.47). In order to do this, by following [Bay62], it is appropriate to consider the transformation

$$
\begin{aligned}
G_{\Theta}(z\,p;z'\,q)&\equiv\left(\frac{d\Theta(z)}{dz}\right)^{\frac{1}{4}}G(\Theta(z)\,p;\Theta(z')\,q)\left(\frac{d\Theta(z')}{dz'}\right)^{\frac{1}{4}},\\
D_{\Theta}(z\,\mu,z'\,\nu)&\equiv\left(\frac{d\Theta(z)}{dz}\right)^{\frac{1}{2}}D(\Theta(z)\,\mu,\Theta(z')\,\nu)\left(\frac{d\Theta(z')}{dz'}\right)^{\frac{1}{2}},\\
M^{\mu}_{\Theta;pq}(z)&\equiv M^{\mu}_{pq}(\Theta(z))\,,\\
w_{\Theta;pqst}(z)&\equiv w_{pqst}(\Theta(z))\,.
\end{aligned}
$$

where $\Theta(z)$ is a contour-time function satisfying $\Theta(t_0-\imath\beta)=t_0-\imath\beta$ and $\Theta(t_{0-})=t_{0-}$ such that $d\Theta(z)/dz\neq 0$. The Ψ-functional is invariant under this transformation since the factor $d\Theta(z)/dz$, which is found at each internal vertex either because of four G-lines connecting to a w-line or due to two G-lines and a D-line being attached at a M-vertex, cancels in the change of the integration variable $z\to\Theta(z)$. As before, by substituting the first variations

$$
\begin{aligned}
\delta M^{\mu}_{pq}(z)&=\Theta(z)\dot{M}^{\mu}_{pq}(z)\,,\\
\delta w_{pqst}(z)&=\Theta(z)\dot{w}_{pqst}(z)\,,
\end{aligned}
$$

$$\delta G(z\,p;z'\,q) = \Big(\frac{1}{4}\dot{\Theta}(z) + \frac{1}{4}\dot{\Theta}(z') + \Theta(z)\partial_z + \Theta(z')\partial_{z'}\Big)G(z\,p;z'\,q)\,,$$
$$\delta D(z\,\mu,z'\,\nu) = \Big(\frac{1}{2}\dot{\Theta}(z) + \frac{1}{2}\dot{\Theta}(z') + \Theta(z)\partial_z + \Theta(z')\partial_{z'}\Big)D(z\,\mu,z'\,\nu)\,,$$

into the equation $0 = \delta\Psi$, it follows, by a relabeling of the summation indices and by using partial integration, that

$$\begin{aligned}
0 = \int_C dz\,\Bigg(&-\frac{1}{4}\sum_{pq}\int_C dz'\,\frac{d}{dz}\big(G(z\,p;z'\,q)\Sigma_{\backslash\mathrm{epMF}}(z'\,q;z\,p) + \Sigma_{\backslash\mathrm{epMF}}(z\,p;z'\,q)G(z'\,q;z\,p)\big)\\
&+\sum_{pq}\int_C dz'\,\big(\partial_z G(z\,p;z'\,q)\Sigma_{\backslash\mathrm{epMF}}(z'\,q;z\,p) + \Sigma_{\backslash\mathrm{epMF}}(z\,p;z'\,q)\partial_z G(z'\,q;z\,p)\big)\\
&+\frac{1}{4}\sum_{\mu\nu}\int_C dz'\,\frac{d}{dz}\big(D(z\,\mu,z'\,\nu)\Pi(z'\,\nu,z\,\mu) + \Pi(z\,\mu,z'\,\nu)D(z'\,\nu,z\,\mu)\big)\\
&-\frac{1}{2}\sum_{\mu\nu}\int_C dz'\,\big(\partial_z D(z\,\mu,z'\,\nu)\Pi(z'\,\nu,z\,\mu) + \Pi(z\,\mu,z'\,\nu)\partial_z D(z'\,\nu,z\,\mu)\big)\\
&+\imath^{1/2}\sum_{\mu}\sum_{pq}\Lambda(z\,\mu;z\,p;z^+\,q)\dot{M}^{\mu}_{qp}(z) - \frac{\imath}{2}\sum_{pqst}G_2(z\,p,z\,q;z^+\,s,z^+\,t)\dot{w}_{stqp}(z)\Bigg)\Theta(z)\,.
\end{aligned}$$

Here, it has been taken advantage of the fact that the boundary terms which arise from the partial integrations vanish since the electron and phonon propagators and self-energies satisfy the Kubo-Martin-Schwinger boundary conditions. It then must be, since $\Theta(z)$ is arbitrary, that the integrand of the outer integral vanishes identically and hence, by a substitution to Eq. (4.48), it is found that

$$\begin{aligned}
\frac{d}{dz}E(z) = &-\imath\sum_{pq}\dot{h}_{pq}(z)G(z\,q;z^+\,p)\\
&+\imath\sum_{\mu\nu}\dot{\Omega}_{\mu\nu}(z)\big(D(z\,\nu,z^+\,\mu) - \imath\phi(z\,\nu)\phi(z\,\mu)\big)\\
&+\sum_{\mu}\dot{F}_{\mu}(z)\phi(z\,\mu)\\
&-\imath^{3/2}\sum_{pq}\sum_{\mu}\dot{M}^{\mu}_{pq}(z)\big(\Lambda(z\,\mu;z\,q;z^+\,p) + \imath^{-1/2}\phi(z\,\mu)G(z\,q;z^+\,p)\big)\\
&+\frac{1}{2}\sum_{pqst}\dot{w}_{pqst}(z)G_2(z\,t,z\,s;z^+\,q,z^+\,p)\,,
\end{aligned}$$

which shows that Eq. (4.47) is recovered. Here, it was also assumed that $G_2(z\,p,z\,q;z^+\,s,z^+\,t) = -G_2(z\,q,z\,p;z^+\,s,z^+\,t) = -G_2(z\,p,z\,q;z^+\,t,z^+\,s)$ without which, in general, an unambiguous continuity equation is not obtained.

Part II

Numerical Methods

5 Solving Kadanoff-Baym Equations

Solving the Kadanoff-Baym equations is a task which in all, but perhaps in the simplest, cases has to be delegated to a computer for which, due to the rarity of equations with a similar two-time integro-differential structure, no commercial software is presently available to do the task, and hence, a dedicated software has to be self programmed. It is the latter, amongst other reasons, which has influenced how wide-spread the method has become and spurred several, not all perfectly independent, documented computer implementations [KKY99, Bal07, SDL09b, FVA10b, SBP16]. In Pubs. **I-III**, the results concerning the studied many-body approximations have been obtained by solving the Kadanoff-Baym equations, or just the Dyson equations, with a computer program which is based on the one developed by several post-graduate and -doctoral, in particular Dr. N. E. Dahlen, students of Prof. R. van Leeuwen [DL05, SDL09a, SDL09b]. It however has to be said that the author has revised the original program by implementing alternative numerical integration schemes, a hybrid openMP/MPI parallelization and by including the possibility to study, by implementing the numerical integration of the phonon field and propagator and the self-energies of Sec. 4.4.1, systems with electron-phonon interactions. In the course of this, most of the original program code has been rewritten in the C++ programming language with some more minor features added and some removed which is why an overview of the main features of the implementation is documented in this chapter. In what follows, the implementation is reviewed by first describing how the problem is posed to a computer and then proceeding to document how the equilibrium, boundary-value problem associated with the imaginary-time propagators is solved and finally how the real- or mixed-time propagators are obtained by numerical integration of an initial-value problem.

5.1 Discrete Representation

In what follows, it is described, in general terms, how the fields, propagators and self-energies which appear in the Kadanoff-Baym equations are described on a computer and moreover, it is specified how the equations themselves are represented. In order to address the first part, it is noted that, in a reasonable computer implementation, the one- and two-time Keldysh functions are described spatially as finite-dimensional vectors or matrices. In particular, here, the phonon field is referred to by the column vector $\phi(z)$, such that $\big[\phi(z)\big]_\mu = \phi_\mu(z)$, and the phonon and electron propagators are referred to by the square matrices $D(z,z')$ and $G(z;z')$, such that $[D(z,z')]_{\mu\nu} = D_{\mu\nu}(z,z')$ and $[G(z;z')]_{pq} = G_{pq}(z;z')$ respectively, for which all operations familiar from linear algebra are readily at ones disposal. Moreover, in the following, the-non-interacting field and propagators and the phonon and electron self-energies are referred to by an analogous notation. Instead of then solving the integro-differential equations of Eqs. (5.6) directly, they are first preprocessed into another, at least in some cases, numerically preferable form. It is, for one, found useful to isolate the time-local, mean-field part of the electron self-energy, which is defined as the sum of the electron-phonon, see Eq. (4.28), and electron-electron interaction, see Eq. (4.29), induced mean-field self-energies or

equivalently as

$$\begin{aligned}\big[\Sigma_{\mathrm{MF}}(z;z')\big]_{pq} &= \Sigma_{\mathrm{MF};pq}(z;z') \\ &\equiv \delta(z,z')v_{\mathrm{epMF}}(z) + \delta(z,z')v_{\mathrm{eeMF}}(z)\end{aligned}$$

where

$$\begin{aligned}\big[v_{\mathrm{epMF}}(z)\big]_{pq} &\equiv v_{\mathrm{epMF};pq}(z) \\ &\equiv \sum_{\mu} M^{\mu}_{pq}(z)\phi_{\mu}(z)\,, \\ \big[v_{\mathrm{eeMF}}(z)\big]_{pq} &\equiv v_{\mathrm{eeMF};pq}(z) \\ &\equiv -\imath\sum_{st} w_{pstq}(z)G^{<}_{ts}(z;z) + \imath\sum_{st} w_{psqt}(z)G^{<}_{ts}(z;z)\,,\end{aligned}$$

are the corresponding mean-field potentials. It is then possible to treat the mean-field self-energy by including the mean-field potentials into the definition of the mean-field, electron one-body Hamiltonian matrix

$$h_{\mathrm{MF}}(z) \equiv h(z) + v_{\mathrm{epMF}}(z) + v_{\mathrm{eeMF}}(z) \tag{5.1}$$

such that the electron self-energy contributing to the collision integrals reduces to the time-nonlocal eXchange-Correlation self-energy $\Sigma_{\mathrm{XC}}(z;z') \equiv \Sigma(z;z') - \Sigma_{\mathrm{MF}}(z;z')$. It follows, by applying the Langreth rules of Sec. 4.5.1 to Eq. (4.19b), that the phonon field determining the electron-phonon interaction induced mean-field electron self-energy is given by

$$\phi_{\mu}(t) = \sum_{\nu}\big[d^{R}_{\mu\nu} \bullet F_{\mathrm{MF};\nu}\big](t) + \sum_{\nu}\big[d^{]}_{\mu\nu} \star F^{M}_{\mathrm{MF};\nu}\big](t)\,, \tag{5.2a}$$

$$\begin{aligned}\phi^{M}_{\mu} &\equiv \phi^{M}_{\mu}(\tau) \\ &= \sum_{\nu}\big[d^{M}_{\mu\nu} \star F^{M}_{\mathrm{MF};\nu}\big](\tau)\,,\end{aligned} \tag{5.2b}$$

where it is to be understood that ϕ^{M}_{μ} is independent of the imaginary time $\tau \in [0,\beta]$. Moreover, in these equations, the one-time Keldysh function

$$F_{\mathrm{MF};\mu}(z) \equiv F_{\mu}(z) - \imath\sum_{pq} M^{\mu}_{pq}(z)G^{<}_{qp}(z;z)\,,$$

henceforth referred to as the mean-field generalized force, was introduced. In order to evaluate the Keldysh components of the phonon field, in fact only the imaginary-time component is needed here, it is necessary to be able to evaluate the non-interacting phonon propagator. Here, it is thus briefly reviewed how the non-interacting phonon and electron propagators can be obtained in a closed form by solving Eqs. (4.39) and (4.40) in the absence of the electron-phonon and electron-electron interactions. It is possible to do this by defining the time-evolution matrices U and V as the solutions to the contour-time differential equation pairs

$$\begin{aligned}\imath\partial_{z}U(z,z') &= h(z)U(z,z')\,, \\ -\imath\partial_{z'}U(z,z') &= U(z,z')h(z')\,,\end{aligned}$$

and

$$\begin{aligned}\imath\partial_{z}V(z,z') &= \bar{\Omega}(z)\alpha V(z,z')\,, \\ -\imath\partial_{z'}V(z,z') &= V(z,z')\bar{\Omega}(z')\alpha\,,\end{aligned}$$

with the initial conditions $U(t_0,t_0)=1$ and $V(t_0,t_0)=1$. In Sec. 4.1, analogous equations were considered, and by an identical way, here the formal solutions

$$U(z,z')=\begin{cases} T\exp\Big(-\imath\int_{C(z,z')}d\bar{z}\;h(\bar{z})\Big) & z\geq z' \\ \bar{T}\exp\Big(\imath\int_{C(z',z)}d\bar{z}\;h(\bar{z})\Big) & z<z' \end{cases}$$

and

$$V(z,z')=\begin{cases} T\exp\Big(-\imath\int_{C(z,z')}d\bar{z}\;\bar{\Omega}(\bar{z})\alpha\Big) & z\geq z' \\ \bar{T}\exp\Big(\imath\int_{C(z',z)}d\bar{z}\;\bar{\Omega}(\bar{z})\alpha\Big) & z<z' \end{cases},$$

can be introduced in terms of the contour-time ordered exponentials in the arguments of which $C(z,z')$ refers to the contour from z' to z. It is then possible to express the non-interacting electron propagator formally in terms of the time-evolution operator U as

$$g(z;z')=-\imath U(z,t_0)\Big(\theta(z,z')-f_+\big(\beta h^M\big)\Big)U(t_0,z')\,, \tag{5.3}$$

cf., [SL13], and similarly, the non-interacting phonon propagator can be written formally in terms of the time-evolution operator V as

$$d(z;z')=-\imath\alpha V(z,t_0)\Big(\theta(z,z')+f_-\big(\beta\bar{\Omega}^M\alpha\big)\Big)V(t_0,z')\,, \tag{5.4}$$

where θ is to be understood as the Heaviside function multiplying an identity matrix and $f_\pm$ denote the matrix-valued Fermi-Dirac $(+)$ and Bose-Einstein $(-)$ distribution functions. It is straightforward to verify, by checking that the correct equations of motion and the Kubo-Martin-Schwinger boundary conditions are obeyed, that these equations hold. It now follows by using the imaginary-time component of the non-interacting phonon propagator of Eq. (5.4), cf., Eq.(5.8), to evaluate the convolution integral of Eq. (5.2b) that the imaginary-time component of the phonon field can be written as

$$\phi^M=-{\bar{\Omega}^M}^{-1}\Big(F^M-\imath\mathrm{tr}\big(M^M G^M(0^-)\big)\Big)\,, \tag{5.5a}$$

where it is assumed that $\bar{\Omega}^M$ is invertible and by the trace it is meant a trace over the electronic indices only. It is noted that this result can also be obtained by solving Eqs. (4.32a) with the help of the variation of constants formula and by requiring that the Kubo-Martin-Schwinger boundary conditions are satisfied. In order to solve the imaginary-time components of the phonon and electron propagators, a similar strategy is adopted, that is the imaginary-time integro-differential equations are converted into integral equations which are solved numerically. It is possible to carry-out this conversion in a way resembling in idea the preconditioning of linear algebraic equations which can be introduced, for instance, to improve the convergence of an iterative technique [Saa03]. In here, the so-called static phonon field ϕ_S and phonon d_S and electron g_S propagators are introduced by demanding that they satisfy Eqs. (4.31) with the so-called static phonon Π_S and electron Σ_S self-energies and with some closely related Hamiltonian operator the elements of which, e.g., h_S and Ω_S, are referred to by the subscript S. It is moreover required that the static field and propagators satisfy the same Kubo-Martin-Schwinger boundary conditions as the field and propagators of interest. It is then possible to recast the imaginary-time integro-differential equations for the phonon and electron propagators of interest, by using the corresponding equations for the static propagators, as the integral Dyson equations

$$D^M(\tau)=d_S^M(\tau)+\big[d_S^M\star\bar{\Pi}^M\star D^M\big](\tau)\,, \tag{5.5b}$$

$$G^M(\tau) = g_S^M(\tau) + \big[g_S^M \star \bar{\Sigma}^M \star G^M\big](\tau)\,, \tag{5.5c}$$

where $\bar{\Pi}^M(\tau) \equiv \imath\delta(\tau)\big(\bar{\Omega}^M - \bar{\Omega}_S^M\big) + \Pi^M(\tau) - \Pi_S^M(\tau)$ and $\bar{\Sigma}^M(\tau) \equiv \imath\delta(\tau)\big(h_{\mathrm{MF}}^M - h_{S;\mathrm{MF}}^M\big) + \Sigma_{\mathrm{XC}}^M(\tau) - \Sigma_{S;\mathrm{XC}}^M(\tau)$ denote the effective phonon and electron self-energies. It is remarked that in [SDL09a, Bal07], where purely electronic systems are considered, the electron propagator in the Hartree-Fock approximation plays the role of the static propagator. It is already in this simple case, i.e., when the Hartree-Fock is chosen over the non-interacting propagator as the static electron propagator, that the shift of the spectrum caused by the interaction in the particle-hole symmetric Hubbard model is taken into account automatically alleviating the convergence substantially. As far as the rest of the equations are concerned, it remains to conclude that the real- and mixed-time components of the electron propagator are obtained by numerically integrating the integro-differential equations

$$\big(\imath\partial_t - h_{\mathrm{MF}}(t)\big)G^{\gtrless}(t;t') = \big[\Sigma_{\mathrm{XC}}^R \bullet G^{\gtrless} + \Sigma_{\mathrm{XC}}^{\gtrless} \bullet G^A + \Sigma_{\mathrm{XC}}^{\rceil} \star G^{\lceil}\big](t;t')\,, \tag{5.6a}$$

$$\big(\imath\partial_t - h_{\mathrm{MF}}(t)\big)G^{\rceil}(t;\tau) = \big[\Sigma_{\mathrm{XC}}^R \bullet G^{\rceil} + \Sigma_{\mathrm{XC}}^{\rceil} \star G^M\big](t;\tau)\,, \tag{5.6b}$$

where the differential operator ∂_t is to be understood to be proportional to the identity matrix. In order to be complete, the real- and mixed-time components of the phonon field and propagator are solved by integrating the equations

$$\big(\imath\alpha\partial_t - \bar{\Omega}(t)\big)\phi(t) = F(t) - \imath\mathrm{tr}\big(M(t)G^<(t;t)\big)\,, \tag{5.6c}$$

and

$$\big(\imath\alpha\partial_t - \bar{\Omega}(t)\big)D^{\gtrless}(t;t') = \big[\Pi^R \bullet D^{\gtrless} + \Pi^{\gtrless} \bullet D^A + \Pi^{\rceil} \star D^{\lceil}\big](t;t')\,, \tag{5.6d}$$

$$\big(\imath\alpha\partial_t - \bar{\Omega}(t)\big)D^{\rceil}(t;\tau) = \big[\Pi^R \bullet D^{\rceil} + \Pi^{\rceil} \star D^M\big](t;\tau)\,, \tag{5.6e}$$

which are the same as those written down in Sec. 4.5.2. It remains, in order to facilitate a numerical solution, to introduce the imaginary M_{I} and real-time M_{R} meshes on which the imaginary-, mixed- and real-time components are discretized. Firstly, the imaginary-time components are discretized on a non-uniform mesh to take into account the exponential dependence of the propagators, cf., Eqs. (5.8) and (5.9), on the imaginary-time arguments [SDL09a, Bal07]. Moreover, in order to take full advantage of the symmetries of the imaginary- and mixed-time-components, the mesh is chosen to span the interval $[0,\beta]$ and to be symmetric with respect to $\beta/2$. The imaginary-time meshes used in the present work are the uniform power and geometric meshes. It is referred to [Bal07, SDL09a] for the description of the former, which is used in **III** [SML12], while the latter, which is used in **I** [SPAL15a] and **II** [SPAL15b], is defined as

$$M_{\mathrm{I}}(\beta;a,b) \equiv \{\tau_k, \beta - \tau_k \in [0,\beta] : \tau_0 = 0, \tau_{k+1} = \tau_k + ab^k \,\forall\, k \in \mathbb{Z}_{\geq 0}\}\,, \tag{5.7}$$

where $a \in]0,\infty[$ and $b \in [1,\infty[$ are grid parameters. and could, for instance, look like

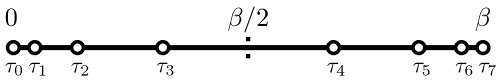

with only eight mesh points. Henceforth, as suggested above, the elements of an imaginary-time mesh are referred to by τ_k such that $\tau_0 = 0$, $\tau_{k+1} > \tau_k$ and $\tau_{|M_{\mathrm{I}}|-1} = \beta$ for $k \in [0, |M_{\mathrm{I}}|[\cap\mathbb{Z}$ where $|M_{\mathrm{I}}|$ denotes the number of the mesh points. Secondly, in order that the collision integrals are efficiently evaluable, the mixed- and real-time components are discretized on direct product meshes, i.e., $M_{\mathrm{R}} \times M_{\mathrm{I}}$ and $M_{\mathrm{R}} \times M_{\mathrm{R}}$ for the right and greater/lesser components respectively. In the present work, the real time mesh M_{R} is uniform, that is

$$M_{\mathrm{R}}(T;h) = \{t_k \in [t_0,T] : t_0 = 0, t_{k+1} = t_k + h \,\forall\, k \in \mathbb{Z}_{\geq 0}\}\,,$$

such that, e.g.,

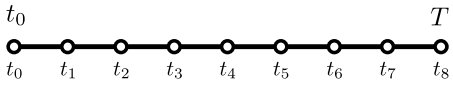

where $h \in]0, \infty]$ is the spacing between neighboring mesh points which is often referred to as the step size in the context of numerical integration. In the following, the elements of a real-time mesh are referred to by t_k such that $t_{k+1} > t_k$ for $k \in [0, |M_\mathrm{R}|[\cap\mathbb{Z}$ where $|M_\mathrm{R}|$ denotes the number of the mesh points. It is further convenient to introduce the abbreviation

$$z_n \equiv \begin{cases} t_n & n \in [0, |M_\mathrm{R}|[\cap\mathbb{Z}, z_n \in C^\pm \\ t_0 - \imath\tau_{|n|} & n \in]-|M_\mathrm{I}|, 0[\cap\mathbb{Z} \end{cases}$$

since it can be used to introduce the short-hand ϕ_n to denote an approximation to the field at z_n as well as the short-hands $G_{n;m}$ and $D_{n;m}$ to denote approximations to the propagators at $(z_n; z_m)$. Here, it is noteworthy that a subscript $\pm$ for a discrete contour time or its indexing integer, e.g., $D_{n_\pm;m_\mp}$ for $n, m \geq 0$, refers to the contour time on the $\pm$ branches. It is the purpose of the following sections to described how the above introduced approximations to the field and propagators for the discrete contour-times can be obtained in practice.

5.2 Imaginary-time, Boundary-Value Problem

In order to solve the initial-value problem associated with the real- and mixed-time components, the initial values of these components, which are determined by the boundary-value problem for the imaginary-time components, need to be solved first, cf., Sec. 4.5.2. It is stressed that instead of solving the imaginary-time integro-differential equations of Sec. 4.5.2 directly, the equivalent integral equations of Eqs. (5.5) are solved in order to obtain the imaginary-time components. In the present work, this is done by relying on the method of fixed-point iterations in which a convergent sequence of approximations to the imaginary-time components is generated by introducing and subsequently using a mapping the fixed-point of which the components are. In other words, by defining the functions

$$\begin{aligned} y_1 &\equiv \phi\,, \\ y_2 &\equiv (D, G)\,, \end{aligned}$$

and by regarding y_1 as a functional of y_2, it is the aim to introduce a map $\mathcal{F}$ with the fixed-point $y_2 = \mathcal{F}(y_2)$ such that the sequence of approximations $(y_2^k : y_2^{k+1} = \mathcal{F}(y_2^k), k \in [0, \infty[\cap\mathbb{Z})$ converges to the solution y_2 up to a controllable numerical error. Here, it is to be understood that the codomain of y_2 is the direct product of the matrix algebras of the propagators such that Eqs. (5.5) can be abbreviated as

$$\begin{aligned} y_2 &= y_{2;S} + y_{2;S} \circ k_2^1[y_2] \circ y_2 \\ &= y_{2;S} + k_2^2[y_2] \circ y_2 \circ y_{2;S}\,, \end{aligned}$$

where $y_{2;S} \equiv (d_S, g_S)$ and

$$\begin{aligned} k_2^1[y_2](\mathsf{y}_1, \mathsf{y}_2) &\equiv (\bar{\Pi}[G, D]\mathsf{y}_1, \bar{\Sigma}[G, D]\mathsf{y}_2)\,, \\ k_2^2[y_2](\mathsf{y}_1, \mathsf{y}_2) &\equiv (\mathsf{y}_1\bar{\Pi}[G, D], \mathsf{y}_2\bar{\Sigma}[G, D])\,, \end{aligned}$$

define the linear operators $k_2^\nu[y_2]$ for $\nu \in \{1, 2\}$. In the following, a schematic review of an algorithm, or its implementation, using a map $\mathcal{F}$ based on the above equations and aimed at solving

for the imaginary-time component of y_2 is documented. It is remarked that due to the symmetries, cf., Sec. 4.5.2, only the function values for τ such that $-\tau \in [0,\beta]$ are considered.

I Initial Guess:
In practice, it is possible to choose the zeroth iterate $y_2^0 \equiv (D^0, G^0)$, i.e., make the initial guess, by choosing

i the non-interacting propagator

$$d^M(-\tau) = -\imath\alpha f_-\big(\beta\bar{\Omega}^M\alpha\big)e^{\bar{\Omega}^M\alpha\tau}\,, \tag{5.8}$$

where $\tau \in [0,\beta]$, cf., Eq. (5.4)

ii any propagator satisfying Eq. (5.5b) and obtained numerically in a previous calculation

as the initial phonon D^0 propagator and by choosing

iii the non-interacting propagator

$$g^M(-\tau) = \imath f_+\big(\beta h^M\big)e^{h^M\tau}\,, \tag{5.9}$$

where $\tau \in [0,\beta]$, cf., Eq. (5.3)

iv the mean-field propagator g^M_{MF} obtained by replacing in Eq. (5.9) h^M with h^M_{MF} of Eq. (5.1) and by demanding that the self-consistency condition $-\imath g^M_{\mathrm{MF}}(0^-) = f_+\big(\beta h^M_{\mathrm{MF}}\big)$ is satisfied

v any propagator satisfying Eq. (5.5c) and obtained numerically in a previous calculation

as the initial electron G^0 propagator.

II Fixed-Point Iteration:
It is noted that the static phonon and electron propagators, which appear below contained in $y_{2;S}$, can be chosen to be any of the I.i-ii labeled phonon and I.iii-v labeled electron propagators available as the initial guesses. In Pubs. **I-III**, only the options I.i and I.iii-iv have been used.

For $k = 0 \ldots \infty$

i In order to obtain the next $(k+1)$th iterate from the previous kth iterate the map $\mathcal{F}$ is used such that $y_2^{k+1} = \mathcal{F}(y_2^k)$. In practice, $\mathcal{F}$ is defined via Eqs. (5.5) by either linearizing them so that

$$y_2^{k+1} = y_{2;S} + y_{2;S} \circ k_2^1[y_2^k] \circ y_2^{k+1}\,,$$

from which the imaginary-time component of y_2^{k+1} is solved for τ s.t. $-\tau \in M_{\mathrm{I}}$ by using the Bi-Conjugate Gradient Stabilized (BiCGStab) method similarly to what is described in [Bal07, SDL09a, Uim15], or by introducing the function

$$y_2^{k+1} = y_{2;S} + y_{2;S} \circ k_2^1[y_2^k] \circ y_2^k\,,$$

from which the imaginary-time component of y_2^{k+1} is obtained by evaluating it for τ s.t. $-\tau \in M_{\mathrm{I}}$. In **III** [SML12], the former, and in **I** [SPAL15a] and **II** [SPAL15b], the latter of the two methods has been used.

ii In order to evaluate imaginary-time convolution integrals of the form

$$\imath[a^M \star b^M](-\tau) = \int_0^\tau d\bar{\tau}\; a^M(-\bar{\tau})b^M(\bar{\tau}-\tau)$$

$$\pm \int_{\tau}^{\beta} d\bar{\tau}\; a^{M}(-\bar{\tau}) b^{M}(\bar{\tau}-\tau-\beta)\,, \qquad\qquad \tau \in M_{\mathrm{I}}\,,$$

where b^M satisfies either the fermionic $(-)$ or non-fermionic $(+)$ boundary conditions and neither a^M nor b^M have local components, clamped cubic spline interpolation [PTVF92] is used. Firstly, the interpolants of a^M and b^M are constructed by using the available function values on $-M_{\mathrm{I}}$. Secondly, by using these interpolants, the interpolants of the integrands are respectively constructed for $\bar{\tau} \in M_{\mathrm{I}}(\tau) \cap [0,\tau]$ and $\bar{\tau} \in M_{\mathrm{I}}(\tau+\beta) \cap [\tau,\beta]$ where $M_{\mathrm{I}}(\tau) \equiv \{\bar{\tau} : \bar{\tau}, \tau - \bar{\tau} \in M_{\mathrm{I}}\}$. It is then possible to approximate the integrals above by evaluating the integral of the obtained piece-wise defined cubic spline polynomial. If M is a mesh defined above and f is the corresponding integrand then this amounts to

$$\int_{x_0}^{x_{|M|-1}} dx\; f(x) \approx \frac{1}{2} \sum_{k=0}^{|M|-2} h_k \big(f_{k+1} + f_k - h_k^2 (f_{k+1}^{''} + f_k^{''})/12 \big)\,,$$

where $h_k \equiv x_{k+1} - x_k > 0$ is the mesh spacing, f_k is the function value at x_k and $f_k^{''}$ is the second derivative of the interpolating polynomial at x_k [PTVF92] where $x_k \in M$ for all $k \in [0, |M|[\cap \mathbb{Z}$. It is noted that it is also possible to only construct the interpolants for a^M and b^M and integrate by using an adaptive integration routine, e.g., from the Gnu Scientific Library [Gou09], which has been observed to be faster in some cases.

iii It is possible to accelerate the convergence of the fixed-point iterations by using a method called Direct Inversion of Iterative Subspace (DIIS) which is often known, in the context of self-consistent field iterations, as Pulay mixing [Pul80]. In the method, an optimized iterate defined as

$$\bar{y}_2^k \equiv \sum_{i=0}^{h_k} c_i y_2^{k-i}\,,$$

where $h_k \equiv \min(k, h-1)$ and h is the maximum number of previous iterates to be used, is constructed by demanding that the coefficients c_i minimize the residual norm $\|\bar{y}_2^k - \mathcal{F}(\bar{y}_2^k)\|^2$ under the constraint that c_i sum up to unity. Here, the norm $\|a\| \equiv \sqrt{\langle a|a\rangle}$ is defined in terms of an inner product $\langle a|b\rangle$ to be specified. It then follows, by assuming that $\bar{y}_2^k - \mathcal{F}(\bar{y}_2^k) \approx -\sum_{i=0}^{h_k} c_i r_{k-i}$ where $r_{k-i} \equiv \mathcal{F}(y_2^{k-i}) - y_2^{k-i}$, which is reasonable close to the fixed-point, from the constrained optimization problem that the coefficients c_i, which are the components of the vector c, satisfy the equation

$$\begin{pmatrix} R_k & -1 \\ -1^T & 0 \end{pmatrix} \begin{pmatrix} c \\ \mu \end{pmatrix} = \begin{pmatrix} 0 \\ -1 \end{pmatrix}$$

where 0 on the right-hand side and 1 on the left-hand side are vectors while R_k is a matrix such that $R_{k;ij} \equiv \langle r_{k-i} | r_{k-j} \rangle$. Moreover, μ is the Lagrange multiplier which enforces the equality constraint. In **I** [SPAL15a] and **II** [SPAL15b], we have used the inner product

$$\langle a|b\rangle = \int_0^{\beta} d\tau\; \mathrm{tr}\big(a^{\dagger}(-\tau) b(-\tau)\big)$$

to define the norm, but it is mentioned here that also the inner-product

$$\langle a|b\rangle = \sum_i \int_0^{\beta} d\tau\; a_{ii}^{*}(-\tau) b_{ii}(-\tau)\,,$$

which would imply, at least in the exact theory, the positivity of $R_{k;ij}$, could be used similarly to [TR08]. In either case, the matrix R_k is guaranteed to be real symmetric if it

is guaranteed that the propagators are anti-hermitian with respect to the spatial indices. In the end, also pure mixing is applied such that the next $(k+1)$th iterate is given by

$$\begin{aligned} y_2^{k+1} &= C\mathcal{F}[\bar{y}_2^k] + (1-C)\bar{y}_2^k \\ &\approx C\sum_{i=0}^{h_k} c_i r_{k-i} + \bar{y}_2^k \,, \end{aligned}$$

where $C \in]0,1]$ is an empirically chosen parameter. It is to be noted that no convergence acceleration has been used in **III** [SML12] amounting to the choice $y_2^{k+1} = \mathcal{F}[y_2^k]$.

It is when the solution has converged, or a maximum number of allowed iterations is reached, that the iteration loop is terminated. In **III** [SML12], by a converged solution, it is meant that the change in the total energy $|E^{k+1} - E^k|$ from kth to $(k+1)$th iteration round is less than a chosen tolerance. In **I** [SPAL15a] and **II** [SPAL15b], we have moreover required that also the residual norm $R_{k;0\,0}$ defined above is less than the chosen tolerance.

It is noted that it is not guaranteed that the iterative method proposed above converges. However, it is often found to be the case if the initial guesses and static propagators are chosen sufficiently well. It should also be mentioned that alternative methods relying either on a direct solution of the integro-differential equations, e.g., by discretization, or on a solution of an equivalent optimization problem could be potentially useful. Here, by the optimization problem it is referred to, in the case of a Ψ-derivable approximation, the variational principle for the Luttinger-Ward derivable functionals, cf., [SL13].

5.3 Real-time, Initial-Value Problem

If the imaginary-time components of the phonon field and propagator and of the electron propagator have been solved, as described in the previous section, then it is possible to solve the corresponding real- and mixed-time components by numerical integration of the integro-differential equations given by Eqs. (5.6). Here, by numerical integration, it is referred to the standard methodology for solving initial-value problems for ordinary differential [But87, HNW08] or Volterra integro-differential equations [BH86] which is often referred to as the time-propagation in the physics literature. In the following, firstly, the numerical integration method designed to solve the real- and mixed-time components by solving the Kadanoff-Baym equations is described and, secondly, its implementation used in **II** [SPAL15b] is reviewed.

5.3.1 Integration Rule

In what follows, it is the purpose to review a simple and practical version of a more general integration rule, which is motivated and defined later in Ch. 6, in order to solve numerically the real-time Kadanoff-Baym equations given by Eqs. (5.6). It is noted that in **III** [SML12], the numerical method described in [Bal07, SDL09b] has been used, and only in **II** [SPAL15b] and [TSK+16], the method described in the following has been applied. Moreover, it is stressed that only self-energies which are evaluation functionals, i.e., functions of the propagators, such as those introduced in Secs. 4.4.1 and 4.4.2, are considered here. Firstly, in order to arrive at a compact representation, the notation

introduced at the end of Sec. 5.1 and in the beginning of Sec. 5.2 is revised. In particular, a refined real-time mesh is defined by introducing the contour-time mesh points

$$z_{(n,i)_\pm} \equiv t_n + hc_i\,, \qquad\qquad n \in [0, |M_{\rm R}|[\cap\mathbb{Z},\, i \in [1,s]\cap\mathbb{Z}\,,$$

where $c_i \in [0,1]$ denote the (integration) nodes of the method and $s \in \mathbb{Z}_{\geq 1}$ refers to the number of the so-called (internal) stages. It is then useful to define the auxiliary index set $I^s_{\rm I\cup R} \equiv \{n,(m,i) : n \in]-|M_{\rm I}|, |M_{\rm R}|[\cap\mathbb{Z}, m \in [0,|M_{\rm R}|[\cap\mathbb{Z}, i \in [1,s]\cap\mathbb{Z}\}$ since it, for one, allows to define compactly the so-called mean and relative contour-time mesh points

$$\begin{aligned} Z_{N;M} &\equiv \frac{z_N + z_M}{2}\,,\\ \zeta_{N;M} &\equiv z_N - z_M\,. \end{aligned}$$

where $N,M \in I^s_{\rm I\cup R}$. For another, if $N,M \in I^s_{\rm I\cup R}$ then the to be specified approximations ϕ_N to the field at z_N as well as the approximations $G_{N;M}$ and $D_{N;M}$ to the propagators at $(z_N;z_M)$ are conveniently introduced. It is found useful to denote collectively the contour-time mesh points and the aforementioned approximations to the field and propagators similarly to what is done in Sec. 5.2. In addition to the more compact notation achieved in this way, also the thus gained more transparent connection to the literature on numerical integration [But87, HNW08, BH86] favors the collective representation specified in the following. It is defined that if $n,m \in]-|M_{\rm I}|, |M_{\rm R}|[\cap\mathbb{Z}$ then

$$\begin{aligned} y_{1;n} &\equiv (z_n, \phi_n)\,,\\ y_{2;n;m} &\equiv (Z_{n;m}, \zeta_{n;m}, D_{n;m}, G_{n;m})\,, \end{aligned}$$

refer to the desired approximations on the primary mesh $M_{\rm I}\cup M_{\rm R}$. Moreover, if $n \in]0,|M_{\rm R}|[\cap\mathbb{Z}$, $m \in]-|M_{\rm I}|, n]\cap\mathbb{Z}$ and $i \in [1,s]\cap\mathbb{Z}$ then

$$\begin{aligned} Y_{1;n,i} &\equiv (z_{n,i}, \phi_{n,i})\,,\\ Y_{2;n,i;n,i} &\equiv (Z_{n,i;n,i}, \zeta_{n,i;n,i}, D_{n,i;n,i}, G_{n,i;n,i})\,,\\ Y_{2;n,i;m} &\equiv (Z_{n,i;m}, \zeta_{n,i;m}, D_{n,i;m}, G_{n,i;m})\,,\\ Y_{2;m;n,i} &\equiv (Z_{m;n,i}, \zeta_{m;n,i}, D_{m;n,i}, G_{m;n,i})\,, \end{aligned}$$

refer to the auxiliary approximations at the refined mesh points known henceforth as the stage approximations in agreement with the standard terminology used in the literature on numerical integration. Here, the vectors $y_{1;n}$ and $y_{2;n,m}$, as well as the stage approximations, are to be understood as the elements of the direct products of the vector spaces for the contour-times, field and propagators. In order to evaluate the approximations for y_1 and y_2, henceforth abbreviated simply as y, the numerical integration rule 6.1.2, which has been derived by relying in particular on the ideas behind the Runge-Kutta methods for the numerical integration of one-dimensional Volterra integro-differential equations [WP68, Lub82, BH86], is specialized to obtain a class of practical methods. It is noted that although the notation chosen here might appear abstract at the moment to some readers, it will be further clarified in the next chapter in which this notation arises more naturally. Moreover, in contrast to what is done in the next chapter, here it is the intention to motivate the integration rule also by relating it to the existing methods for solving the real-time Kadanoff-Baym equations [Bal07, SDL09b, FVA10b]. Having said that, in order to specify the numerical methods, it is proposed that if $n \in [0,|M_{\rm R}|[\cap\mathbb{Z}$ such that $y_{1;k}$ and $y_{2;k;l}$ are known for all $k,l \in]-|M_{\rm I}|, n]\cap\mathbb{Z}$ then in order to solve for $y_{1;n+1}$ and $y_{2;n+1;,n+1}$, $y_{2;n+1,m}$ and $y_{2;m;n+1}$ for all $m \in]-|M_{\rm I}|, n]\cap\mathbb{Z}$, the integration rule

$$y_{1;n+1} = u_{1;n}y_{1;n} + h\sum_{j=1}^{s} b_{1;n,j}N_{1;n,j}\,,$$

$$
\begin{aligned}
y_{2;n+1;n+1} &= u_{2;n} y_{2;n;n} + h \sum_{j=1}^{s} b_{2;n,j} N_{2;n,j;n,j} \,, \\
y_{2;n+1;m} &= u^1_{2;n} y_{2;n;m} + h \sum_{j=1}^{s} b^1_{2;n,j} N^1_{2;n,j;m} \,, \\
y_{2;m;n+1} &= u^2_{2;n} y_{2;m;n} + h \sum_{j=1}^{s} b^2_{2;n,j} N^2_{2;m;n,j} \,,
\end{aligned}
$$

where

$$
\begin{aligned}
Y_{1;n,i} &= v_{1;n,i} y_{1;n} + c_i h \sum_{j=1}^{i-1} a^j_{1;n,i} N_{1;n,j} \,, \\
Y_{2;n,i;n,i} &= v_{2;n,i} y_{2;n;n} + c_i h \sum_{j=1}^{i-1} a^j_{2;n,i} N_{2;n,j;n,j} \,, \\
Y_{2;n,i;m} &= v^1_{2;n,i} y_{2;n;m} + c_i h \sum_{j=1}^{i-1} a^{1;j}_{2;n,i} N^1_{2;n,j;m} \,, \\
Y_{2;m;n,i} &= v^2_{2;n,i} y_{2;m;n} + c_i h \sum_{j=1}^{i-1} a^{2;j}_{2;n,i} N^2_{2;m;n,j} \,,
\end{aligned}
$$

can be used, as has been done in **II** [SPAL15b] and [TSK+16]. Here, it needs to be understood that to obtain the greater and lesser components, all pairs of contour-time indices on the left and right hand sides are to be attached branch labels equivalently, e.g., for $Y_{2;n,i;m}$, if $(n,i)_\pm; m_\mp$ then also $n_\pm; m_\mp$ and $(n,j)_\pm; m_\mp$. It is evident that the above integration rule has a structure which resembles the structure of the Runge-Kutta methods for ordinary differential equations [But87, HNW08]. The so-called weights of the method, which are defined for $\mu, \nu \in \{1,2\}$ by

$$
\begin{aligned}
u^{(\nu)}_{\mu;n} &\equiv u(hL^{(\nu)}_{\mu;n,1}, \ldots, hL^{(\nu)}_{\mu;n,s}) \,, \\
b^{(\nu)}_{\mu;n,j} &\equiv b_j(hL^{(\nu)}_{\mu;n,1}, \ldots, hL^{(\nu)}_{\mu;n,s}) \,,
\end{aligned}
$$

and

$$
\begin{aligned}
v^{(\nu)}_{\mu;n,i} &\equiv v_i(c_i hL^{(\nu)}_{\mu;n,1}, \ldots, c_i hL^{(\nu)}_{\mu;n,i-1}) \,, \\
a^{(\nu);j}_{\mu;n,i} &\equiv a_{ij}(c_i hL^{(\nu)}_{\mu;n,1}, \ldots, c_i hL^{(\nu)}_{\mu;n,i-1}) \,,
\end{aligned}
$$

were introduced in a close analogy to what is done in [Bal07, SDL09b, FVA10b] when time-evolution operators are introduced. In fact, in the definitions of the weights, the linear operators L defined by

$$
\begin{aligned}
L_{1;n,i}(\mathsf{y}_1, \mathsf{y}_2) &\equiv L_1(Y_{1;n,i}, Y_{2;n,i;n,i})(\mathsf{y}_1, \mathsf{y}_2) \\
&= -\imath\big(0, \underbrace{\alpha\bar{\Omega}(z_{n,i})}_{\equiv\, \bar{\Omega}_{n,i}} \mathsf{y}_2\big) \,, \\
L_{2;n,i}(\mathsf{y}_1, \mathsf{y}_2, \mathsf{y}_3, \mathsf{y}_4) &\equiv L^1_{2;n,i}(\mathsf{y}_1, \mathsf{y}_2, \mathsf{y}_3, \mathsf{y}_4) + L^2_{2;n,i}(\mathsf{y}_1, \mathsf{y}_2, \mathsf{y}_3, \mathsf{y}_4) \,, \\
L^1_{2;n,i}(\mathsf{y}_1, \mathsf{y}_2, \mathsf{y}_3, \mathsf{y}_4) &\equiv L^1_2(Y_{1;n,i}, Y_{2;n,i;n,i})(\mathsf{y}_1, \mathsf{y}_2, \mathsf{y}_3, \mathsf{y}_4) \\
&= -\imath\big(0, 0, \alpha\bar{\Omega}(Z_{n,i;n,i})\mathsf{y}_3, \underbrace{h_{\mathrm{MF}}(Z_{n,i;n,i}, \phi_{n,i}, G_{n,i;(n,i)^+})}_{\equiv\, h_{\mathrm{MF};n,i}} \mathsf{y}_4\big) \,, \\
L^2_{2;n,i}(\mathsf{y}_1, \mathsf{y}_2, \mathsf{y}_3, \mathsf{y}_4) &\equiv L^2_2(Y_{1;n,i}, Y_{2;n,i;n,i})(\mathsf{y}_1, \mathsf{y}_2, \mathsf{y}_3, \mathsf{y}_4)
\end{aligned}
$$

$$= \imath\big(0, 0, \mathsf{y}_3\bar{\Omega}(Z_{n,i;n,i})\alpha, \mathsf{y}_4 h_{\mathrm{MF}}(Z_{n,i;n,i}, \phi_{n,i}, G_{n,i;(n,i)^+})\big)\,,$$

contain the one-body electron and phonon Hamiltonian matrices which are the generators of time-evolution. Moreover, the weight functions u, v_i, b_j and a_{ij} introduced above are to be later specified which is analogous to specifying the approximations for the time-evolution operators in [Bal07, SDL09b, FVA10b]. In addition to the weights of the method, the integrations rules depend on the non-linear functions N defined by

$$\begin{aligned}
N_{1;n,i} &\equiv N_1(Y_{2;n,i;n,i}, I_{1;n,i} + Z_{1;n,i}) \\
&= \big(1, -\imath\alpha\underbrace{F_{\mathrm{MF}}(Z_{n,i;n,i}, G_{n,i;(n,i)^+})}_{\equiv F_{\mathrm{MF};n,i}}\big)\,, \\
N_{2;n,i;n,i} &\equiv N_2^1(Y_{2;n,i;n,i}, I^1_{2,1;n,i;n,i} + Z^1_{2,1;n,i;n,i}, I^1_{2,2;n,i;n,i} + Z^1_{2,2;n,i;n,i}) \\
&\quad + N_2^2(Y_{2;n,i;n,i}, I^2_{2,1;n,i;n,i} + Z^2_{2,1;n,i;n,i}, I^2_{2,2;n,i;n,i} + Z^2_{2,2;n,i;n,i}) \\
&\equiv (1,0,0,0) + \sum_{\nu,\mu=1}^{2} (I^\mu_{2,\nu;n,i;n,i} + Z^\mu_{2,\nu;n,i;n,i})\,, \\
N^1_{2;n,i;m} &\equiv N_2^1(Y_{2;n,i;m}, I^1_{2,1;n,i;m} + Z^1_{2,1;n,i;m}, I^1_{2,2;n,i;m}) \\
&\equiv (1/2,1,0,0) + \sum_{\nu=1}^{2} I^1_{2,\nu;n,i;m} + Z^1_{2,1;n,i;m}\,, \\
N^2_{2;m;n,i} &\equiv N_2^2(Y_{2;m;n,i}, I^2_{2,1;m;n,i}, I^2_{2,2;m;n,i} + Z^2_{2,2;m;n,i}) \\
&\equiv (1/2,-1,0,0) + \sum_{\nu=1}^{2} I^2_{2,\nu;m;n,i} + Z^2_{2,2;m;n,i}\,,
\end{aligned}$$

where I and Z denote quadrature approximations to the collision integrals. It is noted that in contrast to what is done at least in [SDL09b] here by Z it is referred to the approximations for the real-time collision integrals from t_n to $t_n + c_i h$ whereas the so-called lag quadrature I include the remaining contributions from t_0 to t_n. It is possible to complete the definition of the integration rule by specifying the form of these quadrature rules. In order to do so, the linear operators k referring to the integral kernels, cf., Sec. 5.2, are introduced such that

$$\begin{aligned}
k^1_{2;n,i;M}(\mathsf{y}_1,\mathsf{y}_2,\mathsf{y}_3,\mathsf{y}_4) &\equiv k_2^1(Y_{2;n,i;M}, Y_{2;M;n,i})(\mathsf{y}_1,\mathsf{y}_2,\mathsf{y}_3,\mathsf{y}_4) \\
&= -\imath\big(0,0,\alpha\underbrace{\Pi(Z_{n,i;M}, \zeta_{n,i;M}, G_{n,i;M}, G_{M;n,i})}_{\equiv \Pi_{n,i;M}}\mathsf{y}_3, \\
&\qquad \Sigma(Z_{n,i;M}, \zeta_{n,i;M}, D_{n,i;M}, G_{n,i;M}, G_{M;n,i})\mathsf{y}_4\big)\,, \\
k^2_{2;M;n,i}(\mathsf{y}_1,\mathsf{y}_2,\mathsf{y}_3,\mathsf{y}_4) &\equiv k_2^2(Y_{2;M;n,i}, Y_{2;n,i;M})(\mathsf{y}_1,\mathsf{y}_2,\mathsf{y}_3,\mathsf{y}_4) \\
&= \imath\big(0,0,\mathsf{y}_3\Pi(Z_{M;n,i}, \zeta_{M;n,i}, G_{M;n,i}, G_{n,i;M})\alpha, \\
&\quad \mathsf{y}_4\underbrace{\Sigma(Z_{M;n,i}, \zeta_{M;n,i}, D_{M;n,i}, G_{M;n,i}, G_{n,i;M})}_{\equiv \Sigma_{\mathrm{XC};M;n,i}}\big)\,,
\end{aligned}$$

where $M \in \{m, (n,i) : m \in]-|M_{\mathrm{I}}|, n] \cap \mathbb{Z}\}$, making it explicit what is meant when the self-energies are required to be evaluation functionals. In terms of these kernels, and by assuming the convention that $c^{r/a}_{2;k_\pm;l_b} = c^{r/a}_{2;k_b;l_\pm} \equiv \delta_{b\pm}(c_{2;k_{+/-};l_{-/+}} - c_{2;k_{-/+};l_{+/-}})$ for a two-time Keldysh function c_2, the quadrature Z are defined by

$$\sum_{\nu=1}^{2} Z^1_{2,\nu;n,i;n,i} \equiv c_i h \sum_{b\in\{\pm\}} b(d_{ii}k^1_{2;(n,i)_b;(n,i)_{-b}} Y_{2;(n,i)_{-b};(n,i)_b} + d_{i1}k^1_{2;(n,i)_b;n_{-b}} Y_{2;n_{-b};(n,i)_b})\,,$$

$$\sum_{\nu=1}^{2} Z^{2}_{2,\nu;n,i;n,i} \equiv c_i h \sum_{b\in\{\pm\}} b(d_{ii} k^{2}_{2;(n,i)_{-b};(n,i)_b} Y_{2;(n,i)_b;(n,i)_{-b}} + d_{i1} k^{2}_{2;n_{-b};(n,i)_b} Y_{2;(n,i)_b;n_{-b}}) \,,$$

$$Z^{1}_{2,1;n,i;m} \equiv c_i h \sum_{b\in\{\pm\}} (d_{ii} k^{1\,r}_{2;n,i;(n,i)_b} Y_{2;(n,i)_b;m} + d_{i1} k^{1\,r}_{2;n,i;n_b} Y_{2;(n,1)_b;m}) \,,$$

$$Z^{2}_{2,2;m;n,i} \equiv c_i h \sum_{b\in\{\pm\}} (d_{ii} k^{2\,a}_{2;(n,i)_b;n,i} Y_{2;m;(n,i)_b} + d_{i1} k^{2\,a}_{2;n_b;n,i} Y_{2;m;(n,1)_b}) \,,$$

and the so-called lag, or tail, quadrature I by

$$\sum_{\nu=1}^{2} I^{1}_{2,\nu;n,i;n,i} \equiv \underbrace{[k^{1}_{2} \star Y_2]_{n,i;n,i} + h \sum_{b\in\{\pm\}} \sum_{l=0}^{n} b w^{l}_{n;n} k^{1}_{2;(n,i)_b;l_{-b}} Y_{2;l_{-b};(n,i)_b}}_{\equiv [k^{1}_{2} \circ Y_2]_{n,i;n,i}} \,,$$

$$\sum_{\nu=1}^{2} I^{2}_{2,\nu;n,i;n,i} \equiv \underbrace{[k^{2}_{2} \star Y_2]_{n,i;n,i} + h \sum_{b\in\{\pm\}} \sum_{l=0}^{n} b w^{l}_{n;n} k^{2}_{2;l_{-b};(n,i)_b} Y_{2;(n,i)_b;l_{-b}}}_{\equiv [k^{2}_{2} \circ Y_2]_{n,i;n,i}} \,,$$

$$\sum_{\nu=1}^{2} I^{1}_{2,\nu;n,i;m} \equiv \underbrace{[k^{1}_{2} \star y_2]_{n,i;m} + h \sum_{b\in\{\pm\}} \sum_{l=0}^{n} (w^{l}_{n;n} k^{1\,r}_{2;n,i;l_b} y_{2;l_b;m} + w^{l}_{n;m} k^{1}_{2;n,i;l_b} y^{a}_{2;l_b;m})}_{\equiv [k^{1}_{2} \circ y_2]_{n,i;m}} \,,$$

$$\sum_{\nu=1}^{2} I^{2}_{2,\nu;m;n,i} \equiv \underbrace{[k^{2}_{2} \star y_2]_{m;n,i} + h \sum_{b\in\{\pm\}} \sum_{l=0}^{n} (w^{l}_{n;m} k^{2}_{2;l_b;n,i} y^{r}_{2;m;l_b} + w^{l}_{n;n} k^{2\,a}_{2;l_b;n,i} y_{2;m;l_b})}_{\equiv [k^{2}_{2} \circ y_2]_{m;n,i}} \,,$$

where $[k^{1}_{2} \star Y_2]_{n,i;n,i}$, $[k^{2}_{2} \star Y_2]_{n,i;n,i}$ and $[k^{1}_{2} \star y_2]_{n,i;m}$ and $[k^{2}_{2} \star y_2]_{m;n,i}$ refer to approximations to the imaginary-time collision integrals based respectively on the values $k^{1}_{2;n,i;l} Y_{2;l;n,i}$. $k^{2}_{2;l;n,i} Y_{2;n,i;l}$ and $k^{1}_{2;n,i;l} y_{2;l;m}$ and $k^{2}_{2;l;n,i} y_{2;m;l}$ for all $l \in]-|M_{\mathrm{I}}|, 0] \cap \mathbb{Z}$. Finally, the real numbers d_{ij} denote the to be specified quadrature weights of the method whereas $w^{l}_{n;m}$ denote the quadrature weights for the lag integrals which can be determined by using the Newton-Cotes formulas [PTVF92].

In order to illustrate how this integration rule works, the meaning of the approximate solutions y_2 and stage approximations Y_2, as well as the related quadrature rules, is demonstrated graphically in Fig. 5.3.1. It is noted that the meaning of the corresponding objects for y_1 is instead clear from the context of the Runge-Kutta methods for ordinary differential [But87, HNW08] and Volterra integro-differential [BH86] equations. It follows from the definitions introduced above that a numerical method based on the defined integration rule is fully determined when its nodes, weight functions and quadrature weights have been chosen. It is possible to choose appropriate nodes and weights by motivating them and by demanding that the so-called order conditions are satisfied. In Sec. 6.3, in particular, a well-motivated class of methods with two internal stages is introduced by requiring that it meets the second-order order conditions derived in App. 6.A. Here, it is found convenient to introduce the nodes and weights of these methods by introducing their Butcher's tables [But87, BH86]. In the case of the above introduced integration rule, a Butcher's table can be written as

$$\begin{array}{c|c|c|c} c & v & a & d \\ \hline & u & b & \end{array} \equiv \begin{array}{c|c|ccc|ccc} c_1 & v_1 & a_{11} & \dots & a_{1s} & d_{11} & \dots & d_{1s} \\ \vdots & \vdots & \vdots & \ddots & \vdots & \vdots & \ddots & \vdots \\ c_s & v_s & a_{s1} & \dots & a_{ss} & d_{s1} & \dots & d_{ss} \\ \hline & u & b_1 & \dots & b_s & & & \end{array}$$

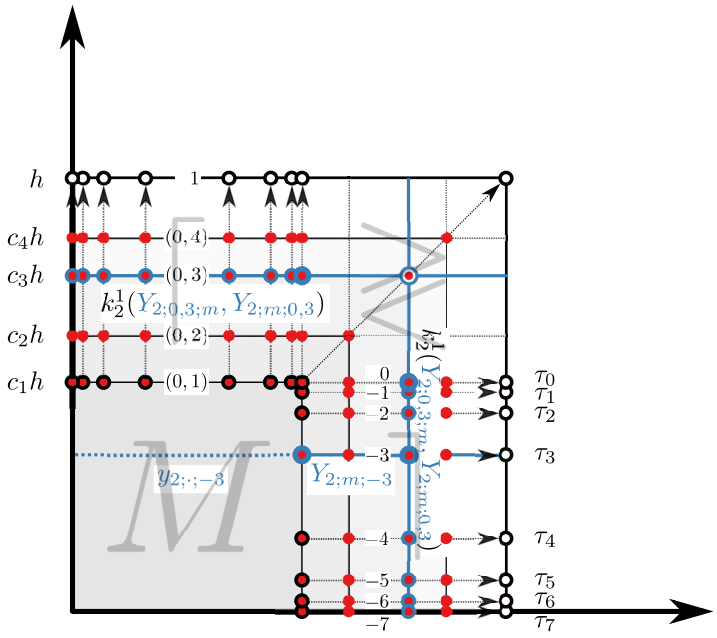

Figure 5.3.1: The numerical integration rule defined in Sec. 5.3.1 is illustrated graphically for y_2 by using a mesh with $|M_{\mathrm{R}}| = 2$ real- and $|M_{\mathrm{I}}| = 8$ imaginary-time points for a method with $s = 4$ internal stages. The possibly overlaying black circles and red bullets denote the mesh points $(z_n; z_m)$ and $(z_{n,i}; z_{n,i})$, $(z_{n,i}; z_m)$, $(z_m; z_{n,i})$, respectively. In blue, by the possibly overlaying small/large circles joined by solid lines and by the dashed lines, it is referred respectively to the stage approximations $Y_{2;0,3;m}$, $Y_{2;0,3;m}$ and the initial values $y_{2;\cdot;-3}$, i.e., the Matsubara (M) components, required to evaluate the collision integrals contained in $N^1_{2;0,3;-3}$. In this context, the large and small circles refer to the stage approximations required by the quadrature $Z^1_{2;0,3;-3}$ and by the lag quadrature $\sum_{\nu=1}^{2} I^1_{2,\nu;0,3;-3}$, respectively. Finally, the black dashed lines with arrows indicate the directions along which the (stage) approximations for the greater/lesser ($\gtrless$), right ($\rceil$) and left ($\lceil$) components are integrated. In the figure, t_0 is set to zero for simplicity.

where, in contrast to the standard case, the weight functions u, v_i, b_j and a_{ij} are to be understood as functions of at most s linear operators. It is due to this difference that, in order to use a Butcher's table to define a method, it is found convenient to introduce some short-hand notations. Firstly, in the following, the operand $\circ$ refers to function composition and, secondly, $\langle \alpha_1, \ldots, \alpha_k|$ refers to a function of k linear operators such that $\langle \alpha_1, \ldots, \alpha_k|(z_1, \ldots, z_k) \equiv \sum_{j=1}^{k} \alpha_j z_j$ where α_j are real numbers. It is then possible to re-express the methods derived in Secs. 6.3.1 and 6.3.2 in terms of their Butcher's tables by introducing

i the one-stage $s = 1$ method

0	1	0	0
	φ_0	φ_1	

which is, in another context, known as the Lie-Euler method

ii the two-stage $s = 2$ method

0	1	0	0	0	0
c	φ_0	φ_1	0	d	$1-d$
	$\varphi_0 \circ \langle b, 1-b|$	$b\varphi_1 \circ \langle b, 1-b|$	$(1-b)\varphi_1 \circ \langle b, 1-b|$		

where $b = 1 - 1/2c$ is a fixed and $c \in]0,1]$ and $d \in [0,1]$ free real parameters

where $\varphi_0(z) \equiv \exp(z)$ and $\varphi_1(z) \equiv (\exp(z)-1)/z$. In **II** [SPAL15b] and [TSK+16], the method ii has been used with the choice that $c = 1$ and $d = 1/2$ for which it reduces to a method which closely resembles the one described in [Bal07, SDL09b]. It is noted that both methods are consistent, cf., Sec. 6.2, since it follows from the choices of the weight functions that

$$\begin{aligned} z_{n+1} &= z_n + h\,, \\ Z_{n+1;n+1} &= Z_{n;n} + h\,, \quad Z_{n+1;m} = Z_{n;m} + h/2\,, \quad Z_{m;n+1} = Z_{m;n} + h/2\,, \\ \zeta_{n+1;n+1} &= \zeta_{n;n}\,, \quad \zeta_{n+1,m} = \zeta_{n;m} + h\,, \quad \zeta_{m;n+1} = \zeta_{m;n} - h\,, \end{aligned}$$

and

$$\begin{aligned} z_{n,i} &= z_n + c_i h\,, \\ Z_{n,i;n,i} &= Z_{n;n} + c_i h\,, \quad Z_{n,i;m} = Z_{n;m} + c_i h/2\,, \quad Z_{m;n,i} = Z_{m;n} + c_i h/2\,, \\ \zeta_{n,i;n,i} &= \zeta_{n;n}\,, \quad \zeta_{n,i;m} = \zeta_{n;m} + c_i h\,, \quad \zeta_{m;n,i} = \zeta_{m;n} - c_i h\,, \end{aligned}$$

for all $m \in]-|M_\mathrm{I}|, n]$ and $n \in [0, |M_\mathrm{R}|[$ which ensures that with the correct initial conditions the contour times are integrated exactly. It is finally hypothesized that the specialized integration rule defined here is not suitable, or at least is inefficient, for the purpose of deriving methods with a high-order of consistency 6.2.3. For one, this is because the quadrature Z are too sparse, i.e., the matrix d is too sparse, to describe the integrals from t_n to $t_n + c_i h$ well, cf., Fig.5.3.1. For another, this is due to the fact that, without an explicit starting procedure, it is not possible to improve the quality of the lag integrals I involved in the first few integration steps beyond the first one. It is for these reasons, amongst some others, that a more versatile integration rule is described and proposed in Sec. 6.1.2.

5.3.2 Overview of Numerical Method

Here, it is the purpose to summarize the main steps of the algorithm implementing the numerical integration methods introduced in the previous section. It is noted that the described method is adapted from the methods described in [Bal07, SDL09b] and that only selected steps are reviewed in a schematic fashion.

I Initial Values:
In order to solve Eqs. (5.6) the real- and mixed-time components contained in $y_{1;0}$ and $y_{2;0;m}$ and $y_{2;m;0}$ are initialized according to Eqs. (4.33) for all $m \in]-|M_\mathrm{I}|, 0] \cap \mathbb{Z}$. In addition, the contour times are initialized such that $z_0 = Z_{0;0} = t_0$, $Z_{0;m} = Z_{m;0} = t_0 - \imath\tau_{|m|}/2$, $\zeta_{0;0} = 0$ and $\zeta_{0;m} = -\zeta_{m;0} = \imath\tau_{|m|}$ for all $m \in]-|M_\mathrm{I}|, 0] \cap \mathbb{Z}$.

II Numerical Integration:
For $n = 0, \ldots, |M_\mathrm{R}| - 2$

i For $i = 1, \ldots, s$

a In order to evaluate the stage approximations $Y_{1;n,i}$, $Y_{2;n,i,m}$ and $Y_{2;m;n,i}$ for all $m \in]-|M_\mathrm{I}|, n] \cap \mathbb{Z}$, i.e., for all off-diagonal times, the weights $v_{1;n,i}$, $v^{\nu}_{2;n,i}$, $a^{j}_{1;n,i}$ and $a^{\nu;j}_{2;n,i}$ of the method are needed for all $\nu \in \{1,2\}$ and $j \in [1, i[\cap \mathbb{Z}$. In the case that either the method i or ii is used, this can be done by taking advantage of the block-diagonal form of the linear operators L such that if $l \in \{0,1\}$ then

$$\varphi_l(\mathsf{L}_{1;n})(\mathsf{y}_1, \mathsf{y}_2) = \big(\mathsf{y}_1, \varphi_l(-\imath\alpha\bar{\Omega}_n)\mathsf{y}_2\big)\,,$$

$$\varphi_l(\mathsf{L}^1_{2;n})(\mathsf{y}_1,\mathsf{y}_2,\mathsf{y}_3,\mathsf{y}_4) = \big(\mathsf{y}_1,\mathsf{y}_2,\varphi_l(-\imath\mathsf{h}_{\mathrm{MF};n})\mathsf{y}_3,\varphi_l(-\imath\alpha\bar{\Omega}_n)\mathsf{y}_4\big)\,,$$
$$\varphi_l(\mathsf{L}^2_{2;n})(\mathsf{y}_1,\mathsf{y}_2,\mathsf{y}_3,\mathsf{y}_4) = \big(\mathsf{y}_1,\mathsf{y}_2,\mathsf{y}_3\varphi_l(\imath\mathsf{h}_{\mathrm{MF};n}),\mathsf{y}_4\varphi_l(\imath\bar{\Omega}_n\alpha)\big)\,,$$

where $\mathsf{L}^{(\nu)}_{\mu;n} \equiv \sum_{k=1}^{s}\eta_k L^{(\nu)}_{\mu;n,k}$ for $\mu,\nu\in\{1,2\}$, $\mathsf{h}_{\mathrm{MF};n}\equiv\sum_{k=1}^{s}\eta_k h_{\mathrm{MF};n,k}$ and $\bar{\Omega}_n \equiv \sum_{k=1}^{s}\eta_k\bar{\Omega}_{n,k}$ with any $\eta_k\in\mathbb{R}$. Moreover, for the system studied in **II** [SPAL15b], both of the matrices $\mathsf{h}_{\mathrm{MF};n}$ and $\alpha\bar{\Omega}_n$ are diagonalizable and hence the corresponding φ-functions have been evaluated by using their diagonal representation [MVL03]. Similarly, in order to evaluate the time-diagonal stage approximation $Y_{2;n,i;n,i}$, the weights $v_{2;n,i}$ and $a^j_{2;n,i}$ of the method are needed for all $j\in[1,i[\cap\mathbb{Z}$. If either the method i or ii is used then this can be done, for instance, by taking advantage of the Taylor series of the φ-functions from which it follows for $l\in\{0,1\}$ that

$$\varphi_l(\mathsf{L}_{2;n})(\mathsf{y}_1,\mathsf{y}_2,\mathsf{y}_3,\mathsf{y}_4) = \left(\mathsf{y}_1,\mathsf{y}_2,\sum_{k=0}^{\infty}\frac{1}{(k+l)!}\mathrm{l}^k_{-\imath\mathsf{h}_{\mathrm{MF};n}}(\mathsf{y}_3),\sum_{k=0}^{\infty}\frac{1}{(k+l)!}\mathrm{l}^k_{-\imath\alpha\bar{\Omega}_n}(\mathsf{y}_4)\right),$$

where the linear operators $\mathrm{l}^k_{\mathsf{x}}$ are defined recursively by $\mathrm{l}^0_{\mathsf{x}}(\mathsf{y})\equiv\mathsf{y}$, $\mathrm{l}^{k+1}_{\mathsf{x}}(\mathsf{y})\equiv\mathsf{x}\mathrm{l}^k_{\mathsf{x}}(\mathsf{y})+\mathrm{l}^k_{\mathsf{x}}(\mathsf{y})\mathsf{x}^\dagger$ for any square matrices x and y of equal dimensions. In practice, in order to preserve the order of consistency of the method, the series need to be truncated at an integer number which is at least as large as the order of consistency of the method. It is noted that in **II** [SPAL15b], the φ-functions have been instead evaluated by diagonalizing the linear operators $\mathsf{L}_{2;n,i}\equiv\mathsf{L}^1_{2;n,i}+\mathsf{L}^2_{2;n,i}$ directly which is however not a suitable approach for larger systems. Independent of the method used to evaluate the weights of the method, if either the method i or ii is used, as done in **II** [SPAL15b], then v_i need not to be evaluated since the identities

$$v^{(\nu)}_{\mu;n,i} = \mathbb{1} + c_i h\sum_{j=1}^{i-1}a^{(\nu;)j}_{\mu;n,i}L^{(\nu)}_{\mu;n,j}\,,\qquad\qquad \mu,\nu\in\{1,2\}\,,$$

where $\mathbb{1}$ is the identity operator, can be instead used. It is also noteworthy that a corresponding relation exists between $u^{(\nu)}_{\mu;n}$ and $b^{(\nu)}_{\mu;n,j}$ for the method i and, provided that $c=1$, for the method ii.

b The exchange-correlation self-energies contained in $k^{\nu}_{2;n,i;n,i}$, $k^1_{2;n,i;m}$ and $k^2_{2;m;n,i}$, which are functions of the stage approximations obtained in step a, are evaluated for all $\nu\in\{1,2\}$ and $m\in]-|M_{\mathrm{I}}|,n]\cap\mathbb{Z}$.

c In order to evaluate the collision integrals $[k^{\nu}_2\circ Y_2]_{n,i;n,i}$, $[k^1_2\circ y_2]_{n,i;m}$ and $[k^2_2\circ y_2]_{m;n,i}$ for all $\nu\in\{1,2\}$ and $m\in]-|M_{\mathrm{I}}|,n]$, firstly, the imaginary-time integrals $[k^{\nu}_2\star Y_2]_{n,i;n,i}$, $[k^1_2\star y_2]_{n,i;m}$ and $[k^2_2\star y_2]_{m;n,i}$ are approximated by using clamped cubic spline interpolation, as described in Sec. 5.2. Secondly, to approximate the corresponding real-time integrals, the quadrature weights $w^l_{n;m}$ are chosen such that

$$\int_0^{hm}dt\;f(t_0+t)\approx h\sum_{l=0}^{n}w^l_{n,m}f(t_0+hl)+\mathcal{O}(h^{q_{n;m}})\,,\qquad\qquad n\geq m\,,$$

where f is a sufficiently continuously differentiable function and $q_{n;m}\in\mathbb{Z}_{\geq 1}$ denotes the order of the quadrature rule. It is due to the uniform mesh spacing h that the Newton-Cotes quadrature [PTVF92] is used in the implementation.

1 If $m<3$ then $w^l_{n;m}=0$ for $l>N^n_m$ and

$$w^l_{n;m}\equiv\int_0^m d\vartheta\;\ell_l^{N^n_m}(\vartheta)\,,l\leq N^n_m\,,$$

where $N_m^n \equiv \min(n, m+2)$ and $\ell_k^{N_m^n}(\vartheta) \equiv \prod_{l=0,l\neq k}^{N_m^n}(\vartheta - l)/(k-l)$ denote the Lagrange cardinal polynomials. In particular, the weights

n	m	$w^0_{n,m}$	$w^1_{n,m}$	$w^2_{n,m}$	$w^3_{n,m}$	$w^4_{n,m}$
1	1	1/2	1/2			
2	1	5/12	2/3	−1/12		
	2	1/3	4/3	1/3		
3	1	3/8	19/24	−5/24	1/24	
	2	1/3	4/3	1/3	0	
	3	3/8	9/8	9/8	3/8	
4	1	251/720	323/360	−11/30	53/360	−19/720
	2	29/90	62/45	4/15	2/45	−1/90
	3	27/80	51/40	9/10	21/40	−3/80
	4	14/45	64/45	8/15	64/45	14/45

which have been obtained by using Mathematica [WR10], are used in the implementation. It is worth a mention that the open Newton-Cotes rules listed here enable higher order quadrature also close to one of the time-axes of the two-time plane.

2 If $m \geq 3$ then $w^l_{n;m} = 0$ for $l > m$. For $l \leq m$, if $m \in \{3, 4\}$ then $w^l_{n;m} = w^l_{m;m}$, where $w^l_{m;m}$ are listed above, else if $m \in [5, 9] \cap \mathbb{Z}$ a composite, or extended, Newton-Cotes rule with the quadrature weights

$w^0_{n;m}$ $w^m_{n;m}$	$w^1_{n;m}$ $w^{m-1}_{n;m}$	$w^l_{n;m}$
5/12	13/12	1

where $l \in \{2, m-2\}$, is used, and otherwise a composite rule with the quadrature weights

$w^0_{n;m}$ $w^m_{n;m}$	$w^1_{n;m}$ $w^{m-1}_{n;m}$	$w^2_{n;m}$ $w^{m-2}_{n;m}$	$w^3_{n;m}$ $w^{m-3}_{n;m}$	$w^4_{n;m}$ $w^{m-4}_{n;m}$	$w^l_{n;m}$
95/288	317/240	23/30	793/720	157/160	1

where $l \in [5, m-5] \cap \mathbb{Z}$, is used. It is noted that these quadrature weights can be found from [PTVF92] for the cases with $m < 10$ while the weights for $m \geq 10$ can be found from [Bak70].

d In order to evaluate the linear operators $L_{1;n,i}$ and $L^{(\nu)}_{2;n,i}$ for $\nu \in \{1, 2\}$, the mean-field one-body electron Hamiltonian $h_{\mathrm{MF};n,i}$ is evaluated by using the stage approximations. Moreover, the non-linear functions $N_{1;n,i}$, $N_{2;n,i;n,i}$, $N^1_{2;n,i;m}$ and $N^2_{2;m;n,i}$ are obtained for all $m \in]-|M_\mathrm{I}|, n] \cap \mathbb{Z}$ by evaluating the mean-field generalized force $F_{\mathrm{MF};n,i}$ and by using the collision integrals which were evaluated in step c.

ii The approximations $y_{1;n+1}$, $y_{2;n+1;n+1}$, $y_{2;n+1;m}$ and $y_{2;m;n+1}$ are evaluated for all $m \in]-|M_\mathrm{I}|, n] \cap \mathbb{Z}$. In order to do this, the weights $u_{1;n}$, $b_{1;n,j}$, $u^{(\nu)}_{2;n}$ and $b^{(\nu)}_{2;n,j}$ are evaluated for all $\nu \in \{1, 2\}$ and $j \in [1, s] \cap \mathbb{Z}$ as described in the step i.a for the weights v and a. All of the required linear operators L and non-linear functions N have been evaluated in the steps i.d.

iii All time-local observables are evaluated, and subsequently printed to a file, from the knowledge of $y_{1;n+1}$ and $y_{2;n+1;n+1}$. The exchange-correlation part of the interaction energy is

evaluated by using all of the newly obtained $y_{2;n+1;m}$ and $y_{2;m;n+1}$ for $m \in]-|M_{\mathrm{I}}|, n+1]\mathbb{Z}$ and the quadrature rules listed in step i.c to evaluate the lesser components of the collision integrals at $(t_{n+1}; t_{n+1})$.

It is noted that instead of solving for all of the components, for instance, only $Y_{2;n,i;m}$ and $y_{2;n+1;m}$ are solved for $i \in [1, s] \cap \mathbb{Z}$ and $m \in]-|M_{\mathrm{I}}|, n] \cap \mathbb{Z}$ while $Y_{2;m;n,i}$ and $y_{2;m;n+1}$ are obtained by using the symmetries of Eqs. (4.30). Moreover, due to the consistency of the method contour times are not solved explicitly.

III Post Processing:
In the end, the greater, lesser and right components of the electron and phonon propagators contained in $y_{2;n;m}$ are printed to a file for all $(n, m) \in \{(k, l), (l, k) : k \in]0, |M_{\mathrm{R}}|[\cap\mathbb{Z}, l \in [-|M_{\mathrm{I}}|, |M_{\mathrm{R}}|[\cap\mathbb{Z}\}$.

It is noted here that if $c = 1$, as in **II** [SPAL15b], then, in principle, the only difference between the proposed method and the one described in [Bal07, SDL09b] is how the weight functions on the time-diagonal are evaluated and how the integrals are discretized.

5.4 Hybrid (MPI/openMP) Parallel Implementation

In the previous sections, it has been described how the Kadanoff-Baym equations are posed and solved numerically in the present work. In practice, it is found by solving them that the two-time structure of the real-time equations leads to a quadratic scaling of the memory requirements and a cubic scaling of the computational time with respect to both the spatial and temporal dimensions. It is then quickly observed that solving for the real- and mixed-time components is a computationally intensive task already for simple model systems such as those studied in **II** [SPAL15b] and **III** [SML12]. In order to alleviate the constraints set by the complexity of the problem, it is possible to implement a parallel algorithm relying on distributed memory parallelism as described in [Bal11]. In what follows, some of the main points of this algorithm are summarized, while trying to complement the discussion in the original work [Bal11], and the performance of our implementation is illustrated by showing its scaling characteristics.

Message Passing Interface (MPI) [MPIF15] is a specification describing in essence how data is to be transfered from one MPI process, henceforth simply referred to as a process, to another in a (distributed) parallel programming model. OpenMP Application Programming Interface (API) [OARB15] is instead defined as a specification of a collection of directives, routines, and variables which provide a (shared) parallel programming model. In the following, a hybrid parallel algorithm, which relies on an MPI implementation to realize parallelism on a distributed memory architecture and OpenMP to realize shared memory parallelism (threading) on each node of the distributed memory system, is described. In **II** [SPAL15b], our results were obtained by running the parallel program based on this algorithm on a Cray XC40 supercomputer currently consisting of 1688 compute nodes each with two 12-core Intel (Xeon) Haswell processors operating @2.6GHz and 64GB of shared memory. [1] On the other hand, in **III** [SML12], our results were obtained by using the predecessors of the program, algorithm and supercomputer [2] mentioned above. In order to proceed to describe the algorithm, it is good to keep in mind that it is designed such that self-energies which are evaluation functionals can be evaluated locally, i.e., no parallel communication is needed, and once the self-energies are made available, by the means of parallel communication, to all processes then also the collision integrals

[1] Sisu at CSC (Center for Scientific Computing https://www.csc.fi/)
[2] Louhi at CSC (decommissioned in May 2013)

can be evaluated locally. In the following, by revisiting the steps outlined in Secs. 5.2 and 5.3.2, it is reviewed how this is accomplished in practice

If `tasks` (> 1) MPI processes labeled uniquely by the integers $\texttt{id} \in [0, \texttt{tasks}[\cap \mathbb{Z}$ are given then the algorithm assigned with $\texttt{itpts} = |M_\mathrm{I}| \in 2\mathbb{Z}$ imaginary- and $\texttt{rtpts} = |M_\mathrm{R}|$ real-time points proceeds as follows.

A Imaginary-Time Problem:
It is noted that, due to a focus of the author towards the real-time problem, the imaginary-time problem has been only partially parallelized using MPI while OpenMP is used ubiquitously via `#pragma omp parallel for` to parallelize for-loops over mainly temporal indices. Nonparallel stages are indicated below with 'serial'.

I Initial Guess:
All processes initialize the zeroth iterate y_2^0 with the initial guess for all $\tau_p \in -M_\mathrm{I}$ (serial).

II Fixed-Point Iteration:
For $k = 0, \ldots, \infty$

i All processes evaluate the mapping $\mathcal{F}(y_2^k)$ for all $\tau_p \in -M_\mathrm{I}$ (serial)

ii The process with the rank `id` evaluates the integral $\imath[a \star b](-\tau_p)$ for all

$$p \in \mathbb{Z} \cap [\texttt{beg}_\texttt{id}, \texttt{beg}_\texttt{id} + \texttt{tpts}_\texttt{id}[\,.$$

such that if [3]

$$\begin{aligned} \texttt{id}_0 &= \texttt{itpts} \bmod \texttt{tasks}\,, \\ \texttt{tpts} &= \texttt{itpts}/\texttt{tasks}\,, \end{aligned}$$

then

$$\texttt{tpts}_\texttt{id} = \begin{cases} \texttt{tpts} + 1 & \texttt{id} < \texttt{id}_0 \\ \texttt{tpts} & \text{otherwise} \end{cases},$$
$$\texttt{beg}_0 = 0\,, \quad \texttt{beg}_\texttt{id} = \texttt{beg}_{\texttt{id}-1} + \texttt{tpts}_{\texttt{id}-1}\,, \quad \texttt{id} \neq 0\,,$$

e.g., if $\texttt{tasks} = 4, \texttt{itpts} = 8$ then graphically

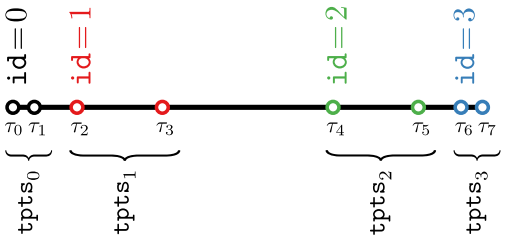

In the end, all integrals made available to all processes by using `MPI_Allgatherv`.

iii All processes evaluate the new iterate y_2^{k+1} by possibly using DIIS (serial).

B Real-Time Problem:
Assign the rank 0 in `MPI_COMM_WORLD` to 'diagonal' and the rest to 'off-diagonal' `MPI_Group`

[3] If $n, k \in \mathbb{Z}$ then n mod k equals to the remainder $r \in \mathbb{Z}_{\geq 0}$ and, if written in the `monospace` font, `n/k` equals to the quotient $q \in \mathbb{Z}$ which are defined by $n = kq + r$ where $r < |k|$. Note that in C++ the sign of the remainder given by the operand % is implementation dependent.

such that in the latter each process is labeled uniquely by the integers $\mathtt{id} \in [0, \mathtt{tasks} - 1[\cap \mathbb{Z}$. In the algorithm, work is distributed to the processes belonging to 'off-diagonal' as evenly as possible by following the principle that the process with the rank $\mathtt{id} + 1$ has less, or an equal amount of data than, the process with the rank $\mathtt{id}$.

I Initial Values:
The 'diagonal' process stores the initial values of the local and lesser/greater components indexed by 0 and $(0;0)$. In 'off-diagonal', the process with the rank $\mathtt{id}$ stores the initial values of the right component indexed by $(0;-p)$ for all

$$p \in \mathbb{Z} \cap \begin{cases} [\mathtt{beg}_{\mathtt{id}}, \mathtt{beg}_{\mathtt{id}} + \mathtt{tpts}_{\mathtt{id}}[& p < \mathtt{itpts}/2 \\ [\mathtt{itpts} - \mathtt{beg}_{\mathtt{id}} - \mathtt{tpts}_{\mathtt{id}} - 1, \mathtt{itpts} - \mathtt{beg}_{\mathtt{id}}[& \text{otherwise} \end{cases} .$$

such that if

$$\begin{aligned} \mathtt{id}_0 &= (\mathtt{itpts}/2) \bmod (\mathtt{tasks} - 1) , \\ \mathtt{tpts} &= (\mathtt{itpts}/2)/(\mathtt{tasks} - 1) , \end{aligned}$$

then

$$\mathtt{tpts}_{\mathtt{id}} = \begin{cases} \mathtt{tpts} + 1 & \mathtt{id} < \mathtt{id}_0 \\ \mathtt{tpts} & \text{otherwise} \end{cases} ,$$

$$\mathtt{beg}_{\mathtt{id}_0} = 0 , \quad \mathtt{beg}_{\mathtt{id}} = \mathtt{beg}_{(\mathtt{id}+1) \bmod (\mathtt{tasks}-1)} + \mathtt{tpts}_{(\mathtt{id}+1) \bmod (\mathtt{tasks}-1)} , \quad \mathtt{id} \neq \mathtt{id}_0 ,$$

e.g., if $\mathtt{tasks} = 4, \mathtt{itpts} = 8$ then graphically

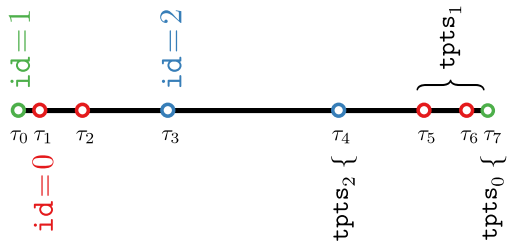

In 'off-diagonal', the process with the rank $\mathtt{id}_0$ stores the initial values of the lesser/greater and left components indexed by $(0;0)$ and $(-p;0)$ for all $p \in [0, \mathtt{itpts}[\cap \mathbb{Z}$.

II Numerical Integration:
For $n = 0, \ldots \mathtt{rtpts} - 2$:

i For $i = 1, \ldots, s$:

a The 'diagonal' process evaluates and stores the stage approximations for the local and lesser/greater components indexed by (n, i) and $(n, i; n, i)$. In 'off-diagonal', the process with the rank $\mathtt{id}$ evaluates and stores the stage approximations for the right components indexed by $(n, i; -p)$ for all p defined in step I. In 'off-diagonal', for all $q \in [0, n]$, the process with the rank $(\mathtt{id}_0 + q) \bmod (\mathtt{tasks} - 1)$ evaluates and stores the stage approximations for the lesser/greater components indexed by $(n, i; q)$. In the end, all of the evaluated stage approximations for the left and lesser/greater components are communicated by using `MPI_Isend`/`MPI_Irecv` to the process with the rank $(\mathtt{id}_0 + n + i) \bmod (\mathtt{tasks} - 1)$ which stores them. For example, if $\mathtt{tasks} = 4$, $\mathtt{itpts} = 8$, $n = 4$ and $i = 1$ then graphically for the local component

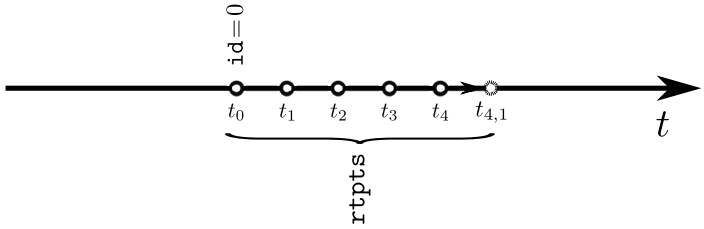

and for the left, right and lesser/greater components [4]

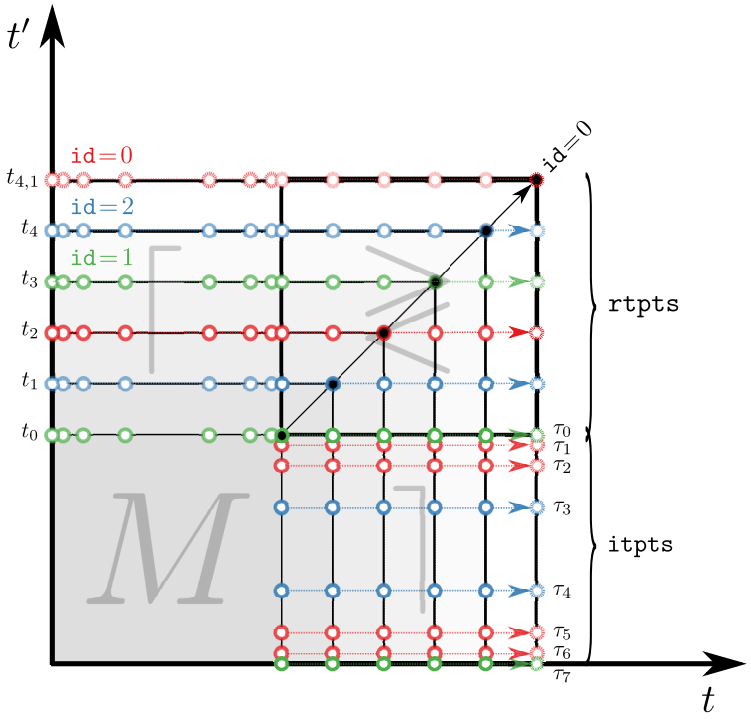

where $t_{4,1} \equiv t_4 + c_i h$ and the rank $id = 0$ typeset in black refers to the 'diagonal' process.

b The self-energies are evaluated 'locally' as follows. The 'diagonal' process evaluates the local components of the self-energies indexed by (n, i). In 'off-diagonal', each processes evaluates the right and lesser/greater components of the self-energies indexed respectively by $(n, i; -p)$ and $(n, i; q)$ for the same p and q as in step a. In the end, all processes communicate the evaluated local, right and lesser/-greater components of the self-energies to all processes by using `MPI_Bcast` and `MPI_Allgatherv`.

c In 'off-diagonal', each process evaluates and stores the right and lesser/greater components of the collision integrals 'locally', i.e., as done in step b for the self-energies. In the end, the process with the rank $(\texttt{id}_0+n+i) \mod (\texttt{tasks}-1)$ in 'off-diagonal' communicates the lesser/greater components of the collision integrals to the process 'diagonal'.

d All processes evaluate and store the linear operators L. All processes evaluate and

[4] In contrast to what the figure suggests, both the greater and right components are stored and evaluated on the edge (t, t_0) and (t, τ_0) in the current implementation and hence the data distribution agrees with the logic of the algorithm.

store the local, right and lesser/greater components of the non-linear functions N 'locally', i.e., as done in the step b for the self-energies.

ii All processes evaluate and store the approximations y as done in the step i.a but with n, i replaced by $n+1$. In the end, the components are instead communicated to the process wit the rank $(\texttt{id}_0 + n + 1) \bmod (\texttt{tasks} - 1)$ in 'off-diagonal'.

iii In 'off-diagonal', each process evaluates the integrands of the lesser components of the collision integrals 'locally', i.e., as in the step i.a for the self-energies but with n, i replaced by $n+1$, and communicates the result to the process 'diagonal' by using `MPI_Isend/MPI_Irecv`. The process 'diagonal' evaluates and writes, by using the HDF5 library [THG16], all time-local observables and the exchange-correlation part of the interaction energy to a file in binary format.

III Post-Processing:
All processes write the left and lesser/greater components to a file in binary format by using the parallel interface to the HDF5 library.

In what follows, it is verified that the algorithm and its implementation indeed speed up the calculations. In order to do this, it is shown how the run wall time behaves when the implementation is given more resources to handle a fixed workload and when additional resources are introduced to handle a simultaneously increasing workload. In other words, both the strong and weak scaling of the implementation is demonstrated. A strong scaling test shows how big of a portion of the work is performed in parallel and how the parallel communication overhead scales with the resources while a weak scaling test indicates how the overhead scales with the workload. In the tests, the programs run wall times are recorded with different numbers of CPU cores (n) and the speed up t_N/t_n, where t_N is a reference wall time run with N cores, is used as a measure of the strong scaling. In theory, the speed up is limited by Amdahl's law [Amd67] which states that if p denotes the parallelizable portion of the serial program then

$$S_{N,n} \equiv \frac{1-p+p/N}{1-p+p/n}\,, \tag{5.10}$$

is the maximum attainable speed up. Instead, the weak scaling test is performed by recording the run wall times when the number of cores n is increased while the ratio $\texttt{rtpts}/n$ is kept a constant. If the run wall time shows then, instead of a cubic, a quadratic dependence on `rtpts` then it is said that the implementation scales ideally.

In order to use relevant data sets for the scaling tests, the imaginary- and real-time mesh sizes have been chosen such that they are comparable to the ones used in **II** [SPAL15b]. In the same spirit, the spatial basis size is set to two but instead of the two-site Holstein model, due to a more recent focus of the author towards open systems, cf., [TSK+16], the exact setup is that of a single quantum mechanical harmonic oscillator coupled to two environments also consisting of harmonic oscillators. The physical parameters, although not very relevant for the scaling, are equal to the ones used in Fig. 3(b) of [TSK+16] with the substitution $T_L = T_R = T_C = 1$. It is instead relevant to illustrate the effect of the mesh sizes to the scaling and hence the two setups, 'small' with $\texttt{itpts} = 98$ and $\texttt{rtpts} \in \{96, 384, 1536\}$, and 'large' with $\texttt{itpts} = 976$ and $\texttt{rtpts} \in \{960, 3840, 15360, 30720\}$, are specified. Also, these sets have been chosen so that the computations fit comfortably within the core 576(18400) and 576, and wall time 30min(4h) and 12h limits of 'test(_large)' and 'small' queues of Sisu at CSC where the scalability tests have been conducted. On Sisu, the code has been compiled with

```
# compiler
icpc (ICC) 15.0.2 20150121
# compiler flags
-DNDEBUG -O3 -opt-prefetch -unroll-aggressive
-fno-alias -align -fp-model precise -openmp
```

where `-openmp` has been neglected when compiling a non-hybrid (MPI) program. In the non-hybrid (MPI) 'small' case with 2-96 cores, additional cores have been utilized by allowing for more MPI processes such that the program is run by specifying

```
# slurm options
--exclusive
# aprun options
-ss -cc cpu
```

In the the hybrid (MPI+OpenMP) case, additional cores have been utilized by allowing more threads until 24 cores have been reached beyond which more MPI processes have been added each of which adds another 12 cores. If $n \in 2\mathbb{Z}_+$ cores are given then this requires instead

```
# slurm options
--exclusive
# threading options
OMP_NUM_THREADS=min(n/2,12);OMP_MAX_ACTIVE_LEVELS=2;OMP_SCHEDULE="guided,1";
OMP_NESTED=TRUE;OMP_THREAD_LIMIT=min(n/2,12);KMP_DETERMINISTIC_REDUCTION=yes;
KMP_AFFINITY="granularity=fine,compact,1"
# aprun options
-ss -cc numa_node
```

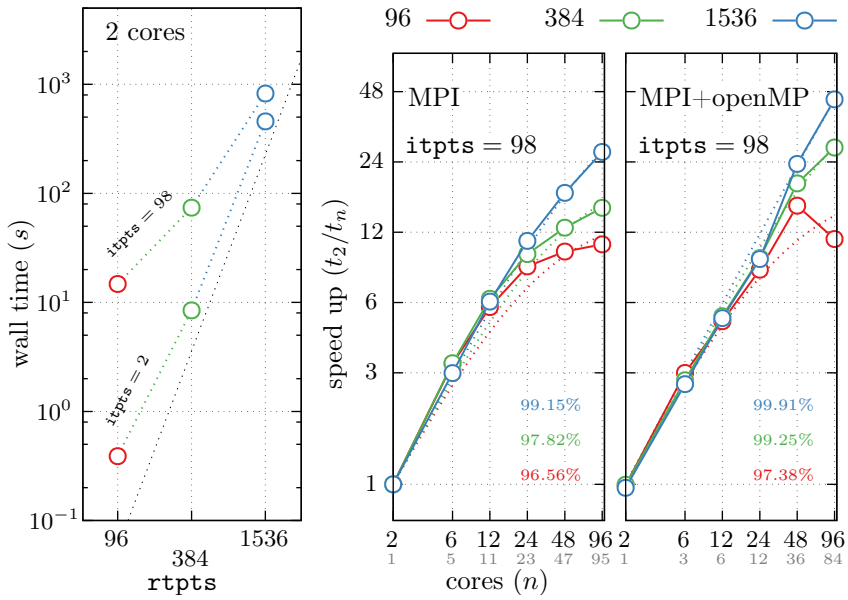

n	MPI -n
2	2
6	6
12	12
24	24
48	48
96	96

n	MPI+openMP -d	MPI+openMP -n
2	1	2
6	3	2
12	6	2
24	12	2
48	12	4
96	12	8

Figure 5.4.1: Illustration of the strong scaling for 2-96 CPU cores in the 'small' case. The left panel shows the wall times for the references calculations with 2 cores where the dashed line indicates a cubic scaling. The middle panels show the speed up t_2/t_n, where t_n is the wall time with n cores, for the cases in which parallelism is achieved by the non-hybrid (MPI) and hybrid (MPI+openMP) schemes. Here, the smaller tic labels count the cores assigned to 'off-diagonal' and the dashed lines are Gnuplot fits to the Amdahl's law of Eq. (5.10) with the corresponding degrees p of parallelism shown with a matching color code in the lower right corners of the graphs. In the tables, the relations between core (n), thread (`-d`) and task (`-n`) numbers given, in addition to `-j 1 -S` $\min(n/2, 12)$ `-N` $\min(n, 24)$, to aprun are shown.

It is remarked, before proceeding to discuss the results of the scaling tests, that it is possible that the speed ups shown below give a distorted picture of the (absolute) strong scaling as the used

reference wall time is obtained by using the same parallel program and by using either 2 or 60 cores instead of a single core. That said, in Fig. 5.4.1, the scalability results are shown for the 'small' case for 2-96 CPU cores. In the left panel, the wall times are shown for the reference runs with 2 cores demonstrating that for a fixed number of cores, in particular when `itpts` = 2 which is shown for reference, the wall times tend to roughly cubic scaling with respect to `rtpts`. In the middle panels, it is shown that in the 'small' case the implementation achieves a reasonably good speed up for almost all core numbers independently of whether parallelism is realized by using the non-hybrid (MPI) or hybrid (MPI+OpenMP) schemes. It is remarked here that t_2 is chosen as the smaller of the wall times for the non-hybrid and hybrid schemes. Notice also that the super ideal scaling observed for 6-12 cores does not appear if 'off-diagonal' cores, shown with smaller tic labels, are used which supports the conclusion that it is an artifact of the reference wall time. Nevertheless, the main observation is that the speed up and the approximate degree of parallelism p of Eq.(5.10) shown in percentages are the higher the larger the ratio $(\texttt{rtpts} + \texttt{itpts})/n$. This agrees with the expectation that the collision integrals, which are performed parallel and there is no parallel overhead involved, become the most time consuming part of the algorithm for a sufficiently large `rtpts` + `itpts`. In the hybrid implementation, the task of evaluating the collision integrals is distributed within a given MPI process among the available threads/cores by using OpenMP. It is hence reasonable to expect that the wall time spend evaluating the collision integrals is not noticeably affected, whereas the overhead associated with parallel communication is reduced, when processes are replaced with threads. In congruence with the above, it is observed that for the higher numbers $48, 96$ of cores and for `rtpts` $= 384, 1536$ the hybrid scheme scales better than the non-hybrid implementation

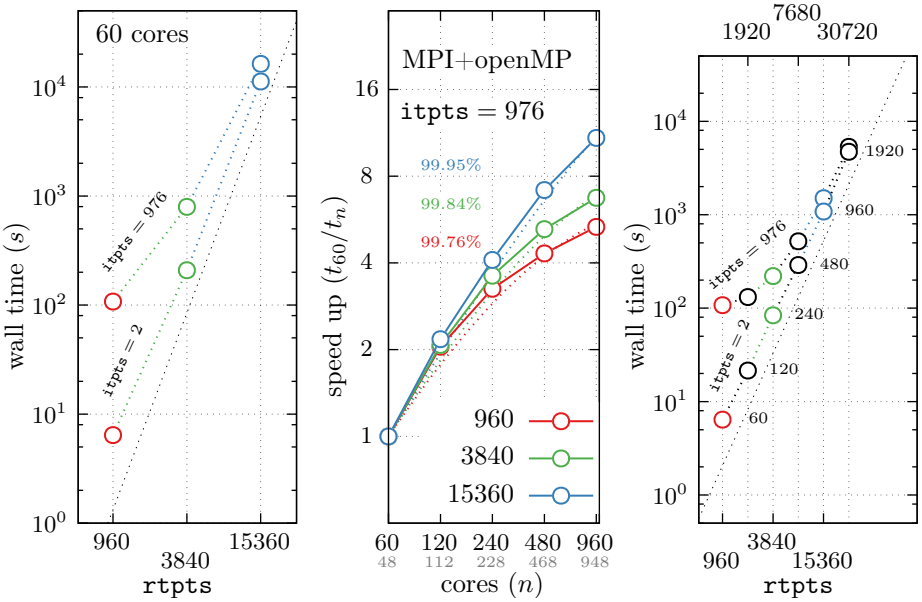

Figure 5.4.2: Illustration of the strong and weak scaling for 60-960(1920) CPU cores in the 'large' case. The left panel shows the wall times for the references calculations with 60 cores where the dashed line indicates a cubic scaling. The middle panel shows the speed up t_{60}/t_n, where t_n is the wall time with n cores, for the cases in which parallelism is achieved by the hybrid (MPI+openMP) scheme. Here, the smaller tic labels count the cores assigned to 'off-diagonal' and the dashed lines are Gnuplot fits to the Amdahl's law of Eq. (5.10) with the corresponding degrees p of parallelism shown with a matching color code in the upper left part of the graph. The right panel shows the wall time when both n, denoted with labels next to points in the graph, and `rtpts` are increased. Additional aprun options are `-n` $(1 + \lfloor n/12 \rfloor)$ `-d 12 -j 2 -S 1 -N 2` where $\lfloor\rfloor$ is the floor function.

In Fig. 5.4.2, the scalability results are shown for the 'large' case for 60-960(1920) cores and only for the hybrid scheme due to the observation that it scales better than the non-hybrid scheme for the 'small' case. In the left panel, the reference wall times obtained with 60 cores are shown and, in the middle panel, the speed up for 60-960 cores together with the approximate degree of parallelism p obtained by fitting the data to Eq. (5.10) is shown. It is observed that the speed up behaves qualitatively as in the 'small' case and, although communication overhead is expected to be larger, since there is more data to communicate, a high percentage of the approximate degree of parallelism is achieved. In the right panel, to mimic weak scaling, it is shown that there exists a relatively large region (cores $\times$ workload) in which the cubic scaling, shown in the right panel, can be roughly transformed into a quadratic scaling by scaling the number of cores equally as `rtpts` is increased.

Overall, it has been shown that the algorithm and its implementation have relatively good scaling characteristics which improve when the ratio $(\texttt{rtpts} + \texttt{itpts})/n$ increases. This is in agreement with the scaling tests performed in [Bal11]. It is also expected, by the design of the algorithm, that neither good strong nor weak scaling can be achieved for $(\texttt{rtpts} + \texttt{itpts})/n \ll 1$ which means that the current method is not ideal for problems with large spatial bases and comparatively small imaginary- or real-time meshes. It may be possible to circumvent this bottleneck by extending the parallelism to spatial dimensions by distributing the columns of the propagator matrices to different processes which should preserve most of the favorable characteristics of the discussed algorithm.

6 Numerical Integration of Integro-Differential Equations

It is the purpose of this chapter to justify the numerical method described in Sec. 5.3.1 and used in **II** [SPAL15b] to solve the real-time Kadanoff-Baym equations. Instead, it is referred to [Bal07, SDL09b] for the justification of the numerical method used in **III** [SML12], although due to the similarities between the two methods, also the latter finds some of its motivation in the following. It is noted in advance, in the manner of a disclaimer, that the numerical method proposed in the following is, strictly speaking, only motivated as no complete convergence theory is provided. However, an attempt is made to justify the method as completely as was possible in the time-frame available for compiling this work and the documentation of this task in its full extent is left to future work. That said, in what follows, a numerical integration rule, which encompasses the methods introduced in Sec. 5.3.1, is proposed to solve the real-time Kadanoff-Baym equations. In order to do this, it is found convenient, for the sake of clarity and generality, to switch to a more general notation. It follows, by switching to the collective notation in terms of y_1 and y_2 introduced in Sec. 5.3.1, or to be more precise by generalizing it for the real- and mixed time components, that the real-time Kadanoff-Baym equations, with a self-energy which is an evaluation functional, constitute to an initial value problem which can be outlined as follows.

It is said that y_1 and y_2 solve the initial value problem with the initial conditions ϕ_1 and ϕ_2, if it holds that $y_1(t) = \phi_1(t)$ and $y_2(t;t') = \phi_2(t;t')$ for all $t, t' \in [t_0 - \tau, t_0]$ where $\tau \geq 0$ such that for $t \in [t_0, T[$ and $(t, t') \in [t_0-\tau, T[\times[t_0-\tau, T[\setminus [t_0-\tau, t_0[\times[t_0-\tau, t_0[$ where $T \geq 0$ the integro-differential equations

$$\begin{aligned} \frac{d}{dt} y_1(t) &= F_1(y_1(t), y_2(t;t), I_1(t)) \,, \\ I_1(t) &\equiv \int_{t_0-\tau}^{t} d\bar{t}\; K_1(y_2(t;\bar{t}), y_1(\bar{t})) \,, \end{aligned} \tag{6.1a}$$

$$\frac{\partial}{\partial t} y_2(t;t') = F_2^1(y_1(t), y_2(t;t), y_2(t;t'), I_{2,1}^1(t;t'), I_{2,2}^1(t;t')) \,, \tag{6.1b}$$

$$\frac{\partial}{\partial t'} y_2(t;t') = F_2^2(y_1(t'), y_2(t';t'), y_2(t;t'), I_{2,1}^2(t;t'), I_{2,2}^2(t;t')) \,, \tag{6.1c}$$

$$\begin{aligned} I_{2,1}^{\nu}(t;t') &\equiv \int_{t_0-\tau}^{t} d\bar{t}\; K_{2,1}^{\nu}(y_2(t;\bar{t}), y_2(\bar{t};t')) \,, \\ I_{2,2}^{\nu}(t;t') &\equiv \int_{t_0-\tau}^{t'} d\bar{t}\; K_{2,2}^{\nu}(y_2(t;\bar{t}), y_2(\bar{t};t')) \,, \end{aligned}$$

are satisfied. In particular, due to the structure of the real-time Kadanoff-Baym equations in the presence of time-local mean-field self-energies, it is relevant to considered the case that the vector fields F_1 and F_2^{ν} are given explicitly by

$$F_1(y_1(t), y_2(t;t), I_1(t))$$

$$= L_1(y_1(t), y_2(t;t))y_1(t) + N_1(y_2(t;t), I_1(t))\,, \qquad t \geq t_0\,, \tag{6.2a}$$

$$F_2^1(y_1(t), y_2(t;t), y_2(t;t'), I_{2,1}^1(t;t').I_{2,2}^1(t;t'))$$
$$= L_2^1(y_1(t), y_2(t;t))y_2(t;t') + N_2^1(y_2(t;t'), I_{2,1}^1(t;t'), I_{2,2}^1(t;t'))\,, \qquad t \geq t', t \geq t_0\,, \tag{6.2b}$$

$$F_2^2(y_1(t'), y_2(t';t'), y_2(t;t'), I_{2,1}^2(t;t'), I_{2,2}^2(t;t'))$$
$$= L_2^2(y_1(t'), y_2(t';t'))y_2(t;t') + N_2^2(y_2(t;t'), I_{2,1}^2(t;t'), I_{2,2}^2(t;t'))\,, \qquad t' \geq t, t' \geq t_0\,, \tag{6.2c}$$

where, for $\nu, \mu \in \{1, 2\}$, L_1 and $L_\mu^{(\nu)}$ denote linear operators and N_1 and N_μ^ν are possibly non-linear functions. Here, by linearity of L it is meant that $L_\mu^{(\nu)}(y_1(t), y_2(t,t))$ are linear operators.

It is seen, when the equations are rephrased like above, that the real-time Kadanoff-Baym equations can be understood as coupled one- [BH86, Cor91] and, a variant of, two-dimensional Volterra integro-differential equations. It is then also proposed that they can be solved by methods which can be derived by using, or by extending into two dimensions, the principles behind the derivation of numerical integration methods for one-dimensional Volterra integro-differential equations. In particular, here, it is the purpose to follow the ideas behind the derivation of one-step Runge-Kutta methods for one-dimensional Volterra integro-differential equations [WP68]. In what follows, in order to pursue this idea, a motivation for the structure of the integration rule is presented followed by an introduction to the concepts of consistency and convergence similarly to [Lub82], where a systematic theory for one-step Runge-Kutta methods was developed. In the end, by requiring that the so-called order conditions are satisfied, the class of second order methods introduced in Sec. 5.3.1, whose variant has been used in **II** [SPAL15b], is justified.

6.1 Numerical Integration Rule

6.1.1 Motivation

Here, the structure of a class of one-step methods designed to numerically solve the initial value problem outlined above is motivated, cf., [WP68]. In order to solve for y, it must be possible to evaluate the derivatives of y_1 and y_2, i.e., the vector fields F and consequently the integrals I, at t and (t, t') which requires the knowledge of y_2 at $\{(t, \bar{t}), (\bar{t}, t') : \bar{t} \in [t_0 - \tau, \max(t, t')]\}$ as has been illustrated in the context of Sec. 5.3.1 in Fig. 5.3.1. Hence, in order to apply numerical quadrature effectively, by making the solution available at all quadrature points, it is preferable to design an integration rule which results into y_2 being represented on a two-dimensional mesh which is a direct product of the one-dimensional mesh chosen to represent y_1 with itself. To begin with, it is assumed, in congruence with this idea, that the initial values of y_2 are available on the mesh $M_\mathrm{I}^2 \equiv M_\mathrm{I} \times M_\mathrm{I}$ where M_I consists of the mesh points referred to by $t_n \in [t_0 - \tau, t_0]$ such that $t_{n+1} > t_n$ and $n \in]-|M_\mathrm{I}|, 0] \cap \mathbb{Z}$. It is noted that the mesh M_I can be refined arbitrarily independent of the integration rule to be specified so that, by opting to discretize the initial values of the solution here, no real restriction on the method is posed. It then holds that if the given initial values of y_1 on M_I are augmented with an approximation for y_1 at $t_0 + h_0$ then it is consistent with the above to augment the initial values of y_2 with approximations for y_2 at $(t_0 + h_0, t)$, $(t, t_0 + h_0)$ and $(t_0 + h_0, t_0 + h_0)$ where $t \in M_\mathrm{I}$ such that the direct product structure is guaranteed. In Fig. 6.1.1, an illustration of this logic, with a possible choice for the mesh M_I, is presented. In agreement with the principles of the numerical integration of initial value problems, it is then possible to recursively continue this process in order to generate a sequence of approximations for y_1 at $t_1 \equiv t_0 + h_0, t_2 \equiv t_1 + h_1, \ldots$ and simultaneously for y_2 on the corresponding direct product mesh.

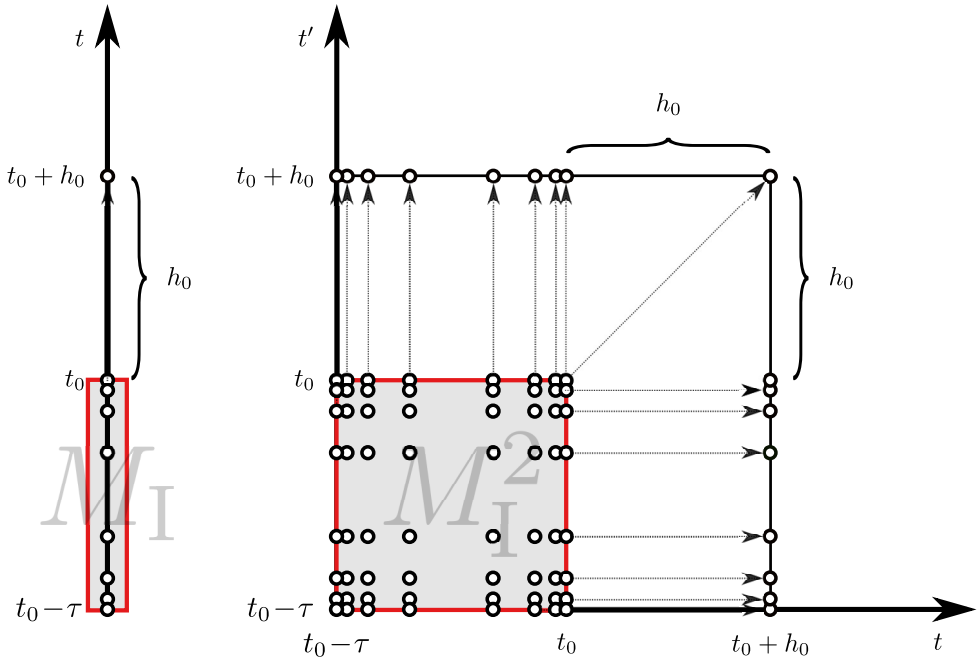

Figure 6.1.1: An illustration of the one- and two-dimensional meshes after the first integration step of a potential numerical method designed to solve the coupled one and two-dimensional Volterra integro-differential equations. Here, h_0 denotes the step size while M_{I} and $M_{\mathrm{I}}^2 \equiv M_{\mathrm{I}} \times M_{\mathrm{I}}$ denote the one- and two-dimensional meshes which are used to discretize the initial values enclosed in the figure within the red borders. In the figure, an example with $|M_{\mathrm{I}}| = 8$ mesh points is shown of a possible choice for M_{I}. It is noted that the new mesh points at $t_0 + h_0$ preserve the direct product structure of the two dimensional mesh.

It is then the task to motivate how the first step of this recursive process can be realized. In order to do so, the considered integro-differential equations are converted into integral equations which, by mimicking how the Runge-Kutta methods can be motivated in the case of the one-dimensional ordinary differential or Volterra integro-differential equations, are discretized by using the $s \in \mathbb{Z}_{\geq 1}$ integration nodes $c_i \in [0,1]$ for $i \in [1,s] \cap \mathbb{Z}$. However, instead of trivially integrating the equations, to carry-out the conversion to an integral equation, it is possible to exploit the special structure of the vector fields similarly to what is done when the so-called exponential integrators are derived for semi-linear ordinary differential equations [HO10]. In the case of the exponential integrators, it follows from the semi-linear structure of the equations, i.e., $F = Ly + N$, that a variation of constants formula can be introduced and it is discretized instead of the trivial integral equation. In order to proceed analogously here, it is first noted that it is possible to rewrite the considered integro-differential equations in terms of the formally equivalent system of the coupled differential and integral equations

$$\begin{aligned} \partial_z u^{(\nu)}_{\mu;0,i}(z;z_0) &= c_i \underbrace{L^{(\nu)}_{\mu}(t_0 + c_i z)}\, u^{(\nu)}_{\mu;0,i}(z;z_0)\,, \qquad (6.3a)\\ &\equiv L^{(\nu)}_{\mu}(y_1(t_0 + c_i z), y_2(t_0 + c_i z; t_0 + c_i z)) \\ \partial_z u_{2;0,ij}(z;z_0) &= \Big(c_i L^1_2(t_0 + c_i z) + c_j L^2_2(t_0 + c_j z)\Big) u_{2;0,ij}(z;z_0)\,, \qquad (6.3b) \end{aligned}$$

and

$$y_1(t_0 + c_1 h_0) = u_{1;0,i}(h_0;0) y_1(t_0)$$

$$+ c_i \int_0^{h_0} dz\; u_{1;0,i}(h_0;z)\underbrace{N_1(t_0+c_iz)}_{\equiv N_1(y_2(t_0+c_iz;t_0+c_iz),I_1(t_0+c_iz;t_0+c_iz))}, \tag{6.3c}$$

$$\begin{aligned} y_2(t_0+c_ih_0;t_0+c_jh_0) &= u_{2;0,ij}(h_0;0)y_2(t_0;t_0) \\ &\quad + c_i\int_0^{h_0} dz\; u_{2;0,ij}(h_0;z)N_2^1(t_0+c_iz;t_0+c_jz) \\ &\quad + c_j\int_0^{h_0} dz\; u_{2;0,ij}(h_0;z)N_2^2(t_0+c_iz;t_0+c_jz)\,, \end{aligned} \tag{6.3d}$$

$$y_2(t_0+c_ih_0;t_n) = u^1_{2;0,i}(h_0;0)y_2(t_0;t_n) + c_i\int_0^{h_0} dz\; u^1_{2;0,i}(h_0;z)\underbrace{N_2^1(t_0+c_iz;t_n)}_{\equiv N_2^1(y_2(t_0+c_iz;t_n),I^1_{2,1}(t_0+c_iz;t_n),I^1_{2,2}(t_0+c_iz;t_n))}, \tag{6.3e}$$

$$y_2(t_n;t_0+c_ih_0) = u^2_{2;0,i}(h_0;0)y_2(t_n;t_0) + c_i\int_0^{h_0} dz\; u^2_{2;0,i}(h_0;z)\underbrace{N_2^2(t_n;t_0+c_iz)}_{\equiv N_2^2(y_2(t_n;t_0+c_iz),I^2_{2,1}(t_n;t_0+c_iz),I^2_{2,2}(t_n;t_0+c_iz))}, \tag{6.3f}$$

for all $\nu,\mu\in\{1,2\}$, $i,j\in[1,s]\cap\mathbb{Z}$, $n\in]-|M_I|,0]\cap\mathbb{Z}$ and $z\geq z_0\in[0,h_0]$. Moreover, the equations for $u^{(\nu)}_{\mu;0,i}$ and $u_{2;0,ij}$ are to be complemented with the initial conditions $u^{(\nu)}_{\mu;0,i}(z_0;z_0)=\mathbb{1}$ and $u_{2;0,ij}(z_0;z_0)=\mathbb{1}$ where $\mathbb{1}$ denote the identity operators. It is readily verified by differentiating the integral equations for y with respect to h_0 and by using the initial conditions and differential equations for u that these equations hold. It is then proposed that it is this system of equations which is discretized by using the mesh $\{c_ih_0\in[0,h_0]:i\in[1,s]\cap\mathbb{Z}\}$ in order to arrive at a system of algebraic equations for the so-called stage approximations. Here, the stage approximations $Y_{1;0,i}$ and $Y_{2;0,i;0,j}$, $Y_{2;0,i;n}$ and $Y_{2;n;0,i}$ can be understood to approximate the solutions y_1 at $t_0+c_ih_0$ and y_2 at $(t_0+c_ih_0;t_0+c_jh_0)$, $(t_0+c_ih_0;t_n)$ and $(t_n;t_0+c_ih_0)$. In the end, it is however the purpose to only use these approximations to introduce the approximations $y_{1;1}$ and $y_{2;1;1}$, $y_{2;1;n}$ and $y_{2;n;1}$ for the desired solutions y_1 at (t_0+h_0) and y_2 at $(t_0+h_0;t_0+h_0)$, $(t_0+h_0;t_n)$ and $(t_n;t_0+h_0)$. In order to proceed with the discretization, the Lagrange cardinal polynomials $\ell_i(x)=\prod_{j=1,j\neq i}^s(x-c_j)/(c_i-c_j)$ are introduced for $i\in[1,s]\cap\mathbb{Z}$ such that, in the spirit of the collocation methods [HNW08, Zan99], the approximations

$$L^{(\nu)}_\mu(t_0+c_iz)\approx\sum_{k=1}^s \ell_k(c_iz/h_0)\underbrace{L^{(\nu)}_{\mu;0,k}}_{\equiv L^{(\nu)}_\mu(Y_{1;0,k},Y_{2;0,k;0,k})},$$

and

$$N_1(t_0+c_iz)\approx\sum_{k=1}^s \ell_k(c_iz/h_0)\underbrace{N_{1;0,k}}_{\equiv N_1(Y_{2;0,k;0,k},I_1(t_0+c_kh_0))},$$

$$N^\nu_2(t_0+c_iz;t_0+c_jz)\approx\sum_{k,l=1}^s \ell_k(c_iz/h_0)\ell_l(c_jz/h_0)\underbrace{N^\nu_{2;0,k;0,l}}_{\equiv N^\nu_2(Y_{2;0,k;0,l},I^\nu_{2,1}(t_0+c_kh_0;t_0+c_lh_0),I^\nu_{2,2}(t_0+c_kh_0;t_0+c_lh_0))},$$

$$
\begin{aligned}
N_2^1(t_0 + c_i z; t_n) &\approx \sum_{k=1}^{s} \ell_k(c_i z/h_0) \underbrace{N_{2;0,k;n}^1}, \\
&\equiv N_2^1(Y_{2;0,k;n}, I_{2,1}^1(t_0 + c_k h_0; t_n), I_{2,2}^1(t_0 + c_k h_0; t_n)) \\
N_2^2(t_n; t_0 + c_i z) &\approx \sum_{k=1}^{s} \ell_k(c_i z/h_0) \underbrace{N_{2;n;0,k}^2}, \\
&\equiv N_2^2(Y_{2;n;0,k}, I_{2,1}^2(t_n; t_0 + c_k h_0), I_{2,2}^2(t_n; t_0 + c_k h_0))
\end{aligned}
$$

can be introduced for $z \in [0, h_0]$ and for all $\mu, \nu \in \{1, 2\}$, $i, j \in [1, s] \cap \mathbb{Z}$ and $n \in]-|M_{\mathrm{I}}|, 0] \cap \mathbb{Z}$. It follows by substituting the interpolants of L into Eqs. (6.3) that $u_{\mu;0,i}^{(\nu)}(z h_0; z_0 h_0)$ can be written a function of z, z_0 and $\{c_i h_0 L_{\mu;0,k}^{(\nu)} : k \in [1, s] \cap \mathbb{Z}\}$ and similarly that $u_{2;0,ij}(z h_0; z_0 h_0)$ can be written a function of z, z_0, and $\{c_i h_0 L_{2;0,k}^1, c_j h_0 L_{2;0,k}^2 : k \in [1, s] \cap \mathbb{Z}\}$ such that the dependence on t_0 and h_0 enters only through the terms which are proportional to $L_{\mu;0,k}^{(\nu)}$. It is in particular this observation which makes its convenient to define the so-called weight functions v and a, i.e., the set $\{v_{1;i}, v_{2,ij}, a_{1;i}^k, a_{2;ij}^{kl} : i, j, k, l \in [1, s] \cap \mathbb{Z}\}$ of multivariate functions, by demanding that the relations

$$
\begin{aligned}
v_{1;i}(c_i h_0 L_{\mu;0,1}^{(\nu)}, \ldots, c_i h_0 L_{\mu;0,s}^{(\nu)}) &\equiv u_{\mu;0,i}^{(\nu)}(h_0; 0)\,, \\
a_{1;i}^k(c_i h_0 L_{\mu;0,1}^{(\nu)}, \ldots, c_i h_0 L_{\mu;0,s}^{(\nu)}) &\equiv \int_0^1 dz\; u_{\mu;0,i}^{(\nu)}(h_0; h_0 z) \ell_k(c_i z)\,,
\end{aligned}
$$

and

$$
\begin{aligned}
v_{2;ij}(c_i h_0 L_{2;0,1}^1, \ldots, c_i h_0 L_{2;0,s}^1; c_j h_0 L_{2;0,1}^2, \ldots, c_j h_0 L_{2;0,s}^2) &\equiv u_{2;0,ij}(h_0; 0)\,, \\
a_{2;ij}^{kl}(c_i h_0 L_{2;0,1}^1, \ldots, c_i h_0 L_{2;0,s}^1; c_j h_0 L_{2;0,1}^2, \ldots, c_j h_0 L_{2;0,s}^2) &\equiv \int_0^1 dz\; u_{2;0,ij}(h_0; h_0 z) \ell_k(c_i z) \ell_l(c_j z)\,,
\end{aligned}
$$

are satisfied for all $i, j, k, l \in [1, s] \cap \mathbb{Z}$. It remains to use these definitions and to substitute the interpolants of N into Eqs. (6.3) in order to show that the stage approximations satisfy the algebraic equations

$$
\begin{aligned}
Y_{1;0,i} &= v_{1;i}(c_i h_0 L_{1;0,1}, \ldots, c_i h_0 L_{1;0,s}) y_{1;0} \\
&\quad + c_i h_0 \sum_{k=1}^{s} a_{1;i}^k(c_i h_0 L_{1;0,1}, \ldots, c_i h_0 L_{1;0,s}) N_{1;0,k}\,, \qquad (6.4a) \\
Y_{2;0,i;0,j} &= v_{2;ij}(c_i h_0 L_{2;0,1}^1, \ldots, c_i h_0 L_{2;0,s}^1; c_j h_0 L_{2;0,1}^2, \ldots, c_j h_0 L_{2;0,s}^2) y_{2;0;0} \\
&\quad + c_i h_0 \sum_{k,l=1}^{s} a_{2;ij}^{kl}(c_i h_0 L_{2;0,1}^1, \ldots, c_i h_0 L_{2;0,s}^1; c_j h_0 L_{2;0,1}^2, \ldots, c_j h_0 L_{2;0,s}^2) N_{2;0,k;0,l}^1 \\
&\quad + c_j h_0 \sum_{k,l=1}^{s} a_{2;ij}^{kl}(c_i h_0 L_{2;0,1}^1, \ldots, c_i h_0 L_{2;0,s}^1; c_j h_0 L_{2;0,1}^2, \ldots, c_j h_0 L_{2;0,s}^2) N_{2;0,k;0,l}^2\,, \qquad (6.4b) \\
Y_{2;0,i;n} &= v_{1;i}(c_i h_0 L_{2;0,1}^1, \ldots, c_i h_0 L_{2;0,s}^1) y_{2;0,n} \\
&\quad + c_i h_0 \sum_{k=1}^{s} a_{1;i}^k(c_i h_0 L_{2;0,1}^1, \ldots, c_i h_0 L_{2;0,s}^1) N_{2;0,k;n}^1\,, \qquad (6.4c) \\
Y_{2;n;0,i} &= v_{1;i}(c_i h_0 L_{2;0,1}^2, \ldots, c_i h_0 L_{2;0,s}^2) y_{2;n;0} \\
&\quad + c_i h_0 \sum_{k=1}^{s} a_{1;i}^k(c_i h_0 L_{2;0,1}^2, \ldots, c_i h_0 L_{2;0,s}^2) N_{2;n;0,k}^2\,. \qquad (6.4d)
\end{aligned}
$$

for all $i, j \in [1, s] \cap \mathbb{Z}$ and $n \in]-|M_{\mathrm{I}}|, 0] \cap \mathbb{Z}$. It is then possible to proceed analogously in order to show that the desired approximate solutions $y_{1;1}$ and $y_{2;1;1}$, $y_{2;1;n}$ and $y_{2;n;1}$ can be evaluated from

the knowledge of the stage approximations. For one, by letting $u_{\mu;0}^{(\nu)}$ and $u_{2;0}$ denote the solutions of Eqs. (6.3a) and (6.3b) obtained by setting $c_i = c_j = 1$ and using the interpolants of L, the weight functions u and b, i.e., the set $\{u_\mu, b_1^k, b_\nu^{kl} : \mu \in \{1,2\}, k,l \in [1,s] \cap \mathbb{Z}\}$ of multivariate functions, can be defined by demanding that

$$\begin{aligned} u_1(h_0 L_{\mu;0,1}^{(\nu)}, \dots, h_0 L_{\mu;0,s}^{(\nu)}) &\equiv u_{\mu;0}^{(\nu)}(h_0;0)\,, \\ b_1^k(h_0 L_{\mu;0,1}^{(\nu)}, \dots, h_0 L_{\mu;0,s}^{(\nu)}) &\equiv \int_0^1 dz\; u_{\mu;0}^{(\nu)}(h_0; h_0 z)\ell_k(z)\,, \end{aligned}$$

and

$$\begin{aligned} &u_2(h_0 L_{2;0,1}^1, \dots, h_0 L_{2;0,s}^1; h_0 L_{2;0,1}^2, \dots, h_0 L_{2;0,s}^2) \\ &\quad \equiv u_1(h_0(L_{2;0,1}^1 + L_{2;0,1}^2), \dots, h_0(L_{2;0,s}^1 + h_0 L_{2;0,s}^2) \equiv u_{2;0}(h_0;0)\,, \\ &b_2^{kl}(h_0 L_{2;0,1}^1, \dots, h_0 L_{2;0,s}^1; h_0 L_{2;0,1}^2, \dots, h_0 L_{2;0,s}^2) \\ &\quad \equiv b_1^{kl}(h_0(L_{2;0,1}^1 + L_{2;0,1}^2), \dots, h_0(L_{2;0,s}^1 + L_{2;0,s}^2)) \equiv \int_0^1 dz\; u_{2;0}(h_0; h_0 z)\ell_k(z)\ell_l(z)\,, \end{aligned}$$

for all $k,l \in [1,s] \cap \mathbb{Z}$. It is noteworthy that it is due to the definition of $u_{2;0}$ that the functions u_2 and b_2^{kl} could be defined in terms of the functions u_1 and b_1^{kl}. For another, by defining $y_{1;1}$ and $y_{2;1;1}$, $y_{2;1;n}$ and $y_{2;n;1}$ respectively as the left-hand sides of Eq. (6.3c) and Eqs. (6.3d), (6.3e) and (6.3f) obtained by setting $c_i = c_j = 1$ and by using the interpolants of N and the definitions of the weight functions, it follows for all $n \in]-|M_\mathrm{I}|, 0] \cap \mathbb{Z}$ that

$$\begin{aligned} y_{1;1} &= u_1(h_0 L_{1;0,1}, \dots, h_0 L_{1;0,s}) y_{1;0} \\ &\quad + h_0 \sum_{k=1}^s b_1^k(h_0 L_{1;0,1}, \dots, h_0 L_{1;0,s}) N_{1;0,k}\,, \qquad (6.5a) \\ y_{2;1;1} &= u_2(h_0 L_{2;0,1}^1, \dots, h_0 L_{2;0,s}^1; h_0 L_{2;0;1}^2, \dots, h_0 L_{2;0,s}^2) y_{2;0;0} \\ &\quad + h_0 \sum_{k,l=1}^s b_2^{kl}(h_0 L_{2;0.1}^1, \dots, h_0 L_{2;0,s}^1; h_0 L_{2;0,1}^2, \dots, h_0 L_{2;0,s}^2) N_{2;0,k;0,l}^1 \\ &\quad + h_0 \sum_{k,l=1}^s b_2^{kl}(h_0 L_{2;0.1}^1, \dots, h_0 L_{2;0,s}^1; h_0 L_{2;0,1}^2, \dots, h_0 L_{2;0,s}^2) N_{2;0,k;0,l}^2\,, \qquad (6.5b) \\ y_{2;1;n} &= u_1(h_0 L_{2;0,1}^1, \dots, h_0 L_{2;0,s}^1) y_{2;0;n} \\ &\quad + h_0 \sum_{k=1}^s b_1^k(h_0 L_{2;0,1}^1, \dots, h_0 L_{2;0,s}^1) N_{2;0,k;n}^1\,, \qquad (6.5c) \\ y_{2;n;1} &= u_1(h_0 L_{2;0,1}^2, \dots, h_0 L_{2;0,s}^2) y_{2;n;0} \\ &\quad + h_0 \sum_{k=1}^s b_1^k(h_0 L_{2;0,1}^2, \dots, h_0 L_{2;0,s}^2) N_{2;n;0,k}^2\,, \qquad (6.5d) \end{aligned}$$

which together with the equations for the stage approximations form a closed set of equations provided that the integrals I can be somehow evaluated. It hence remains to supplement Eqs. (6.4) and (6.5) with a quadrature rule for the integrals I appearing as the arguments of the vector fields N. In order to do this, by following [WP68, Lub82, BH86], each of the integrals I is split into an integral from $t_0 - \tau$ to t_0 and to the remaining integral from t_0 to $t_0 + c_i h_0$. In particular, the integrals of the latter type, i.e., the integrals from t_0 to $t_0 + c_i h$, are approximated with a quadrature rule motivated here by using Lagrange interpolation. It follows by approximating for $z \in [0, h_0]$ the

integral kernels K with the interpolants

$$K_1(y_2(t_0+c_ih_0;t_0+z),y_1(t_0+z)) \approx \sum_{k=1}^{s} \ell_k(z/h_0)\underbrace{K_{1;0,i;0,k}}_{\equiv K_1(Y_{2;0,i;0,k},Y_{1;0,k})},$$

$$K^\nu_{2,\mu}(y_2(t_0+c_ih_0;t_0+z),y_2(t_0+z;t_0+c_jh_0)) \approx \sum_{k=1}^{s} \ell_k(z/h_0)\underbrace{K^\nu_{2,\mu;0,i;0,k;0,j}}_{\equiv K^\nu_{2,\mu}(Y_{2;0,i;0,k},Y_{2;0,k;0,j})},$$

$$K^1_{2,\nu}(y_2(t_0+c_ih_0;t_0+z),y_2(t_0+z;t_n)) \approx \sum_{k=1}^{s} \ell_k(z/h_0)\underbrace{K^1_{1,\nu;0,i;0,k;n}}_{\equiv K^1_{2,\nu}(Y_{2;0,i;0,k},Y_{2;0,k;n})},$$

$$K^2_{2,\nu}(y_2(t_n;t_0+z),y_2(t_0+z;t_0+c_ih_0)) \approx \sum_{k=1}^{s} \ell_k(z/h_0)\underbrace{K^2_{2,\nu;n;0,k;0,i}}_{K^2_{2,\nu}(Y_{2;n;0,k},Y_{2;0,k;0,i})},$$

for all $\nu,\mu \in \{1,2\}$, $i,j \in [1,s]\cap\mathbb{Z}$ and $n \in]-|M_\mathrm{I}|,0]$ that the integrals I can be approximated with the quadrature rules

$$I_1(t_0+c_ih_0) \approx I_{1;0,i} + \underbrace{h_0\sum_{k=1}^{s} c_id_i^kK_{1;0,i;0,k}}_{\equiv Z_{1;0,i}}, \tag{6.6a}$$

$$I^\nu_{2,\mu}(t_0+c_ih_0;t_0+c_jh_0) \approx I^\nu_{2,\mu;0,i;0,j} + \underbrace{h_0\sum_{k=1}^{s}(c_id_i^k\delta_{\mu\,1}+c_jd_j^k\delta_{\mu\,2})K^\nu_{2,\mu;0,i;0,k;0,j}}_{\equiv Z^\nu_{2,\mu;0,i;0,j}}, \tag{6.6b}$$

$$I^\nu_{2,\mu}(t_0+c_ih_0;t_n) \approx I^\nu_{2,\mu;0,i;n} + \underbrace{h_0\sum_{k=1}^{s}\delta_{\mu\,1}c_id_i^kK^\nu_{2,\mu;0,i;0,k;n}}_{\equiv Z^\nu_{2,\mu;0,i;n}}, \tag{6.6c}$$

$$I^\nu_{2,\mu}(t_n;t_0+c_ih_0) \approx I^\nu_{2,\mu;n;0,i} + \underbrace{h_0\sum_{k=1}^{s}\delta_{\mu\,2}c_id_i^kK^\nu_{2,\mu;n;0,k;0,i}}_{\equiv Z^\nu_{2,\mu;n;0,i}}, \tag{6.6d}$$

where $d_i^j \equiv \int_0^1 dz\ \ell_j(c_iz)$ denote the so-called quadrature weights of the method. Here, by $I_{i;0,i}$ and $I^\nu_{2,\mu;0,i;0,j}$, $I^\nu_{2,\mu;0,i,n}$ and $I^\nu_{2,\mu;n;0,i}$ approximations to the integrals from $t_0-\tau$ to t_0, i.e., the so-called lag or tail integrals, are denoted. In an agreement with the idea of mixed quadrature methods [Lub82, BH86], it is proposed that the lag integrals are approximated by

$$I_{1;0,i} \equiv \sum_{m=-|M_\mathrm{I}|+1}^{0} w_{0;m}K_1(Y_{2;0,i;m},y_{1;m}), \tag{6.7a}$$

$$I^\nu_{2,\mu;0,i;0,j} \equiv \sum_{m=-|M_\mathrm{I}|+1}^{0} w_{0;m;0}K^\nu_{2,\mu}(Y_{2;0,i;m},Y_{2;m;0,j}), \tag{6.7b}$$

$$I^\nu_{2,\mu;0,i;n} \equiv \sum_{m=-|M_\mathrm{I}|+1}^{0} w_{0;m;n}K^\nu_{2,\mu}(Y_{2;0,i;m},y_{2;m;n}), \tag{6.7c}$$

$$I^{\nu}_{2,\mu;n;0,i} \equiv \sum_{m=-|M_{\mathrm{I}}|+1}^{0} w_{n;m;0} K^{\nu}_{2,\mu}(y_{2;n;m}, Y_{2;m;0,i}) \,, \tag{6.7d}$$

where $w_{0;m}$, $w_{0;m;0}$, $w_{0;m;n}$ and $w_{n;m;0}$ denote real-valued quadrature weights. In order to conclude, it is noted that these quadrature weights can be chosen by acknowledging the possible (derivative) discontinuities of the integral kernels and for instance by requiring that the associated quadrature rule integrates exactly polynomials of a given degree [Atk89].

6.1.2 Statement of the Integration Rule

In the preceding discussion, a numerical method epitomizing to the integration rules of Eqs. (6.4), (6.5), (6.6) and (6.7) has been motivated by extending into two dimensions, several ideas familiar from the numerical integration of ordinary differential as well as Volterra integro-differential equations in a single dimension. In the following, this numerical method is defined formally by extending the motivated rules beyond the first integration step and by relaxing some of the constraints concerning the introduced weight functions and quadrature weights. It quickly becomes clear when trying to extend the proposed integration rules to the second integration step, which involves the integration from $t_1 = t_0 + h_0$ to $t_1 + h_1$, that, without an explicit starting procedure, it is not possible to devise methods whose precision can be systematically improved if only the approximations at t_0 and t_1 are available to evaluate the lag integrals from t_0 onward. In order to go around this issue, a mixed integration rule, in which y_1 and y_2 are respectively approximated on the refined meshes M_N^S and $(M_N^S \cup M_{\mathrm{I}})^2 \setminus M_{\mathrm{I}}^2$, is proposed here by following [Lub82, BH86]. Here, $M_N^S \equiv \{t_n + \theta_i h_n : t_{n+1} = t_n + h_n, h_n \in]0,\infty[, \theta_i \in]0,1[\forall i < S, \theta_S = 1$ for all $n \in [0, N[\cap\mathbb{Z}, i \in [1,S] \cap \mathbb{Z}\ \}$ defines the refined mesh, the elements of which, i.e., the mesh points, are referred to as $t_{n,i} \equiv t_n + \theta_i h_n$ and $t_{n+1} \equiv t_{n,S}$ in the following. Moreover, it is useful to define the index set $i(M_N^S \cup M_{\mathrm{I}}) \equiv \{n, (m,i) : n \in]-|M_{\mathrm{I}}|, 0] \cap \mathbb{Z}, m \in [0, N[\cap\mathbb{Z}, i \in [1,S] \cap \mathbb{Z}\}$ for indexing the mesh points. It is the advantage of a mixed integration rule that more precise approximations for the lag integrals can be introduced by increasing the number $S \in \mathbb{Z}_{\geq 1}$ of the approximations $y_{1;n,i}$ and $y_{2;n,i;n,j}$, $y_{2;n,i;M}$ and $y_{2;M;n,j}$ to the solutions y_1 at $t_{n,i}$ and y_2 at $(t_{n,i}; t_{n,j})$, $(t_{n,i}; t_M)$ and $(t_M; t_{n,j})$ for all $M \in i(M_n^S \cup M_{\mathrm{I}})$, respectively. It is noteworthy that this issue could also potentially be solved by defining an extended integration rule in which the stage approximations would be stored and used to evaluate the lag integrals [Lub82, BH86]. However, it is felt that a mixed rule is more appropriate since it allows, in principle, one to choose better which function values are stored. In Fig. 6.1.2, an example of the refined mesh is shown in order to illustrate how the lag integrals are evaluated and how the additional mesh points are to be understood.

In order to solve for the above introduced approximations $y_{1;n,i}$ and $y_{2;n,i;n,j}$, $y_{2;n,i;M}$ and $y_{2;M;n,j}$ at the secondary mesh points for which $i,j \in [1,S[\cap\mathbb{Z}$, the integration rules given in Eqs. (6.5) need to be extended to rules which resemble the integration rules of Eqs. (6.4) for the stage approximations. In addition to having to introduce additional weight functions u and b to do this, it is chosen here, in analogy to how the Runge-Kutta methods are stated [But87, BH86], to disregard the explicit forms of the weight functions of the previous section and only demand that they are defined as as follows.

Definition 6.1.1 (Weight Functions)**.** *The weight functions of a s-stage mixed method with $S-1$ secondary mesh points are the multivariate functions*

$$u_{1;i}(z_1, \ldots, z_s) \,,$$
$$b^k_{1;i}(z_1, \ldots, z_s) \,,$$

$$v_{1;k}(z_1, \ldots, z_s) \,,$$

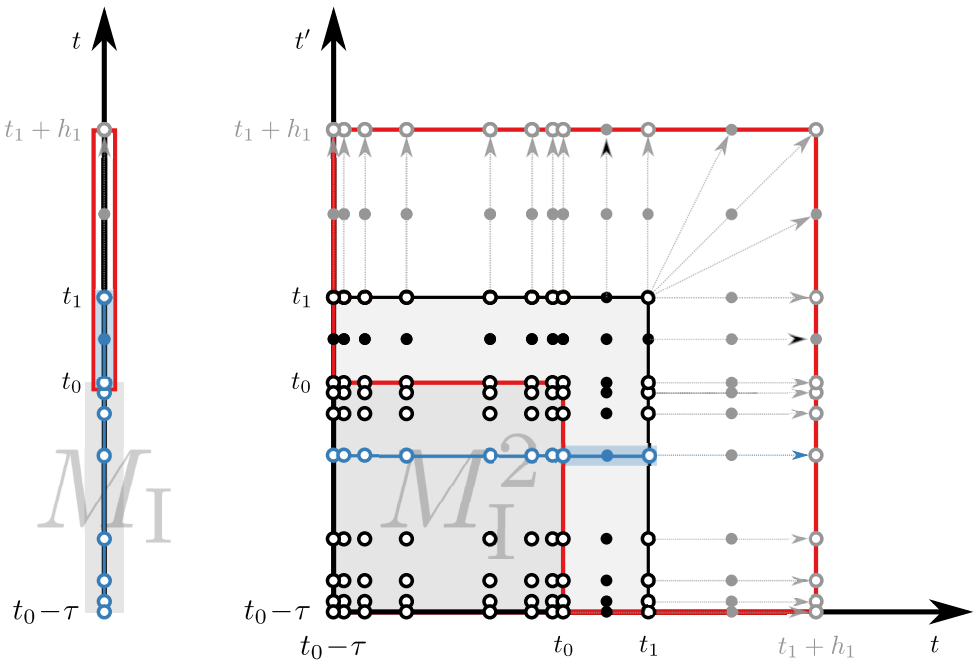

Figure 6.1.2: An example of the refined one-dimensional mesh M_N^S, and of the corresponding two-dimensional mesh $(M_N^S \cup M_\mathrm{I})^2 \setminus M_\mathrm{I}^2$, with one ($S = 2$) secondary (bullets) and two ($N = 2$) primary (circles) mesh points highlighted with an enclosing red border is shown. The initial mesh M_I with $|M_\mathrm{I}| = 8$ mesh points is the same as in Fig. 6.1.1. The gray circles and bullets denote the mesh points for which y_1 and y_2 are obtained in the second integration step. In addition, the mesh points at which y_1 and y_2 are needed in order to evaluate the lag integrals in the second integration step from $(t_1; t_{-3})$ to $(t_1 + \theta_i h_1; t_{-3})$ are highlighted with blue such that the part of the integral from t_0 to t_1 is shown on a blue background.

$$a^l_{1;k}(z_1, \ldots, z_s)\,,$$

and

$$\begin{aligned} u_{2;ij}(z_1, \ldots, z_s; z'_1, \ldots, z'_s) &= u_{2;ji}(z'_1, \ldots, z'_s; z_1, \ldots, z_s)\,,\\ b^{kl}_{2;ij}(z_1, \ldots, z_s; z'_1, \ldots, z'_s) &= b^{lk}_{2;ji}(z'_1, \ldots, z'_s; z_1, \ldots, z_s)\,, \end{aligned}$$

$$\begin{aligned} v_{kl}(z_1, \ldots, z_s; z'_1, \ldots, z'_s) &= v_{lk}(z'_1, \ldots, z'_s; z_1, \ldots, z_s)\,,\\ a^{pq}_{kl}(z_1, \ldots, z_s; z'_1, \ldots, z'_s) &= a^{qp}_{lk}(z'_1, \ldots, z'_s; z_1, \ldots, z_s)\,, \end{aligned}$$

such that

$$\begin{aligned} u_{2;ii}(z_1, \ldots, z_s; z'_1, \ldots, z'_s) &= u_{1;i}(z_1 + z'_1, \ldots, z_s + z'_s)\,,\\ b^{kl}_{2;ii}(z_1, \ldots, z_s; z'_1, \ldots, z'_s) &= \delta_{kl} b^k_{1;i}(z_1 + z'_1, \ldots, z_s + z'_s)\,, \end{aligned}$$

$$\begin{aligned} v_{2;kk}(z_1, \ldots, z_s; z'_1, \ldots, z'_s) &= v_{1;k}(z_1 + z'_1, \ldots, z_s + z'_s)\,,\\ a^{pq}_{2;kk}(z_1, \ldots, z_s; z'_1, \ldots, z'_s) &= \delta_{pq} a^p_{1;k}(z_1 + z'_1, \ldots, z_s + z'_s)\,, \end{aligned}$$

where $i, j \in [1, S] \cap \mathbb{Z}$ *and* $k, l, p, q \in [1, s] \cap \mathbb{Z}$.

It is noted that the minimal constraints, which have been imposed on the weight functions in their definition above, can be motivated, e.g., by examining the explicit weight functions of the previous section. It is possible that if the constraints connecting the weight functions for y_1, Y_1 and y_2, Y_2 would be relaxed then more efficient methods could be realized. Nevertheless, here it is proceeded to generalize the integration rules introduced in the previous section by extending them to cover the approximations at the secondary mesh points and by disregarding the explicit form of the previously defined quadrature weights d.

Definition 6.1.2 (Numerical Integration Rule)**.** *If $s \in \mathbb{Z}_{\geq 1}$ is the number of stages, $S-1 \in \mathbb{Z}_{\geq 0}$ the number of secondary mesh points, $i,j \in [1,S] \cap \mathbb{Z}$, $n \in [0,N[\cap\mathbb{Z}$ and $M \in i(M_n^S \cup M_{\mathrm{I}})$ then*

$$
\begin{aligned}
y_{1;n,i} &= u_{1;n,i} y_{1;n} + \theta_i h_n \sum_{k=1}^{s} b_{1;n,i}^{k} N_{1;n,k}\,,\\
y_{2;n,i;n,j} &= u_{2;n,ij} y_{2;n;n} + \theta_i h_n \sum_{k,l=1}^{s} b_{2;n,ij}^{kl} N_{2;n,k;n,l}^{1} + \theta_j h_n \sum_{k,l=1}^{s} b_{2;n,ij}^{kl} N_{2;n,k;n,l}^{2}\,,\\
y_{2;n,i;M} &= u_{2;n,i}^{1} y_{2;n;M} + \theta_i h_n \sum_{k=1}^{s} b_{2;n,i}^{1;k} N_{2;n,k;M}^{1}\,,\\
y_{2;M;n,i} &= u_{2;n,i}^{2} y_{2;M;n} + \theta_i h_n \sum_{k=1}^{s} b_{2;n,i}^{2;k} N_{2;M;n,k}^{2}\,,
\end{aligned}
$$

where $\theta_i \in]0,1]$ and $h_n \in]0,\infty[$ is the step size, approximate y_1 at $t_n+\theta_i h_n$ and y_2 at $(t_n+\theta_i h_n; t_n+\theta_j h_n)$, $(t_n+\theta_i h_n; t_M)$ and $(t_M; t_n+\theta_i h_n)$ with $t_M \in M_n^S \cup M_{\mathrm{I}}$ respectively. Here, c_k are the real-valued nodes of the method and if $k,l \in [1,s]\cap\mathbb{Z}$ then

$$
\begin{aligned}
Y_{1;n,k} &= v_{1;n,k} y_{1;n} + c_k h_n \sum_{l=1}^{s} a_{1;n,k}^{l} N_{1;n,l}\,,\\
Y_{2;n,k;n,l} &= v_{2;n,kl} y_{2;n;n} + c_k h_n \sum_{p,q=1}^{s} a_{2;n,kl}^{pq} N_{2;n,p;n,q}^{1} + c_l h_n \sum_{p,q=1}^{s} a_{2;n,kl}^{pq} N_{2;n,p;n,q}^{2}\,,\\
Y_{2;n,k;M} &= v_{2;n,k}^{1} y_{2;n;M} + c_k h_n \sum_{l=1}^{s} a_{2;n,k}^{1;l} N_{2;n,l;M}^{1}\,,\\
Y_{2;M;n,k} &= v_{2;n,k}^{2} y_{2;M;n} + c_k h_n \sum_{l=1}^{s} a_{2;n,k}^{2;l} N_{2;M;n,l}^{2}\,,
\end{aligned}
$$

are the stage approximations. If $\nu,\mu \in \{1,2\}$ then the weights of the method

$$
\begin{aligned}
u_{\mu;n,i}^{(\nu)} &\equiv u_{1;i}(\theta_i h_n L_{\mu;n,1}^{(\nu)}, \ldots, \theta_i h_n L_{\mu;n,s}^{(\nu)})\,,\\
b_{\mu;n,i}^{(\nu);k} &\equiv b_{1;i}^{k}(\theta_i h_n L_{\mu;n,1}^{(\nu)}, \ldots, \theta_i h_n L_{\mu;n,s}^{(\nu)})\,,
\end{aligned}
$$

$$
\begin{aligned}
v_{\mu;n,k}^{(\nu)} &\equiv v_{1;k}(c_k h_n L_{\mu;n,1}^{(\nu)}, \ldots, c_k h_n L_{\mu;n,s}^{(\nu)})\,,\\
a_{\mu;n,k}^{(\nu);l} &\equiv a_{1;k}^{l}(c_k h_n L_{\mu;n,1}^{(\nu)}, \ldots, c_k h_n L_{\mu;n,s}^{(\nu)})\,,
\end{aligned}
$$

and

$$
\begin{aligned}
u_{2;n,ij} &\equiv u_{2;ij}(\theta_i h_n L_{2;n,1}^{1}, \ldots, \theta_i h_n L_{2;n,s}^{1}; \theta_j h_n L_{2;n,1}^{2}, \ldots, \theta_j h_n L_{2;n,s}^{2})\,,\\
b_{2;n,ij}^{kl} &\equiv b_{2;ij}^{kl}(\theta_i h_n L_{2;n,1}^{1}, \ldots, \theta_i h_n L_{2;n,s}^{1}; \theta_j h_n L_{2;n,1}^{2}, \ldots, \theta_j h_n L_{2;n,s}^{2})\,,
\end{aligned}
$$

$$v_{2;n,kl} \equiv v_{2;kl}(c_k h_n L^1_{2;n,1}, \ldots, c_k h_n L^1_{2;n,s}; c_l h_n L^2_{2;n,1}, \ldots, c_l h_n L^2_{2;n,s}) ,$$
$$a^{pq}_{2;n,kl} \equiv a^{pq}_{2;kl}(c_k h_n L^1_{2;n,1}, \ldots, c_k h_n L^1_{2;n,s}; c_l h_n L^2_{2;n,1}, \ldots, c_l h_n L^2_{2;n,s}) .$$

where $p, q \in [1, s] \cap \mathbb{Z}$, are defined in terms of the weight functions 6.1.1. Here,

$$L^{(\nu)}_{\mu;n,k} \equiv L^{(\nu)}_{\mu}(Y_{1;n,k}, Y_{2;n,k;n,k})$$

denote the linear operators and, above,

$$N_{1;n,k} \equiv N_1(Y_{2;n,k;n,k}, I_{1;n,k} + Z_{1;n,k}) ,$$
$$N^{\nu}_{2;n,k;n,l} \equiv N^{\nu}_2(Y_{2:n,k;n,l}, I^{\nu}_{2,1;n,k;n,l} + Z^{\nu}_{2,1;n,k;n,l}, I^{\nu}_{2,2;n,k;n,l} + Z^{\nu}_{2,2;n,k;n,l}) ,$$
$$N^1_{2;n,k;M} \equiv N^1_2(Y_{2:n,k;M}, I^1_{2,1;n,k;M} + Z^1_{2,1;n,k;M}, I^1_{2,2;n,k;M}) ,$$
$$N^2_{2;M;n,k} \equiv N^2_2(Y_{2;M;n,k}, I^2_{2,1;M;n,k}, I^2_{2,2;M;n,k} + Z^2_{2,2;M;n,k}) ,$$

the non-linear functions. Moreover, by

$$I_{1;n,k} \equiv \sum_{R \in i[M^S_n \cup M_I]} w_{n;R} K_1(Y_{2;n,k;R}, y_{1;R}) ,$$
$$I^{\nu}_{2,\mu;n,k;n,l} \equiv \sum_{R \in i[M^S_n \cup M_I]} w^{\mu}_{n;R;n} K^{\nu}_{2,\mu}(Y_{2;n,k;R}, Y_{2;R;n.l}) ,$$
$$I^{\nu}_{2,\mu;n,k;M} \equiv \sum_{R \in i[M^S_n \cup M_I]} w^{\mu}_{n;R;M} K^{\nu}_{2,\mu}(Y_{2;n,k;R}, y_{2;R;M}) ,$$
$$I^{\nu}_{2,\mu;M;n,k} \equiv \sum_{R \in i[M^S_n \cup M_I]} w^{\mu}_{M;R;n} K^{\nu}_{2,\mu}(y_{2;M;R}, Y_{2;R;n,k}) ,$$

where $w_{n;R}$, $w^{\mu}_{n;R;n}$, $w^{\mu}_{n;R;M}$ and $w^{\mu}_{M;R;n}$ are real-valued quadrature weights, and by

$$Z_{1;n,k} = h_n \sum_{l=1}^{s} c_k d^l_k K_1(Y_{2;n,k;n,l}, Y_{1;n,l}) ,$$
$$Z^{\nu}_{2,\mu;n,k;n,l} = h_n \sum_{p=1}^{s} (\delta_{\mu\,1} c_k d^p_k + \delta_{\mu\,2} c_l d^p_l) K^{\nu}_{2,\mu}(Y_{2;n,k;n,p}, Y_{2;n,p;n,l}) ,$$
$$Z^{\nu}_{2,\mu;n,k;M} = h_n \sum_{l=1}^{s} \delta_{\mu\,1} c_k d^l_k K^{\nu}_{2,\mu}(Y_{2;n,k;n,l}, Y_{2;n,l;M}) ,$$
$$Z^{\nu}_{2,\mu;M;n,k} = h_n \sum_{l=1}^{s} \delta_{\mu\,2} c_k d^l_k K^{\nu}_{2,\mu}(Y_{2;M;n,l}, Y_{2;n,l;n,k}) ,$$

where d^l_k are the real-valued quadrature weights of the method, approximations for the (lag) integrals are denoted.

It then remains to build specific numerical methods relying on this integration rule by choosing the nodes, weight functions and quadrature weights appropriately. In the next sections, it is shown how this can be done in practice.

6.2 Consistency and Convergence

A numerical method designed to integrate an initial value problem is useful only if it is convergent, i.e., roughly speaking, the numerical solution defined on a mesh converges to the exact solution when

the mesh is refined. In the case of Volterra integral and integro-differential equations, the convergence, or the order of convergence, of a one-step method with respect to a uniform step size h is usually proven in two steps: by proving that the method has a certain local order, or an order of consistency, and subsequently by establishing the convergence by using the local order [Lub82, HLN83, BH86]. In particular, in the context of the Runge-Kutta methods, it holds that a method which has an order of consistency p is convergent of order p, i.e., the error with respect to the step size h is $\mathcal{O}(h^p)$. Here, it is specified, by following [Lub82, HLN83, BH86], what is meant, in the case of the integration rule defined in 6.1.2, by the order of consistency and convergence. Also, the criteria, i.e., the so-called order conditions, to construct methods which have an order of consistency of two are introduced but a proof connecting the order of consistency to the order of convergence, or to the converge in general, is not provided. It is recapitulated that here by a numerical method is is meant the integration rule 6.1.2 supplemented with a fixed set of nodes, quadrature weights and weight functions.

In order to require that the method has a certain order of consistency, it is mandatory to introduce some additional constrains for the weight functions. In the following, it is assumed that the weight functions of the method introduced in 6.1.1, as well as the multivariate linear operators L, vector fields F and N, and functions K are continuously differentiable to a sufficiently high order and possess partial derivatives to the equivalent order whenever required. It is meant by differentiability, cf., [But87], that if f is a map between two normed vector spaces then provided that the map Df, which takes an element of a vector space to an element of the associated space of linear operators, such that

$$\lim_{\|h\|\to 0} \|h\|^{-1} \|f(z+h) - f(z) - Df(z)(h)\| = 0\,,$$

exits then f is differentiable and the linear operator $Df(z)$ is called the derivative of f at z. Moreover, by using the abbreviation $(h_i)_1^{k-1} \equiv h_1, \ldots, h_{k-1}$, if the map $D^k f$, such that

$$\lim_{\|h\|\to 0} \|h\|^{-1} \|D^{k-1} f(z+h)((h_i)_1^{k-1}) - D^{k-1} f(z)((h_i)_1^{k-1}) - D^k f(z)((h_i)_1^{k-1}, h)\| = 0\,,$$

holds uniformly on a bounded set, exits then f is k times differentiable and the symmetric k-linear operator $D^k f(z)$ is the kth derivative of f at z. It is possible, in an analogous manner, to define that the k-linear operator $D^k_{j_1,\ldots,j_k} f(z_1, \ldots, z_s)$ is a kth order partial derivative, where the subscript j_i refers to a derivative with respect to the $j_i \in [1, s] \cap \mathbb{Z}$th argument, of the multivariate function f at $(z_1, \ldots, z_s)$ [Lan93]. In what follows, if f denotes a sufficiently differentiable multivariate function of s arguments, for the sake of brevity, the short-hands

$$f \equiv f(z_1, \ldots, z_s)\big|_{z_i = 0 \forall i \in [1,s] \cap \mathbb{Z}}\,,$$

and

$$f_{j_1,\ldots,j_k} \equiv D^k_{j_1,\ldots,j_k} f(z_1, \ldots, z_s)\big|_{z_i = 0 \forall i \in [1,s] \cap \mathbb{Z}}\,,$$

are introduced to denote the function values and partial derivatives at the origin. Although this notation can be ambiguous in general, its meaning should be clear in the context in which it is used the remaining chapter including App. 6.A. It is then possible to proceed to define what is meant when it is said that a method is consistent or internally consistent. In particular, if a method is consistent and internally consistent then the independent variables t and (t, t') are integrated exactly when a non-autonomous system is mapped into an autonomous system, cf., Sec. 5.3.1. Another reason for introducing the notion of consistency is that in the context of the Runge-Kutta methods for one-dimensional Volterra integro-differential equations consistency is a prerequisite for achieving convergence.

Definition 6.2.1 ((Internal) Consistency). *Given a set of weight functions 6.1.1, an associated s-stage method with $S-1$ secondary mesh points using the integration rule 6.1.2 is said to be consistent, if for all $i,j \in [1,S]\cap\mathbb{Z}$ and $k,l \in [1,s]\cap\mathbb{Z}$, the weight functions satisfy*

$$\begin{aligned} v_{2;kl} &= \mathbb{1}\,, \\ u_{2;ij} &= \mathbb{1}\,, \\ u_{2;ij;k}(z) &= \mathsf{u}_{2;ij;k} z\,, \\ b^{kl}_{2;ij} &= \mathsf{b}^{kl}_{2;ij}\mathbb{1}\,, \end{aligned}$$

such that

$$\sum_{k=1}^{s} \mathsf{u}_{2;ij;k} = 1\,, \tag{1.1}$$

$$\sum_{k,l=1}^{s} \mathsf{b}^{kl}_{2;ij} = 1\,, \tag{1.2}$$

where $\mathbb{1}$ is the identity operator and $\mathsf{u}_{2;ij;k}$ and $\mathsf{b}^{kl}_{2;ij}$ are real numbers. Moreover, the method is said to be internally consistent, if for all $k,l,p,q \in [1,s]\cap\mathbb{Z}$, the weight functions further satisfy

$$a^{pq}_{2;kl} = \mathsf{a}^{pq}_{2;kl}\mathbb{1}\,,$$

such that

$$c_k \sum_{p,q=1}^{s} \mathsf{a}^{pq}_{2;kl} = c_k\,, \tag{1.3}$$

where $\mathsf{a}^{pq}_{2;kl}$ are real numbers and $\{c_k : k \in [1,s]\cap\mathbb{Z}\}$ denote the nodes of the method.

It is also shown below that a method which is consistent and internally consistent has an order of consistency of at least one. In order to define what is meant by the order of consistency, it must first be defined what is meant by a local approximation obtained by a local application of a method based on the proposed numerical integration rule.

Definition 6.2.2 (Local Application/Approximation). *Let a method with s stages, $S-1$ secondary mesh points and a set of secondary mesh nodes $\{\theta_i \in]0,1] : i \in [1,S]\cap\mathbb{Z}\}$ based on the integration rule 6.1.2 be given. If y_1 and y_2 are given respectively on $[t_0-\tau,t_n]$ and $[t_0-\tau,t_n]^2$ then $y_{1;n,i}$ and $y_{2;n,i;n,j}$, $y_{2;n,i;t}$ and $y_{2;t;n,i}$ obtained by using the integration rule with the indices labeled by $M \in i(M_n^S \cup M_{\mathrm{I}})$ replaced by the continuous variable $t \in [t_0-\tau,t_n]$ and the lag integrals redefined as*

$$\begin{aligned} I_{1;n,k} &\equiv \int_{t_0-\tau}^{t_n} dt\; K_1(Y_{2;n,k;t}, y_1(t))\,, \\ I^{\nu}_{2,\mu;n,k;n,l} &\equiv \int_{t_0-\tau}^{t_n} dt\; K^{\nu}_{2,\mu}(Y_{2;n,k;t}, Y_{2;t;n,l})\,, \\ I^{\nu}_{2,\mu;n,k;t} &\equiv \int_{t_0-\tau}^{\delta_{\mu 1}t_n+\delta_{\mu 2}t} dt'\; K^{\nu}_{2,\mu}(Y_{2;n,k;t'}, y_2(t';t))\,, \\ I^{\nu}_{2,\mu;t;n,k} &\equiv \int_{t_0-\tau}^{\delta_{\mu 1}t+\delta_{\mu 2}t_n} dt'\; K^{\nu}_{2,\mu}(y_2(t;t'), Y_{2;t';n,k})\,, \end{aligned}$$

are referred to as the local approximations to the solutions y_1 at $t_n+\theta_i h_n$ and y_2 at $(t_n+\theta_i h_n, t_n+\theta_j h_n)$, $(t_n+\theta_i h_n, t)$ and $(t, t_n+\theta_i h_n)$ for all $t \in [t_0-\tau,t_n]$ where h_n is the step size. It is this process of obtaining the local approximations which is referred to as the local application of a method based on the integration rule 6.1.2 at t_n.

In other words, by a local application, it is referred to a more formal process in which the obtained local approximation has an error following purely from the local discretization of the integro-differential equations. It is noted that the notion of a local application, or approximation, is also used in an analogous way in the context of one-dimensional Volterra integro-differential equations [Lub82]. It is now possible, by taking advantage of the concept of a local approximation, to describe how a method based on the integration rule 6.1.2 behaves when the mesh is refined locally by reducing the step size. It is the order of consistency which describes how the error in the local approximation is bound in terms of the step size.

Definition 6.2.3 (Order of Consistency)**.** *Given a method based on the integration rule 6.1.2, let $\bar{y}_1$ and $\bar{y}_2$ denote the local approximations obtained by its local application 6.2.2 at $t_n \geq t_0$ with $S-1$ secondary mesh points, a set of secondary mesh nodes $\{\theta_i \in]0,1] : i \in [1,S] \cap \mathbb{Z}\}$ and a step size h_n. If there exists a real-valued constant $C > 0$ such that*

$$\begin{aligned}
\|\bar{y}_{1;n,i} - y_1(t_n + \theta_i h_n)\| &\leq C h_n^{p+\delta_{i\,S}}\,, \\
\|\bar{y}_{2;n,i;n,j} - y_2(t_n + \theta_i h_n; t_n + \theta_j h_n)\| &\leq C h_n^{p+\delta_{i\,S}\delta_{j\,S}}\,, \\
\|\bar{y}_{2;n,i;t} - y_2(t_n + \theta_i h_n; t)\| &\leq C h_n^{p+\delta_{i\,S}}\,, \\
\|\bar{y}_{2;t;n,i} - y_2(t; t_n + \theta_i h_n)\| &\leq C h_n^{p+\delta_{i\,S}}\,,
\end{aligned}$$

hold for all $t \in [t_0 - \tau, t_n]$ then the method on which the local application is based on is said to have an order of consistency of, or a local order, $p \in \mathbb{Z}_{\geq 0}$.

In order to guarantee that a method has a certain local order one demands that the Taylor expansions of the exact and approximate solutions with respect to the step size match up to the required order of consistency. This leads to an increasing number of algebraic conditions for the nodes, quadrature weights and weight functions of the method, which are referred to as the order conditions, for the increasing order of consistency. In the case of one-dimensional ordinary differential and Volterra integro-differential equations, the complexity of determining the order conditions can be alleviated elegantly for various numerical methods, which includes the class of the Runge-Kutta methods, by taking advantage of graph theory [But87, HNW08, BH86]. However, as only low order methods are considered here, it suffices to conduct the Taylor expansions by brute force. In the following, the order conditions are stated up to second order, i.e., to achieve an order of consistency of at least two.

Order Conditions (1st order)**.** *If a method based on the integration rule 6.1.2 satisfies the consistency conditions 6.2.1 then it has an order of consistency of at least one.*

Order Conditions (2nd order)**.** *If a method with s stages and $S-1$ secondary mesh points based on the integration rule 6.1.2 meets the first-order order conditions and further its weight functions 6.1.1 satisfy for $i = j = S$ and for all $k, l, p, q \in [1, s] \cap \mathbb{Z}$ the conditions*

$$\begin{aligned}
v_{2;kl;p}(z) &= \mathsf{v}_{2;kl;p} z\,, \\
b^{kl}_{2;ij;p}(z) &= \mathsf{b}^{kl}_{2;ij;p} z\,, \\
u_{2;ij;k,l}(z,z) &= \mathsf{u}_{2;ij;k,l} z^2\,, \\
u_{2;ij;k,l'}(z,z') &= \frac{1}{2}\mathsf{u}_{2;ij;k,l'}(zz' + z'z)\,,
\end{aligned}$$

where $\mathsf{v}_{2;kl;p}$, $\mathsf{b}^{kl}_{2;ij;p}$ and $\mathsf{u}_{2;ij;k,l^{(\prime)}}$ are real numbers such that

$$\sum_{k,l=1}^{s} \mathsf{u}_{2;ij;k,l} = 1\,, \tag{2.1}$$

$$\sum_{k,l=1}^{s} \mathsf{u}_{2;ij;k,l'} = 1\,, \tag{2.2}$$

$$\sum_{k,l=1}^{s} \mathsf{u}_{2;ij;k} c_k \mathsf{v}_{2;kk;l} = \frac{\theta_i}{2}\,, \tag{2.3}$$

$$\sum_{k=1}^{s} \mathsf{u}_{2;ij;k} c_k = \frac{\theta_i}{2}\,, \tag{2.4}$$

$$\sum_{k,l,p=1}^{s} \mathsf{b}^{kl}_{2;ij;p} = \frac{1}{2}\,, \tag{2.5}$$

$$\sum_{k,l,p=1}^{s} \mathsf{b}^{kl}_{2;ij} c_k \mathsf{v}_{2;kk;p} = \frac{\theta_i}{2}\,, \tag{2.6}$$

$$\sum_{k,l,p=1}^{s} \mathsf{b}^{kl}_{2;ij} c_k \mathsf{v}_{2;kl;p} = \frac{\theta_i}{2}\,, \tag{2.7}$$

$$\sum_{k,l=1}^{s} \mathsf{b}^{kl}_{2;ij} c_k = \frac{\theta_i}{2}\,, \tag{2.8}$$

$$\sum_{k,l,p=1}^{s} \mathsf{b}^{kl}_{2;ij} c_k d^p_k = \frac{\theta_i}{2}\,, \tag{2.9}$$

then the method has an order of consistency of at least two. Here, a primed index l' with $l \in [1,s]\cap\mathbb{Z}$ is to be understood as the index $s+l$.

It is referred to App. 6.A for the derivation of these order conditions and noted here that these conditions are to be understood together with the relations imposed in the definition 6.1.1 of the weight functions. As said, ff a method satisfies the first, second or even higher order order conditions then its local applications have an error which can be controlled by adjusting the step size. However, a given order of consistency does not explicitly describe how the numerical error behaves or accumulates when the fully discrete integration rule is applied successively. It is concluded here by outlining what is meant by the order of convergence, which describes how the desired global error behaves as a function of the step sizes, and by commenting how a given order of convergence can be potentially achieved. A method based on the integration rule 6.1.2 is said to have an order of convergence of $p \in \mathbb{Z}_{\geq 0}$ if there exists $h^* \in [0,\infty[$ such that it holds that $\|y_{1;n} - y_1(t_n)\| \leq c + Ch^p$ for all $n \in]0,N]\cap\mathbb{Z}$ and that $\|y_{2;n;m} - y_2(t_n;t_m)\| \leq c + Ch^p$ for all $(n,m) \in (]-M_\mathrm{I},N]^2 \setminus M_\mathrm{i}^2)\cap\mathbb{Z}^2$ where $c>0$ and $C>0$ are real valued constants and $h \equiv \max_{n\in[0,N]} h_n \in [0,h^*[$ is the maximal step size. Moreover, the constant c is required to tend to zero when the error in the initial conditions and in the discretization of the integrals from $t_0-\tau$ to t_0 on the initial mesh M_I tends to zero. It is stressed that in the case of the one-dimensional Volterra integro-differential equations, at this point, it can be proven that a Runge-Kutta method which has an order of consistency of p and whose lag integrals are discretized by using a quadrature rule of order p has also an order of convergence of p [Lub82, BH86]. It is due to the similarity with this standard case that it is possible that the same can be proven for a method based on the integration rule 6.1.2. However, it is emphasized that no such proof is presented in this thesis and hence it remains as an open problem to prove the convergence of a method based on the proposed integration rule.

6.3 Construction of Low Order Methods

In what follows, the first and second-order order conditions introduced in the previous section are applied to derive the one- and two-stage methods which have been introduced in Sec. 5.3.1. In order to do this, first, the mesh points and weight functions are chosen, and then, it is shown that by fixing the remaining parameters appropriately the second-order order conditions can be satisfied. Firstly, the mesh is chosen based on the following criterium. In order to reduce the computational complexity, it is desirable to minimize the number of the secondary mesh points and hence, as already two adjacent mesh points are sufficient to obtain second order numerical quadrature, only methods without $S = 1$ secondary mesh points are considered here. It is shown below, similarly to the case of ordinary differential [But87, HNW08] and Volterra integro-differential equations [BH86], that if a method is implicit then the second-order order conditions can be met with a single $s = 1$ internal stage while for an explicit method, at least two $s = 2$ internal stages are required. Here, by an explicit method it is meant a method whose weights satisfy for all $k, l, p, q \in [1, s] \cap \mathbb{Z}$ the conditions

$$\begin{aligned} v_{2;kl}(z_1, \dots, z_s; z'_1, \dots, z'_s) &\equiv v_{2;kl}(z_1, \dots, z_{\bar{s}}; z'_1, \dots, z'_{\bar{s}}) \,, \\ c_k a^{pq}_{2;kl}(z_1, \dots, z_s; z'_1, \dots, z'_s) &\equiv \begin{cases} 0 & \max(p,q) > \bar{s} \\ c_k a^{pq}_{2;kl}(z_1, \dots, z_{\bar{s}}; z'_1, \dots, z'_{\bar{s}}) & \text{otherwise} \end{cases} \,, \\ c_k d^l_k &= 0 \,, \qquad\qquad l > k \,, \end{aligned}$$

where $\bar{s} \equiv \max(k, l) - 1$, and by an implicit method it is referred to a method which is not explicit. Secondly, the weight functions of the method are specified by following closely the motivation of the integration rule presented in Sec. 6.1.1. It was shown that after the polynomial interpolation, the weight functions u and v could be deduced from the solutions of linear ordinary differential equations of the form $d\mathsf{y}_1(z)/dz = a(z)\mathsf{y}_1$ such that $\mathsf{y}_1(0) = 1$. It is possible, for example, to write the solution of this initial value problem as

$$\begin{aligned} \mathsf{y}_1(z) &= \varphi_0(\Omega(z)) \,, \\ \frac{d}{dz}\Omega(z) &= \sum_{k=0}^{\infty} \frac{B_k}{k!} \mathrm{ad}^k_{\Omega(z)} a(z) \,, \qquad\qquad \Omega(0) = 0 \,, \end{aligned}$$

where $\varphi_0(z) \equiv \exp(z)$, $\mathrm{ad}_a b \equiv ab - ba$ and B_k are Bernoulli numbers [IMKNZ05, BCOR09]. It is then natural to choose, although also other equally well-motived choices are possible, the weight functions u and v by truncating the expansion obtained by applying Picard iterations to Ω, i.e., applying the Magnus expansion [IMKNZ05, BCOR09], at a sufficiently high order to be able to construct second-order methods. In an analogous way, it is possible to choose the weight functions b and a from the knowledge of the solutions of the inhomogeneous differential equation $d\mathsf{y}_2(z)/dz = a(z)\mathsf{y}_2(z) + b(z)$ such that $\mathsf{y}_2(0) = 0$. In this case, it holds that the solution can be, for example, written as

$$\begin{aligned} \mathsf{y}_2(z) &= \varphi_1(\Omega_1(z))\Omega_2(z) \,, \\ \frac{d}{dz}(\Omega_1(z), \Omega_2(z)) &= \sum_{k=0}^{\infty} \frac{B_k}{k!} \mathrm{ad}^k_{(\Omega_1(z), \Omega_2(z))}(a(z), b(z)) \,, \qquad (\Omega_1(0), \Omega_2(0)) = (0, 0) \,, \end{aligned}$$

where $\varphi_1(z) \equiv (\exp(z) - 1)/z$ and $\mathrm{ad}_{(a_1,b_1)}(a_2, b_2) \equiv (a_1 a_2 - a_2 a_1, a_1 b_2 - a_2 b_1)$ [Min04, IMKNZ05]. In practice, in order to specify the weight functions b and a, the expansion above is truncated similarly to what is done in the case of Ω. In fact, as it is the purpose here to derive only second-order methods, it suffices to consider the simplest truncated equations $d\Omega(z)/dz = a(z)$ and $d(\Omega_1(z), \Omega_2(z))/dz = (a(z), b(z))$ for the weight functions u, v and b, a, respectively.

6.3.1 One-Stage Methods

It is instructive to first consider briefly methods which have a single $s = 1$ internal stage. In this case, the interpolating polynomials of Sec. 6.1.1 are just constant functions which corresponds, in the motivation above, to the cases $\Omega(z) = az$ and $(\Omega_1(z), \Omega_2(z)) = (az, bz)$ where a and b are independent of z. It is hence natural to choose the weight functions

$$\begin{aligned} u_{2;11}(z;z') &= v_{2;11}(z;z') \\ &= \varphi_0(z+z')\,, \\ b^{11}_{2;11}(z;z') &= a^{11}_{2;11}(z;z') \\ &= \int_0^1 d\vartheta\ \exp((z+z')(1-\vartheta)) \\ &= \varphi_1(z+z')\,, \end{aligned}$$

where the integral form of φ_1 is shown to highlight the connection to Sec. 6.1.1. It is then straightforward to verify, by using the derivatives

$$\begin{aligned} \varphi_k(z)\big|_{z=0} &= \frac{\mathbb{1}}{k!}\,, \\ D\varphi_k(z)\big|_{z=0}(z_1) &= \frac{z_1}{(k+1)!}\,, \\ D^2\varphi_k(z)\big|_{z=0}(z_1,z_2) &= \frac{z_1 z_2 + z_2 z_1}{(k+2)!}\,, \end{aligned}$$

which hold for all of the so-called φ-functions

$$\varphi_k(z) \equiv \int_0^1 d\vartheta\ \exp((1-\vartheta)z)\frac{\vartheta^{k-1}}{(k-1)!}\,, \qquad\qquad k \in \mathbb{Z}_{>0}\,,$$

that the first-order order conditions, i.e., the consistency conditions 6.2.1, which require that $u_{2;11} = v_{2;11} = \mathsf{u}_{2;11;1} = \mathbb{1}$ and $b^{11}_{2;11} = a^{11}_{2;11} = \mathbb{1}$ are satisfied independent of the choice of c_1. In particular, the choice $c_1 = 0$ leads to an explicit, first-order method, i.e., the method labeled by $\underline{\mathrm{i}}$ in Sec. 5.3.1, which resembles the forward (Lie-)Euler method familiar from the context of ordinary differential equations. If $c_1 > 0$ instead then the method is implicit and, for instance, the choice $c_1 = 1$ leads to a first-order method known in the context of ordinary differential equations as the backward (Lie-)Euler method. It is finally noted that since $\mathsf{v}_{2;11;1} = \mathsf{u}_{2;11;1,1^{(\prime)}} = 1$ and $\mathsf{b}^{11}_{2;11;1} = 1/2$, also the second-order order conditions are met provided that $c_1 = 1/2$ and $d^1_1 = 1$ which in turn leads to a method resembling the midpoint method for ordinary differential equations.

6.3.2 Class of Explicit Two-Stage Methods

In what follows, the class of explicit two-stage methods labeled by $\underline{\mathrm{ii}}$ in Sec. 5.3.1 is derived by requiring that the second-order order conditions are satisfied. First of all, since explicit methods are of interest, it is chosen that $c_1 = 0$ which implies that the first stage approximations labeled by $n, 1$ and $(n, 1; n, 1)$, $(n, i; M)$ and $(M; n, 1)$ can be seen to approximate the solutions at t_n and $(t_n; t_n)$, $(t_n; t_M)$ and $(t_M; t_n)$ for all $M \in i(M^S_n \cap M_{\mathrm{I}})$, respectively. It is then geometrically well-justified to choose the weight functions such that for y_2 the stage approximations labeled by $(n, 2; n, 1)$ and $(n, 1; n, 2)$ equal to the stage approximations labeled by $(n, 2; n)$ and $(n; n, 2)$, respectively. Second of all, in the case that $s = 2$, the interpolating polynomials of Sec. 6.1.1, are linear functions such that

when determining the weight functions, it would in principle be necessary to consider higher order truncations of Ω, Ω_1 and Ω_2 than in the previous section on one-stage methods. However, as most of the corrections related to a higher order truncation would lead to third or higher order corrections with respect to the step size h_n for y_1 and y_2, it is proposed that the form of the weight functions is the same as in the previous section. It then follows from these propositions that

$$
\begin{aligned}
u_{2;11}(z_1, z_2; z_1', z_2') &= \varphi_0\left(\sum_{r=1}^{2} u_r(z_r + z_r')\right), \\
v_{2;kl}(z_1, z_2; z_1', z_2') &= \varphi_0\left(\sum_{r=1}^{2} v^r_{\max(k,l)}(z_r + z_r')\right), \\
b^{kl}_{2;11}(z_1, z_2; z_1', z_2') &= \delta_{kl} b_k \varphi_1\left(\sum_{r=1}^{2} u_r(z_r + z_r')\right), \\
a^{pq}_{2;kl}(z_1, z_2; z_1', z_2') &= \begin{pmatrix} \delta_{pq} & \delta_{p1} \\ \delta_{q1} & \delta_{pq} \end{pmatrix}_{kl} a^{\max(p,q)}_{\max(k,l)} \varphi_1\left(\sum_{r=1}^{2} v^r_{\max(k,l)}(z_r + z_r')\right),
\end{aligned}
$$

are the weight function candidates for the second order methods. Here, u_k, v^l_k, b_k and a^l_k such that $v^l_k = a^l_k = 0$ for $l \geq k$ denote real parameters which are to be determined by enforcing the order conditions. It follows from these choices that $\mathsf{u}_{2;11} = \mathsf{v}_{2;kl} = 1$, $\mathsf{u}_{2;11;k} = u_k$, $\mathsf{b}^{kl}_{2;11} = \delta_{kl} b_k$, $\mathsf{a}^{pq}_{2;kk} = \delta_{pq} a^p_k$ and $\mathsf{a}^{pq}_{2;12} = \mathsf{a}^{qp}_{2;21} = \delta_{p1} a^q_2$ which means that the consistency conditions 6.2.1, and as a consequence the first-order order conditions, reduce to

$$\sum_{k=1}^{2} u_k = 1\,, \tag{1.1}$$

$$\sum_{k=1}^{2} b_k = 1\,, \tag{1.2}$$

$$a^1_2 = 1\,. \tag{1.3}$$

It remains to supplement these conditions with the second-order order conditions which can potentially be satisfied as it follows from the choice of the weight functions that $\mathsf{v}_{2;kl;p} = v^p_{\max(k,l)}$, $\mathsf{b}^{kl}_{2;11;p} = \delta_{kl} b_k u_p/2$ and $\mathsf{u}_{2;11;k,l^{(\prime)}} = u_k u_l$. It is then found, by using the first-order conditions, that the second-order order conditions reduce to

$$u_2 c_2 v^1_2 = \frac{1}{2}\,, \tag{2.3}$$

$$u_2 c_2 = \frac{1}{2}\,, \tag{2.4}$$

$$b_2 c_2 v^1_2 = \frac{1}{2}\,, \tag{2.6-7}$$

$$b_2 c_2 = \frac{1}{2}\,, \tag{2.8}$$

$$\sum_{k=1}^{2} b_2 c_2 d^k_2 = \frac{1}{2}\,, \tag{2.9}$$

where, similarly to the case of the first-order conditions, the equation labels refer to the enumerated order conditions of the previous section. It is then possible to conclude that the first- and second-order order conditions can be satisfied by choosing $u_2 = b_2 = 1/2c_2$, $u_1 = b_1 = 1 - b_2 = 1 - 1/2c_2$, $v^1_2 = 1$ and $d^1_2 = 1 - d^2_2$ where c_2 and d^2_2 are regarded as free parameters. It has been thus shown explicitly that the integration rule ii of Sec. 5.3.1, which is used in **II** [SPAL15b], is well-motivated and, furthermore, satisfies the second-order order conditions.

Appendix

6.A Derivation of 1st- and 2nd-Order, Order Conditions

In what follows, the order conditions of Sec. 6.2 are derived by evaluating the Taylor expansions of the exact solution y and a local approximation $\bar{y}$ up to second order with respect to the step size. It follows from the definition 6.2.3 that a method with s stages and $S-1$ secondary mesh points has an order of consistency of two if the Taylor coefficients of the local approximations $\bar{y}_{1;n,i}$ and $\bar{y}_{2;n,i;n,j}$, $\bar{y}_{2;n,i;t}$ and $\bar{y}_{1;t;n,i}$ equal respectively to the Taylor coefficients of y_1 at $t_{n,i}$ and y_2 at $(t_{n,i}, t_{n,j})$, $(t_{n,i}, t)$ and $(t, t_{n,i})$ up to first order for all $i, j \in [1, S[\cap\mathbb{Z}$ and up to second order for $i = j = S$ with respect to h_n. In order to evaluate these coefficients, it is useful to introduce the short-hands

$$\begin{aligned} y_{1;n} &\equiv y_1(t_n)\,, \\ y_{2;n;n} &\equiv y_2(t_n; t_n)\,, \\ y_{2;n;t} &\equiv y_2(t_n; t)\,, \\ y_{2;t;n} &\equiv y_2(t; t_n)\,, \end{aligned}$$

$$\begin{aligned} L^{(\nu)}_{\mu;n} &\equiv L^{(\nu)}_{\mu}(y_{1;n}, y_{2;n;n})\,, \\ (L^{\nu}_2 y_2)_{n;n} &\equiv L^{\nu}_{2;n} y_{2;n;n}\,, \\ (L^{1}_2 y_2)_{n;t} &\equiv L^{1}_{2;n} y_{2;n;t}\,, \\ (L^{2}_2 y_2)_{t;n} &\equiv L^{2}_{2;n} y_{2;t;n}\,, \end{aligned}$$

and

$$\begin{aligned} N_{1;n} &\equiv N_1(y_{2;n;n}, I_1(t_n))\,, \\ N^{\nu}_{2;n;n} &\equiv N^{\nu}_2(y_{2;n;n}, I^{\nu}_{2,1}(t_n; t_n), I^{\nu}_{2,2}(t_n; t_n))\,, \\ N^{1}_{2;n;t} &\equiv N^{1}_2(y_{2;n;t}, I^{1}_{2,1}(t_n; t), I^{1}_{2,2}(t_n; t))\,, \\ N^{2}_{2;t;n} &\equiv N^{2}_2(y_{2;t;n}, I^{2}_{2,1}(t; t_n), I^{2}_{2,2}(t; t_n))\,, \end{aligned}$$

where $\nu \in \{1, 2\}$ and $t \in [t_0 - \tau, t_0]$. Moreover, also

$$\begin{aligned} K_{1;n;n} &\equiv K_1(y_{2;n;n}, y_{1;n})\,, \\ K^{\nu}_{2,\mu;n;n;n} &\equiv K^{\nu}_{2,\mu}(y_{2;n;n}, y_{2;n;n})\,, \\ K^{1}_{2,\mu;n;n;t} &\equiv K^{1}_{2,\mu}(y_{2;n;n}, y_{2;n;t})\,, \end{aligned}$$

and

$$\begin{aligned} \{D_1 K_1(z)\}_n &\equiv \int_{t_0-\tau}^{t_n} dt\; D_1 K_1(y_{2;n;t}, y_1(t))(z_{n;t})\,, \\ \{D_1 K^{\nu}_{2,\mu}(z)\}_{n;n} &\equiv \int_{t_0-\tau}^{t_n} dt\; D_1 K^{\nu}_{2,\mu}(y_{2;n;t}, y_{2;t;n})(z_{n;t})\,, \end{aligned}$$

$$\{D_2K^{\nu}_{2,\mu}(z)\}_{n;n} \equiv \int_{t_0-\tau}^{t_n} dt\; D_2K^{\nu}_{2,\mu}(y_{2;n;t}, y_{2;t;n})(z_{t;n})\,,$$
$$\{D_1K^{1}_{2,\mu}(z)\}_{n;t} \equiv \int_{t_0-\tau}^{\delta_{\mu\,1}t_n+\delta_{\mu\,2}t} dt'\; D_1K^{1}_{2,\mu}(y_{2;n;t'}, y_2(t';t))(z_{n;t'})\,,$$

where $\nu, \mu \in \{1, 2\}$ are useful abbreviations in order to keep the equations as short as possible, It is then possible to proceed to list compactly the first and second derivatives of the solutions $y_{1;n,i}$, $y_{2;n,i;n,j}$ and $y_{2;n,i;t}$ with respect to the step size h_n for $h_n = 0$. It is noted that since the integration rule 6.1.2 treats $\bar{y}_{2;n,i;t}$ and $\bar{y}_{2;t;n,i}$ symmetrically, the latter gives rise to the same order conditions as the former, and hence the derivatives of $y_{2;t;n,i}$ are not listed explicitly in the following.

If $y_{1;n,i} \equiv y_1(t_{n,i})$ then

$$\frac{d}{dh_n} y_{1;n,i}\bigg|_0$$
$$= \theta_i L_{1;n} y_{1;n} \tag{A1.1}$$
$$+ \theta_i N_{1;n}\,, \tag{A1.2}$$
$$\frac{d^2}{dh_n^2} y_{1;n,i}\bigg|_0$$
$$= \theta_i^2 D_1 L_{1;n}(L_{1;n}y_{1;n})y_{1;n} \tag{A2.1}$$
$$+ \theta_i^2 D_1 L_{1;n}(N_{1;n})y_{1;n} \tag{A2.2}$$
$$+ \theta_i^2 D_2 L_{1;n}(L^1_{2;n}y_{2;n;n})y_{1;n} \tag{A2.3}$$
$$+ \theta_i^2 D_2 L_{1;n}(L^2_{2;n}y_{2;n;n})y_{1;n} \tag{A2.4}$$
$$+ \theta_i^2 D_1 L_{1;n}(N^1_{2;n;n})y_{1;n} \tag{A2.5}$$
$$+ \theta_i^2 D_1 L_{1;n}(N^2_{2;n;n})y_{1;n} \tag{A2.6}$$
$$+ \theta_i^2 L_{1;n} L_{1;n} y_{1;n} \tag{A2.7}$$
$$+ \theta_i^2 L_{1;n} N_{1;n} \tag{A2.8}$$
$$+ \theta_i^2 D_1 N_{1;n}(L^1_{2;n}y_{2;n;n}) \tag{A2.9}$$
$$+ \theta_i^2 D_1 N_{1;n}(L^2_{2;n}y_{2;n;n}) \tag{A2.10}$$
$$+ \theta_i^2 D_1 N_{1;n}(N^1_{2;n;n}) \tag{A2.11}$$
$$+ \theta_i^2 D_1 N_{1;n}(N^2_{2;n;n}) \tag{A2.12}$$
$$+ \theta_i^2 D_2 N_{1;n}(\{D_1K_1(L^1_2y_2)\}_n) \tag{A2.13}$$
$$+ \theta_i^2 D_2 N_{1;n}(\{D_1K_1(N^1_2)\}_n) \tag{A2.14}$$
$$+ \theta_i^2 D_2 N_{1;n}(K_{1;n;n})\,. \tag{A2.15}$$

If $y_{2;n,i;n,j} \equiv y_2(t_{n,i}; t_{n,j})$ then

$$\frac{d}{dh_n} y_{2;n,i;n,j}\bigg|_0$$
$$= \theta_i L^1_{2;n} y_{2;n;n} \tag{B1.1}$$
$$+ \theta_j L^2_{2;n} y_{2;n;n} \tag{B1.2}$$
$$+ \theta_i N^1_{2;n;n} \tag{B1.3}$$
$$+ \theta_j N^1_{2;n;n}\,, \tag{B1.4}$$
$$\frac{d^2}{dh_n^2} y_{2;n,i;n,j}\bigg|_0$$
$$= \theta_i^2 D_1 L^1_{2;n}(L_{1;n}y_{1;n})y_{2;n;n} \tag{B2.1}$$
$$+ \theta_i^2 D_1 L^1_{2;n}(N_{1;n})y_{2;n;n} \tag{B2.2}$$
$$+ \theta_i^2 D_2 L^1_{2;n}(L^1_{2;n}y_{2;n;n})y_{2;n;n} \tag{B2.3}$$
$$+ \theta_i^2 D_2 L^1_{2;n}(L^2_{2;n}y_{2;n;n})y_{2;n;n} \tag{B2.4}$$
$$+ \theta_i^2 D_2 L^1_{2;n}(N^1_{2;n;n})y_{2;n;n} \tag{B2.5}$$
$$+ \theta_i^2 D_2 L^1_{2;n}(N^2_{2;n;n})y_{2;n;n} \tag{B2.6}$$
$$+ \theta_i^2 L^1_{2;n} L^1_{2;n} y_{2;n;n} \tag{B2.7}$$
$$+ \theta_i\theta_j L^1_{2;n} L^2_{2;n} y_{2;n;n} \tag{B2.8}$$
$$+ \theta_i^2 L^1_{2;n} N^1_{2;n;n} \tag{B2.9}$$
$$+ \theta_i\theta_j L^1_{2;n} N^2_{2;n;n} \tag{B2.10}$$
$$+ \theta_j^2 D_1 L^2_{2;n}(L_{1;n}y_{1;n})y_{2;n;n} \tag{B2.11}$$
$$+ \theta_j^2 D_1 L^2_{2;n}(N_{1;n})y_{2;n;n} \tag{B2.12}$$
$$+ \theta_j^2 D_2 L^2_{2;n}(L^1_{2;n}y_{2;n;n})y_{2;n;n} \tag{B2.13}$$
$$+ \theta_j^2 D_2 L^2_{2;n}(L^2_{2;n}y_{2;n;n})y_{2;n;n} \tag{B2.14}$$
$$+ \theta_j^2 D_2 L^2_{2;n}(N^1_{2;n;n})y_{2;n;n} \tag{B2.15}$$
$$+ \theta_j^2 D_2 L^2_{2;n}(N^2_{2;n;n})y_{2;n;n} \tag{B2.16}$$
$$+ \theta_i\theta_j L^2_{2;n} L^1_{2;n} y_{2;n;n} \tag{B2.17}$$
$$+ \theta_j^2 L^2_{2;n} L^2_{2;n} y_{2;n;n} \tag{B2.18}$$
$$+ \theta_i\theta_j L^2_{2;n} N^1_{2;n;n} \tag{B2.19}$$
$$+ \theta_j^2 L^2_{2;n} N^2_{2;n;n} \tag{B2.20}$$
$$+ \theta_i^2 D_1 N^1_{2;n;n}(L^1_{2;n}y_{2;n;n}) \tag{B2.21}$$
$$+ \theta_i\theta_j D_1 N^1_{2;n;n}(L^2_{2;n}y_{2;n;n}) \tag{B2.22}$$
$$+ \theta_i^2 D_1 N^1_{2;n;n}(N^1_{2;n;n}) \tag{B2.23}$$
$$+ \theta_i\theta_j D_1 N^1_{2;n;n}(N^2_{2;n;n}) \tag{B2.24}$$
$$+ \theta_i^2 D_{\nu+1} N^1_{2;n;n}(\{D_1K^1_{2,\nu}(L^1_2y_2)\}_{n;n}) \tag{B2.25}$$
$$+ \theta_i^2 D_{\nu+1} N^1_{2;n;n}(\{D_1K^1_{2,\nu}(N^1_2)\}_{n;n}) \tag{B2.26}$$
$$+ \theta_i\theta_j D_{\nu+1} N^1_{2;n;n}(\{D_2K^1_{2,\nu}(L^2_2y_2)\}_{n;n}) \tag{B2.27}$$
$$+ \theta_i\theta_j D_{\nu+1} N^1_{2;n;n}(\{D_2K^1_{2,\nu}(N^2_2)\}_{n;n}) \tag{B2.28}$$
$$+ \theta_i^2 D_2 N^1_{2;n;n}(K^1_{2,1;n;n;n}) \tag{B2.29}$$
$$+ \theta_i\theta_j D_3 N^1_{2;n;n}(K^1_{2,2;n;n;n}) \tag{B2.30}$$
$$+ \theta_i\theta_j D_1 N^2_{2;n;n}(L^1_{2;n}y_{2;n;n}) \tag{B2.31}$$
$$+ \theta_j^2 D_1 N^2_{2;n;n}(L^2_{2;n}y_{2;n;n}) \tag{B2.32}$$
$$+ \theta_i\theta_j D_1 N^2_{2;n;n}(N^1_{2;n;n}) \tag{B2.33}$$
$$+ \theta_j^2 D_1 N^2_{2;n;n}(N^2_{2;n;n}) \tag{B2.34}$$
$$+ \theta_i\theta_j D_{\nu+1} N^2_{2;n;n}(\{D_1K^2_{2,\nu}(L^1_2y_2)\}_{n;n}) \tag{B2.35}$$
$$+ \theta_i\theta_j D_{\nu+1} N^2_{2;n;n}(\{D_1K^2_{2,\nu}(N^1_2)\}_{n;n}) \tag{B2.36}$$

$$+\theta_j^2 D_{\nu+1} N^2_{2;n;n}(\{D_2 K^2_{2,\nu}(L^2_2 y_2)\}_{n;n}) \quad \text{(B2.37)}$$
$$+\theta_j^2 D_{\nu+1} N^2_{2;n;n}(\{D_2 K^2_{2,\nu}(N^2_2)\}_{n;n}) \quad \text{(B2.38)}$$
$$+\theta_i\theta_j D_2 N^2_{2;n;n}(K^2_{2,1;n;n;n}) \quad \text{(B2.39)}$$
$$+\theta_j^2 D_3 N^2_{2;n;n}(K^2_{2,2;n;n;n})\,. \quad \text{(B2.40)}$$

If $y_{2;n,i;t} \equiv y_2(t_{n,i};t)$ then

$$\left.\frac{d}{dh_n} y_{2;n,i;t}\right|_0$$
$$= \theta_i L^1_{2;n} y_{2;n;t} \quad \text{(C1.1)}$$
$$+\theta_i N^1_{2;n;t}\,, \quad \text{(C1.2)}$$
$$\left.\frac{d^2}{dh_n^2} y_{2;n,i;t}\right|_0$$
$$= \theta_i^2 D_1 L^1_{2;n}(L_{1;n} y_{1;n}) y_{2;n;t} \quad \text{(C2.1)}$$
$$+\theta_i^2 D_1 L^1_{2;n}(N_{1;n}) y_{2;n;t} \quad \text{(C2.2)}$$
$$+\theta_i^2 D_2 L^1_{2;n}(L^1_{2;n} y_{2;n;n}) y_{2;n;t} \quad \text{(C2.3)}$$
$$+\theta_i^2 D_2 L^1_{2;n}(L^2_{2;n} y_{2;n;n}) y_{2;n;t} \quad \text{(C2.4)}$$
$$+\theta_i^2 D_2 L^1_{2;n}(N^1_{2;n;n}) y_{2;n;t} \quad \text{(C2.5)}$$
$$+\theta_i^2 D_2 L^1_{2;n}(N^2_{2;n;n}) y_{2;n;t} \quad \text{(C2.6)}$$
$$+\theta_i^2 L^1_{2;n} L^1_{2;n} y_{2;n;t} \quad \text{(C2.7)}$$
$$+\theta_i^2 L^1_{2;n} N^1_{2;n;t} \quad \text{(C2.8)}$$
$$+\theta_i^2 D_1 N^1_{2;n;t}(L^1_{2;n} y_{2;n;t}) \quad \text{(C2.9)}$$
$$+\theta_i^2 D_1 N^2_{2;n;t}(N^1_{2;n;t}) \quad \text{(C2.10)}$$
$$+\theta_i^2 D_{\nu+1} N^1_{2;n;t}(\{D_1 K^1_{2,\nu}(L^1_2 y_2)\}_{n;t}) \quad \text{(C2.11)}$$
$$+\theta_i^2 D_{\nu+1} N^1_{2;n;t}(\{D_1 K^1_{2,\nu}(N^1_2)\}_{n;t}) \quad \text{(C2.12)}$$
$$+\theta_i^2 D_2 N^1_{2;n;t}(K^1_{2,1;n;n;t})\,. \quad \text{(C2.13)}$$

In the equations above, the indices $\nu \in \{1,2\}$ labeling the integral kernels and in addition, in the equations below, all internal indices $k,l,p,q \in [1,s]\cap\mathbb{Z}$ are to be understood to be summed over. In order to require that the Taylor expansions of the exact y and approximate $\bar{y}$ solutions agree up to a given order, it is demanded that

$$\begin{aligned} u_{1;i} &= \mathbb{1}\,, \\ v_{1;k} &= \mathbb{1}\,, \\ u_{2;ij} &= \mathbb{1}\,, \\ v_{2;kl} &= \mathbb{1}\,, \end{aligned}$$

for all $i,j \in [1,S]\cap\mathbb{Z}$ and $k,l \in [1,s]\cap\mathbb{Z}$ since then

$$\begin{aligned} \bar{y}_{1;n,i}|_0 &= \bar{Y}_{1;n,k}|_0 \\ &= y_{1;n}\,, \end{aligned} \qquad \begin{aligned} \bar{y}_{2;n,i;t}|_0 &= \bar{Y}_{2;n,k;t}|_0 \\ &= y_{2;n;t}\,, \end{aligned}$$

$$\begin{aligned} \bar{y}_{2;n,i;n,j}|_0 &= \bar{Y}_{2;n,k;n,l}|_0 \\ &= y_{2;n;n}\,, \end{aligned}$$

and $\bar{y}_{2;t;n,i}|_0 = \bar{Y}_{2;t;n,k}|_0 = y_{2;t;n}$ for all $i,j \in [1,S]\cap\mathbb{Z}$ and $k,l \in [1,s]\cap\mathbb{Z}$. It is then possible to compare the Taylor coefficients of the exact y and approximate $\bar{y}$ solutions by first listing the first and second derivatives of the local approximations $\bar{y}_{1;n,i}$, $\bar{y}_{2;n,i;n,j}$ and $\bar{y}_{2;n,i;t}$ with respect to the step size h_n for $h_n = 0$. It is noted that below, by a primed index k' referring to a derivative of $u_{2;ij}$, $v_{2;kl}$, $b^{kl}_{2;ij}$ or $a^{pq}_{2;kl}$, it is meant that the derivative is taken with respect to the $(s+k)$th argument. Also, the abbreviations $(v_{1;k;l}(L^1_2)z)_{n,t} \equiv v_{1;k;l}(L^1_{2;n})z_{n,t}$ and $(v_{1;k;l}(L^2_2)z)_{t,n} \equiv v_{1;k;l}(L^2_{2;n})z_{t,n}$ are used below.

If $\bar{y}_{1;n,i}$ is considered then

$$\left.\frac{d}{dh_n}\bar{y}_{1;n,i}\right|_0$$
$$= \theta_i u_{1;i;k}(L_{1;n}) y_{1;n} \quad \text{(A1.1)}$$
$$+\theta_i b^k_{1;i} N_{1;n}\,, \quad \text{(A1.2)}$$
$$\left.\frac{d^2}{dh_n^2}\bar{y}_{1;n,i}\right|_0$$
$$= \theta_i^2 u_{1;i;k,l}(L_{1;n}, L_{1;n}) y_{1;n} \quad \text{(A2.7)}$$
$$+2\theta_i u_{1;i;k}(D_1 L_{1;n}(c_k v_{1;k;l}(L_{1;n}) y_{1;n})) y_{1;n} \quad \text{(A2.1)}$$
$$+2\theta_i u_{1;i;k}(D_1 L_{1;n}(c_k a^l_{1;k} N_{1;n})) y_{1;n} \quad \text{(A2.2)}$$

$$+ 2\theta_i u_{1;i;k}(D_2 L_{1;n}(c_k v_{2;kk;l}(L^1_{2;n}) y_{2;n;n}))y_{1;n} \quad \text{(A2.3)}$$
$$+ 2\theta_i u_{1;i;k}(D_2 L_{1;n}(c_k v_{2;kk;l'}(L^2_{2;n}) y_{2;n;n}))y_{1;n} \quad \text{(A2.4)}$$
$$+ 2\theta_i u_{1;i;k}(D_2 L_{1;n}(c_k a^{lp}_{2;kk} N^1_{2;n;n}))y_{1;n} \quad \text{(A2.5)}$$
$$+ 2\theta_i u_{1;i;k}(D_2 L_{1;n}(c_k a^{lp}_{2;kk} N^2_{2;n;n}))y_{1;n} \quad \text{(A2.6)}$$
$$+ 2\theta_i^2 b^k_{1;i;l}(L_{1;n}) N_{1;n} \quad \text{(A2.8)}$$
$$+ 2\theta_i b^k_{1;i} D_1 N_{1;n}(c_k v_{2;kk;l}(L^1_{2;n}) y_{2;n;n}) \quad \text{(A2.9)}$$
$$+ 2\theta_i b^k_{1;i} D_1 N_{1;n}(c_k v_{2;kk;l'}(L^2_{2;n}) y_{2;n;n}) \quad \text{(A2.10)}$$
$$+ 2\theta_i b^k_{1;i} D_1 N_{1;n}(c_k a^{lp}_{2;kk} N^1_{2;n;n}) \quad \text{(A2.11)}$$
$$+ 2\theta_i b^k_{1;i} D_1 N_{1;n}(c_k a^{lp}_{2;kk} N^2_{2;n;n}) \quad \text{(A2.12)}$$
$$+ 2\theta_i b^k_{1;i} D_2 N_{1;n}(c_k \{D_1 K_1(v_{1;k;l}(L^1_2) y_2)\}_n \quad \text{(A2.13)}$$
$$+ 2\theta_i b^k_{1;i} D_2 N_{1;n}(c_k \{D_1 K_1(a^l_{1;k} N^1_2)\}_n \quad \text{(A2.14)}$$
$$+ 2\theta_i b^k_{1;i} D_2 N_{1;n}(c_k d^l_k K_{1;n;n}) \,. \quad \text{(A2.15)}$$

If $\bar{y}_{2;n,i;n,j}$ is considered then

$$\left.\frac{d}{dh_n}\bar{y}_{2;n,i;n,j}\right|_0$$
$$= \theta_i u_{2;ij;k}(L^1_{2;n}) y_{2;n;n} \quad \text{(B1.1)}$$
$$+ \theta_j u_{2;ij;k'}(L^2_{2;n}) y_{2;n;n} \quad \text{(B1.2)}$$
$$+ \theta_i b^{kl}_{2;ij} N^1_{2;n;n} \quad \text{(B1.3)}$$
$$+ \theta_j b^{kl}_{2;ij} N^2_{2;n;n} \,, \quad \text{(B1.4)}$$
$$\left.\frac{d^2}{dh_n^2}\bar{y}_{2;n,i;n,j}\right|_0$$
$$= \theta_i^2 u_{2;ij;k,l}(L^1_{2;n}, L^1_{2;n}) y_{2;n;n} \quad \text{(B2.7)}$$
$$+ 2\theta_i\theta_j u_{2;ij;k,l'}(L^1_{2;n}, L^2_{2;n}) y_{2;n;n} \quad \text{(B2.(8,17))}$$
$$+ 2\theta_i u_{2;ij;k}(D_1 L^1_{2;n}(c_k v_{1;k;l}(L_{1;n}) y_{1;n}))y_{2;n;n} \quad \text{(B2.1)}$$
$$+ 2\theta_i u_{2;ij;k}(D_1 L^1_{2;n}(c_k a^l_{1;k} N_{1;n}))y_{2;n;n} \quad \text{(B2.2)}$$
$$+ 2\theta_i u_{2;ij;k}(D_2 L^1_{2;n}(c_k v_{2;kk;l}(L^1_{2;n}) y_{2;n;n}))y_{2;n;n} \quad \text{(B2.3)}$$
$$+ 2\theta_i u_{2;ij;k}(D_2 L^1_{2;n}(c_k v_{2;kk;l'}(L^2_{2;n}) y_{2;n;n}))y_{2;n;n} \quad \text{(B2.4)}$$
$$+ 2\theta_i u_{2;ij;k}(D_2 L^1_{2;n}(c_k a^{lp}_{2;kk} N^1_{2;n;n}))y_{2;n;n} \quad \text{(B2.5)}$$
$$+ 2\theta_i u_{2;ij;k}(D_2 L^1_{2;n}(c_k a^{lp}_{2;kk} N^2_{2;n;n}))y_{2;n;n} \quad \text{(B2.6)}$$
$$+ \theta_j^2 u_{2;ij;k',l'}(L^2_{2;n}, L^2_{2;n}) y_{2;n;n} \quad \text{(B2.18)}$$
$$+ 2\theta_j u_{2;ij;k'}(D_1 L^2_{2;n}(c_k v_{1;k;l}(L_{1;n}) y_{1;n}))y_{2;n;n} \quad \text{(B2.11)}$$
$$+ 2\theta_j u_{2;ij;k'}(D_1 L^2_{2;n}(c_k a^l_{1;k} N_{1;n}))y_{2;n;n} \quad \text{(B2.12)}$$
$$+ 2\theta_j u_{2;ij;k'}(D_2 L^2_{2;n}(c_k v_{2;kk;l}(L^1_{2;n}) y_{2;n;n}))y_{2;n;n} \quad \text{(B2.13)}$$
$$+ 2\theta_j u_{2;ij;k'}(D_2 L^2_{2;n}(c_k v_{2;kk;l'}(L^2_{2;n}) y_{2;n;n}))y_{2;n;n} \quad \text{(B2.14)}$$
$$+ 2\theta_j u_{2;ij;k'}(D_2 L^2_{2;n}(c_k a^{lp}_{2;kk} N^1_{2;n;n}))y_{2;n;n} \quad \text{(B2.15)}$$
$$+ 2\theta_j u_{2;ij;k'}(D_2 L^2_{2;n}(c_k a^{lp}_{2;kk} N^2_{2;n;n}))y_{2;n;n} \quad \text{(B2.16)}$$
$$+ 2\theta_i^2 b^{kl}_{2;ij;p}(L^1_{2;n}) N^1_{2;n;n} \quad \text{(B2.9)}$$
$$+ 2\theta_i\theta_j b^{kl}_{2;ij;p'}(L^2_{2;n}) N^1_{2;n;n} \quad \text{(B2.19)}$$
$$+ 2\theta_i b^{kl}_{2;ij} D_1 N^1_{2;n;n}(c_k v_{2;kl;p}(L^1_{2;n}) y_{2;n;n}) \quad \text{(B2.21)}$$
$$+ 2\theta_i b^{kl}_{2;ij} D_1 N^1_{2;n;n}(c_l v_{2;kl;p'}(L^2_{2;n}) y_{2;n;n}) \quad \text{(B2.22)}$$
$$+ 2\theta_i b^{kl}_{2;ij} D_1 N^1_{2;n;n}(c_k a^{pq}_{2;kl} N^1_{2;n;n}) \quad \text{(B2.23)}$$
$$+ 2\theta_i b^{kl}_{2;ij} D_1 N^1_{2;n;n}(c_l a^{pq}_{2;kl} N^2_{2;n;n}) \quad \text{(B2.24)}$$
$$+ 2\theta_i b^{kl}_{2;ij} D_{\nu+1} N^1_{2;n;n}(c_k \{D_1 K^1_{2,\nu}(v_{1;k;p}(L^1_2) y_2)\}_{n;n}) \quad \text{(B2.25)}$$
$$+ 2\theta_i b^{kl}_{2;ij} D_{\nu+1} N^1_{2;n;n}(c_k \{D_1 K^1_{2,\nu}(a^p_{1;k} N^1_2)\}_{n;n}) \quad \text{(B2.26)}$$
$$+ 2\theta_i b^{kl}_{2;ij} D_{\nu+1} N^1_{2;n;n}(c_l \{D_2 K^1_{2,\nu}(v_{1;l;p}(L^2_2) y_2)\}_{n;n}) \quad \text{(B2.27)}$$
$$+ 2\theta_i b^{kl}_{2;ij} D_{\nu+1} N^1_{2;n;n}(c_l \{D_2 K^1_{2,\nu}(a^p_{1;l} N^2_2)\}_{n;n}) \quad \text{(B2.28)}$$
$$+ 2\theta_i b^{kl}_{2;ij} D_2 N^1_{2;n;n}(c_k d^p_k K^1_{2,1;n;n;n}) \quad \text{(B2.29)}$$
$$+ 2\theta_i b^{kl}_{2;ij} D_3 N^1_{2;n;n}(c_l d^p_l K^1_{2,2;n;n;n}) \quad \text{(B2.30)}$$
$$+ 2\theta_i\theta_j b^{kl}_{2;ij;p}(L^1_{2;n}) N^2_{2;n;n} \quad \text{(B2.10)}$$
$$+ 2\theta_j^2 b^{kl}_{2;ij;p'}(L^2_{2;n}) N^2_{2;n;n} \quad \text{(B2.20)}$$
$$+ 2\theta_j b^{kl}_{2;ij} D_1 N^2_{2;n;n}(c_k v_{2;kl;p}(L^1_{2;n}) y_{2;n;n}) \quad \text{(B2.31)}$$
$$+ 2\theta_j b^{kl}_{2;ij} D_1 N^2_{2;n;n}(c_l v_{2;kl;p'}(L^2_{2;n}) y_{2;n;n}) \quad \text{(B2.32)}$$
$$+ 2\theta_j b^{kl}_{2;ij} D_1 N^2_{2;n;n}(c_k a^{pq}_{2;kl} N^1_{2;n;n}) \quad \text{(B2.33)}$$
$$+ 2\theta_j b^{kl}_{2;ij} D_1 N^2_{2;n;n}(c_l a^{pq}_{2;kl} N^2_{2;n;n}) \quad \text{(B2.34)}$$
$$+ 2\theta_j b^{kl}_{2;ij} D_{\nu+1} N^2_{2;n;n}(c_k \{D_1 K^2_{2,\nu}(v_{1;k;p}(L^1_2) y_2)\}_{n;n}) \quad \text{(B2.35)}$$
$$+ 2\theta_j b^{kl}_{2;ij} D_{\nu+1} N^2_{2;n;n}(c_k \{D_1 K^2_{2,\nu}(a^p_{1;k} N^1_2)\}_{n;n}) \quad \text{(B2.36)}$$
$$+ 2\theta_j b^{kl}_{2;ij} D_{\nu+1} N^2_{2;n;n}(c_l \{D_2 K^2_{2,\nu}(v_{1;l;p}(L^2_2) y_2)\}_{n;n}) \quad \text{(B2.37)}$$
$$+ 2\theta_j b^{kl}_{2;ij} D_{\nu+1} N^2_{2;n;n}(c_l \{D_2 K^2_{2,\nu}(a^p_{1;l} N^2_2)\}_{n;n}) \quad \text{(B2.38)}$$
$$+ 2\theta_j b^{kl}_{2;ij} D_2 N^2_{2;n;n}(c_k d^p_k K^2_{2,1;n;n;n}) \,, \quad \text{(B2.39)}$$
$$+ 2\theta_j b^{kl}_{2;ij} D_3 N^2_{2;n;n}(c_l d^p_l K^2_{2,2;n;n;n}) \,. \quad \text{(B2.40)}$$

If $\bar{y}_{2;n,i;t}$ is considered then

$$\left.\frac{d}{dh_n}\bar{y}_{2;n,i;t}\right|_0$$
$$= \theta_i u_{1;i;k}(L^1_{2;n}) y_{2;n;t} \quad \text{(C1.1)}$$
$$+ \theta_i b^k_{1;i} N^1_{2;n;t} \,, \quad \text{(C1.2)}$$
$$\left.\frac{d^2}{dh_n^2}\bar{y}_{2;n,i;t}\right|_0$$
$$= \theta_i^2 u_{1;i;k,l}(L^1_{2;n}, L^1_{2;n}) y_{2;n;t} \quad \text{(C2.7)}$$
$$+ 2\theta_i u_{1;i;k}(D_1 L^1_{2;n}(c_k v_{1;k;l}(L_1) y_{1;n}))y_{2;n;t} \quad \text{(C2.1)}$$
$$+ 2\theta_i u_{1;i;k}(D_1 L^1_{2;n}(c_k a^l_{1;k} N_{1;n}))y_{2;n;t} \quad \text{(C2.2)}$$
$$+ 2\theta_i u_{1;i;k}(D_2 L^1_{2;n}(c_k v_{2;kk;l}(L^1_{2;n}) y_{2;n;n}))y_{2;n;t} \quad \text{(C2.3)}$$
$$+ 2\theta_i u_{1;i;k}(D_2 L^1_{2;n}(c_k v_{2;kk;l'}(L^2_{2;n}) y_{2;n;n}))y_{2;n;t} \quad \text{(C2.4)}$$
$$+ 2\theta_i u_{1;i;k}(D_2 L^1_{2;n}(c_k a^{lp}_{2;kk} N^1_{2;n;n}))y_{2;n;t} \quad \text{(C2.5)}$$
$$+ 2\theta_i u_{1;i;k}(D_2 L^1_{2;n}(c_k a^{lp}_{2;kk} N^2_{2;n;n}))y_{2;n;t} \quad \text{(C2.6)}$$
$$+ 2\theta_i^2 b^k_{1;i;l}(L^1_{2;n}) N^1_{2;n;t} \quad \text{(C2.8)}$$

$$+ 2\theta_i b^k_{1;i} D_1 N^1_{2;n;t}(c_k v_{1;k;l}(L^1_2) y_{2;n;t}) \tag{C2.9}$$
$$+ 2\theta_i b^k_{1;i} D_1 N^1_{2;n;t}(c_k a^l_{1;k} N^1_{2;n;t}) \tag{C2.10}$$
$$+ 2\theta_i b^k_{1;i} D_{\nu+1} N^1_{2;n;t}(c_k \{D_1 K^1_{2,\nu}(v_{1;k;l}(L^1_2) y_2)\}_{n;t}) \tag{C2.11}$$
$$+ 2\theta_i b^k_{1;i} D_{\nu+1} N^1_{2;n;t}(c_k \{D_1 K^1_{2,\nu}(a^l_{1;k} N^1_2)\}_{n;t}) \tag{C2.12}$$
$$+ 2\theta_i b^k_{1;i} D_2 N^1_{2;n;t}(c_k d^l_k K^1_{2,1;n;n;t}) \,. \tag{C2.13}$$

It is possible to guarantee that the $k \in \{1,2\}$th order derivatives of the local approximations $\bar{y}_1$ and $\bar{y}_2$ agree with the corresponding derivatives of the solutions y_1 and y_2 by requiring that for all $j \in \mathbb{Z}_{\geq 1}$ the terms labeled by $Ak.j$ and $Bk.j$, $Ck.j$ contributing to the derivatives of $\bar{y}_1$ and $\bar{y}_2$ reduce to the equivalently labeled terms contributing to the derivatives of y_1 and y_2. It follows by taking into account the symmetries of the weight functions 6.1.1 that in order to do this for the first order derivatives, it is sufficient to require that the weight functions satisfy

$$u_{1;i;k}(z) = \mathsf{u}_{1;i;k} z \,, \qquad \text{((A,C)(1.1,2.(1-6)))}$$
$$b^k_{1;i} = \mathsf{b}^k_{1;i} \mathbb{1} \,, \qquad \text{((A,C)1.2,A2.(9-15),C2.(9-13))}$$
$$u_{2;ij;k}(z) = \mathsf{u}_{2;ij;k} z \,, \qquad \text{(B(1.(1-2),2.(1-6,11-16)))}$$
$$b^{kl}_{2;ij} = \mathsf{b}^{kl}_{2;ij} \mathbb{1} \,, \qquad \text{(B(1.(3-4),2.(21-40)))}$$

for all $i, j \in [1, S] \cap \mathbb{Z}$ and $k, l \in [1, s] \cap \mathbb{Z}$ such that

$$1 = \sum_{k=1}^{s} \mathsf{u}_{1;i;k} \,, \qquad \text{((A,C)1.1)}$$
$$1 = \sum_{k=1}^{s} \mathsf{b}^k_{1;i} \,, \qquad \text{((A,C)1.2)}$$
$$1 = \sum_{k=1}^{s} \mathsf{u}_{2;ij;k} \,, \qquad \text{(B1.(1-2))}$$
$$1 = \sum_{k,l=1}^{s} \mathsf{b}^{kl}_{2;ij} \,, \qquad \text{(B1.(3-4))}$$

where $\mathbb{1}$ denotes the identity operator and $\mathsf{u}_{1;i;k}$, $\mathsf{u}_{2;ij;k}$, $\mathsf{b}^k_{1;i}$ and $\mathsf{b}^{kl}_{2;ij}$ are real numbers. Here, and in the following, the equation labels refer to the terms for which the condition of the equation is required. Similarly, in order to match the second order derivatives, it is sufficient to demand that the weight functions satisfy

$$u_{1;i;k,l}(z,z) = \mathsf{u}_{1;i;k,l} z^2 \,, \qquad \text{((A,C)2.7)}$$
$$b^k_{1;i;l}(z) = \mathsf{b}^k_{1;i;l} z \,, \qquad \text{((A,C)2.8)}$$
$$v_{1;k;l}(z) = \mathsf{v}_{1;k;l} z \,, \qquad \text{(A2.(1,13),C2.(1,9,11),B2.(1,11,25,27,35,37))}$$
$$a^l_{1;k} = \mathsf{a}^l_{1;k} \mathbb{1} \,, \qquad \text{(A2.(2,14),C2.(2,10,12),B2.(2,12,26,28,36,38))}$$
$$u_{2;ij;k,l}(z,z) = \mathsf{u}_{2;ij;k,l} z^2 \,, \qquad \text{(B2.(7,18))}$$
$$2u_{2;ij;k,l'}(z,z') = \mathsf{u}_{2;ij;k,l'}(zz' + z'z) \,, \qquad \text{(B2.(8,17))}$$
$$b^{kl}_{2;ij;p}(z) = \mathsf{b}^{kl}_{2;ij;p} z \,, \qquad \text{(B2.(9-10,19-20))}$$
$$v_{2;kl;p}(z) = \mathsf{v}_{2;kl;p} z \,, \qquad \text{(A2.(3-4,9-10),C2.(3-4),B2.(3-4,13-14,21-22,31-32))}$$
$$a^{pq}_{2;kl} = \mathsf{a}^{pq}_{2;kl} \mathbb{1} \,, \qquad \text{(A2.(5-6,11-12),C2.(5-6),B2.(5-6,15-16,23-24,33-34))}$$

for all $i, j \in [1, S] \cap \mathbb{Z}$ and $k, l, p, q \in [1, s] \cap \mathbb{Z}$ such that

$$1 = \sum_{k,l=1}^{s} \mathsf{u}_{1;i;k,l} \,, \qquad \text{((A,C)2.7)}$$
$$\theta_i = 2 \sum_{k,l=1}^{s} \mathsf{u}_{1;i;k} c_k \mathsf{v}_{1;k;l} \,, \qquad \text{((A,C)2.1)}$$

$$\theta_i = 2\sum_{k,l=1}^{s} \mathsf{u}_{1;i;k} c_k \mathsf{a}^l_{1;k}\,, \qquad \text{((A,C)2.2)}$$

$$\theta_i = 2\sum_{k,l=1}^{s} \mathsf{u}_{1;i;k} c_k \mathsf{v}_{2;kk;l}\,, \qquad \text{((A,C)2.(3-4))}$$

$$\theta_i = 2\sum_{k,p,q=1}^{s} \mathsf{u}_{1;i;k} c_k \mathsf{a}^{pq}_{2;kk}\,, \qquad \text{((A,C)2.(5-6))}$$

$$1 = 2\sum_{k,l=1}^{s} \mathsf{b}^k_{1;i;l} \qquad \text{((A,C)2.8)}$$

$$\theta_i = 2\sum_{k,l=1}^{s} \mathsf{b}^k_{1;i} c_k \mathsf{v}_{1;k;l} \qquad \text{(A2.13,C2.(9,11))}$$

$$\theta_i = 2\sum_{k,l=1}^{s} \mathsf{b}^k_{1;i} c_k \mathsf{a}^l_{1;k} \qquad \text{(A2.14,C2.(10,12))}$$

$$\theta_i = 2\sum_{k,l=1}^{s} \mathsf{b}^k_{1;i} c_k \mathsf{v}_{2;kk:l} \qquad \text{(A2.(9-10))}$$

$$\theta_i = 2\sum_{k,p,q=1}^{s} \mathsf{b}^k_{1;i} c_k \mathsf{a}^{pq}_{2;kk} \qquad \text{(A2.(11-12))}$$

$$\theta_i = 2\sum_{k,l=1}^{s} \mathsf{b}^k_{1;i} c_k d^l_k \qquad \text{(A2.15,C2.13)}$$

$$1 = \sum_{k,l=1}^{s} \mathsf{u}_{2;ij;k,l}\,, \qquad \text{(B2.(7,18))}$$

$$\theta_i = 2\sum_{k,l=1}^{s} \mathsf{u}_{2;ij;k} c_k \mathsf{v}_{1;k;l}\,, \qquad \text{(B2.(1,11))}$$

$$\theta_i = 2\sum_{k,l=1}^{s} \mathsf{u}_{2;ij;k} c_k \mathsf{a}^l_{1;k}\,, \qquad \text{(B2.(2,12))}$$

$$\theta_i = 2\sum_{k,l=1}^{s} \mathsf{u}_{2;ij;k} c_k \mathsf{v}_{2;kk;l}\,, \qquad \text{(B2.(3-4,13-14))}$$

$$\theta_i = 2\sum_{k,p,q=1}^{s} \mathsf{u}_{2;ij;k} c_k \mathsf{a}^{pq}_{2;kk}\,, \qquad \text{(B2.(5-6,15-16)}$$

$$1 = \sum_{k,l=1}^{s} \mathsf{u}_{2;ij;k,l'}\,, \qquad \text{(B2.(8,17))}$$

$$1 = 2\sum_{k,l,p=1}^{s} \mathsf{b}^{kl}_{2;ij;p}\,, \qquad \text{(B2.(9-10,19-20)}$$

$$\theta_i = 2\sum_{k,l,p=1}^{s} \mathsf{b}^{kl}_{2;ij} c_k \mathsf{v}_{1;k;p}\,, \qquad \text{(B2.(25,27,35,37))}$$

$$\theta_i = 2\sum_{k,l,p=1}^{s} \mathsf{b}^{kl}_{2;ij} c_k \mathsf{a}^p_{1;k}\,, \qquad \text{(B2.(26,28,36,38))}$$

$$\theta_i = 2\sum_{k,l,p=1}^{s} \mathsf{b}^{kl}_{2;ij} c_k \mathsf{v}_{2;kl;p}\,, \qquad \text{(B2.(21-22,31-32))}$$

$$\theta_i = 2\sum_{k,l,p,q=1}^{s} \mathsf{b}^{kl}_{2;ij} c_k a^{pq}_{2;kl}\,, \qquad \text{(B2.(23-24,33-34))}$$

$$\theta_i = 2\sum_{k,l,p=1}^{s} \mathsf{b}^{kl}_{2;ij} c_k d^p_k\,, \qquad \text{(B2.(29-30,39-40))}$$

where $\mathsf{u}_{1;i;k,l}$, $\mathsf{u}_{2;ij;k,l}$, $\mathsf{u}_{2;ij;k,l'}$, $\mathsf{b}^l_{1;i;k}$, $\mathsf{b}^{kl}_{1;ij;p}$, $\mathsf{v}_{1;k;l}$, $\mathsf{v}_{2;kl;p}$, $\mathsf{a}^l_{1;k}$ and $\mathsf{a}^{pq}_{2;kl}$ are real numbers. It then only remains to use the definitions of the weight functions 6.1.1 and the consistency conditions 6.2.1 in order to reduce the above derived conditions to the order conditions summarized in Sec. 6.2.

Part III

Applications

7 Kadanoff-Baym Approach to Linear Response Functions

It is well-known that in addition to directly solving for a linear response function, it is possible to evaluate it in time-domain by perturbing the system weakly and recording the desired observable from which, if desired, the response function can be deduced. In time-dependent density functional theory, for instance, this is done routinely to calculate, in essence, density response functions [SLR+12]. It is analogously possible to do the same by using time-dependent many-body perturbation theory as demonstrated, e.g., in [KB00, BGK+01, DLS06, DL07, AGM11, SML12, BHB12, HBB12, SPAL15b, SP16] where also the density response function is considered. It is however remarked that, to the best knowledge of the author, how this is done, has not been described in the literature in the case of the many-body perturbation theory. In what follows, it is therefore documented, how by solving the Kadanoff-Baym equations, we have obtained the density(-density) response functions shown in **II** [SPAL15b] and **III** [SML12]. It is noted that the numerical method which is described in the following is not due to the author but has been originally implemented by previous members of the research group. In addition to a documentation of this method, at the end of this chapter, it is shown explicitly that a density response function $\delta n/\delta v$ obtained by the numerical method satisfies the Bethe-Salpeter equation with the kernel $\delta\Sigma/\delta G$, cf., [KB00]. It is due to the nature of the aforementioned topics that this chapter is rather technical and an uninterested reader is referred to the next chapter regarding the applications of the here documented method.

7.1 Linear Density Response Relation

It is first reminded that in the spin-position $(r\,\sigma)$ basis, the retarded density-density response function of a system described by the unperturbed Hamiltonian operator $\widehat{H}$ is defined as $\chi^R(r\,\sigma,t;r'\,\sigma',t') \equiv -\imath\theta(t-t')\langle[\hat{n}_H(r\,\sigma,t),\hat{n}_H(r'\,\sigma',t')]_-\rangle$ where $\hat{n}$ is the density operator, cf., Sec. 3.3.2. Moreover, it is a response function which is particularly interesting as it is directly related, e.g., to photoabsorption and electron energy loss spectra [ORR02]. In a time-dependent approach, it can be extracted by perturbing the system with a weak one-body potential $v(r\,\sigma,t)$ and by subsequently recording how the electron density $n(r\,\sigma,t)$ fluctuates in response to the perturbation. In a general basis, on the other hand, the density response function can be evaluated from the knowledge of the retarded response function $\chi^R_{pq,st}(t;t') \equiv -\imath\theta(t-t')\langle[\widehat{\gamma}_{Hpq}(t),\widehat{\gamma}_{Hst}(t')]_-\rangle$ where $\widehat{\gamma}_{pq} \equiv \hat{c}^\dagger_q\hat{c}_p$ is the one-body reduced density matrix operator. It is the basis of the time-dependent approach that if $\delta\gamma_{pq}$ is the first variation of the density matrix and $\widehat{V}(t) \equiv \sum_{pq} v_{pq}(t)\hat{c}^\dagger_p\hat{c}_q$ the applied potential then the response relation

$$\delta\gamma_{pq}(t) = \sum_{st}\int_{t_0}^{\infty} dt'\; \chi^R_{pq,st}(t;t')v_{ts}(t')\,.$$

relates the potential described by $v_{pq}(t)$ to the induced density matrix variation for $t \geq t_0$. In order to extract the response function by using this relation, it is possible, instead of modeling a realistic electric field with a finite bandwidth, to excite all frequencies simultaneously by applying a

perturbation of the temporal form $v_{pq}(t) = v_{pq}\delta(t - t_0^+)$ where v_{pq} is a time-independent amplitude and t_0 the initial time. Moreover, when the unperturbed system is invariant under time translations, i.e., it is described by a time-independent Hamiltonian operator $\widehat{H}$ which commutes with the initial state statistical density operator, the response function is a function of the time-difference only. It then follows from the resulting response relation

$$\delta\gamma_{pq}(t) = \sum_{st} \chi^R_{pq,st}(t - t_0)v_{ts} \tag{7.1}$$

that the retarded response function of Eq. (3.1) is given by

$$\chi^R_{pq,st}(t - t_0) = \left.\frac{\partial\gamma_{pq}(t)}{\partial v_{ts}}\right|_{v=0}, \tag{7.2}$$

where v denotes a norm of the matrix with the components v_{pq}. It then remains to document how the density matrix $\gamma_{pq}(t)$ can be obtained in the exact and many-body perturbation theories.

7.2 Numerical Method for Evaluating Response Function

Here, it is first described how the retarded response function of Eq. (3.1) can be obtained in time-domain in the exact theory in which the time-evolution of a quantum state is governed by the time-dependent Schrödinger equation and then in the approximate theory in which the time-evolution of the density matrix is due to the Kadanoff-Baym equations. In either case, it is usually possible to evaluate the response function $\chi^R_{pq,\bar{s}\bar{t}}(t - t_0)$ for all p, q and for fixed $\bar{s}, \bar{t}$ to a desired accuracy by choosing $v_{ts} = v\delta_{s\bar{s}}\delta_{t\bar{t}}$ and by replacing the derivative in Eq. (7.2) with a difference quotient. It is a prerequisite, in order to do this, that the amplitude v can be chosen such that the induced response $\gamma_{pq}(t) - \gamma_{pq}(t_0^-)$ is linear in v to a sufficient accuracy for all times t of interest. It is possible to accomplish all this by realizing the temporal delta function potential as described below.

7.2.1 In Exact Theory

In the case of the exact theory, in a finite dimensional Hilbert space, it is appropriate to treat the time-dependent Schrödinger equation as a linear, ordinary differential equation. It is clear that none of the standard theorems regarding the existence and uniqueness of the solutions, or regarding the continuous dependence of the solutions on parameters, of ordinary differential equations [HS74] apply when the vector field, i.e., the right-hand side of the equation, contains distributions such as a delta function. It is noted that there are several ways to deal with such impulsive vector fields, e.g., by replacing the delta function with a mollifier, i.e., an approximation to the identity, and taking the appropriate limit in the end [NO12]. However, here it is not purposeful to strive for such rigor and, instead, the method is only motivated and shown to lead to the desired response relation.

It is proposed that in the exact theory, it is possible to obtain a one-body reduced density matrix satisfying the response relation of Eq. (7.1) for the more general case that the initial state statistical density operator $\widehat{\rho}$ does not necessarily commute with the Hamiltonian operator $\widehat{H}$ by

i choosing an ensemble $\{|\Psi_k\rangle\}$,

ii preparing the states $|\Phi_k\rangle = \exp\big(-\imath\widehat{V}\big)|\Psi_k\rangle$ where $\widehat{V} \equiv \sum_{pq} v_{pq}\hat{c}_p^\dagger\hat{c}_q$,

iii solving for $|\Psi_k(t)\rangle$ by using $\imath\partial_t|\Psi_k(t)\rangle = \widehat{H}|\Psi_k(t)\rangle$ with $|\Psi_k(t_0)\rangle = |\Phi_k\rangle$,

iv constructing $\gamma_{pq}(t) = \sum_{ij}\rho_{ij}\langle\Psi_j(t)|\widehat{\gamma}_{pq}|\Psi_i(t)\rangle$ where $\rho_{ij} \equiv \langle\Psi_i|\widehat{\rho}|\Psi_j\rangle$

from which it follows for $t \geq t_0$ that

$$\gamma_{pq}(t) = \gamma_{0;pq}(t) - \imath\sum_{st}\sum_{ij}\rho_{ij}\langle\Psi_j|\left[\widehat{\gamma}_{Hpq}(t),\widehat{\gamma}_{st}\right]_-|\Psi_i\rangle v_{ts} + \mathcal{O}(v^2)$$

where γ_0 is the density matrix of the unperturbed system, and hence the response relation is satisfied. It is noted that in this thesis and in the enclosed publications the ensemble of step i consists only of a non-degenerate ground state.

In order to motivate steps ii and iii, it is briefly argued, by using essentially a gauge transformation from the length to velocity gauge, that if $U(t;t')$ is the time-evolution operator evolving under $\widehat{H}(t) \equiv \widehat{H} + \delta(t-t_0)\widehat{V}$ then the result $U(t;t_0^-) = U_0(t;t_0)\exp(-\imath\widehat{V})$, where $U_0(t;t_0)$ is the time-evolution operator of the unperturbed system evolving under $\widehat{H}$, can be used. It is possible to justify this result by introducing the transformation

$$\mathcal{U}(t;t_i) \equiv e^{\imath\widehat{V}\theta(t-t_0)}U(t;t_i)\,,$$

where $t_i < t_0$ such that $U(t_i;t_i) = \mathbb{1}$, from which it follows that $\mathcal{U}$ is the solution to the initial value problem

$$\begin{aligned}\mathcal{U}(t_i;t_i) &= \mathbb{1}\,,\\ \imath\partial_t\mathcal{U}(t;t_i) &= \hat{\mathcal{H}}(t)\mathcal{U}(t;t_i)\,,\end{aligned}$$

where $\hat{\mathcal{H}}(t) \equiv \exp(\imath\widehat{V}\theta(t-t_0))\widehat{H}\exp(-\imath\widehat{V}\theta(t-t_0))$ is the transformed Hamiltonian operator. It then holds, by Carathéodory's theorem [Fil88], that this solution is absolutely continuous, i.e.,

$$\mathcal{U}(t;t_i) = \mathbb{1} + \int_{t_i}^{t} dt'\;\hat{\mathcal{H}}(t')\mathcal{U}(t';t_i)\,,$$

and hence the unitary transformation $\exp(\imath\widehat{V}\theta(t-t_0))$ has countered the delta-function induced discontinuity of the time-evolution operator $U(t;t_i)$ at t_0. It then follows by inverting the transformation that $U(t_0^+;t_0^-) = \exp(-\imath\widehat{V})$ from which the result $U(t;t_0^-) = U_0(t;t_0)\exp(-\imath\widehat{V})$ and, subsequently, the method summarized above by steps i-iv follow straightforwardly.

7.2.2 In Many-Body Perturbation Theory

In the approximate case, there is no underlying quantum state and the one-body reduced density matrix is instead given by $\gamma_{pq}(t) = -\imath G^<_{pq}(t;t)$ where the lesser electron propagator $G^<_{pq}(t;t)$ together with the other components and phononic quantities satisfies the Kadanoff-Baym equations. It is therefore natural to motivate the approach by considering how the phonon field and the electron and phonon propagators behave under the delta function perturbation. In the following, this is done by relying on the results derived in the previous section for the exact case.

It is proposed that in many-body perturbation theory, it is possible to obtain a one-body reduced density matrix corresponding to the grand canonical density operator $\exp(-\beta\widehat{H}^M)/Z$ which satisfies the response relation of Eq. (7.1) by

i solving for the imaginary-time components of ϕ, D and G by solving the Dyson equations of Eqs. (5.5) corresponding to the Hamiltonian operator of Eq. (2.1)

ii preparing the propagators

$$\begin{aligned} G^{\gtrless}_{0;pq} &\equiv \sum_{st} \left[e^{-\imath v}\right]_{ps} \left[e^{\imath v}\right]_{tq} G^{M}_{st}(0^{\pm}) \,, \\ G^{\rceil}_{0;pq}(\tau) &\equiv \sum_{s} \left[e^{-\imath v}\right]_{ps} G^{M}_{sq}(-\tau) \,, \\ G^{\lceil}_{0;pq}(\tau) &\equiv \sum_{s} \left[e^{\imath v}\right]_{sq} G^{M}_{ps}(\tau) \,, \end{aligned}$$

iii solving for the real- and mixed-time components of ϕ, D and G by solving the Kadanoff-Baym equations of Eqs. (5.6) corresponding to the Hamiltonian operator of Eq. (2.1) with the modified initial conditions $G^{\gtrless}_{pq}(t_0;t_0) = G^{\gtrless}_{0;pq}$, $G^{\rceil}_{pq}(t_0;\tau) = G^{\rceil}_{0;pq}(\tau)$ and $G^{\lceil}_{pq}(\tau;t_0) = G^{\lceil}_{0;pq}(\tau)$

iv evaluating $\gamma_{pq}(t) = -\imath G^{<}_{pq}(t;t)$

from which it follows that the response relation for $\delta\gamma_{pq}(t)$ is satisfied with

$$\chi^{R}_{pq,st}(t-t_0) \equiv -\imath \frac{\partial G^{<}_{pq}(t;t)}{\partial v_{ts}}\bigg|_{v=0}$$

being the response function. In the next section, it is further shown that this response function is well-defined in the sense that it satisfies the Bethe-Salpeter equation.

In order to motivate step ii, it is convenient to carry out the gauge transformation used in the exact case which was considered in the previous section. In other words, the real-time time-evolution operator is written as $U(t;t_0^-) = \exp(-\imath \widehat{V}\theta(t-t_0))\hat{\mathcal{U}}(t;t_0)$ such that the Heisenberg picture operators become

$$\begin{aligned} \widehat{\phi}_{H\mu}(t) &= \widehat{\phi}_{\mathcal{H}\mu}(t) \,, \\ \hat{c}_{Hp}(t) &= \sum_{q} \left[e^{-\imath v\theta(t-t_0)}\right]_{pq} \hat{c}_{\mathcal{H}q} \,, \end{aligned}$$

for the real times whereas they are left invariant by the gauge transformation for the imaginary times. It is then possible to re-express the phonon field and the phonon and electron propagators compactly as

$$\phi_{\mu}(z) = \langle \widehat{\phi}_{\mathcal{H}\mu}(z) \rangle \,, \tag{7.3a}$$

$$D_{\mu\nu}(z;z') = \frac{1}{\imath} \langle T\{\widehat{\phi}_{\mathcal{H}\mu}(z)\widehat{\phi}_{\mathcal{H}\nu}(z')\}\rangle \,, \tag{7.3b}$$

$$G_{pq}(z;z') = \frac{1}{\imath} \sum_{p'q'} \left[e^{-\imath v\theta(t_{0+},z)}\right]_{pp'} \left[e^{\imath v\theta(t_{0+},z')}\right]_{q'q} \langle T\{\hat{c}_{\mathcal{H}p'}(z)\hat{c}^{\dagger}_{\mathcal{H}q'}(z')\}\rangle \,, \tag{7.3c}$$

where as usual t_{0+} refers to a contour-time on the backward branch. It is, for one, then clear that the imaginary-time components are not affected by the potential which was expected. For another, it follows from these equations that the real- and mixed-time components satisfy the initial conditions

$$\begin{aligned} \lim_{t\to t_0^+} \phi_{\mu}(t) &= \phi^{M}_{\mu} \,, \\ \lim_{t,t'\to t_0^+} D^{\gtrless}_{\mu\nu}(t;t') &= D^{M}_{\mu\nu}(0^{\pm}) \,, \end{aligned}$$

$$\lim_{t\to t_0^+} D^{\rceil}_{\mu\nu}(t;\tau) = D^M_{\mu\nu}(-\tau)\,,$$
$$\lim_{t\to t_0^+} D^{\lceil}_{\mu\nu}(\tau;t) = D^M_{\mu\nu}(\tau)\,,$$
$$\lim_{t,t'\to t_0^+} G^{\gtrless}_{pq}(t;t') = \sum_{st}\big[e^{-\imath v}\big]_{ps}\big[e^{\imath v}\big]_{tq} G^M_{st}(0^{\pm})\,,$$
$$\lim_{t\to t_0^+} G^{\rceil}_{pq}(t;\tau) = \sum_{s}\big[e^{-\imath v}\big]_{ps} G^M_{sq}(-\tau)\,,$$
$$\lim_{t\to t_0^+} G^{\lceil}_{pq}(\tau;t) = \sum_{s}\big[e^{\imath v}\big]_{sq} G^M_{ps}(\tau)\,,$$

which shows explicitly that the electron propagators are discontinuous at t_0 which was also expected. It remains to conclude that the equations of motion for the field and propagators are invariant for $z \gtrless t_{0+}$ which means that both steps ii and iii are well-motivated.

7.3 Equivalence of Method with Bethe-Salpeter Approach

In the following, it is shown explicitly that the one-body reduced density matrix $\gamma_{pq}(t)$ obtained according to steps i-iv of Sec. 7.2.2 by using a self-consistent self-energy approximation Σ fulfills the response relation of Eq. (7.1) such that the response function $-\imath\partial G^{<}_{pq}(t;t)/\partial v_{ts}\big|_{v=0}$ satisfies the Bethe-Salpeter equation corresponding to the four-point kernel $\delta\Sigma/\delta G$, cf., Sec. (4.3.4). It is noted that the justification given below is specific to the delta function potential and hence, is meant to complement the standard arguments given, e.g., in [KB00, DL07]. To begin with, it is found convenient to take advantage of the matrix notation of Sec. 5.1 when possible and to use the contour-time equations of motion to avoid overcrowding the derivation with unnecessary indices and equations. It then holds by step iii of Sec. 7.2.2 that the field and propagators satisfy the unperturbed equations of motion for $z \neq t_{0\pm}$. In particular, the electron propagator satisfies the equations

$$\imath\partial_z G(z;z') = \delta(z,z') + hG(z;z') + \int_C d\bar{z}\; \Sigma(z;\bar{z})G(\bar{z};z')\,,$$
$$-\imath\partial_{z'} G(z;z') = \delta(z,z') + G(z;z')h + \int_C d\bar{z}\; G(z;\bar{z})\Sigma(\bar{z};z')\,,$$

and its imaginary-time component satisfies the boundary conditions $G^M(\tau) = -G^M(\tau-\beta)$ whereas its mixed- and real-time components satisfy the initial or discontinuity conditions given by step ii of Sec. 7.2.2. In contrast, the phonon field and propagator satisfy both the standard boundary, i.e., $\phi^M(0) = \phi^M(\beta)$ and $D^M(\tau) = D^M(\tau-\beta)$, and initial conditions the latter of which are given in Eqs. (4.33). In order to proceed, it is noted that since the only explicit dependence on the potential v lies in the initial conditions for the electron propagator, it is found convenient in the following to treat the electron self-energy $\Sigma(z;z') \equiv \Sigma[G](z;z')$ as a functional of the electron propagator only. It then holds that if $G_0(z;z')$ denotes the equilibrium electron propagator, i.e., the electron propagator of the unperturbed system, then the first variation δG, which is equal to

$$\delta G_{pq}(z;z') = \sum_{st} \frac{\partial G_{pq}(z;z')}{\partial v_{st}}\bigg|_{v=0} v_{st}\,, \tag{7.4}$$

satisfies the equations of motion

$$\imath\partial_z \delta G(z;z') = h\delta G(z;z') + \int_C d\bar{z}\; \Sigma_0(z;\bar{z})\delta G(\bar{z},z') + \int_C d\bar{z}\; \delta\Sigma(z;\bar{z})G_0(\bar{z};z')\,,$$

$$-\imath\partial_{z'}\delta G(z;z') = \delta G(z;z')h + \int_C d\bar{z}\ \delta G(z;\bar{z})\Sigma_0(\bar{z};z') + \int_C d\bar{z}\ G_0(z;\bar{z})\delta\Sigma(\bar{z},z')\,.$$

Here, $\Sigma_0(z;z') \equiv \Sigma[G_0](z;z')$ is the equilibrium electron self-energy and if

$$K_{ps,qt}(z,\bar{z};z',\underline{z}) \equiv -\frac{\delta\Sigma_{pq}(z;z')}{\delta G_{ts}(\underline{z};\bar{z})}\bigg|_{G_0} \tag{7.5}$$

denotes the four-point kernel, see Sec. 4.3.4, then

$$\delta\Sigma_{pq}(z;z') = -\sum_{st}\int_C d\bar{z}d\underline{z}\ K_{ps,qt}(z,\underline{z};z',\bar{z})\delta G_{ts}(\bar{z};\underline{z})\,, \tag{7.6}$$

is the first variation of the electron self-energy. It is readily checked that the above introduced equations of motion admit the formal particular solution

$$\delta G_p(z;z') = \int_C d\bar{z}d\underline{z}\ G_0(z;\bar{z})\delta\Sigma(\bar{z};\underline{z})G_0(\underline{z};z')\,,$$

the imaginary-time component of which vanishes since $\delta\Sigma^M = 0$ which is in an agreement with the requirement that $\delta G^M = 0$. However, for the same reason, the real- and mixed-time components tend to zero as z and/or z' tend to $t_{0\pm}$ which is not compatible with the correct initial conditions for the real- and mixed-time components given in step ii of Sec. 7.2.2. It is therefore not possible that this particular solution is the sought solution. In order to find a solution which satisfies the correct initial conditions, i.e., has the correct discontinuity, it is suggested that the general solution is a sum of a homogeneous solution δG_h and of the above defined particular solution δG_p. In other words, by using Eq. (7.6) and by defining

$$L_{0;pq,st}(z,\bar{z};\underline{z},z') \equiv G_{0;pt}(z;z')G_{0;qs}(\bar{z};\underline{z})\,,$$

it holds that a solution of the integral equation

$$\begin{aligned}\delta G_{pq}(z;z') = {}& \delta G_{h;pq}(z;z') \\ & - \sum_{p'q's't'}\int_C d\bar{z}d\underline{z}d\bar{z}'d\underline{z}'\ L_{0;pq',qp'}(z,\bar{z};z',\underline{z})K_{p's',q't'}(\underline{z},\underline{z}';\bar{z},\bar{z}')\delta G_{t's'}(\bar{z}';\underline{z}')\,,\end{aligned}$$

is also a solution of the equations of motion if the homogeneous equations

$$\begin{aligned}\imath\partial_z\delta G_h(z;z') &= h\delta G_h(z;z') + \int_C d\bar{z}\ \Sigma_0(z;\bar{z})\delta G_h(\bar{z};z')\,, \\ -\imath\partial_{z'}\delta G_h(z;z') &= \delta G_h(z;z')h + \int_C d\bar{z}\ \delta G_h(z;\bar{z})\Sigma_0(\bar{z};z')\end{aligned}$$

determining the homogeneous solution are satisfied. In addition, it is possible to enforce the correct initial conditions for the real- and mixed-time components of δG and to guarantee that $\delta G^M = 0$ by requiring that

$$\delta G_{h;pq}(z;z') = \sum_{st} L_{0;pt,qs}(z;z')v_{st}\,, \tag{7.7}$$

where the functions $L_{0;pt,qs}(z;z')$ satisfy

$$\begin{aligned}L^{\gtrless}_{0;pt,qs}(t_0;t_0) &= -\imath\big(\delta_{ps}G^M_{0;tq}(0^\pm) - \delta_{tq}G^M_{0;ps}(0^\pm)\big)\,, \\ L^{\rceil}_{0;pt,qs}(t_0;\tau) &= -\imath\delta_{ps}G^M_{0;tq}(-\tau)\,,\end{aligned}$$

$$L^{\ulcorner}_{0;pt,qs}(\tau;t_0) = \imath\delta_{tq}G^{M}_{0;ps}(\tau)\,.$$
$$L^{M}_{0;pt,qs}(\tau;\tau') = 0\,.$$

and naturally also solve the above introduced homogeneous equations for all s,t. Here, it is noteworthy that $L^{>}_{0;pt,qs}(t_0;t_0) = L^{<}_{0;pt,qs}(t_0;t_0)$ and it is emphasized that these (initial) conditions follow straightforwardly from steps $\underline{i}$ and $\underline{\text{ii}}$ of Sec. 7.2.2. In order to solve for these functions, it is rather suggested that

$$L_{0;pt,qs}(z;z') = L_{0;pt,qs}(z,t_{0-};z',t_{0-}) - L_{0;pt,qs}(z,t_{0+};z',t_{0+})$$

are the sought solutions such that, by treating them as trial solutions, it remains to verify that this is the case. For one, the (initial) conditions are shown to be satisfied by

$$\begin{aligned}
L^{\gtrless}_{0;pt,qs}(t_0;t_0) &= \big(G^{<}_{0;ps}(t_0;t_0) - \imath\delta_{ps}\big)G^{<}_{0;tq}(t_0;t_0) - G^{<}_{0;ps}(t_0;t_0)\big(G^{<}_{0;tq}(t_0;t_0) - \imath\delta_{tq}\big)\\
&= -\imath\big(\delta_{ps}G^{M}_{0;tq}(0^-) - \delta_{tq}G^{M}_{0;ps}(0^-)\big)\,,\\
L^{\urcorner}_{0;pt,qs}(t_0;\tau) &= \big(G^{>}_{0;ps}(t_0;t_0) - G^{<}_{0;ps}(t_0;t_0)\big)G^{\urcorner}_{0;tq}(t_0;\tau)\\
&= -\imath\delta_{ps}G^{M}_{0;tq}(-\tau)\,,\\
L^{\ulcorner}_{0;pt,qs}(\tau;t_0) &= G^{\ulcorner}_{0;ps}(\tau;t_0)\big(G^{<}_{0;tq}(t_0;t_0) - G^{>}_{0;tq}(t_0;t_0)\big)\\
&= \imath\delta_{tq}G^{M}_{0;ps}(\tau)\,,\\
L^{M}_{0;pt,qs}(\tau;\tau') &= G^{M}_{0;ps}(\tau)G^{M}_{0;tq}(-\tau') - G^{M}_{0;ps}(\tau)G^{M}_{0;tq}(-\tau')\\
&= 0\,,
\end{aligned}$$

and, for another, the Kadanoff-Baym equations for the real- and mixed-time components are also satisfied, as shown by

$$\begin{aligned}
\sum_{p'}\big(\imath\delta_{pp'}\partial_t - h_{pp'}\big)L^{\gtrless}_{0;p't,qs}(t;t') &= \sum_{p'}[\Sigma_{0;pp'}\circ G_{0;p's}]^{>}(t;t_0)G^{<}_{0;tq}(t_0;t')\\
&\quad - \sum_{p'}[\Sigma_{0;pp'}\circ G_{0;p's}]^{<}(t;t_0)G^{>}_{0;tq}(t_0;t')\\
&= \sum_{p'}[\Sigma^{R}_{0;pp'}\bullet L^{\gtrless}_{0;p't,qs}](t;t') + \sum_{p'}[\Sigma^{\urcorner}_{0;pp'}\star L^{\ulcorner}_{0;p't,qs}](t;t')\,,\\
\sum_{q'}\big(-\imath\delta_{q'q}\partial_{t'} - h_{q'q}\big)L^{\gtrless}_{0;pt,q's}(t;t') &= \sum_{q'}G^{>}_{0;ps}(t;t_0)[G_{0;tq'}\circ\Sigma_{0;q'q}]^{<}(t_0;t')\\
&\quad - \sum_{q'}G^{<}_{0;ps}(t;t_0)[G_{0;tq'}\circ\Sigma_{0;q'q}]^{>}(t_0;t')\\
&= \sum_{q'}[L^{\gtrless}_{0;pt,q's}\bullet\Sigma^{A}_{0;q'q}](t;t') + \sum_{q'}[L^{\urcorner}_{0;pt,q's}\star\Sigma^{\ulcorner}_{0;q'q}](t;t')\,,\\
\sum_{p'}\big(\imath\delta_{pp'}\partial_t - h_{pp'}\big)L^{\urcorner}_{0;p't,qs}(t;\tau) &= \sum_{p'}[\Sigma_{0;pp'}\circ G_{0;p's}]^{>}(t;t_0)G^{\urcorner}_{0;tq}(t_0;\tau)\\
&\quad - \sum_{p'}[\Sigma_{0;pp'}\circ G_{0;p's}]^{<}(t;t_0)G^{\urcorner}_{0;tq}(t_0;\tau)\\
&= \sum_{p'}[\Sigma^{R}_{0;pp'}\bullet L^{\urcorner}_{0;p't,qs}](t;\tau)\,,\\
\sum_{q'}\big(-\imath\delta_{q'q}\partial_t - h_{q'q}\big)L^{\ulcorner}_{0;pt,q's}(\tau;t) &= \sum_{q'}G^{\ulcorner}_{0;ps}(\tau;t_0)[G_{0;tq'}\circ\Sigma_{0;q'q}]^{<}(t_0;t)\\
&\quad - \sum_{q'}G^{\ulcorner}_{0;ps}(\tau;t_0)[G_{0;tq'}\circ\Sigma_{0;q'q}]^{>}(t_0;t)
\end{aligned}$$

$$= \sum_{q'} [L^{\lceil}_{0;pt,q's} \bullet \Sigma^{A}_{0;q'q}](\tau;t)\,,$$

where it is to be acknowledged that $L^{M}_{0;pt,qs} = 0$ and that $L^{R/A}_{0;pt,qs} = 0$ since $L^{>}_{0;pt,qs} = L^{<}_{0;pt,qs}$. This shows explicitly that the functions $L_{0;pt,qs}(z,t_{0-};z',t_{0-}) - L_{0;pt,qs}(z,t_{0+};z',t_{0+})$ and consequently $\delta G_{h;pq}(z;z')$ satisfy both the homogeneous equation and the correct (initial) conditions. It then follows from Eq. (7.7) that the response function $\partial G_{pq}(z;z')/\partial v_{st}\big|_{v=0}$, which is obtained in a self-consistent self-energy approximation Σ by following steps i-iv of Sec. 7.2.2 and which naturally fulfills the response relation of Eq. (7.4), satisfies the equation

$$\begin{aligned}\left.\frac{\partial G_{pq}(z;z')}{\partial v_{st}}\right|_{v=0} &= L_{0;pt,qs}(z,t_{0-};z',t_{0-}) - L_{0;pt,qs}(z,t_{0+};z',t_{0+}) \\ &\quad - \sum_{p'q's't'} \int_C d\bar{z}d\underline{z}d\bar{z}'d\underline{z}'\; L_{0;pq',qp'}(z,\bar{z};z',\underline{z}) K_{p's',q't'}(\underline{z},\underline{z}';\bar{z},\bar{z}') \left.\frac{\partial G_{t's'}(\bar{z};\underline{z}')}{\partial v_{st}}\right|_{v=0},\end{aligned}$$

which is nothing but the Bethe-Salpeter equation for the generalized electronic response function $L_{pt,qs}(z,t_{0-};z',t^{+}_{0-}) - L_{pt,qs}(z,t^{-}_{0+};z',t_{0+})$, cf., Sec. 4.3.4. In particular, tt is then possible to conclude that

$$\begin{aligned}-\imath \left.\frac{\partial G^{\gtrless}_{pq}(t;t)}{\partial v_{st}}\right|_{v=0} &= -\imath\big(L_{pt,qs}(t_{\pm},t_{0-};t_{\mp},t^{+}_{0-}) - L_{pt,qs}(t_{\pm},t^{-}_{0+};t_{\mp},t_{0+})\big) \\ &= \chi^{R}_{pq,ts}(t-t_0)\,,\end{aligned}$$

which justifies the argument that the retarded response function obtained as described in the steps i-iv of Sec. 7.2.2 satisfies the Bethe-Salpeter equation with the four-point kernel of Eq. (7.5). In Secs. 8.3.2 and 8.3.3, in the context of the results, a few examples are provided of the four-point kernels which result by using simple self-energy approximations such as the ones used in the publications.

8 Summary of the Results of the Publications

It has been the aim of this work to take part in the development of the methodology based on solving the Kadanoff-Baym equations for systems of electrons interacting with themselves or with phonons in particular. In the previous chapters, the focus has been on the theoretical and computational developments while in this chapter the focus shifts to understanding what can be expected from the many-body approximations introduced in Sec. 4.4. In what follows, the results of the publications **I-III** concerning the properties of these many-body approximations in the selected model systems outlined in Sec. 2.3 are briefly summarized.

In the publications, as usual, various smaller problems are described, analyzed and, in the end, explanations to understand them are proposed. In what follows, the reader is in addition to the details concerning the assessment of the quality of the many-body approximations encouraged to keep in mind that the work contained in the publications can be seen in a wider scope as a study concerning time-domain solutions of the Bethe-Salpeter equation, see Ch. 7. In [KB00], to the best knowledge of the author, the Bethe-Salpeter equation was solved for the first time by solving the Kadanoff-Baym equations in a time-nonlocal self-energy approximation for a system subject to a weak perturbation. In addition to demonstrating the correlation induced redshift and broadening of the plasmon peak for the homogeneous electron gas in the second Born approximation, it was pointed out that if a self-consistent self-energy Σ is used then the obtained response function $\delta n/\delta v$ satisfies the Bethe-Salpeter equation corresponding to the four-point kernel $\delta\Sigma/\delta G$. It was also concluded that if Σ is in addition density conserving then $\delta n/\delta v$ satisfies the f-sum rule and it was shown that in the opposite case large violations of the sum rule are possible. It was recognized, e.g., in [ORR02], that this alternative way of solving the Bethe-Salpeter equation is appealing due to not having to deal with four-point objects, but it was also speculated that already the two-point structure could quickly lead via memory effects to computational restrictions for realistic systems. Inhomogeneous systems were for the first time addressed in [DLS06, DL07], also by using the second Born approximation, where the polarizability of the beryllium atom was calculated to illustrate that the method could be successfully applied in the context of atomic and molecular physics. It was repeated that considering larger systems would be computationally difficult but instead calculations involving model Hamiltonians would certainly be feasible, e.g., to investigate electron correlation on a fundamental level. It was only a few years after that the work compiled in Pubs. **I-III** was initiated starting with a study of the electronic excitation spectra of small finite model systems. In the course of this work, it was further shown, by us and others, that the second Born approximation has the potential to describe electronic states with a doubly-excited state character and that also spurious excitations without a clear physical origin could be observed [BHB12]. Moreover, in [HBB12], it was shown that double excitations could be also described by using the second Born approximation when the Kadanoff-Baym equations were reduced to a single-time equation for the one-body reduced density matrix by invoking the Generalized Kadanoff-Baym Ansatz (GKBA) [LvV86]. In addition, the generalized Kadanoff-Baym ansatz has been used in several earlier studies of the optical absorption of semiconductor quantum dot systems which involve the quantum kinetic equations, see e.g. [LNS+06a, LNS+06b]. It should also be noted that, besides by using this ansatz, by considering time-local self-energy approximations, only one-time objects are involved and thus the methodology can be applied in the ab-initio context as has

been demonstrated recently, e.g., in [AGM11]. In addition to further ab-initio studies, it is a possible future direction to apply the methodology discussed here to solve the Bethe-Salpeter equation to obtain the density response with respect to a non-equilibrium state, although also other approaches have been recently made available [PSMS15], as done, e.g., in [SP16] where plasmon-accompanied optical absorption has been studied.

In order to outline our contributions, it first is noted that in **I** [SPAL15a], we studied the properties of the equilibrium electron and phonon propagators for the two-site, two-electron Holstein model by using the self-energy approximations of Sec. 4.4.1. In particular, we studied and proposed explanations for how the used approximations cope with the electron-phonon interaction induced tendency for symmetry-breaking. In **II** [SPAL15b], we extended these studies by further analyzing the neutral and non-neutral excitation spectra of the same model by using the same many-body approximations. In particular, we illustrated how the properties of the multiple, possibly symmetry-broken, equilibrium solutions found in **I** [SPAL15a] affect the properties, e.g., the boundedness, of the density response functions obtained as the solutions of the corresponding Bethe-Salpeter equations. Instead, in the last publication **III** [SML12], we studied the self-energy approximations of Sec. 4.4.2 by using the few-site Hubbard and Pariser-Parr-Pople models. It is was shown by an example that it is possible to describe neutral excitation spectra with contributions from doubly-excited states by solving the Bethe-Salpeter equation by using the simplest correlated second Born self-energy approximation.

8.1 Models

In what follows, the two lattice models which have been used in Pubs. **I-III** to study the many-body approximations and solutions to the Bethe-Salpeter equation are introduced. In the publications, the Bethe-Salpeter equation has been solved by considering the time-dependent generalizations

$$\widehat{H}(t) \equiv \widehat{H} + \sum_i \sum_\sigma v_i \delta(t) \hat{n}_{i\sigma} \, ,$$

of the corresponding model Hamiltonians $\widehat{H}$ which are introduced below. Here, v_i denote the amplitudes of the impulsive external field, i.e., a field which is proportional to a delta function, acting on the electrons. The reader is referred to Sec. 2.3 for the definitions of the operators and parameters which are not introduced explicitly in the following.

8.1.1 Two-site Holstein Model

The homogeneous, two-site Holstein model with two electrons is a minimal model for a system in which electrons move between two identical molecules and interact indirectly via coupling to the vibrational modes of the molecules. It has been said to be relevant [Ber07], e.g., for modeling bipolaronic physics in Ti_4O_7 crystals where bipolarons are associated with Ti^{3+}-Ti^{3+} pairs and explain the properties of a semi-conducting intermediate phase [LSC+76]. Identical or nearly equivalent models appear with slightly modified interpretations, e.g., in semi-classical [VSA06, KVS14] as well as in fully quantum mechanical [PC06] treatments of electronic transport. It is also noteworthy that by adopting a completely different physical picture, i.e., by interchanging the two molecules with a two- or three-level system and the vibrational with electromagnetic field modes, one arrives at formally identical quantum optics models, i.e., the Rabi [Rab36, Rab37] or Dicke [Dic54] models. It is common to these systems, and referred to by 'formally' above, that under some restrictions to their Hilbert

spaces their Hamiltonian operators are isomorphic. In the original context, the Hamiltonian operator is a simplified version of the one given in Eq. (2.5) such that if

$$\widehat{H}_e = -t_{\text{kin}} \sum_{\sigma} \left(\hat{c}^{\dagger}_{1\sigma} \hat{c}_{2\sigma} + \hat{c}^{\dagger}_{2\sigma} \hat{c}_{1\sigma} \right) ,$$

is the Hamiltonian operator describing the electrons then

$$\widehat{H} = \widehat{H}_e + \omega_0 \sum_{i=1}^{2} \hat{a}^{\dagger}_i \hat{a}_i - g \sum_{i=1}^{2} (\hat{a}^{\dagger}_i + \hat{a}_i) \hat{n}_i \, ,$$

describes the full system as illustrated in the left panel of Fig. 8.1.1. Here, t_{kin}, ω_0 and g are respectively the electron hopping amplitude, bare vibrational frequency and electron-phonon interaction strength. It can be shown that the vibrational mode defined by the operator $\widehat{A} \equiv (\hat{a}_1 + \hat{a}_2)/\sqrt{2}$ couples only to the electron number which, as a good quantum number, can be fixed, and hence it is useful to consider only the relative vibrational mode defined by the operator $\hat{a} \equiv (\hat{a}_1 - \hat{a}_2)/\sqrt{2}$. If only the relative mode is considered then the Hamiltonian operator

$$\widehat{H} = \widehat{H}_e + \omega_0 \hat{a}^{\dagger} \hat{a} - \frac{g}{\sqrt{2}} (\hat{a}^{\dagger} + \hat{a}) (\hat{n}_1 - \hat{n}_2) \, ,$$

is instead obtained. The Hilbert space of this Hamiltonian operator contains only a single oscillator mode which makes it better suited to the computationally more demanding calculations. It is noted that in **II** [SPAL15b] the representation in terms of the relative mode only is used while in **I** [SPAL15a] the full Hamiltonian operator is used. Independent of the representation chosen, the properties of the model can be characterized in terms of two parameters: the adiabatic ratio $\gamma \equiv \omega_0/t_{\text{kin}}$, which sets the relative energy scale between electrons and nuclei, and the effective interaction $\lambda \equiv 2g^2/t_{\text{kin}}\omega_0$, which is a dimensionless measure of the interaction between the two constituents. In particular, the latter equals the ratio between the bipolaron energy and the energy of two free electrons.

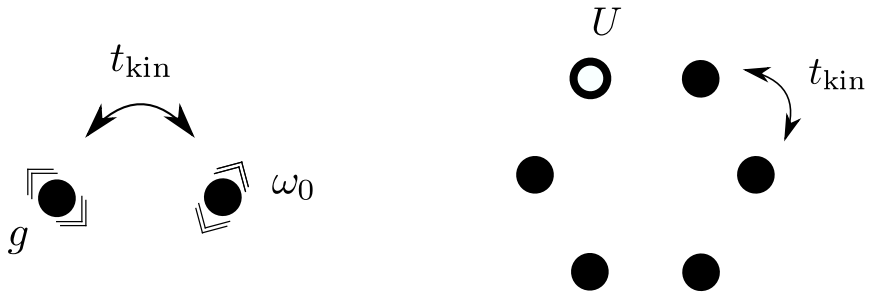

Figure 8.1.1: The two-site Holstein and a six-site Hubbard model illustrated graphically. Here, t_{kin} is the electron hopping amplitude, ω_0 the bare vibrational frequency, and g and U the local electron-phonon and electron-electron interaction strengths.

8.1.2 Few-site Hubbard Models

Few-site Hubbard models are minimal models for describing systems in which a possibly strong, short-range electron-electron interaction plays a significant role. It is, for one, the simplicity of the Hubbard model, in particular its low number of the degrees of freedom, which has made it ubiquitous in different fields of physics, e.g., in the study of ultracold gases [BDZ08] and quantum transport [RGSC09].

In the simplest case of a homogeneous system, the Hamiltonian operator is given by

$$\widehat{H} = -t_{\mathrm{kin}} \sum_{\langle i,j\rangle_N} \sum_{\sigma} \left(\hat{c}^{\dagger}_{i\sigma}\hat{c}_{j\sigma} + \hat{c}^{\dagger}_{j\sigma}\hat{c}_{i\sigma}\right) + U \sum_{i=1}^{N} \hat{n}_{i\uparrow}\hat{n}_{i\downarrow} \,,$$

where by $\langle i,j\rangle_N$ it is referred to that the sum goes only over the neighboring sites on a N site lattice, cf., Eq. (2.4). Moreover, by t_{kin} and U, the electron hopping amplitude and the local electron-electron interaction strength are denoted. It is then the ratio U/t_{kin} describing the competition between delocalization and localization brought upon the kinetic and interaction energies which determines the properties of the system. In **III** [SML12], we have only considered one-dimensional systems and, in the following, only results for periodic lattices, which are henceforth referred to as rings and obtained by choosing the sites i and $(i+1)$ mod N for $i \in [1,N] \cap \mathbb{Z}$ as neighbors, are shown. In the right panel of Fig. 8.1.1, the topology of the six-site ring together with the meaning of the parameters is illustrate graphically. It is also noted that in a ring, electron correlation is pronounced in the sense that, due to the periodicity and homogeneity of the system, a mean-field description of the ground state is equivalent to the non-interacting description. Finally, it is of practical interest that the four-index interaction

$$\frac{1}{2} \sum_{ijkl} \sum_{\alpha\beta\alpha'\beta'} w_{i\alpha,j\beta,k\beta',l\alpha'} \hat{c}^{\dagger}_{i\alpha}\hat{c}^{\dagger}_{j\beta}\hat{c}_{k\beta'}\hat{c}_{l\alpha'} \,,$$

reduces to the interaction of the Hubbard model either by imposing a spin-dependent or -independent interaction. In [SB16], the spin-dependent approach is described whereas in this work, the spin-independent interaction, i.e., $w_{i\alpha,j\beta,k\beta',l\alpha'} = U\delta_{ij}\delta_{jk}\delta_{kl}\delta_{\alpha\alpha'}\delta_{\beta\beta'}$, is used. However, both interactions are equivalent for the many-body approximations used here since the spin-symmetry respected [FVA09].

8.2 Ground State Properties (Pub. I)

In **I** [SPAL15a], we have studied the zero-temperature equilibrium, henceforth also referred to as the ground state, solutions to the Dyson equation for the two-site, two-electron Holstein model of Sec. 8.1.1 in the Hartree (H) and partially (Gd) and fully (GD) self-consistent Born approximations. Our purpose has been to analyze how these approximations deal with the strong localizing effect of the electron-phonon interaction in order to understand when the approximations can be considered to be predictive. Moreover, it is a prerequisite to understand the equilibrium solutions well to be able to solve the Bethe-Salpeter equation for the density response function as described in Sec. 7.2.2.

8.2.1 Obtaining a Physical Picture by Exact Diagonalization

In order to understand the behavior of the many-body approximations, we have analyzed the properties of the two-site, two-electron Holstein model by solving the time-independent Schrödinger equation. In the analysis, we have focused on the cross-over of the system from two nearly free electrons to a bound state of two electrons and an accompanying nuclear displacement referred to as the bipolaron. It is imperative for understanding how the many-body approximations behave to quantify when the system can be described well in terms of the bipolaron. However, since one deals with a cross-over, there is no sharp boundary between bipolaronic and non-bipolaronic systems, and hence different measures lead inevitably to different notions to which degree the system is bipolaronic. That said, the measures chosen by us consist of the binding energy, double occupancy and ultimately the

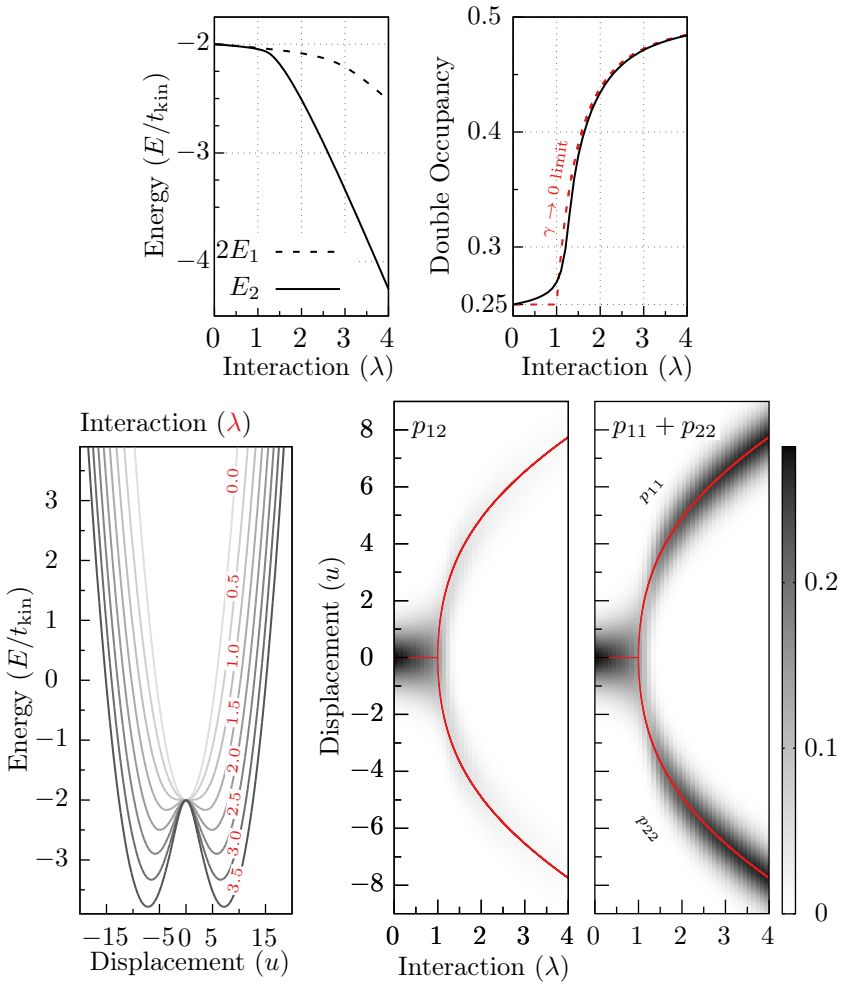

Figure 8.2.1: Illustration of the ground state properties of the two-site, two-electron Holstein model in the adiabatic case $\gamma = 1/8$. In the upper left panel, the ground state energy $(2E_1)$ E_2 of the (one-electron) two-electron system, and in the upper right panel, the double occupancy $\langle \hat{n}_{1\uparrow}\hat{n}_{1\downarrow}\rangle$ together with its $\gamma \to 0$ limit are shown. In the lower left panel, the adiabatic ground state potential energy surface $E_{\mathrm{BO}}(u)$ is shown for selected interactions (λ). In the lower right panels, the joint probability densities p_{12} and $p_{11} + p_{22}$, and in red, the position of the minimum (minima) of the potential energy surface E_{BO} are shown. Note that although the sum $p_{11} + p_{22}$ is shown, after the splitting of the probability density, the two branches correspond to p_{11} and p_{22}, as indicated by their labels, increasingly well as λ is increased.

joint probabilities for finding electrons together with a given nuclear displacement. In Fig. 8.2.1, some numerical results, on which the analysis presented in **I** [SPAL15a] is based on, are summarized. Needless to say, the original work **I** [SPAL15a] is referred to for a more thorough discussion and additional details. In the top panels, it is shown that both the binding energy $2E_1 - E_2$, where E_n is the ground-state energy of the n-electron system, and the double occupancy $\langle \hat{n}_{1\uparrow}\hat{n}_{1\downarrow}\rangle$ increase as a function of the interaction λ indicating that in the adiabatic case $\gamma = 1/8$, the electrons form a bound state in which they prefer to reside on the same site. Moreover, there is a more abrupt change around $\lambda \sim 1$ and, as suggested by the shown double occupancy for $\gamma \to 0$, the degree of the abruptness increases as the adiabatic ratio decreases. It is possible to further analyze these qualitative changes

by associating the adiabatic ground state potential energy surface $E_{\mathrm{BO}}(u)$ with the joint probability densities $p_{11}(u)$, $p_{22}(u)$ and $p_{12}(u)$ to find the two electrons either on the same or different sites and the nuclei with a given relative displacement u. The ground state potential energy surface E_{BO} is shown in the lower left panel of Fig. 8.2.1 for selected interactions to show that a double well structure forms in the potential energy surface for $\lambda > 1$. In the lower right panels, instead the joint probability densities p_{12} and $p_{11} + p_{22}$, which are used by us as ingredients of a working definition of a dominantly bipolaronic state, are shown. It is seen that the initially Gaussian joint probability densities split into probability densities with two maxima as a function of the interaction. As this happens, it becomes less likely to find the electrons in neighboring sites, and vice versa more likely to find the electrons in the same site and with a non-zero relative displacement. Moreover, it is shown that as the interaction is increased, the individual probability densities p_{11} and p_{22} become centered roughly around the potential energy surface minima, which are shown with red contour lines, and that they approach a Gaussian line shape. It is then understood that the system becomes dominantly bipolaronic, i.e., it is described well by a bound state of two electrons and an accompanying displacement, and that, for the adiabatic case $\gamma = 1/8$, this cross-over is strongly correlated with the formation of the double well structure at $\lambda = 1$ in the adiabatic ground state potential energy surface. In **I** [SPAL15a], it is further shown that although the system becomes bipolaronic for sufficiently large interactions also for other values of the adiabatic ratio, in the anti-adiabatic case $\gamma \gg 1$, the cross-over is not by any means abrupt and the electron-pair forms with a less distinct lattice polarization.

8.2.2 Characterization of Equilibrium Solutions in Many-Body Approximations

In what follows, the results on the character of the ground state solutions in the Hartree and partially and fully self-consistent Born approximations published in **I** [SPAL15a] are summarized. In the process, some relevant remarks connecting these results to ones presented in **II** [SPAL15b] are made.

First of all, we have solved the ground state problem analytically in the Hartree approximation by solving the associated mean-field, equilibrium Hartree equations. It was found that while for $\lambda < 1$ a unique solution exists, three solutions co-exist for $\lambda > 1$ independent of the adiabatic ratio, and that the additional solutions, which are fixed-points of the time-dependent Hartree equations, as shown in **II** [SPAL15b], emerge in the manner of a supercritical pitchfork bifurcation. It is characteristic to these solutions that one of them has a symmetric (s), i.e., homogeneous density $n_s = 1$ while other two have asymmetric (a), i.e., inhomogeneous densities $n_{a\pm} = 1 \pm \sqrt{1 - \lambda^{-2}}$, and since $u_i = \sqrt{2} g n_i / \omega_0$, also the displacements are symmetric and asymmetric, respectively. Moreover, it is useful to point out that if the mean-field problem is seen as an optimization problem then by solving the electronic part it remains to optimize a potential energy surface for the nuclei which equals to $E_{\mathrm{BO}}(u)$ shown in Fig. 8.2.1. It is then intuitively clear that the asymmetric solutions emerge for $\lambda > 1$ since the potential energy surface forms a double well structure, and that the asymmetric solutions correspond to the degenerate minima of the surface while the symmetric solution exists as a saddle point.

In contrast to the mean-field case, we have been restricted to a numerical solution in the partially and fully self-consistent Born approximations. In order to illustrate convergence and show how the numerical solution depends on the (inverse) temperature (β) and the mesh parameters (a,b of Eq.(5.7)), the change in the quantum interaction energy $E_{\mathrm{epQ}} \equiv E_{\mathrm{ep}} + g \sum_{i=1}^{2} u_i n_i$ is shown in Fig. 8.2.2 as a function of these parameters for the adiabatic ratio $\gamma = 1/8$ and for the fully self-consistent Born approximation. It is noted that by a solution, we mean here and in the publications that the electron and phonon propagators satisfy the Dyson equation up to a numerical tolerance of 10^{-8}, cf., the appendix of **I** [SPAL15a]. In the left panel, it is shown for fixed mesh parameters that by choosing

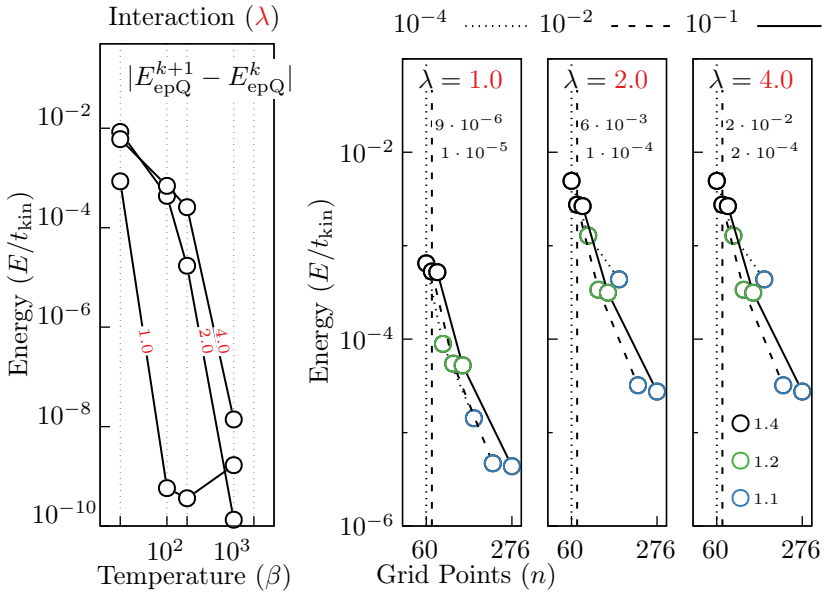

Figure 8.2.2: Illustration of convergence of the numerical solution in the fully self-consistent Born approximation for $\gamma = 1/8$ and $\lambda \in \{1, 2, 4\}$. Here, the change in the quantum part of the interaction energy $|E^{k+1}_{\mathrm{epQ}} - E^{k}_{\mathrm{epQ}}|$ is used as a measure of convergence. In the left panel, by k we label the inverse temperatures $\beta_k \in \big(2 \cdot 10^1, 10^2, 2 \cdot 10^2, 10^3, (2 \cdot 10^3)\big)$ with the parameters of the geometric mesh of Eq. (5.7) fixed to $a = 10^{-3}$ and $b = 1.1$. In the right panels, $\beta = 10^3$ is fixed and k labels the parameters of the geometric mesh. The lines (top legend) with circles (bottom right legend) correspond to a fixed a and $b_k \in \big(1.4, 1.2, 1.1, (1.05)\big)$ whereas the vertical lines (top legend) with a label, which indicates the change in the interaction energy, correspond to $b = 1.4$ and $a_k \in \big(10^{-2}, 10^{-3}, (10^{-4})\big)$.

$\beta = 10^3$, it is possible to obtain results for which a doubling of the inverse temperature only changes the energy by $\sim 10^{-8}$. In the right panels, it is further shown by fixing $\beta = 10^3$ that by choosing the mesh parameters $a = 10^{-3}$ and $b = 1.1$, which amounts to 228 grid points, it is possible to obtain results for which a further refinement of the mesh, either to $a = 10^{-4}$ or $b = 1.05$, only changes the energy by $\sim 10^{-4}$ for $\lambda = 4$. It is worth remarking that for $\lambda < 4$, the results are better converged for the same parameters, i.e., by refining the mesh the interaction energy changes even less. Moreover, a much faster convergence with respect to the refinement of the mesh is observed for larger adiabatic ratios, asymmetric solutions, and for the partially self-consistent Born approximation.

We have then found, for appropriate initial guesses, that also the partially and fully self-consistent Born approximations support at least three solutions which can be termed similarly as the symmetric and asymmetric solutions. In Fig. 8.2.3, the main observations on the character of the symmetric and asymmetric solutions in the correlated Born approximations are summarized. In the topmost panel, it is shown that in both Born approximations, the relative density $n \equiv n_1 - n_2$ behaves similarly to the mean-field case. Moreover, as indicated by the vertical dashed lines, which denote the critical interaction λ_C above which the asymmetric solutions have been found to exist, it is observed that the asymmetric solution emerges discontinuously in the fully self-consistent Born approximation, In the panel below, it is shown that unlike in the Hartree approximation, in the Born approximations the critical interaction does depend on the adiabatic ratio such that it increases monotonously as the adiabatic ratio is increased. In **I** [SPAL15a], we further analyze the partially self-consistent Born approximation analytically and propose that it approaches asymptotically the

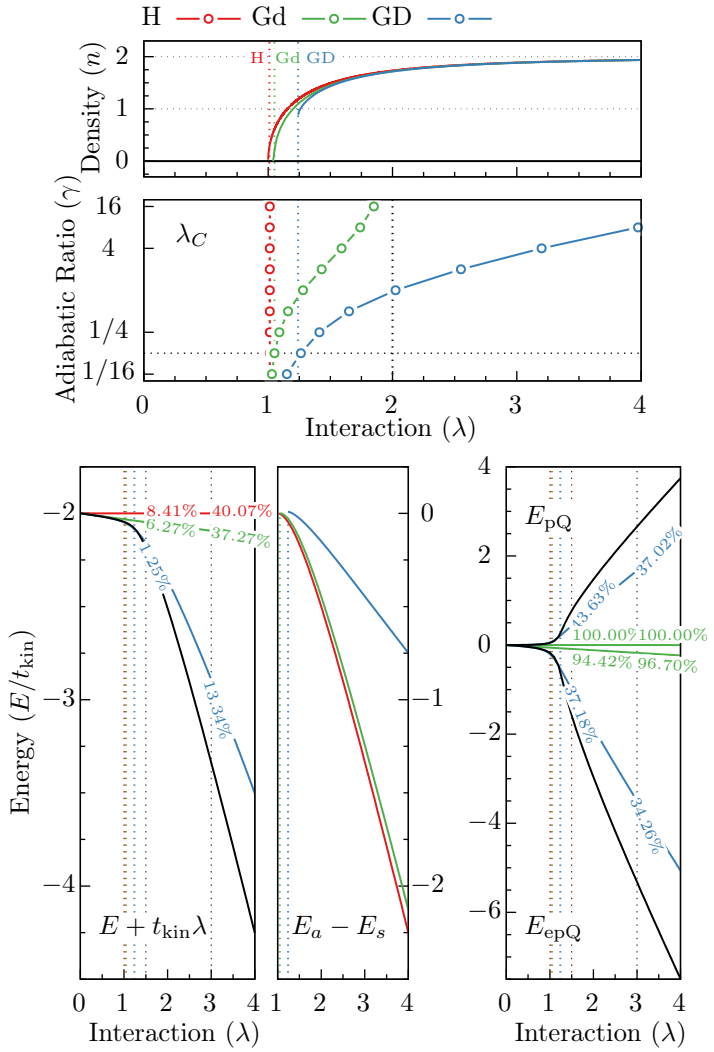

Figure 8.2.3: Illustration of the character of the ground state solutions in the Hartree (H) and partially (Gd) and fully (GD) self-consistent Born approximations. In the top panel, the relative density $n \equiv n_1 - n_2$ is shown for the asymmetric solutions as a function of the interaction λ for the adiabatic ratio $\gamma = 1/8$. The dashed vertical lines, color coded to H, Gd, and GD, denote the critical interactions λ_C. In the middle panel, the critical interaction is shown as a function of the adiabatic ratio. In the bottom left panel, the total energy $E + t_{\rm kin}\lambda$ of the relative Hamiltonian is shown as a function of the interaction. The relative error with respect to the exact total energy is shown in percentages for $\lambda \in \{3/2, 3\}$ which are denoted by dashed lines. The bottom middle panel shows the difference $E_a - E_s$ between the symmetric and asymmetric total energies. In the bottom right panel, the quantum phonon (positive energies) and electron-phonon interaction (negative energies) energies and their relative errors to the exact energy components (percentages, dashed vertical lines) are shown as a function of the interaction for the Born approximations.

Hartree approximation in the limits $\gamma \to 0$ and $\gamma \to \infty$, but in the latter case, i.e., for $\gamma \to \infty$, with the renormalized interaction $\lambda/2$. It can be seen from Fig. 8.2.3 that the numerical results do not exclude this proposition as the critical interaction does not exceed two when the adiabatic ratio γ is increased in the partially self-consistent Born approximation. In the same context, we

propose that the discontinuous emergence of the asymmetric solution for the fully self-consistent Born approximation can be associated with the so-called phonon vacuum instability which occurs if the phonon propagator is dressed with the bare polarization bubble. It is summarized here that this instability occurs for $\lambda > 1$ if the non-interacting electron propagator, or equivalently the symmetric mean-field propagator, is used and does not occur for $\lambda > \lambda_C$ if the asymmetric mean-field propagator is used. In the mean-field case $\lambda_C = 1$, and by thinking in terms of the potential energy surface E_{BO}, it is natural to interpret that the instability follows for the saddle point solution $u = 0$ since the curvature of the surface becomes negative and is prevented by allowing a readjustment to one of the newly formed minima $u \neq 0$. Moreover, based on this, we have hypothesized that in the fully self-consistent Born approximation, it is the shift of the critical interaction as a function of the adiabatic ratio which leads to an interval of interactions for which the asymmetric solutions would not exist. Finally, in the lower left panel of Fig. 8.2.3, it is shown that in the adiabatic case $\gamma = 1/8$, the asymmetric solutions are lower in total energy once they appear. It is also highlighted, by showing the relative errors with respect to the exact total energy, that the symmetric solution of the fully self-consistent Born approximation is in a good agreement with the exact result for the intermediate $\lambda \sim 1$ to border line strong interactions. However, in the bottom right panel, it is shown that if the separate energy components are instead compared then the deviations are much larger, which also illustrates a cancellation of errors.

8.3 Excited State Properties (Pubs. II,III)

In **II** [SPAL15b], we have, for one, studied the zero-temperature equilibrium solutions to the Dyson equation for the two-site, two-electron Holstein model of Sec. 8.1.1 in the Hartree (H) and partially (Gd) and fully (GD) self-consistent Born approximations. It has been the aim to complement our previous study in **I** [SPAL15a], in which only frequency-integrated observables, i.e., densities and energies, are considered, with a study of the frequency-resolved electron and phonon propagators from which, e.g., the non-neutral excitation spectrum follows, cf., Sec. 3.3.1. For another, we have studied, by using the same model, the zero-temperature equilibrium solutions to the Bethe-Salpeter equation obtained in the same (H, Gd, GD) many-body approximations by using the time-domain method documented in Ch. 7. In **III** [SML12], we have instead studied, by using the same method, the zero-temperature equilibrium solutions of the Bethe-Salpeter equation for the few-site Hubbard and Pariser-Parr-Pople models in the Hartree-Fock (HF) and second Born (2B) approximations. In the context of the Bethe-Salpeter equation, it was, in general terms, our purpose to explore what could be expected if the Kadanoff-Baym equations would be applied to obtain neutral excitation spectra, cf., Sec. 3.3.2, by solving for the density-density response functions.

8.3.1 Assessment of Performance of Hartree and Born Approximations

Here, a brief summary of the results and conclusions of **I** [SPAL15a] and **II** [SPAL15b] concerning the quality of the many-body approximations with regard to the equilibrium electron and phonon propagators of the two-site, two-electron Holstein model is provided.

In **II** [SPAL15b], we have compared the phonon propagators obtained in the many-body approximations against the exact phonon propagator. In the Hartree and partially self-consistent Born approximation the phonon propagator is equal to the non-interacting propagator which consists of a single delta function at the bare phonon frequency ω_0 independent of the interaction λ. Instead, the exact propagator has a strong dependence on the interaction and its dominant feature is a low

energy excitation with the frequency ω_p. In Fig. 8.3.1, in the top left panel, it is shown that ω_p tends to zero and, as shown in the top right panel, the corresponding oscillator strength gains intensity as a function of the interaction. In **II** [SPAL15b], we have analyzed that this behavior together with a simultaneously emerging excitation at ω_0 reflects the formation of the double-well structure in the adiabatic ground-state potential energy surface E_{BO}. In addition, due to a strong correlation between the formation of the double-well structure and the cross-over to a dominantly bipolaronic state, cf., Sec. 8.2.1, we have concluded that the aforementioned features can be seen as a spectral fingerprint of a bipolaronic system. In Fig. 8.3.1, it is seen that the fully self-consistent Born approximation describes the low energy excitation partly but it does not reproduce the excitation at ω_0 for $\lambda > 1$, for the studied parameters, and hence the phonon propagator does not exhibit sufficient bipolaronic character.

We have also compared and analyzed in **II** [SPAL15b] the approximate and exact electron propagators in a similar way. Here, in the lower panels of Fig. 8.3.1, it is shown that it is characteristic to the exact electron propagator that spectral weight is redistributed from the excitation at the frequency ω_e to higher-lying excitations as the interaction is increased. In the publication, we have furthermore derived that in the limit $\lambda \gg 1$, in which the system is dominantly bipolaronic, the electron propagator consists of the bare phonon frequency separated peaks with a Poissonian envelope. In the lower left panels of Fig. 8.3.1, it is shown that apart from the asymmetric solutions only the fully self-consistent Born approximation shows a significant loss of intensity of the excitation at ω_e in a qualitative agreement with exact results. However, by remembering that the symmetric solution of the Hartree approximation is equal to the non-interacting solution, it is possible to conclude based on the middle panels that none of the approximations reproduce correctly the frequency distribution of the exact propagator. In the lower right panels, it is moreover shown that none of the approximations display the correct intensity redistribution either. It follows from these observations that the approximate electron propagators cannot be seen to describe a dominantly bipolaronic system.

In **II** [SPAL15b], based on the spectral contents of the propagators, we have concluded that, despite what the frequency-integrated observables suggest in **I** [SPAL15a], none of the approximations show evidence of describing the bipolaronic cross-over even partially. Moreover, by focusing on the fully self- consistent Born approximation, we have concluded on a more quantitative level that a reasonably good agreement with the compared exact results is achieved up to intermediate $\lambda \sim 1$ interactions for the studied adiabatic ratios. In particular, in the case of the electron propagator, cf., Fig. 8.3.1, the fully self-consistent Born approximation breaks down due to a too dense spectrum and an insufficient redistribution of the spectral weight for $\lambda > 1$.

8.3.2 On Solutions of Bethe-Salpeter Equation in Hartree and Born Approximations

In what follows, some findings regarding the density-density response functions of the two-site, two-electron Holstein model are summarized.

In **I** [SPAL15a], we found multiple solutions to the Dyson equation which invoked the question that with respect to which solutions it would be reasonable or even possible to solve the Bethe-Salpeter equation. In the simplest case, in the Hartree approximation, the answer is suggested by the observation that the asymmetric solutions minimize the total energy whereas the symmetric solution is a saddle-point for $\lambda > 1$, cf., Sec. 8.2.2. It is then physically reasonable to regard the asymmetric solutions as the candidates for which the density response function could be obtained as described in Sec. 7.2.2. However, in the partially and fully self-consistent Born approximations, the asymmetric solutions do not, for instance, always have a lower total energy than the symmetric solution and we

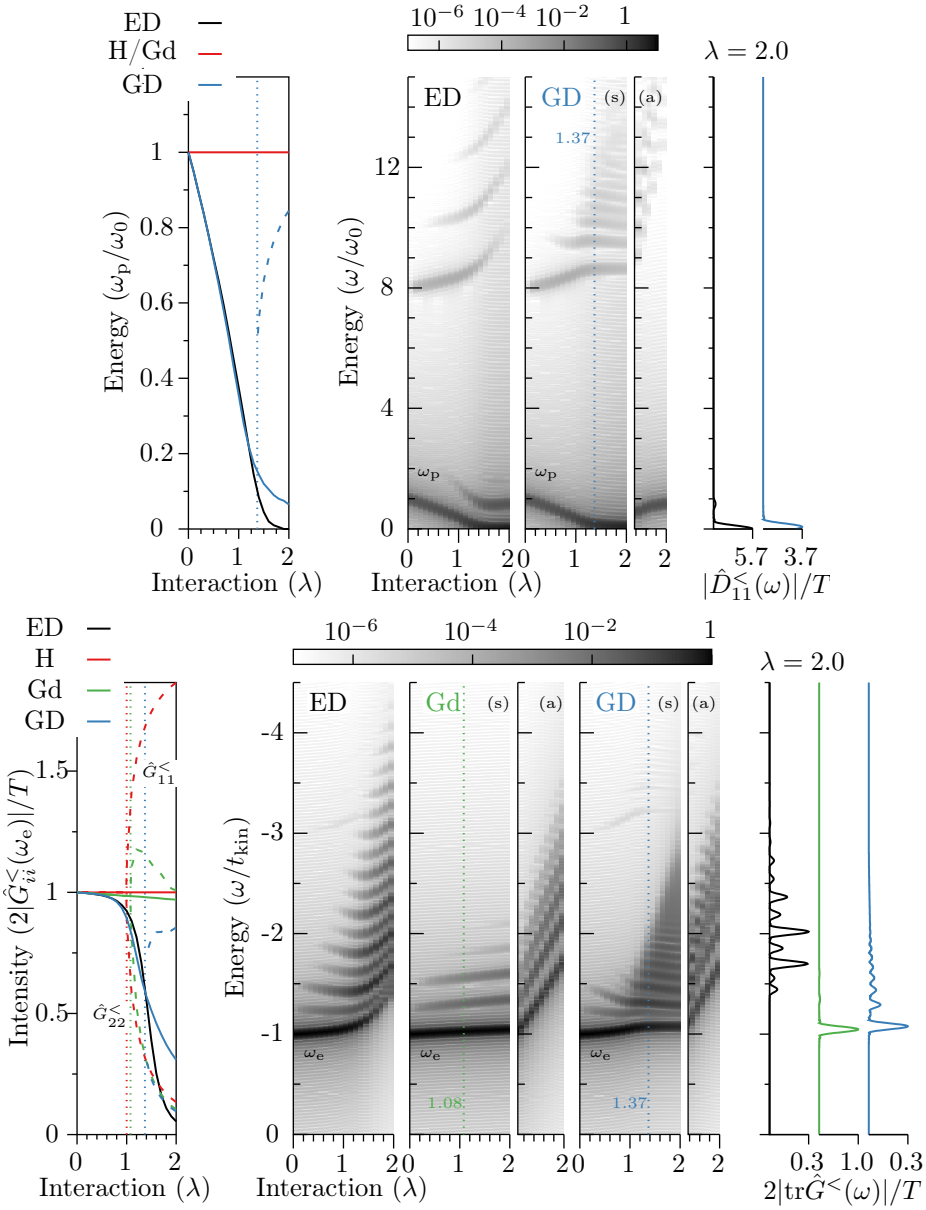

Figure 8.3.1: Illustrations of the ground state electron and phonon propagators of the two-site, two-electron Holstein model in exact diagonalization (ED) and in the Hartree (H) and partially (Gd) and fully (GD) self-consistent Born approximations shown for $\gamma = 1/4$. In the top left panel, the excitation energy ω_p is shown as a function of the interaction λ. In the top middle panel, the phonon propagator $|\hat{D}^>_{11}(\omega)|/T$ is shown on the logarithmic scale and, in the top right panel, on the linear scale for $\lambda = 2$. In the bottom left panel, the intensity corresponding to the excitation energy ω_e is shown. In the bottom middle panel, the electron propagator $2|\mathrm{tr}\hat{G}^<(\omega)|/T$ is shown on the logarithmic scale and, in the bottom right panel, on the linear scale for $\lambda = 2$. Here, results corresponding to the symmetric and asymmetric solutions are denoted respectively by the solid and dashed lines. The thin, vertical dashed lines denote the critical interaction λ_C shown next to the lines, $[\beta/\omega_0^{-1} = 10^3, T/t_{kin}^{-1} = 200]$

were not able to analyze the used total energy functional in order to establish if the solutions are saddle points or global/local minima. Moreover, the equilibrium propagators, which were described in Sec. 8.3.1, give no indication on how to choose the initial propagators with respect to which the density response function is obtained. In **II** [SPAL15b], in order to analyze this problem, we have first solved the density response function analytically in the Hartree approximation by solving the linearized Hartree equations, i.e., the Bethe-Salpeter equation with the Hartree kernel. By doing so, we have shown that the obtained time-domain response function has an oscillating component whose frequency tends to zero and amplitude diverges as $\lambda \to 1^-$. Moreover, if $\lambda > 1$ and the symmetric ground-state solution is used then the response function is an unbounded function but if instead an asymmetric ground-state solution is used then a well-defined, bounded response function is recovered. Here, it is appropriate to refer to App. 8.A.2 for an erratum regarding the equations for the Hartree response function presented in **II** [SPAL15b]. It is also noted here that the found instability of the symmetric ground state solution, which appears as the unboundedness of the corresponding response function, is congruent with the physical picture based on the nature of the solutions as the optimal points of an energy surface. In order to understand the stability characteristics of the ground-state solutions in the Born approximations, instead of a rigorous mathematical analysis, we have only resorted to a chosen numerical working measure of stability. For one, we have proposed by using the chosen working measure that, when they co-exist, the symmetric and asymmetric ground-state solutions of the partially self-consistent Born approximation are stable and unstable such that the corresponding density response functions are bounded and unbounded, respectively. For another, based on the working measure, we have proposed that both the symmetric and asymmetric solutions of the fully self-consistent Born approximation are stable and do not exhibit an unbounded density response function. It is noted that in the energetic picture, cf., E_{BO} in Fig. 8.2.1, it is plausible that the non-interacting phonon propagator, which is related to a Gaussian probability distribution, used in the partially self-consistent Born approximation is not compatible with the formation of the double-well structure. However, it is found less clear that by dressing the phonon propagator self-consistently in the lowest order in the fully self-consistent Born approximation, and hence allowing more complicated probability distributions for the nuclei, the instability related to the $u = 0$ saddle-point of the mean-field energy surface, is not observed for the physical and temporal parameters that we considered.

In **II** [SPAL15b], having identified the candidate ground-state solutions with respect to which it is reasonable to solve the Bethe-Salpeter equation, we further assessed the quality of the density response functions obtained by using the Hartree and the partially and fully self-consistent Born approximations. It is referred to Sec. 8.3.3, for a brief discussion related to the convergence of the frequency-domain density response functions obtained by using the method of Sec. 7.2.2. Instead here, in Fig. 8.3.2, we proceed to summarize our main findings regarding the density response functions obtained by using the stable solutions as the initial conditions when solving the Kadanoff-Baym equations. It is stressed that by the stable solutions, it is referred to the unique symmetric solutions for $\lambda < \lambda_C$, and for all λ in the case of the fully self-consistent Born approximation, as well as to the asymmetric solutions for all $\lambda > \lambda_C$. Moreover, it is noted that the obtained response functions satisfy the Bethe-Salpeter equation with the four-points kernels shown on top of the results in Fig. 8.3.2 as proven in Sec. 7.3. In the leftmost panel, it is shown explicitly that the intensity of the low energy excitation with the frequency ω_p diverges in the Hartree and partially self-consistent Born approximations when $\lambda \to \lambda_C$. In the fully self-consistent Born approximation, although no divergence is found, the intensity becomes monotonously decreasing as a function of the interaction for sufficiently large interactions in a qualitative disagreement with the exact results. In **II** [SPAL15b], we concluded, based in particular on these observations and on the observation that the excitation with the frequency ω_e is the dominant feature of the response function for $\lambda < 1$, cf., Fig. 8.3.2, that the density response function obtained in the fully self-consistent Born approximation is in a reasonably good agreement with the exact response function up to intermediate $\lambda \sim 1$ interactions. In the middle panels of Fig. 8.3.2, it is moreover illustrated that the fully self-consistent Born approx-

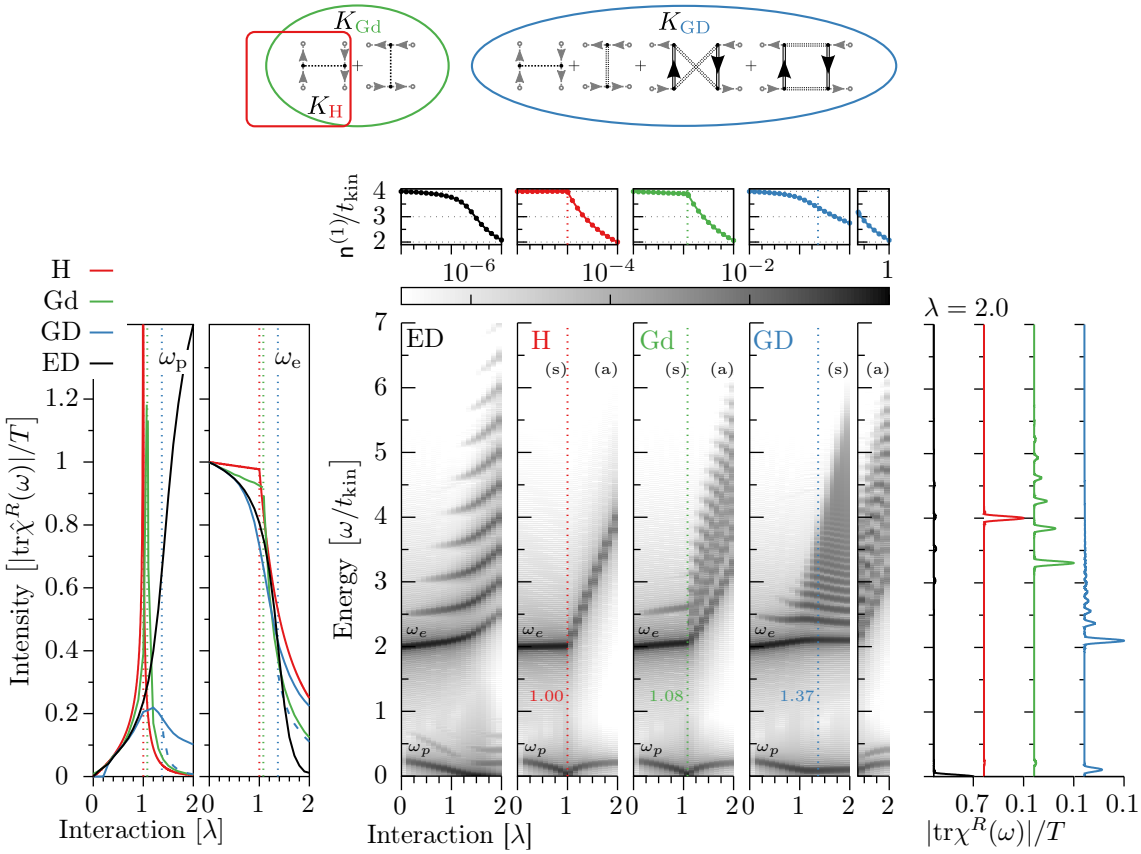

Figure 8.3.2: Illustrations of the retarded density response function of the two-site, two- electron Holstein model obtained by using the exact diagonalization (ED) and the Hartree (H) and partially (Gd) and fully (GD) self-consistent Born approximations for $\gamma = 1/4$. In the left panel, the intensities of the excitations with the frequencies ω_p and ω_e are shown as a function of the interaction λ. In the middle panel, the response function $|\mathrm{tr}\hat{\chi}^R(\omega)|/T$ is shown on the logarithmic scale and, in the right panel, on the linear scale for $\lambda = 2$. In the top panel, the first frequency moment $\mathsf{n}^{(1)}/t_{\mathrm{kin}}$ (points) and the electron energy $E_{\mathrm{e}}/t_{\mathrm{kin}}$ (lines) are shown. Here, by the solid and dashed lines for the GD results in the left and right panels, the results corresponding to the symmetric and asymmetric solutions are denoted, respectively. The thin, vertical dashed lines denote the critical interaction λ_C shown next to the lines, On top of the results, the four-point kernels $K = -\delta\Sigma[G]/\delta G$ corresponding to the self-energy approximations $\Sigma_{\mathrm{H}}[G]$, $\Sigma_{\mathrm{Gd}}[G]$ and $\Sigma_{\mathrm{GD}}[G]$ are shown. It is noted that in the right panel, a longer propagation time T is used in ED to obtain better converged intensities, hence also a more narrow peak is observed. $[\beta/\omega_0^{-1} = 10^3,\ T/t_{\mathrm{kin}}^{-1} = 200]$

imation fails to describe the high-energy spectra for $\lambda > 1$ as it gives rise to a too dense spectrum with an incorrect distribution of the spectral weight which is highlighted by the rightmost panel. It is noted that these observations are consistent with the observations we made about the equilibrium propagators, cf., Sec. 8.3.1.

In the top insets of Fig. 8.3.2, the electron energy $-2E_{\mathrm{e}}$ is shown against the first frequency moment $\mathsf{n}^{(1)}$ of the density response function to illustrate that the approximate density response functions do not exhibit gross violations of the f-sum rule. In fact, in **III** [SML12], we show explicitly, in the context of the electron-electron interactions, that any self-consistent, density conserving, i.e., gauge-invariant, many-body approximation satisfies the f-sum rule in a lattice model. It is noted that a

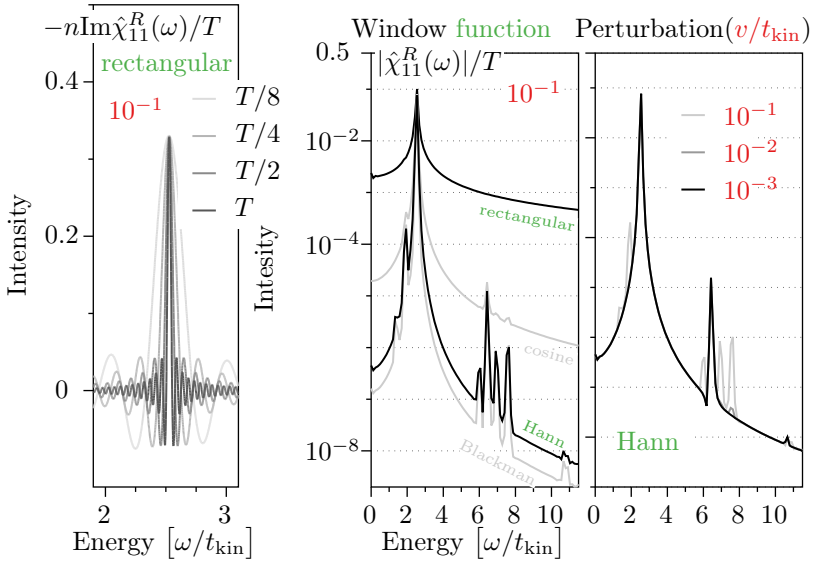

Figure 8.3.3: An illustration of the behavior of the windowed Fourier transform $\hat{\chi}^R_{11}(\omega)$ of $\chi^R_{11}(t) \equiv (n_1(t) - n_1(0))/v$ as a function of selected parameters. In the left panel, the behavior of the transform as a function of the width T/n, where $T/t_{\mathrm{kin}}^{-1} = 150$ and $n \in \{1, 2, 4, 8\}$, of the window function is shown for the rectangular window function when $v/t_{\mathrm{kin}} = 10^{-1}$. In the middle panel, the transform for $v/t_{\mathrm{kin}} = 10^{-1}$ is shown, on the logarithmic scale, also for the cosine, Hann and Blackman window functions. In the right panel, with the same axes as in the middle panel, the convergence of the transform with the Hann window is illustrated as a function of v. The middle and right panels have been plotted by using the Gnuplot option 'smooth bezier' in order to smoothen the original oscillatory curves.

proof of this in the spin-position basis can be found, e.g., in [LD04].

8.3.3 Correlation Induced Double Excitations in Second Born Approximation

In addition to the two-site Holstein model, we have investigated the solutions of the Bethe-Salpeter equation for the few-site Hubbard and Pariser-Parr-Pople models in **III** [SML12]. In what follows, our main finding concerning the second Born approximation is described by using the one-dimensional, periodic, six-site Hubbard model, cf., Sec. 8.1.2.

A few general remarks on the convergence of the density response functions are in order before proceeding to summarize the results. Firstly, the frequency-domain density response functions presented in this thesis have been evaluated by Fourier transforming, by using a window function [AM04], the time-domain response functions obtained as described in Sec. 7.2.2. In Fig. 8.3.3, the convergence of the density response function $\hat{\chi}^R_{11}(\omega)/T$ with respect to the choice and width T, i.e., the time-propagation length, of the window function and to the magnitude v of the perturbation is illustrated. In the figure, the zero-temperature density response function of the two-site, two-electron Hubbard model with $U/t_{\mathrm{kin}} = 1$ obtained in the second Born approximation is shown. In the left panel, it is shown on a linear scale that as T increases the intensity of the peaks in the frequency-domain re-

sponse function $\hat{\chi}^R_{11}$ increases linearly and their width, i.e., the full-width at half maximum, decreases roughly inversely with respect to T. In fact, in the case of the exact response function, it is expected if the rectangular window function $\theta(T-t)$ is used that $-\mathrm{Im}\hat{\chi}^R(\omega) \propto \sin((\omega-\Omega)T)/(\omega-\Omega)$, where Ω is an excitation energy, tends to $\pi\delta(\omega-\Omega)$ when $T\to\infty$ exactly as observed above. In the middle panel, it is illustrated, on a logarithmic scale, for $T/t_{\mathrm{kin}}^{-1}=150$ and $v/t_{\mathrm{kin}}=10^{-1}$ that it is possible to gain intensity resolution by using other window functions, e.g., the Hann window, which reduce the spectral leakage [AM04] at the expense of the frequency resolution in the sense that the spectral peaks gain width. In particular, as shown in Fig. 8.3.3, the other window functions reveal spectral weight with weaker $< 10^{-3}$ intensities. In the right panel, it is shown that when all of the other parameters, in particular the window function, are considered to be fixed then a converged density response function is obtained for $v/t_{\mathrm{kin}}=10^{-3}$. It is noted that there are also other parameters affecting the convergence of the results whose effect has not been checked in the example given in Fig. 8.3.3.

It is then proceeded to review the main result of **III** [SML12] concerning the second Born approximation. In Fig. 8.3.4, the density-density response functions obtained by using exact diagonalization (ED) and many-body perturbation theory in the Hartree-Fock (HF) and second Born (2B) approximations are shown for the six-site Hubbard ring. In the middle top panel, the results for the 1/2-filled ring with $U/t_{\mathrm{kin}}=1$ are shown for reference in order to illustrate a case in which both many-body approximations reproduce the exact spectra qualitatively correctly on the shown linear scale. It is noted that on a more quantitative level, the second Born approximation reproduces the exact response function slightly more accurately than the Hartree-Fock approximation. In the two bottom middle panels, the density response functions are shown for the 1/6-filled ring for $U/t_{\mathrm{kin}}\in\{1,2\}$. It is observed that the Hartree-Fock approximation fails to reproduce some exact excitations (E2) and that it is difficult to relate some exact excitations (E4,E5) to approximate ones. In contrast, it is shown that the second Born approximation is able to qualitatively describe the excitations labeled by E1-E6.

In **III** [SML12], we analyzed the density response functions by defining the so-called weighted occupation numbers to be able to associate populations, in the basis of Hartree-Fock orbitals, to possibly degenerate excited states contributing to the response function. In spite of our intention, these quantities are not suitable for the task since they are not invariant under unitary transformations in the subspace spanned by the degenerate states. In order to use a better suited quantity, the Approximate Excitation Level $\mathrm{AEL}_k=\mathrm{tr}|\gamma_k-\gamma_0|/2$ is used here similarly to [BHB12] to characterize the density response function. Here, γ_k is the one-body reduced ensemble density matrix with the equal weights $1/N_{E_k}$ for all states belonging to the N_{E_k}-fold degenerate subspace with the energy E_k. It is noted that even this definition is arbitrary in the sense that it depends on the used single-particle basis for the density matrix and if there are degeneracies in the chosen basis then different choices within the degenerate subspace lead to different excitation levels. Here, this ambiguity is avoided by further specifying that the reduced density matrix is represented in the single-particle basis $\varphi_{jk}=e^{\imath 2\pi jk/N}/\sqrt{N}$, where $j,k\in[1,N]\cap\mathbb{Z}$ and N is the number of sites, which diagonalizes simultaneously the density matrix and the lattice momentum operator, cf., [SL13]. It is noted that if the value of the approximate excitation level is close to n, it indicates a n-particle excitation. In Fig. 8.3.4, in the right panel, the approximate excitation levels are shown for the excitations labeled by E1-E6 in the 1/6-filled case. It is seen that the Hartree-Fock approximations fails to capture E2 since it arises due to dominantly a doubly excited states. Moreover, as both E5 and E6 have a strong double-excited state character, it is not possible for the mean-field approximation to describe both of them. It is noted that although the second Born approximation does describe the double-excited states qualitatively, its quality deteriorates as the interaction is further increased to $U/t_{\mathrm{kin}}=2$. It is also remarked that a qualitatively equivalent observation was published nearly simultaneously for few-electron quantum dots and the second Born approximation in [BHB12].

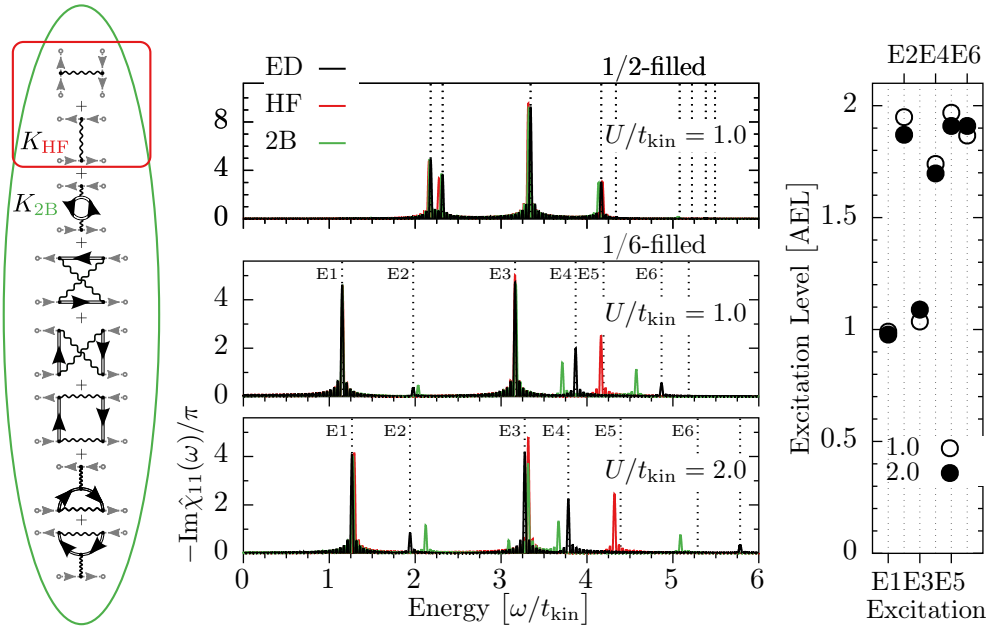

Figure 8.3.4: An illustration of the retarded density response functions for the six-site Hubbard ring in exact diagonalization (ED) and in the Hartree-Fock (HF) and second Born (2B) approximations. In the left panel, the four-point kernels K_{HF} and K_{2B} corresponding to the Hartree-Fock and second Born self-energy approximations are shown diagrammatically. In the middle panels, the density response function $-\mathrm{Im}\hat{\chi}_{11}(\omega)/\pi$ is shown for the 1/2-filled (six electrons) and 1/6-filled (two electrons) cases for selected interactions U/t_{kin}. Low-lying exact excitation energies which have non-zero oscillator strengths are denoted with vertical dashed lines and enumerated with labels E1-E6. In the right panel, the Approximate Excitation Levels (AEL) are shown for these labeled excitations in the 1/6-filled case. $[\beta/t_{\mathrm{kin}}^{-1} = 10^2,\ T/t_{\mathrm{kin}}^{-1} = 150]$

In **III** [SML12], we have also observed that there is a possibly spurious excitation for $U/t_{\mathrm{kin}} = 2$ close to E3 in the second Born density response function. It is noted that a possibly spurious excitation, by taking into account that convergence of the results is not properly checked for all parameters, is also visible for $\omega/t_{\mathrm{kin}} \sim 6 - 7$ in the right panel of Fig. 8.3.3. Although similar observations have been made both prior [RSB+09, SROM11] and after [BHB12] this observation, in particular when the response functions have been shown on a logarithmic scale, a systematic study of such defects has not been published up to present date.

Appendix

8.A Erratum

In the process of writing this thesis, the author has found some errors in the enclosed publications. In addition to the erratum provided below, the reader is referred to Sec. 8.3.3 for a discussion on a miss-definition which is used in **III** [SML12].

8.A.1 Pub. I

i In App. B, the equation

$$\begin{pmatrix} \boldsymbol{R}_k & -1 \\ 1^T & 0 \end{pmatrix} \begin{pmatrix} C \\ \mu \end{pmatrix} = \begin{pmatrix} \bar{0} \\ -1 \end{pmatrix}$$

should be

$$\begin{pmatrix} \boldsymbol{R}_k & -\bar{1} \\ -\bar{1}^T & 0 \end{pmatrix} \begin{pmatrix} \bar{C} \\ \mu \end{pmatrix} = \begin{pmatrix} \bar{0} \\ -1 \end{pmatrix}$$

where the overhead bar denotes a column vector.

ii In App. B, the last equations

$$\begin{aligned} \boldsymbol{G}^M_{k+1} &= d\mathcal{F}_G[\boldsymbol{G}^M_k, \boldsymbol{D}^M_k] + (1-d)\boldsymbol{G}^k_{\text{opt}}\,, \\ \boldsymbol{D}^M_{k+1} &= d\mathcal{F}_D[\boldsymbol{G}^M_k, \boldsymbol{D}^M_k] + (1-d)\boldsymbol{D}^k_{\text{opt}}\,, \end{aligned}$$

should be

$$\begin{aligned} \boldsymbol{G}_{k+1} &= \sum_{i=0}^{N_k} c_i \big(d\mathcal{F}_G[\boldsymbol{G}_{k-i}, \boldsymbol{D}_{k-i}] + (1-d)\boldsymbol{G}_{k-i} \big)\,, \\ \boldsymbol{D}_{k+1} &= \sum_{i=0}^{N_k} c_i \big(d\mathcal{F}_D[\boldsymbol{G}_{k-i}, \boldsymbol{D}_{k-i}] + (1-d)\boldsymbol{D}_{k-i} \big)\,, \end{aligned}$$

where $\boldsymbol{G}_{k+1}$ and $\boldsymbol{D}_{k+1}$ are the new iterates.

8.A.2 Pub. II

i In Fig. 7, in the left panels, all data displaying intensities should be multiplied by $\sqrt{2}$.

ii On p. 14, the equation

$$\chi_{\pm}^{n} = \frac{2t_{\mathrm{kin}}\left(\omega_0^2 - {\omega_{\pm}^{n}}^2\right)^2}{\omega_{\pm}^{n}\left(\left(\omega_0^2 - {\omega_{\pm}^{n}}^2\right)^2 + 4\lambda\omega_0^2 t_{\mathrm{kin}}\right)},$$

should be replaced with

$$\chi_{\pm}^{s} = \frac{2t_{\mathrm{kin}}\left(\omega_0^2 - {\omega_{\pm}^{s}}^2\right)^2}{\omega_{\pm}^{s}\left(\left(\omega_0^2 - {\omega_{\pm}^{s}}^2\right)^2 + 4\lambda\omega_0^2 t_{\mathrm{kin}}^2\right)},$$

$$\chi_{\pm}^{a} = \frac{2t_{\mathrm{kin}}\left(\omega_0^2 - {\omega_{\pm}^{a}}^2\right)^2}{\lambda\omega_{\pm}^{a}\left(\left(\omega_0^2 - {\omega_{\pm}^{a}}^2\right)^2 + 4\omega_0^2 t_{\mathrm{kin}}^2\right)},$$

and similarly for the last equation of the supplemental material.

9 Summary and Outlook

In this thesis, firstly, a summary of the theoretical and computational background behind time-independent and -dependent many-body perturbation theory for the electron-phonon and electron-electron interactions has been presented. In particular, it has been elucidated how time-dependent many-body perturbation theory for the electron and phonon propagators can be accomplished by solving the Kadanoff-Baym equations. Secondly, both the theoretical and numerical methodologies have been applied in three publications with the aims to (i) further develop this time-dependent approach, (ii) explore the quality and properties of realizable approximations and (iii) examine an alternative way to solve the Bethe-Salpeter equation.

In the theory part, an unconventional description of many-body perturbation theory for the electron-phonon interaction in terms of the two-component, displacement and momentum, operators has been presented including, e.g., an alternative proof of Wick's theorem for the phonon propagator. In the process, several points regarding the case of non-vanishing field expectation values have been clarified. A Galitski-Migdal total energy functional has been derived in terms of the two-component propagators for a system with both the electron-phonon and electron-electron interactions. It has also been re-derived by using the chosen representation, i.e., the two-component and a general basis representations, that a Ψ-derivable approximation satisfies the continuity equations for the one-body reduced density matrix and total energy. In the computational part, it has been described how the phonon field and the electron and phonon propagators are obtained by solving the coupled Dyson and Kadanoff-Baym equations. In particular, a numerical integration rule to solve for the real- and mixed-time components of the electron and phonon propagators corresponding to self-energies which are functions of the propagators has been presented. In this context, a class of two-stage methods has been proposed by relying on the ideas familiar from the numerical integration of one-dimensional Volterra integro-differential equations.

In Pubs. **I-III**, the methodologies presented in the theory and computational parts have been applied, in particular, to explore the quality of selected realizable many-body approximations. In **I** [SPAL15a], the equilibrium, in fact the zero-temperature, Hartree and partially and fully self-consistent Born approximations have been studied by benchmarking them against numerically exact results for the two-site and two-electron Holstein model. It has been found that the mean-field Hartree approximation exhibits spontaneous symmetry-breaking once the localizing effect of the electron-phonon interaction exceeds a critical limit. Although the partially self-consistent Born approximation is found to exhibit a similar behavior, albeit with a different critical limit, its fully self-consistent counterpart is not observed to break the symmetry continuously. It is concluded, by comparing against exact diagonalization results, that the fully self-consistent Born approximation is overall, for the considered adiabatic ratios and weak to strong interactions, in best agreement with the exact results when the total energies, energy components and natural occupation numbers are compared. In **II** [SPAL15b], these studies have been extended by considering also the equilibrium spectral functions and density-response functions obtained by solving the Kadanoff-Baym equations in the above mentioned many-body approximations. It has been found, by comparing against exact diagonalization, that although the fully self-consistent Born approximation performs overall the best, the approximate frequency-resolved propagators are in a substantially worse agreement with the exact results than the frequency-integrated observables studied earlier. It is concluded, based on this observation, that the fully self-

consistent Born approximation performs reasonably well up to intermediate interactions and cannot be said to describe, even partially, cf., **I** [SPAL15a], the bipolaronic crossover of the exact system. In this thesis, it has been verified explicitly that a density-response function obtained by solving the Kadanoff-Baym equations with a self-consistent electron self-energy Σ corresponds to a solution of the Bethe-Salpeter equation with the kernel $\delta\Sigma/\delta G$. In **II** [SPAL15b], we have shown that, if the symmetry-breaking is prevented, the density-response function obtained in this way by using the Hartree approximation becomes unbounded once the electron-phonon interaction exceeds the critical limit. In the same situation, we have found numerically, for the accessed time scales and physical parameters, that the density response functions obtained respectively by using the partially and fully self-consistent Born approximations do and do not become unbounded. Hence, we have concluded that the instability associated with the unboundedness of the density response is prevented already by dressing the phonon propagators with the simplest bubble self-energy in a self-consistent manner. In spite that no unboundedness is observed, by comparing against exact diagonalization, we have also concluded that the fully self-consistent Born approximation performs reasonably well only up to intermediate interactions beyond which its quality deteriorates and even qualitative disagreement with the exact results is found. In **III** [SML12], we have studied the Hartree-Fock and second Born approximations by comparing, in particular, the density response functions obtained as above against the exact results for selected few-site Hubbard and Pariser-Parr-Pople models. In doing so, we have observed that the second Born approximation is capable of reproducing qualitatively some of the structure of the exact response function which is not found in the mean-field Hartree-Fock approximation. We have concluded that this additional structure arises due to doubly-excited states which are thus, by a proof of example, possible to describe by using the Second Born approximation. In addition, we have summarized that, for the selected models and parameters, the second Born approximations performs better than the Hartree-Fock approximation but that the signs of possibly spurious excitations call for further research. In the appendix of **III** [SML12], we prove that a density response function obtained by solving the Kadanoff-Baym equations in a gauge-invariant self-energy approximation satisfies the f-sum rule also in a lattice system.

An outlook concerning further pursue of the aims is provided. In order to carry-on developing the time-dependent approach (i) used in this thesis, i.e., solving the Kadanoff-Baym equations, it would be desirable to find a way to alleviate the quadratic/cubic scaling of the method with respect to the temporal dimensions. In order to make the scaling issue concrete, it is noted that the storage of the phonon propagator required more than 100GB of memory for the largest dataset of the scaling tests of Sec. 5.4 which had $\sim$ 30k temporal grid points but a spatial basis with only two elements. It is known that a better scaling can be achieved by utilizing, e.g., the Generalized Kadanoff-Baym Ansatz (GKBA) but also numerical methods relying on efficient evaluation of the lag integrals for decaying integral kernels [Zwo08], which are ubiquitous for open systems, or methods which would use the equations for general initial states [Wag91, MR99, SKB99, LS12, LS13] would be worth a thought. In addition, it would also be useful to find more efficient, possibly adaptive, integration methods by carrying-on the development of the integration rule proposed in this thesis, even though they would not solve the scaling issue. It would be beneficial to work along these lines since it would enable both the application of the existing approximations to more realistic systems and also the development of more sophisticated approximations.

In order that the partially and fully self-consistent Born approximations studied here could be of a more wide interest, in further pursue of aim (ii), their properties should be studied in a truly time-dependent situations to find out if, and to which extent, issues such as the artificial damping documented in [FVA09, FVA10b] are found. In particular, in addition to simply the system size, the effect of the adiabatic ratio, i.e., more generally the relative energy scales of the interacting systems. would be interesting from the view point of applying the approximations to the closely related systems in quantum optoelectronics or optomechanics. Moreover, in these fields, it would be a virtue of the two-component propagators that some more complex interactions, obtained for

instance by neglecting some processes, or quantum mechanical states of light, such as squeezed states, could be modeled. Finally, to pursue the last aim (iii), in addition to expediting the development of the numerical methods, it would be called for to understand better, and to map out more thoroughly, the appearance of the spurious excitations [SROM11, SML12, BHB12] when solving the Kadanoff-Baym equations. In this regard, it would be possibly valuable to find out how more versatile, also non-self-consistent, approximations for the four-point kernel could be realized.

References

[AG98] Aryasetiawan F and Gunnarsson O, The GW method, Reports on Progress in Physics, 61:237 (1998)

[AGD65] Abrikosov A A, Gorkov L P, and Dzyaloshinski I E, Methods of Quantum Field Theory in Statistical Physics, Pergamon Press, 2nd ed. (1965)

[AGM11] Attaccalite C, Grüning M, and Marini A, Real-time approach to the optical properties of solids and nanostructures: Time-dependent Bethe-Salpeter equation, Phys. Rev. B, 84:245110 (2011)

[AKN06] Arnold V I, Kozlov V V, and Neihstadt A I, Mathematical Aspects of Classical and Celestial Mechanics, Spinger-Verlag (2006)

[Alm85] Almbladh C-O, On the theory of photoemission, Physica Scripta, 32:341 (1985)

[Alm06] Almbladh C-O, Photoemission beyond the sudden approximation, Journal of Physics: Conference Series, 35:127 (2006)

[AM04] Allen R L and Mills D W, Signal Analysis: Time, Frequency, Scale and Structure, John Wiley & Sons (2004)

[Amd67] Amdahl G M, Validity of the single processor approach to achieving large scale computing capabilities, in Proceedings of the April 18-20, 1967, Spring Joint Computer Conference, AFIPS '67 (Spring), pp. 483–485, ACM (1967)

[Atk89] Atkins K E, An Introduction to Numerical Analysis, John Wiley & Sons, 2nd ed. (1989)

[Bak70] Bakker A R, An experimental integrated system for application of a computer in shipbuilding industry, Ph.D. thesis, Delft University of Technology (1970)

[Bal07] Balzer K, Nonequilibrium Greens function approach to artificial atoms, Master's thesis, Christian-Albrechts-Universität zu Kiel (2007)

[Bal11] Balzer K, Solving the two-time Kadanoff-Baym equations application to model atoms and molecules, Ph.D. thesis, Christian-Albrechts-Universität zu Kiel (2011)

[Bay62] Baym G, Self-consistent approximations in many-body systems, Phys. Rev., 127:1391 (1962)

[BB09] Balzer K and Bonitz M, Nonequilibrium properties of strongly correlated artificial atoms - A Green's functions approach, Journal of Physics A: Mathematical and Theoretical, 42:214020 (2009)

[BBB10a] Balzer K, Bauch S, and Bonitz M, Efficient grid-based method in nonequilibrium Green's function calculations: Application to model atoms and molecules, Phys. Rev. A, 81:022510 (2010)

[BBB10b] Balzer K, Bauch S, and Bonitz M, Finite elements and the discrete variable representation in nonequilibrium Green's function calculations. atomic and molecular models, Journal of Physics: Conference Series, 220:012020 (2010)

[BBL+09] Balzer K, Bonitz M, van Leeuwen R, Stan A, and Dahlen N E, Nonequilibrium Green's function approach to strongly correlated few-electron quantum dots, Phys. Rev. B, 79:245306 (2009)

[BCOR09] Blanes S, Casas F, Oteo J A, and Ros J, The Magnus expansion and some of its applications, Physics Reports, 470:151 (2009)

[BDZ08] Bloch I, Dalibard J, and Zwerger W, Many-body physics with ultracold gases, Rev. Mod. Phys., 80:885 (2008)

[Ber07] Berciu M, Exact Green's functions for the two-site Hubbard-Holstein hamiltonian, Phys. Rev. B, 75:081101 (2007)

[BF04] Bruus H and Flensberg K, Many-Body Quantum Theory in Condensed Matter Physics, Oxford University Press (2004)

[BGK+01] Bonitz M, Golubnichiy V, Kwong N H, Semkat D, Kremp D, Filinov V S, and Schlanges M, Dielectric properties of correlated quantum plasmas, Contributions to Plasma Physics, 41:155 (2001)

[BGL+01] Betz M, Göger G, Laubereau A, Gartner P, Bányai L, Haug H, Ortner K, Becker C R, and Leitenstorfer A, Subthreshold carrier-LO phonon dynamics in semiconductors with intermediate polaron coupling: A purely quantum kinetic relaxation channel, Phys. Rev. Lett., 86:4684 (2001)

[BH86] Brunner H and van der Houwen P J, The Numerical Solution of Volterra Equations, Elsevier Science (1986)

[BHB12] Balzer K, Hermanns S, and Bonitz M, Electronic double excitations in quantum wells: Solving the two-time Kadanoff-Baym equations, EPL (Europhysics Letters), 98:67002 (2012)

[BJWM00] Beck M H, Jäckle A, Worth G A, and Meyer H-D, The multiconfiguration time-dependent Hartree (MCTDH) method: a highly efficient algorithm for propagating wavepackets, Physics Reports, 324:1 (2000)

[BK61] Baym G and Kadanoff L P, Conservation laws and correlation functions, Phys. Rev., 124:287 (1961)

[Blo67] Blomberg C, Some fundamental aspects of many-body problems in statistical thermodynamics, Ph.D. thesis, Royal Institute of Technology, Stockholm, Sweden (1967)

[BM07] Bartlett R J and Musiał M, Coupled-cluster theory in quantum chemistry, Rev. Mod. Phys., 79:291 (2007)

[But87] Butcher J C, The Numerical Analysis of Ordinary Differential Equations: Runge-Kutta and General Linear Methods, John Wiley & Sons (1987)

[CHR12] Casida M and Huix-Rotllant M, Progress in time-dependent density-functional theory, Annual Review of Physical Chemistry, 63:287 (2012), pMID: 22242728

[CLRRSJ73] Caroli C, Lederer-Rozenblatt D, Roulet B, and Saint-James D, Inelastic effects in photoemission: Microscopic formulation and qualitative discussion, Phys. Rev. B, 8:4552 (1973)

[Cor91] Corduneanu C, Integral Equations and Applications, Cambridge University Press (1991)

[CRR+12] Caruso F, Rinke P, Ren X, Scheffler M, and Rubio A, Unified description of ground and excited states of finite systems: The self-consistent *GW* approach, Phys. Rev. B, 86:081102 (2012)

[CRR+13] Caruso F, Rinke P, Ren X, Rubio A, and Scheffler M, Self-consistent *GW*: All-electron implementation with localized basis functions, Phys. Rev. B, 88:075105 (2013)

[Dan84] Danielewicz P, Quantum theory of nonequilibrium processes, I, Annals of Physics, 152:239 (1984)

[Dic54] Dicke R H, Coherence in spontaneous radiation processes, Phys. Rev., 93:99 (1954)

[DL05] Dahlen N E and van Leeuwen R, Self-consistent solution of the Dyson equation for atoms and molecules within a conserving approximation, The Journal of Chemical Physics, 122:164102 (2005)

[DL07] Dahlen N E and van Leeuwen R, Solving the Kadanoff-Baym equations for inhomogeneous systems: Application to atoms and molecules, Phys. Rev. Lett., 98:153004 (2007)

[DLS06] Dahlen N E, van Leeuwen R, and Stan A, Propagating the Kadanoff-Baym equations for atoms and molecules, Journal of Physics: Conference Series, 35:340 (2006)

[DSL06] Dahlen N E, Stan A, and van Leeuwen R, Nonequilibrium Green function theory for excitation and transport in atoms and molecules, Journal of Physics: Conference Series, 35:324 (2006)

[DVN05] Dickhoff W H and Van Neck D, Many-Body Theory Exposed!, World Scientific Publishing Company (2005)

[Eli60a] Eliashberg G M, Interactions between electrons and lattice vibrations in a superconductor, Sov. Phys. JETP, 11:696 (1960)

[Eli60b] Eliashberg G M, Temperature Green's function for electrons in a superconductor, Sov. Phys. JETP, 12:1000 (1960)

[Fil88] Filippov A F, Differential Equations with Discontinuous Righthand Sides: Control Systems, Kluwer Academic Publishers (1988)

[FVA09] Puig von Friesen M, Verdozzi C, and Almbladh C-O, Successes and failures of Kadanoff-Baym dynamics in Hubbard nanoclusters, Phys. Rev. Lett., 103:176404 (2009)

[FVA10a] Puig von Friesen M, Verdozzi C, and Almbladh C-O, Artificial damping in the Kadanoff-Baym dynamics of small Hubbard chains, Journal of Physics: Conference Series, 220:012016 (2010)

[FVA10b] Puig von Friesen M, Verdozzi C, and Almbladh C-O, Kadanoff-Baym dynamics of Hubbard clusters: Performance of many-body schemes, correlation-induced damping and multiple steady and quasi-steady states, Phys. Rev. B, 82:155108 (2010)

[FW71] Fetter A L and Walecka J D, Quantum Theory of Many-Particle Systems, McGraw-Hill (1971)

[GBH99] Gartner P, Bányai L, and Haug H, Two-time electron-LO-phonon quantum kinetics and the generalized Kadanoff-Baym approximation, Phys. Rev. B, 60:14234 (1999)

[GM58] Galitskii V and Migdal A, Application of quantum field theory methods to the many-body problem, Sov. Phys. JETP, 7:96 (1958)

[GMB57] Gell-Mann M and Brueckner K A, Correlation energy of an electron gas at high density, Phys. Rev., 106:364 (1957)

[Gou09] Gough B, GNU Scientific Library Reference Manual, Network Theory, 3rd ed. (2009)

[GSJ06] Gartner P, Seebeck J, and Jahnke F, Relaxation properties of the quantum kinetics of carrier-LO-phonon interaction in quantum wells and quantum dots, Phys. Rev. B, 73:115307 (2006)

[HBB12] Hermanns S, Balzer K, and Bonitz M, The non-equilibrium Green function approach to inhomogeneous quantum many-body systems using the generalized Kadanoff-Baym ansatz, Physica Scripta, 2012:014036 (2012)

[Hed65] Hedin L, New method for calculating the one-particle Green's function with application to the electron-gas problem, Phys. Rev., 139:A796 (1965)

[HJ08] Haug H and Jauho A-P, Quantum Kinetics in Transport and Optics of Semiconductors, Springer-Verlag (2008)

[HL70] Hedin L and Lundqvist S, Effects of electron-electron and electron-phonon interactions on the one-electron states of solids, Solid State Physics, vol. 23, pp. 1 – 181, Academic Press (1970)

[HL02] Hedin L and Lee J D, Sudden approximation in photoemission and beyond, Journal of Electron Spectroscopy and Related Phenomena, 124:289 (2002), frontiers in photoemission spectroscopy of solids and surfaces

[HLN83] Hairer E, Lubich C, and Nørsett S P, Order of convergence of one-step methods for Volterra integral equations of the second kind, SIAM Journal on Numerical Analysis, 20:569 (1983)

[HNW08] Hairer E, Nørsett S P, and Wanner G, Solving Ordinary Differential Equations I: Non-stiff Problems, Springer-Verlag, 2nd ed. (2008)

[HO10] Hochbruck M and Ostermann A, Exponential integrators, Acta Numerica, 19:209 (2010)

[Hol00a] Holstein T, Studies of polaron motion: Part I. the molecular-crystal model, Ann. Phys., 281:706 (2000)

[Hol00b] Holstein T, Studies of polaron motion: Part II. the "small" polaron, Ann. Phys., 281:725 (2000)

[HS74] Hirsch M W and Smale S, Differential Equations, Dynamical Systems, and Linear Algebra, Academic Press Inc. (1974)

[HSB14] Hermanns S, Schlünzen N, and Bonitz M, Hubbard nanoclusters far from equilibrium, Phys. Rev. B, 90:125111 (2014)

[Hub63] Hubbard J, Electron correlations in narrow energy bands, Proceedings of the Royal Society of London A: Mathematical, Physical and Engineering Sciences, 276:238 (1963)

[IMKNZ05] Iserles A, Munthe-Kaas H Z, Nørsett S P, and Zanna A, Lie-group methods, Acta Numerica, pp. 1–148 (2005)

[Kar07] Kardar M, Statistical Physics of Particles, Cambridge University Press (2007)

[KB62] Kadanoff L P and Baym G, Quantum Statistical Mechanics, W. A. Benjamin (1962)

[KB00] Kwong N-H and Bonitz M, Real-time Kadanoff-Baym approach to plasma oscillations in a correlated electron gas, Phys. Rev. Lett., 84:1768 (2000)

[Kel65] Keldysh L V, Diagram technique for nonequilibrium processes, Sov. Phys. JETP, 20:1018 (1965)

[KKY99] Köhler H S, Kwong N H, and Yousif H A, A Fortran code for solving the Kadanoff-Baym equations for a homogeneous fermion system, Computer Physics Communications, 123:123 (1999)

[KL16] Karlsson D and van Leeuwen R, Partial self-consistency and analyticity in many-body perturbation theory: particle number conservation and a generalized sum rule (2016)

[KSM+15] Kemper A F, Sentef M A, Moritz B, Freericks J K, and Devereaux T P, Direct observation of Higgs mode oscillations in the pump-probe photoemission spectra of electron-phonon mediated superconductors, Phys. Rev. B, 92:224517 (2015)

[KVS14] Kartsev A, Verdozzi C, and Stefanucci G, Nonadiabatic Van der Pol oscillations in molecular transport, Eur. Phys. J. B, 87:1 (2014)

[Lan76] Langreth D, Linear and nonlinear response theory with applications, in Linear and Nonlinear Electron Transport in Solids, edited by Devreese J and van Doren E, NATO Advanced Study Institutes Series, pp. 3–32, Springer US (1976)

[Lan93] Lang S, Real and Functional Analysis, Springer-Verlag, 3th ed. (1993)

[LD04] van Leeuwen R and Dahlen N E, Conserving approximations in nonequilibrium Green function and density functional theory, in The Electron Liquid Paradigm in Condensed Matter Physics, Proc. of the International School of Physics Enrico Fermi, vol. CLVII, IOS Press (2004)

[LNS+06a] Lorke M, Nielsen T R, Seebeck J, Gartner P, and Jahnke F, Influence of carrier-carrier and carrier-phonon correlations on optical absorption and gain in quantum-dot systems, Phys. Rev. B, 73:085324 (2006)

[LNS+06b] Lorke M, Nielsen T R, Seebeck J, Gartner P, and Jahnke F, Quantum kinetic effects in the optical absorption of semiconductor quantum-dot systems, Journal of Physics: Conference Series, 35:182 (2006)

[LS12] van Leeuwen R and Stefanucci G, Wick theorem for general initial states, Phys. Rev. B, 85:115119 (2012)

[LS13] van Leeuwen R and Stefanucci G, Equilibrium and nonequilibrium many-body perturbation theory: a unified framework based on the Martin-Schwinger hierarchy, Journal of Physics: Conference Series, 427:012001 (2013)

[LSC+76] Lakkis S, Schlenker C, Chakraverty B K, Buder R, and Marezio M, Metal-insulator transitions in Ti_4O_7 single crystals: Crystal characterization, specific heat, and electron paramagnetic resonance, Phys. Rev. B, 14:1429 (1976)

[Lub82] Lubich C, Runge-Kutta theory for Volterra integrodifferential equations, Numerische Mathematik, 40:119 (1982)

[LvV86] Lipavský P, Špička V, and Velický B, Generalized Kadanoff-Baym ansatz for deriving quantum transport equations, Phys. Rev. B, 34:6933 (1986)

[Mah00] Mahan G D, Many-Particle Physics, Kluwer Academic/Plenum Publishers (2000)

[Mat55] Matsubara T, A new approach to quantum-statistical mechanics, Progress of Theoretical Physics, 14:351 (1955)

[Mes61a] Messiah A, Quantum Mechanics, vol. I, North-Holland Publishhing Company (1961)

[Mes61b] Messiah A, Quantum Mechanics, vol. II, North-Holland Publishhing Company (1961)

[Mig58] Migdal A B, Interaction between electrons and lattice vibrations in a normal metal, Sov. Phys. JETP, 7:996 (1958)

[Min04] Minchev B V, Exponential integrators for semilinear problems, Ph.D. thesis, University of Bergen (2004)

[MMN+12] Marques M A L, Maitra N T, Nogueira F M S, Gross E K U, and Rubio A, Fundamentals of Time-Dependent Density Functional Theory, Lecture Notes in Physics, vol. 837, Springer-Verlag (2012)

[MPIF15] Message Passing Interface Forum, MPI: A Message-Passing Interface Standard, Version 3.1, Tech. rep. (2015)

[MR99] Morozov V G and Röpke G, The "mixed" Green's function approach to quantum kinetics with initial correlations, Annals of Physics, 278:127 (1999)

[MS59] Martin P C and Schwinger J, Theory of many-particle systems. I, Phys. Rev., 115:1342 (1959)

[MSSL08] Myöhänen P, Stan A, Stefanucci G, and van Leeuwen R, A many-body approach to quantum transport dynamics: Initial correlations and memory effects, EPL (Europhysics Letters), 84:67001 (2008)

[MSSL09] Myöhänen P, Stan A, Stefanucci G, and van Leeuwen R, Kadanoff-Baym approach to quantum transport through interacting nanoscale systems: From the transient to the steady-state regime, Phys. Rev. B, 80:115107 (2009)

[MSSL10] Myöhänen P, Stan A, Stefanucci G, and van Leeuwen R, Kadanoff-Baym approach to time-dependent quantum transport in AC and DC fields, Journal of Physics: Conference Series, 220:012017 (2010)

[MTK+12] Myöhänen P, Tuovinen R, Korhonen T, Stefanucci G, and van Leeuwen R, Image charge dynamics in time-dependent quantum transport, Phys. Rev. B, 85:075105 (2012)

[MVL03] Moler C and Van Loan C, Nineteen dubious ways to compute the exponential of a matrix, twenty-five years later, SIAM Review, 45:3 (2003)

[NBRG07] Nelson W, Bokes P, Rinke P, and Godby R W, Self-interaction in Green's-function theory of the hydrogen atom, Phys. Rev. A, 75:032505 (2007)

[NO12] Nedeljkov M and Oberguggenberger M, Ordinary differential equations with delta function terms, Publications de l'Institut Mathematique, 91:125 (2012)

[OARB15] OpenMP Architecture Review Board, OpenMP Application Program Interface, Version 4.5, Tech. rep. (2015)

[ORR02] Onida G, Reining L, and Rubio A, Electronic excitations: density-functional versus many-body Green's-function approaches, Rev. Mod. Phys., 74:601 (2002)

[PB11] Pathria R K and Beale P D, Statistical Mechanics, Elsevier, 3rd ed. (2011)

[PC06] Paganelli S and Ciuchi S, Tunnelling system coupled to a harmonic oscillator: an analytical treatment, Journal of Physics: Condensed Matter, 18:7669 (2006)

[Pop53] Pople J A, Electron interaction in unsaturated hydrocarbons, Trans. Faraday Soc., 49:1375 (1953)

[PP53a] Pariser R and Parr R G, A semi-empirical theory of the electronic spectra and electronic structure of complex unsaturated molecules. I, The Journal of Chemical Physics, 21:466 (1953)

[PP53b] Pariser R and Parr R G, A semi-empirical theory of the electronic spectra and electronic structure of complex unsaturated molecules. II, The Journal of Chemical Physics, 21:767 (1953)

[PSMS15] Perfetto E, Sangalli D, Marini A, and Stefanucci G, Nonequilibrium Bethe-Salpeter equation for transient photoabsorption spectroscopy, Phys. Rev. B, 92:205304 (2015)

[PTVF92] Press W H, Teukolsky S A, Vetterling W T, and Flannery B P, Numerical Recipes in C: The Art of Scientific Computing, Cambridge University Press, 2nd ed. (1992)

[Pul80] Pulay P, Convergence acceleration in iterative sequences: The case of SCF iteration, J. Chem. Phys. Lett., 73:393 (1980)

[Rab36] Rabi I I, On the process of space quantization, Phys. Rev., 49:324 (1936)

[Rab37] Rabi I I, Space quantization in a gyrating magnetic field, Phys. Rev., 51:652 (1937)

[Ram07] Rammer J, Quantum Field Theory of Non-equilibrium States, Cambridge University Press (2007)

[RGSC09] Ryndyk D A, Gutiérrez R, Song B, and Cuniberti G, Green function techniques in the treatment of quantum transport at the molecular scale, in Energy Transfer Dynamics in Biomaterial Systems, edited by Burghardt I, May V, Micha D A, and Bittner E R, pp. 213–335, Springer-Verlag (2009)

[RSB+09] Romaniello P, Sangalli D, Berger J A, Sottile F, Molinari L G, Reining L, and Onida G, Double excitations in finite systems, The Journal of Chemical Physics, 130:044108 (2009)

[Saa03] Saad Y, Iterative Methods for Sparse Linear Systems, SIAM, 2nd ed. (2003)

[SB16] Schlünzen N and Bonitz M, Nonequilibrium Green functions approach to strongly correlated fermions in lattice systems, Contributions to Plasma Physics, 56:5 (2016)

[SBP16] Schüler M, Berakdar J, and Pavlyukh Y, Time-dependent many-body treatment of electron-boson dynamics: Application to plasmon-accompanied photoemission, Phys. Rev. B, 93:054303 (2016)

[SDL06] Stan A, Dahlen N E, and van Leeuwen R, Fully self-consistent GW calculations for atoms and molecules, EPL (Europhysics Letters), 76:298 (2006)

[SDL09a] Stan A, Dahlen N E, and van Leeuwen R, Levels of self-consistency in the GW approximation, The Journal of Chemical Physics, 130:114105 (2009)

[SDL09b] Stan A, Dahlen N E, and van Leeuwen R, Time propagation of the Kadanoff-Baym equations for inhomogeneous systems, The Journal of Chemical Physics, 130:224101 (2009)

[SKB99] Semkat D, Kremp D, and Bonitz M, Kadanoff-Baym equations with initial correlations, Phys. Rev. E, 59:1557 (1999)

[SKGK16] Sentef M A, Kemper A F, Georges A, and Kollath C, Theory of light-enhanced phonon-mediated superconductivity, Phys. Rev. B, 93:144506 (2016)

[SL13] Stefanucci G and van Leeuwen R, Nonequilibrium Many-Body Theory of Quantum Systems: A Modern Introduction, Cambridge Unversity Press (2013)

[SLR+12] Strubbe D A, Lehtovaara L, Rubio A, Marques M A L, and Louie S G, Response functions in TDDFT: Concepts and implementation, in Fundamentals of Time-Dependent Density Functional Theory, edited by Marques A M, Maitra T N, Nogueira M S F, Gross E K U, and Rubio A, pp. 139–166, Springer-Verlag (2012)

[SML12] Säkkinen N, Manninen M, and van Leeuwen R, The Kadanoff-Baym approach to double excitations in finite systems, New Journal of Physics, 14:013032 (2012)

[SP16] Schüler M and Pavlyukh Y, Second-order bosonic Kadanoff-Baym equations for plasmon-accompanied optical absorption, Journal of Physics: Conference Series, 696:012006 (2016)

[SPAL15a] Säkkinen N, Peng Y, Appel H, and van Leeuwen R, Many-body Green's function theory for electron-phonon interactions: Ground state properties of the Holstein dimer, The Journal of Chemical Physics, 143:234101 (2015)

[SPAL15b] Säkkinen N, Peng Y, Appel H, and van Leeuwen R, Many-body Green's function theory for electron-phonon interactions: The Kadanoff-Baym approach to spectral properties of the Holstein dimer, The Journal of Chemical Physics, 143:234102 (2015)

[SROM11] Sangalli D, Romaniello P, Onida G, and Marini A, Double excitations in correlated systems: A manybody approach, The Journal of Chemical Physics, 134:034115 (2011)

[Str88] Strinati G, Application of the Green's function method to study the optical properties of semiconductors, Rev. Nuovo Cimento, 11:1 (1988)

[THG16] The HDF Group, Hierarchical Data Format, Version 5 (1997-2016)

[TR08] Thygesen K S and Rubio A, Conserving GW scheme for nonequilibrium quantum transport in molecular contacts, Phys. Rev. B, 77:115333 (2008)

[TSK+16] Tuovinen R, Säkkinen N, Karlsson D, Stefanucci G, and van Leeuwen R, Phononic heat transport in the transient regime: An analytic solution, Phys. Rev. B, 93:214301 (2016)

[Uim15] Uimonen A-M, Developments in many-body theory of quantum transport and spectroscopy with non-equilibrium Green's functions and time-dependent density functional theory, Ph.D. thesis, University of Jyväskylä (2015)

[UKS+10] Uimonen A-M, Khosravi E, Stefanucci G, Kurth S, van Leeuwen R, and Gross E K U, Real-time switching between multiple steady-states in quantum transport, Journal of Physics: Conference Series, 220:012018 (2010)

[UKS+11] Uimonen A-M, Khosravi E, Stan A, Stefanucci G, Kurth S, van Leeuwen R, and Gross E K U, Comparative study of many-body perturbation theory and time-dependent density functional theory in the out-of-equilibrium Anderson model, Phys. Rev. B, 84:115103 (2011)

[UY14] Ullrich C A and Yang Z Y, A brief compendium of time-dependent density functional theory, Brazilian Journal of Physics, 44:154 (2014)

[VSA06] Verdozzi C, Stefanucci G, and Almbladh C-O, Classical nuclear motion in quantum transport, Phys. Rev. Lett., 97:046603 (2006)

[Wag91] Wagner M, Expansions of nonequilibrium Green's functions, Phys. Rev. B, 44:6104 (1991)

[WALT14] Wang J-S, Agarwalla B K, Li H, and Thingna J, Nonequilibrium Green's function method for quantum thermal transport, Frontiers of Physics, 9:673 (2014)

[Wic50] Wick G C, The evaluation of the collision matrix, Phys. Rev., 80:268 (1950)

[WP68] Wolfe M A and Phillips G M, Some methods for the solution of non-singular Volterra integro-differential equations, The Computer Journal, 11:334 (1968)

[WR10] Wolfram Research, Mathematica, Version 8.0 (2010)

[WWTR14] Wilner E Y, Wang H, Thoss M, and Rabani E, Nonequilibrium quantum systems with electron-phonon interactions: Transient dynamics and approach to steady state, Phys. Rev. B, 89:205129 (2014)

[Zan99] Zanna A, Collocation and relaxed collocation for the Fer and the Magnus expansions, SIAM Journal on Numerical Analysis, 36:1145 (1999)

[Zwo08] Zwolak M, Numerical ansatz for solving integro-differential equations with increasingly smooth memory kernels: spin-boson model and beyond, Computational Science & Discovery, 1:015002 (2008)